



HAL
open science

Adaptation in an unsteady world - community adaptation and biodiversity-ecosystem functioning relationships, spatial heterogeneity and the evolution of stress tolerance, pulsed migration patterns and local adaptation

Flora Aubree

► **To cite this version:**

Flora Aubree. Adaptation in an unsteady world - community adaptation and biodiversity-ecosystem functioning relationships, spatial heterogeneity and the evolution of stress tolerance, pulsed migration patterns and local adaptation. Populations and Evolution [q-bio.PE]. Université Côte d'Azur, 2021. English. NNT : 2021COAZ6023 . tel-03564467

HAL Id: tel-03564467

<https://theses.hal.science/tel-03564467>

Submitted on 10 Feb 2022

HAL is a multi-disciplinary open access archive for the deposit and dissemination of scientific research documents, whether they are published or not. The documents may come from teaching and research institutions in France or abroad, or from public or private research centers.

L'archive ouverte pluridisciplinaire **HAL**, est destinée au dépôt et à la diffusion de documents scientifiques de niveau recherche, publiés ou non, émanant des établissements d'enseignement et de recherche français ou étrangers, des laboratoires publics ou privés.

THÈSE DE DOCTORAT

Adaptation dans un monde en mouvement :
Adaptation des communautés et relations biodiversité-fonctionnement des
écosystèmes, hétérogénéité spatiale et évolution de la tolérance au stress,
migration pulsée et adaptation locale

Flora AUBREE

Institut Sophia Agrobiotech, INRAE

Présentée en vue de
l'obtention du grade de
docteur en Biologie des
Interactions et Écologie
d'Université Côte d'Azur

Dirigée par :
Vincent CALCAGNO

Soutenue le : 8 Nov. 2021

Devant le jury, composé de :

György BARABÁS, Professeur adjoint, Linköping Uni-
versity

Vincent CALCAGNO, Directeur de Recherche, INRAE

Vincent A.A. JANSEN, Professeur, Royal Holloway Uni-
versity of London

Ludovic MAILLERET, Directeur de Recherche, INRAE

Virginie RAVIGNÉ, Directrice de Recherche, CIRAD

Elisa THÉBAULT, Chargée de Recherche, CNRS

Adaptation dans un monde en mouvement :
Adaptation des communautés et relations
biodiversité-fonctionnement des écosystèmes, hétérogénéité
spatiale et évolution de la tolérance au stress, migration
pulsée et adaptation locale

Jury

Directeur de thèse :

Vincent CALCAGNO – Directeur de Recherche INRAE – Laboratoire ISA (Institut Sophia Agrobiotech) – Université Côte d’Azur

Rapporteurs/trices :

György BARABÁS – Assistant Professor – Department of Physics, Chemistry and Biology, Group of Theoretical Biology – Linköping University

Virginie RAVIGNÉ – Chargée de Recherche CIRAD (HDR) – UMR PHIM (Plant Health Institut Montpellier) Montferrier-sur-lez – Université de Montpellier

Examineurs/trices :

Vincent A.A. JANSEN – Professor – Royal Holloway University of London

Elisa THÉBAULT – Chargée de Recherche CNRS – Laboratoire iEES-Paris (Institut d’Ecologie et des Sciences de l’Environnement de Paris) – Sorbonne université

Ludovic MAILLERET – Directeur de Recherche INRAE – Laboratoires ISA (Institut Sophia Agrobiotech), Inria Sophia Antipolis – Université Côte d’Azur

Adaptation dans un monde en mouvement :

Adaptation des communautés et relations biodiversité-fonctionnement des écosystèmes, hétérogénéité spatiale et évolution de la tolérance au stress, migration pulsée et adaptation locale

Résumé

Le monde change à un rythme sans précédent sous de nombreux aspects interconnectés les uns aux autres, et les écosystèmes sont parmi les premiers systèmes concernés. L'évolution actuelle des conditions environnementales – en partie induite par les activités anthropiques – s'accompagne d'une augmentation de la variabilité temporelle des processus environnementaux, qui vient s'ajouter à la variabilité naturelle existante. Ce travail de thèse fait parti des études qui cherchent à comprendre comment la variabilité de certains processus environnementaux clés va impacter la composition et les propriétés écologiques et évolutives des écosystèmes à différentes échelles. L'accent est mis en particulier sur l'interaction entre cette variabilité et le processus d'adaptation par évolution, qui est un aspect fondamental de la dynamique des écosystèmes. L'adaptation fait partie intégrante du fonctionnement des écosystèmes, mais elle est encore relativement peu considérée. Dans cette thèse, trois échelles biologiques sont considérées : l'échelle de la communauté, l'échelle de l'espèce et l'échelle des populations. Une approche de modélisation théorique est utilisée pour introduire certains aspects de la variabilité et étudier la façon dont les dynamiques écologiques et évolutives sont impactées.

A l'échelle de la communauté, nous questionnons l'impact que des changements dans le niveau de co-adaptation des espèces peuvent avoir sur certaines relations biodiversité-fonctionnement des écosystèmes (BEF ; relations diversité-productivité, diversité-stabilité et diversité-réponse aux invasions). Des communautés aléatoires et co-adaptées sont comparées à l'aide de méthodes de dynamiques adaptatives. Les résultats montrent que la co-adaptation des espèces a un impact sur la plupart des relations BEF, inversant parfois la pente de la relation. À l'échelle de l'espèce, l'évolution de la tolérance au stress, dans le cadre d'un modèle de trade-off tolérance-fécondité, est également explorée via des méthodes de dynamiques adaptatives. Les comportements évolutifs de ce modèle sont déterminés pour différentes intensités de trade-off et différentes distributions de stress. L'hétérogénéité du niveau de stress a un rôle plus important que le niveau de stress moyen dans la détermination de la stabilité de l'équilibre évolutif (contrôlant le branching). L'inverse est observé quant à la détermination de la valeur de la tolérance au stress à l'équilibre évolutif. Enfin, à l'échelle de la population, nous nous intéressons au flux génétique entre des sous-populations d'une même espèce, qui est un déterminant important de la dynamique évolutive. L'impact que des schémas de migrations variables dans le temps peuvent avoir sur le flux de gènes et sur l'adaptation locale est questionné en utilisant à la fois des analyses mathématiques et des simulations stochastiques d'un modèle île-continent. Dans ce modèle, la migration se produit sous forme de "pulses" récurrents. On constate que cette migratoire pulsée peut diminuer ou augmenter le taux de migration effectif selon le type de sélection appliquée. Globalement, la migration pulsée favorise la fixation d'allèles délétères et augmente la maladaptation. Les résultats suggèrent également que la migration pulsée peut laisser une signature détectable dans les génomes.

Pour conclure, ces résultats sont mis en perspective, et des éléments sont proposés pour tester ces prédictions avec des données d'observations. Certaines conséquences pratiques que ces résultats peuvent avoir pour la gestion des écosystèmes et la conservation biologique sont également discutées.

Mots clés : Dynamique adaptative, dynamique éco-évolutive, interactions entre espèces, génétique des populations, migration variable dans le temps, flux génétique, adaptation locale, simulations stochastiques, modélisation.

Adaptation in an unsteady world:
Community adaptation and biodiversity-ecosystem functioning
relationships, spatial heterogeneity and the evolution of stress
tolerance, pulsed migration patterns and local adaptation.

Abstract

The world is changing at an unprecedented rate in many interconnected aspects, and ecosystems are primarily concerned. The current shift in environmental conditions is accompanied by an increase in the temporal variability of environmental processes, which is also driven by anthropogenic activities. This work is part of the effort to understand how variability in key environmental processes impacts ecosystem composition and ecological and evolutionary functioning at different scales. The focus is made in particular on the interplay between such variability and the process of adaptation, which is a key aspect of ecosystem dynamics. Adaptation is integral to the functioning of ecosystems, yet it is still relatively little considered. In this thesis, three biological scales are considered – the scale of the community, the scale of the species, and the scale of populations. A theoretical modeling approach is used to introduce some aspects of variability and investigate how ecological and evolutionary dynamics are impacted.

At the community scale, the impact that changes in the species co-adaptation level may have on some biodiversity-ecosystem functioning (BEF) relationships (diversity-productivity, diversity-stability and diversity-response to invasion relationships) is questioned. Random and co-adapted communities are compared using adaptive dynamics methods. Results show that species co-adaptation impacts most BEF relationships, sometimes inverting the slope of the relationship. At the species scale, the evolution of stress tolerance under a tolerance-fecundity trade-off model is explored using adaptive dynamics as well. The evolutionary outcomes are determined under different trade-offs and different stress distributions. The most critical parameters in determining the evolutionary outcomes (ESS trait value, branching) are highlighted, and they evidence that stress level heterogeneity is more critical than average stress level. At the population scale, gene flow between sub-populations of the same species is an important determinant of evolutionary dynamics. The impact that temporally variable migration patterns have on gene flow and local adaptation is questioned using both mathematical analyses and stochastic simulations of a mainland-island model. In this model, migration occurs as recurrent “pulses”. This migration pulsedness is found to not only decrease, but also increase, the effective migration rate, depending on the type of selection. Overall, migration pulsedness favors the fixation of deleterious alleles and increases maladaptation. Results also suggest that pulsed migration may leave a detectable signature across genomes.

To conclude, these results are put into perspective, and elements are proposed for possible tests of the predictions with observational data. Some practical consequences they may have for ecosystem management and biological conservation are also discussed.

Keywords: Adaptive dynamics, Eco-evolutionary dynamics, Species interactions, Population genetics, Temporally variable migration, Gene flow, Local adaptation, Stochastic simulations

Remerciements

J'ai commencé ma thèse il y a 4 ans, avec le souhait d'explorer de multiples et divers aspects de l'évolution. Et j'ai effectivement exploré des questions très différentes, ce que j'ai beaucoup aimé et ne regrette pas, même si ce n'était rétrospectivement pas le choix le plus facile ! Je tiens à remercier Vincent Calcagno de m'avoir permis de réaliser cette aventure, et fournis un grand nombre d'outils. Merci pour ta présence et ton accompagnement. Je souhaite également remercier Thomas Guillemaud, qui a été mon deuxième directeur de thèse pendant plus de la moitié de ma thèse, et a été d'une aide précieuse dans les moments les moins évidents. Merci également à Ludovic Mailleret, pour les nombreuses discussions, les questionnements et les remises en question toujours bénéfiques.

J'aimerais aussi remercier l'ensemble des deux équipes qui m'ont hébergée pendant ces 4 années. L'équipe M2P2 (moi qui ait eu une bourse de thèse "*jedi*", je ne pouvais pas trouver mieux comme équipe d'accueil !) et l'équipe BPI. Guy, Lydia, Cécile, Louise, Suzanne, Valentina, Élodie, Alexandra, Thibaut & Thibaut, Géraldine, David, Quentin, Maxime, Chloé, Silène, Aurélie, Didier, David, Mélina, Victor, Silène, Marjorie, Samuel, Léo, Bruno, Christine, Séverine, Icham, Pia. Merci pour la présence attentionnée que j'ai apprécié chez beaucoup d'entre vous. Merci également à l'équipe Biocore de l'Inria, pour ces quelques échanges et séminaires partagés.

Merci aux doctorants qui m'ont accueillie lors de mon arrivée, en particulier Victor, Samuel et Marjorie. Et merci aux doctorants arrivés après moi pour votre présence à tous. Merci Dries et Antoine pour cette reprise du Journal Club qui j'espère, pourra continuer sur sa nouvelle lancée ! Merci Mélina, nouvelle co-bureau que le distanciel ne m'aura pas permis de côtoyer autant que j'aurais aimé. Merci pour ta présence, ton regard attentif et ta bienveillance.

Merci à la team musique de l'ISA ! Pour cette évasion en pleine rédaction, et surtout pour tous les bons moments d'écoute et de partage que je garde en mémoire.

Merci à l'ensemble des personnes à l'ISA ou à l'Université avec qui j'ai pu interagir lors des cours et TDs que j'ai pu donné. Cela a toujours été une bonne expérience, et si je ne fais plus d'enseignement pour le moment, je pense que j'y retournerai très probablement un jour.

Merci enfin aux organisations qui m'ont financée ou accueillie : l'Université Côte d'Azur, pour m'avoir fournie une bourse de thèse Idex UCA*jedi*, et l'Institut Sophia Agrobiotech, pour m'avoir hébergée pendant 4 ans. Merci également à toutes les personnes qui ont participé à tout l'administratif qui se cache derrière une thèse !

Pour terminer, je souhaite élargir un peu les horizons des remerciements, à la fois temporellement et spatialement. Ci-dessous, quelques mots, rapides mais non des moindre à mes yeux, pour remercier des personnes qui m'ont inspirée, marquée et/ou accompagnée lors de mon parcours professionnel, mais aussi mon chemin personnel.

Je repense de temps en temps à plusieurs professeur.e.s de collège et de lycée qui m'ont marquée lors de ma scolarité, à quelques professeur.e.s de ma classe prépa et de l'ENS de Lyon. Également, merci à mon premier encadrant de stage de recherche, Bruno Moulia, pour cette première expérience de la recherche qui avait confirmé mon envie d'explorer cette voie.

Ensuite, merci aux danseurs et danseuses pour ces moments de légèreté, aux co-doctorants vallauriens et antibois pour le travail partagé, et aux ami.e.s et membres de ma famille présent.e.s à chaque instants. Merci à toutes les personnes qui sont là et me soutiennent, en étant proche ou à distance. Je ne les citerai pas tou.te.s, ils/elles savent qu'ils/elles sont là derrière ces lignes !

Contents

Introduction	1
1 Ecological systems in an unsteady world	1
1.1 Biological systems and scales considered	1
1.2 Variability encountered	3
2 Adaptation as a response to fluctuations and changes	5
2.1 Definition of adaptation	5
2.2 Manifestations of adaptation	7
2.3 Tools for modeling adaptation	9
3 Questions addressed in the thesis	14
1 How community adaptation impacts biodiversity-functioning relationships	29
1.1 Introduction	31
1.2 Material and methods	32
1.2.1 Ecological scenarios and traits	32
1.2.2 Random and co-adapted communities	35
1.2.3 Biodiversity-functioning relationships	36
1.3 Results	37
1.3.1 Biodiversity-Productivity	37
1.3.2 Species trait composition	38
1.3.3 Biodiversity-Stability	40
1.3.4 Biodiversity-Invasion	40
1.4 Discussion	42
2 Evolution of stress tolerance under a tolerance-fecundity trade-off	53
2.1 Introduction	55
2.2 Model and Method	58
2.2.1 Model definition	58
2.2.2 Analysis	59
2.2.3 Specific definition and functions for numerical analyses	63
2.3 Results	67
2.3.1 Overview of model behavior through sensitivity analysis	67
2.3.2 Evolutionary equilibrium of stress tolerance x^*	70
2.3.3 The evolutionary stability	71
2.3.4 The relative coexistence surface for two species	73
2.3.5 Impact of the dose-response curve asymmetry	73
2.3.6 Evolutionary dynamics with more than one species	74
2.4 Discussion	75

3	Migration pulsedness alters patterns of allele fixation and local adaptation in a mainland-island model	87
3.1	Introduction	89
3.2	Methods	91
3.2.1	Mainland-island model	91
3.2.2	Mathematical analysis	93
3.2.3	Simulations	93
3.3	Results	94
3.3.1	A general criterion to predict the impact of migration pulsedness	94
3.3.2	Neutral alleles	95
3.3.3	Alleles under selection with co-dominance	96
3.3.4	Introducing dominant and recessive alleles	97
3.3.5	Mean fitness and pulsedness load	99
3.3.6	The genomic signature of pulsedness	100
3.4	Discussion	101
	Conclusions & Perspectives	111
	Appendix	123
A	Supplementary information for Chapter 1	123
A.1	Modelling of the four ecological scenarios	123
A.1.1	Niche scenario	123
A.1.2	Body-size scenario	124
A.1.3	Life History Trade-off scenario	124
A.1.4	Trophic scenario: derivation of the Lotka-Volterra form	125
A.2	Parameter sets explored and those plotted in the main article figures	127
A.3	Algorithm of community formation	128
A.4	Metrics used to quantify diversity-functioning relationships	130
A.4.1	Productivity	130
A.4.2	Stability	132
A.4.3	Response to invasion	133
A.4.4	Metrics for trait composition	134
A.5	Magnitude of the difference between random and co-adapted communities	136
A.6	Coefficient of variation of the average interval between trait values	137
A.7	Results with a limit on possible trait change	138
B	Supplementary information for Chapter 2	143
B.1	Equivalence between parameters	143
B.1.1	The fecundity steepness c_s	143
B.1.2	The dose-response steepness β_s	143
B.2	Complements for the dose-response parameter choices	144
B.2.1	Symmetric versions	144
B.2.2	Asymmetric versions	144
B.3	Changes in x^* with the steepness of the fecundity and dose-response functions	145

B.4	Performance of the species at the evolutionary equilibrium	146
C	Supplementary information for Chapter 3	147
C.1	Complements to the method	147
C.1.1	Time scale separation for the mathematical analysis	147
C.1.2	Gillespie algorithm for the simulations	147
C.1.3	Simulation time optimization	148
C.2	Selection values at transitions (figure 4 from the main article)	149
C.3	Finding s_{l1} and slopes of n_l and n_+ around it	149
C.3.1	Finding s_{l1} in frequency-independent selection case	149
C.3.2	Finding the slope of n_+ around s_{l1} as a function of s	150
C.3.3	Finding the slope of n_l , knowing the slope of n_+	151
C.4	Effective migration rate from simulation	153
C.5	Mean number of migration events before fixation	154
C.6	Simulations without time-scale separation and for different popula- tion sizes	155
C.6.1	Large m cases: the “mass” effect	155
C.6.2	Simulations for various m and N	155
C.7	Probability that a mainland allele gets fixed, mean fitness in the island and pulsedness load	157
C.7.1	Probability f_1 that a mainland allele gets fixed	157
C.7.2	Genetic load and pulsedness load	157
C.8	Likelihood and fitting the continuous model on pulsed data	158
C.8.1	Methodology	158
C.8.2	The case of a migrant pool distribution centered on a negative value of s	159
C.8.3	Pulsedness load depending on the allelic distribution of the migrant pool	160
D	Inferring migration pulsedness from a genomic dataset	163
D.1	Type of data needed	163
D.2	Model description	164
D.3	Comparison with stochastic simulations and Chapter 3’s mathemat- ical model	166
D.4	Fit by a maximum likelihood method	167

Introduction

*Logic will get you from A to B.
Imagination will take you everywhere.*

Albert EINSTEIN

1 Ecological systems in an unsteady world

Trying to understand, explain and predict the world in which we live can be approached from many different perspectives and disciplines. A common challenge often lies in the fact that multiple sources of variability may be difficult to grasp and integrate, and the understanding of the living is no exception to the rule (Vasseur & McCann, 2007). Environmental variation is an ubiquitous component of living processes in the natural world. The physical and biological conditions that influence life are continuously changing in time and space, what induces changes in many living characteristics or processes as physiology, behavior, ecology, or also evolution (Ruokolainen *et al.*, 2009). Those many external sources of variability (of biological or physical origin) are more or less predictable and modelizable depending on their nature. In addition, the intrinsic variability of the living complexifies the approach, reducing the reproducibility and the possibility of predicting the outcome of a biological process.

Variability is closely linked to the process of adaptation (Futuyma, 1998; Losos, 2017). Adaptation, and more generally evolution, participates in biological variability, while variability is both a source and a trigger for ecosystem adaptation. A trigger because the forces governing adaptation are more likely to be null without existing changes or fluctuations affecting the system we consider, so that the system would stay where it is. And a source, because adaptation can often be seen as the selection of a beneficial existing variation for the system ; in other words, adaptation relies on some variations to occur. The main interest of this manuscript will be adaptation in living system in relation to variability. More specifically, we will be interested in ecological systems adaptation, what means that we will consider individuals and populations, and not cells or organs within an individual. Before going into the details of what we mean by ecological adaptation, we will first define the relevant biological scales we will consider (from the population to the community), and which variability they may encounter.

1.1 Biological systems and scales considered

Biological scales We are interested in adaptive changes that occur in biological systems ranging from the population to the community, which are the typical focus

of ecology, evolutionary biology and population genetics studies (Losos, 2017). We will not specify which kind of ecosystem in particular, as our modeling approach seeks to obtain general results. A **population** is a group of individuals which live in a particular geographical area and belong to the same species, while a **species** designates the ensemble of all the individuals (on earth) that are (really or potentially) capable of interbreeding and to produce fertile offspring (Futuyma, 1998). A population is sometimes hard to define properly when there exist migration between populations of the same species. We precise here that by migration we mean dispersal, as usually the case in population genetics. Migration provokes a gene flow that may homogenize genes and alleles in different populations, and allow the interbreeding of individuals that come from geographically distinct places. A **community** is a group of populations that all belong to different species, and that live in the same geographical area. There is no possible mating between populations, and populations interact through ecological interactions as competition, mutualism, predation (Futuyma, 1998). The community concept has a botanical origin, but is nowadays largely used for both plant and animal populations interaction. In practice, it is not always easy to define a community isolated from outside interactions, but some delimited systems can be approximated as so (islands, forests, grasslands, etc.). Both the system of study and the question we want to ask will guide the relevant spatial and time scales to consider.

The spatial scales They have to be large enough to contain populations or communities, and small enough to match with the definitions of population or communities (i.e. allowing interbreeding or ecological interactions). Defining a proper spatial scale is often under debate as it may profoundly impact the patterns one finds (Wiens, 1989; Henle & Grobelnik, 2014; Czarniecka-Wiera *et al.*, 2020). Every single study will have to properly define its relevant spatial scale, depending on the organisms and questions considered. For instance, some microbial communities can spread over only a few centimeters or even less (Green & Bohannan, 2006), while a typical grassland community could be of the order of less than a hectare to a few thousand of hectares (Czarniecka-Wiera *et al.*, 2020). Also, a bird population can spread over a few hundred or thousand of square kilometers like on some islands distant from the mainlands (in the Mascarene Islands for instance Milá *et al.*, 2010). In this manuscript, we will not explicitly define any spatial scales as they will be implicit within the definition of population and communities.

The temporal scales The temporal scale and time unit condition the type of questions and evolutionary observations we can make (Gingerich, 2001). Of course, it must be large enough to let changes occur from one generation to the next. Here, we will focus on adaptive evolution occurring over temporal scales that are not too large so that we will be able to see the details of changes, and not only their average or effects over too long periods of time, or not only the results of successive large but rare catastrophic events. In other words, we will be mostly interested in what is classically called microevolution (the short term evolutionary changes within population or species) rather than macroevolution (phenotypic changes usually great enough to allocate the changed lineage and its descendants to a distinct genus or taxon, Futuyma, 1998). We will thus consider time units from a few generation up to a few hundred of generations depending on the questions asked (Gingerich,

2001). Those timescales will then define the type of variable phenomena that have a relevant impact for ecological adaptation. In the following paragraph, we will see some of the several natural sources of variability and contemporary environmental changes that operate on this timescale.

1.2 Variability encountered

In this section, we will briefly expose how variability may affect ecosystems, decomposing the latter into three schematic components. From a large point of view, an ecosystem can be seen as a *structure*, that has different *properties* (or functions), and the potentiality to *evolve*.

Variation affecting ecosystem structure...

An ecosystem is literally a system composed of several entities, which interact together, into an environment. When asking the question of the variability that may affect ecosystems, one has to consider those three aspects: the environment, the entities (ecosystem composition) and the interactions. They all three influence each other, and may of course be impacted by external factors. Because of all the interconnected influences, the list would be long, and is not the purpose of this introduction. We just give here some examples of processes variation affecting the ecosystem structure. Some reviews summarize some of them (Wrona *et al.*, 2006; Miles *et al.*, 2019; Cao *et al.*, 2020; Rogers *et al.*, 2020; Leal Filho *et al.*, 2021).

Global climate is likely to influence local meteorological condition, which in turn affects habitat quality (the “environment”) (Vermeulen *et al.*, 2012; Leal Filho *et al.*, 2021). Habitat quality (soil and water quality) is also impacted by anthropic activities as urbanization, land use and pollution (Zari, 2014; Mahmoud & Gan, 2018; Cao *et al.*, 2020; Tanaka *et al.*, 2021). In turn, habitat quality may affect ecosystem composition (the “entities”) (Wrona *et al.*, 2006), or even species and individuals interactions (Cassidy *et al.*, 2020). Ecosystem composition is also impacted by connectivity which may bring new species or individuals into a specific environment. Connectivity is impacted by many different kind of processes that are potentially highly variable as various geographical barriers (Morris-Pocock *et al.*, 2016) or sea currents (Benestan *et al.*, 2021), meteorological conditions (Jones & Harrison, 2004) and water regimes (Carlton *et al.*, 2017) or even urbanization and land use (Miles *et al.*, 2019) and anthropic transportation (Carlton & Cohen, 2003). Variability affecting connectivity will be more detailed in Chapter 3.

All those processes are potentially highly variable. Any kind of variation in ecosystem structure may then affect ecosystem properties and shape, and in turn, evolution. The two next paragraphs provide some non-exhaustive examples of such impacts.

... with impacts on ecological properties...

Environmental variance may both increase or decrease the long-term population growth (Lawson *et al.*, 2015). Individual growth (nestling growth and development for avian for instance, Sauve *et al.*, 2021) is also impacted by weather variations like variations in wind speed, rainfall, solar radiation and air temperature. Grassland productivity is sensitive to soil-water content variability (Manea & Leishman,

2018). And more generally, all crops productivity and food quality (nutrients) are affected by many climatic factors potentially highly variable as CO₂ concentrations, precipitation, temperature or sunlight, inter-seasonal changes, or even sea level rise (Giulia *et al.*, 2020). Changes in some ecosystem components (as resources) impact ecosystems stability (Olivier *et al.*, 2020). The resilience of ecosystems are also shown to be affected by variability in temperature. For instance, the resilience of ant population is greater when the thermal variability is usually greater (Arnan *et al.*, 2015). On the contrary, Hernández-Padilla *et al.* (2021) found for instance that the resilience of the southeastern Gulf of California ecosystem decreases under high sea surface temperature variability. Moreover, they found that the trophic role of species is changed and reorganized under periods of low or high variability.

... and evolution.

Not surprisingly, evolution is also found to be impacted by environmental variations. Variation in the physical environment is found to impact the rate of diversification in inland water for instance (Hebert, 1998), by altering the mutation rate and modifying the exposure to selection (through genotype by environment interactions). Species as the ginseng are found to be locally adapted to inter-annual variation in temperature, what could modify their adaptation potential to shift in thermal niches (Souther & McGraw, 2011). On the contrary, a stochastic temperature variation may also impede adaptation, as for some RNA viruses (Alto *et al.*, 2013). Leaving in a variable environment may also participate in maintaining a genetic diversity large enough to face future fluctuations or changes, as shown for marine sticklebacks (Shama, 2017). Also, temporal variability in the environment is found to favor generalists rather than specialists (see e.g. ?), provided that the period of temporal changes is not too large compared to the generation time. The period of time changes is critical, and is briefly discussed in the next paragraph.

About the patterns of variation

It is interesting to note the distinction between a change in mean environmental conditions and a fluctuation around a mean. By change we mean the passage from one state to another, without necessarily the possibility of a return. By fluctuation we mean the move now in one direction and now in another, around a mean state. A mean change over a small time period can appear to be part of a fluctuating pattern over a larger timescale. Moreover, mean changes and fluctuations are not disconnected from one another. Fluctuations may sometimes be the same order-of-magnitude as that of changes, as the annual mean temperature from 1970 to 2000 for instance (Lawson *et al.*, 2015). Natural patterns of environmental variations are being modified by climate change (Masson-Delmotte *et al.*, 2018). Fluctuations are also found to interact with mean changes up to alter or even reverse the effects of mean changes (Lawson *et al.*, 2015) so that we need to understand fluctuations consequences both in environment in which the mean conditions are changing or not.

2 Adaptation as a response to fluctuations and changes

An ecosystem subject to fluctuations or changes can respond in different ways. The two main categories of responses are demographic changes (changes in the absolute and relative abundance of different species), including migration processes, and adaptation (changes in the traits/phenotypes of individuals and species) (Futuyma, 1998). We will focus here on the third mechanism, adaptation, and in particular on adaptive evolution (evolution driven by genetic changes and natural selection).

2.1 Definition of adaptation

Adaptation has a relatively broad meaning. The process of adaptation can involve different mechanisms as individual plasticity that is not heritable, or heritable changes of the genome (Futuyma, 1998; Hendry, 2020). We will briefly describe plasticity, before focusing on heritable changes that are the main focus of this manuscript.

Plasticity The term “plasticity” regroups processes through which environmental conditions influence the expression of phenotypic traits for a given genotype. It encompasses phenotypic plasticity, developmental plasticity, environmental induction, acclimation, epigenetics, induced defenses, maternal effects, genotype-by-environment interaction, or also indirect genetic effects (Hendry, 2020). Just to give a few examples, we can cite the phototaxis behavioral response of *Daphnia* to the presence of predators (Parejko & Dodson, 1991). This response to fish kairomones is shown to be a plastic response, that is greater for *Daphnia* that live in lakes with high levels of fish predation. Another example could be that of the morphological plasticity of some plants which develop leaves with smaller area and larger mass in response to an increase in temperature (Gratani, 2014).

Plasticity can be either adaptive as in the previous examples, or non-adaptive when the plasticity process results in a mean phenotypic response that is far from the favoured phenotypic optimum (Ghalambor *et al.*, 2007). This distinction renders more complex the answer to the question of the selective advantage of plasticity and its contribution to adaptive evolution (Ghalambor *et al.*, 2007).

Plasticity is often seen as a non-heritable response of individuals. It is worth to notice that actually, some plasticity processes as epigenetic (genetic changes that do not alter DNA sequences) can be heritable such as the survival of fish at high toxicity levels (hydrogen sulfide-rich springs) due to a stable generational inheritance of certain DNA methylation (Kelley *et al.*, 2021). Those heritable processes could fall under the scope of some of the present manuscript considerations (for Chapter 1 mostly).

Adaptive evolution The main focus of this manuscript remains that of adaptation through heritable changes in the genome, which (may) results in changes in phenotype. Adaptive evolution involves the notion of fitness. The fitness of a given genotype is defined as its contribution to the gene pool of the next generation (Wright, 1931). Genotypes may differ in fitness in many ways, e.g. viability, mating success, fecundity (Orr, 2009). There are several ways to describe and measure

fitness (Endler, 2020). It is usually measured by quantities that are proportional to the mean number of viable, fertile progeny produced by a genotype/phenotype, as survival and reproductive success.

The curve or surface for individual fitness versus individual trait values is called a fitness landscape (idea derived by Wright in 1937 and widely used afterwards; Orr, 2005). This surface may present several local maximum. Adaptation will involve the walk up to the nearest fitness peak (even if not the global optimum). However, adaptation might be a lot constrained by many factors so that most population have their phenotype in some distance from the nearest fitness peak (Hendry, 2020).

This dynamical process involves four main evolutionary forces well described in most of the textbooks about evolution (Endler, 2020; Futuyma, 1998; Losos, 2017). **Mutation** brings new alleles to a population and participates to genetic variation. **Migration** creates gene flow between populations, brings new alleles into a population, enhancing genetic variation. **Genetic drift** randomly changes the frequency of an existing allele in a population (through stochastic death and mating). And **selection** provokes a differential survival and/or reproduction of individuals, guiding which alleles are more probable to be maintained or to disappear. Natural selection is closely linked to the notion of fitness, which can be seen as a within-generation measure of the process of natural selection. However, selection does not always imply “adaptation” in the sense of improved fit between organism and environment (Orr, 2005).

Those four forces are known to interact with each other, what makes all the richness of this process, but also the difficulties to grasp it in all its dimensions. To give just a few examples of such interactions: gene-flow may counteract selection, bringing deleterious alleles and hampering local adaptation (Lenormand, 2002; Bürger, 2014), or being favorable for evolutionary rescue for instance (Tomasini & Peischl, 2020). It also interacts with drift, preventing the random loss of some alleles into small populations (Lenormand, 2002; Blanquart *et al.*, 2012). Similarly, the mutation-selection balance specifies the relative forces of mutation and selection in determining allele frequencies in a population (Crow *et al.*, 1970; Lynch *et al.*, 2016).

Even if mutation is the ultimate source of genetic variation and the fundamental aspect of several theory of evolution (Orr, 2005), it is not the only one. Adaptation can for instance also occur from standing genetic variation¹. In any way, genetic variance is a prerequisite of adaptation. Such a genetic variation is actually found in nature, but the reason why is a fundamental question that has long been unresolved (Rice, 2004). Maynard-Smith highlighted that mutation should probably not be sufficient (rate too low) for maintaining the observed genetic variation in nature. And indeed, other processes as recombination and immigration of new alleles also participate to genetic variation (Rice, 2004). Other mechanisms as habitat choice can help maintaining polymorphism, but is not always necessary depending on the joint effects of density regulation and viability selection (Ravigné *et al.*, 2004). In anyway, polymorphism maintenance requires in some way a frequency-dependent selection² conferring an advantage to rare phenotypes or genotypes (Ravigné *et al.*,

¹Allelic variation that is currently segregating within a population; as opposed to alleles that appear by new mutation events (Orr, 2005).

²Frequency-dependent selection occurs when the fitness of a phenotype or genotype depends on its frequency in a population.

2004).

2.2 Manifestations of adaptation

2.2.1 Adaptation in a single population or species

A population subject to perturbation or changes in its environment can adapt to them. A lot of examples are reported in the literature, where some population or species are seen to adapt (here, to evolve, in the sense of the acquisition of heritable traits) to new or fluctuating conditions. Examples are as diverse as species evolutionary adaptation to urban environment (McDonnell & Hahs, 2015), to pesticides (Hawkins *et al.*, 2019), to altitude for human (Rupert & Hochachka, 2001), to temperature for instance for bacteria (Bennett *et al.*, 1992), or also to salinity (Ahmadi *et al.*, 2016). In the case of environmental variability, evolution is generally expected to favor generalist species (see Wilson & Yoshimura, 1994, for a review), or bet-hedgers (Jansen & Stumpf, 2005).

When considering heterogeneous environments, where several populations of the same species evolve in different environments, we can observe what is called local adaptation. A population is locally adapted when well locally suited compared to other individuals/populations of the same species (Rice, 2004; Hendry, 2020). Many examples exist as the local adaptation of disease vectors to temperature (Sternberg & Thomas, 2014), or of tropical plants to drought (Barton *et al.*, 2020). Local adaptation implies in some way a trade-off, where a population well adapted to an environment will be mal- or less-adapted to another one (Levins, 1968). A population or species that would not be subject to any trade-off and would evolve without any biological constraints is called a Darwinian Demon (Leimar, 2002). Local adaptation can be favored and protected by habitat choice (Johnson *et al.*, 1996). On the contrary, local adaptation might be eventually slowed down or even prevented by gene flow between populations (Lenormand, 2002, but see for instance Walker *et al.*, 2017). For instance, mosquitoes from Corsica did not develop a strong pesticide resistance as expected because of large gene flow from the mainland (Raymond & Marquine, 1994), what is called gene swamping (Lenormand, 2002).

Adaptation (and a fortiori local adaptation) might eventually result in evolutionary divergence and diversification, what participate in adaptive radiation and speciation (Losos, 2017). This can occur when selection maintains (stabilizing selection) or evolves (directional selection) phenotypic differences among populations. Such an adaptive divergence in salt tolerance occurred for instance between coastal perennial and inland annual ecotypes of a yellow monkey-flower in the Western North America (Lowry *et al.*, 2009).

Speciation can also occur in case of a disruptive selection, which increases the variance of a trait and progressively forms two groups. If there exists a reproductive isolation between the two groups, they will finally diverge to form two distinct species (adaptive radiation). Darwin's Finches for instance are supposed to have differentiated through disruptive selection and assortative mating (a kind of reproductive isolation) (Losos, 2017). There exist different types of reproductive isolation, either geographic (potential mates do not meet; referring here to the case of local adaptation), behavioral or sexual isolation, gametic incompatibilities, or hybrid inviability or sterility (Futuyma, 1998; Kirkpatrick & Ravigné, 2002).

2.2.2 Adaptation in an ensemble of populations within a community

Adaptive evolution is also found to affect community assembly (Ricklefs, 1987; Vanoverbeke *et al.*, 2016) as well as reorganization. Community adaptation refers to the reorganization and modification of the traits of the species that belong to the community, in response to a disturbance affecting the species trait (loss or invasion) or the environment. For instance, bacterial communities adaptation examples are numerous, in part because of the rapid generation time and possibilities of evolution. They are shown to adapt to temperature (Pettersson & Bååth, 2003), to nutrient limitation (Hoyos-Santillan *et al.*, 2018). Fungi communities are also found to adapt to temperature (Bárcenas-Moreno *et al.*, 2009) or to soil copper for instance (Chu *et al.*, 2010). At larger scales, there exist studies about adaptation in grasslands communities (van Moorsel *et al.*, 2018) or even within trophic levels (Loeuille, 2010).

What distinguish a community from a population or species is precisely the presence of several species. Evolutionary change of one species is thus influenced and constrained by the evolution of the other species, what is the notion of co-evolution (Losos, 2017; Hendry, 2020). The more species the more constraints, and some theoretical (Mazancourt *et al.*, 2008) and experimental (terHorst *et al.*, 2018; Scheuerl *et al.*, 2020) studies have argued that biodiversity may leave much less room for adaptive evolution. However, other studies argued on the contrary that high functional diversity may promote species diversification due to increased competition (Jousset *et al.*, 2016) in rich communities. The presence of strong co-evolutionary dynamics is suggested to increase the ongoing evolutionary potential because the adaptive peak for a population would be more mobile in a community (Garant *et al.*, 2007). Ecological interactions are known to interplay with evolution, and are thus of great importance when considering adaptation to environmental changes, as the nowadays gradual shift in temperature (Åkesson *et al.*, 2021).

Ecological interactions are shown to be of great importance when considering adaptive evolution. For instance, (Åkesson *et al.*, 2021) highlighted that ecological and evolutionary processes both interplay in adaptation to gradual shift in the temperature.

2.2.3 How rapid is adaptation?

Evolution has long been considered as a slow process relatively to ecological time scales, and therefore has not been considered in concert with ecological studies and questions. However, evolution is now recognized to be relevant even on ecological timescales (Carroll *et al.*, 2007; Ellner *et al.*, 2011; Hendry, 2020; Hart *et al.*, 2019). One famous example is the one of guppies. When moved from one predation environment (high or low) to the other, they experience evolutionary changes (color, life history, behaviors) over only a few generations (Reznick *et al.*, 1997). There are many other examples as the contemporary adaptation of fungi to fungicide (Walker *et al.*, 2017), or of a kind of mosquitoes to variation in temperature (within 3 generations, Foucault *et al.*, 2018). The rate of phenotype change per trait, in cases reported as being rapid evolution cases, has been measured to be in average $1/4$ (and up to $2/3$) the rate of population change per generation (DeLong *et al.*, 2016).

Some studies suggest that fluctuating selection and associated periods of contemporary evolution (i.e. rapid evolution) should probably be the norm rather than exception throughout the history of life (Carroll *et al.*, 2007). Rapid evolution is

moreover found to especially occur after extreme meteorological events (Grant *et al.*, 2017) or in context of global variability such as the current anthropogenic changes in selection and population structure (Carroll *et al.*, 2007). Besides, anthropogenic impacts induce a very particular type of variability at the world scale because it is rather homogeneous across many places. Thus, rapid adaptations that have appeared in some places can easily invade other places (Hufbauer *et al.*, 2012).

Both ecological and evolutionary processes act in concert and for instance, contemporary evolution implies that the maintenance of species diversity may be governed by more than pure ecological processes (Hart *et al.*, 2019). Diversity, in turns, is found to impact rapid evolution outcomes in grassland communities (van Moorsel *et al.*, 2019). Species interaction as competitive population dynamics is also found to be modified by the evolution in response to inter-specific competition (for instance in aquatic plant species over 10–15 generations, Hart *et al.*, 2019).

2.3 Tools for modeling adaptation

The classic Georges E.P. Box’s quote about modelling is not famous for nothing: “All models are wrong, but some are useful”. Models are useful to understand the mechanisms governing some processes, the interaction between parameters, the interaction between forces driving the system changes. They are useful to support, extend, revise or reject some of the narratives we mentally create to explain many kinds of phenomena (Otto & Rosales, 2020) whether for instance physical, biological, societal or financial. Models require that we make assumptions at some levels in order to explore some aspects, forces and interactions acting at other levels. In the following, we will briefly expose some theoretical approaches used to study evolutionary dynamics.

2.3.1 Population genetics

In the early 20th century, Fisher, Wright and Haldane derived a model of evolution whose approach consisted in assigning a fitness to each genotype, and then following the temporal changes in allele frequencies (Rice, 2004; Otto & Day, 2011). This approach works thanks to the relation that exists between genotypes and allele frequencies, and that comes from the Mendel’s laws of inheritance. The simplest – but strongly constrained – relations of this type are the well-known Hardy-Weinberg equations. Introducing the influence of selection or mutation on allele frequencies into their model, the precursors of population genetics fused Darwin’s vision of gradual slight changes with Mendelism.

Each genotype contributes to the next generation according to its fitness and its frequency in the previous generation. Modeling changes in allele frequency (i.e. evolution) involves the use of various mathematical approaches dealing with probabilities (random sampling, Markov chains, random walk, diverse manipulation of probabilities, diffusion theory, etc. ; see for instance Rice, 2004 for an general overview).

In the case of a large population (to the limit of an infinitely large population), we can neglect the stochastic effects due to genetic drift. This allows to study the deterministic variation of alleles frequencies under selection, mutation or migration, at one or two loci, and to study deviations from the Hardy-Weinberg equilibrium. With two loci, we can also study deviation from their independent frequency variation,

what is called a linkage disequilibrium¹ effects (Losos, 2017). From one generation to the other, the change in allele frequencies is described using both the current allele frequencies and fitness, along with mutation and migration rates when needed. This allows to study the equilibrium allele frequencies as resulting from a balance of two (or less often three) evolutionary forces. This is rather simple as we only consider deterministic mechanisms.

When the population size is not large enough, we cannot anymore ignore some stochastic changes in alleles frequencies as genetic drift. Stochastic changes are in general more difficult to model because we must consider at each point the probability of all possible ways the system could change, and we cannot simply know exactly the next (deterministic) step it will go. This is why genetic drift has first been studied at neutral loci. Drift has been considered using different approaches (Rice, 2004). For instance, Markov processes state that the probability to be in a given state only depends on the immediately preceding step, and not on the others. Another way involves Random walk which tells that the expected distance from the starting point goes as the square root of time. A third way considers the covariance between fitness and the number of alleles present in the first generation. This latter approach is a first step to apprehend the joint effects of selection and drift: to form the second generation, we randomly sample alleles in the first generation, with a weight that depends on their fitness (Rice, 2004).

To combine selection and drift in the same model, i.e. both deterministic and stochastic mechanisms, one of the most powerful method is diffusion theory², introduced to population genetic by Wright in 1945, and largely used since then (Kimura, 1983, in its neutral theory of evolution, Kimura, 1964; Gavrillets & Gibson, 2002). This method initially comes from Adolf Fick in 1855 who derived the particle diffusion equation that represents the macroscopic behavior of many micro-particles in Brownian motion. The same equation has been widely used for different purposes in different fields, but still with the same rationale: studying the collective movement of particles in a medium caused by the random motion of each particle. The idea of this theory is that some processes act as a force, acting on the average position of the allele distribution (directional processes, e.g. selection, mutation, migration), while some other processes are spreading factors (non-directional processes, e.g. genetic drift). From those considerations, we can derive a Kolmogorov equation (Kimura, 1964). For this, we first express the probability $\psi(p, t)$ of a given density population with allele frequency p at time t as a function of the probability that a population changes from allele frequency p to frequency $p + \epsilon$ in a given infinitesimal time interval. Then, expressing this probability of change as a function of the rate of directional changes $M(p)$ and the variance in allele frequency due to non directional changes $V(p)$, we end up with a Kolmogorov equation, for instance:

$$\frac{\partial\psi(p, t)}{\partial t} = \frac{\partial\psi(p, t)M(p)}{\partial p} + \frac{1}{2} \frac{\partial^2\psi(p, t)V(p)}{\partial p^2}$$

Another form of this equation exists that explicitly takes into account the initial density population p_0 , and that will be useful to derive alleles fixation probabilities for instance (Kimura, 1962). The diffusion theory approach allows to consider var-

¹Two alleles are in linkage disequilibrium if those two alleles at two loci are associated more frequently (or less frequently) than predicted by their individual frequencies.

²Another one is branching processes (Dawson, 2017)

ious questions as how much or how small must be each of the evolutionary forces to get strong or low effects, what is the maintenance of genetic variation through the four evolutionary forces (Kimura & Crow, 1964), or also, what is the probability of mutant fixation depending on its selection coefficient (Kimura, 1962; Gavrillets & Gibson, 2002).

This approach is elegant and useful. But of course, like any model, it comes with some assumptions. The diffusion approximation needs the population to be large enough for two reasons. First, to be able to consider continuous changes in the variable of interest (that is often discrete by essence, e.g. number of alleles, individuals, etc.). Continuous changes will be more tractable than discrete ones with differential equations. And second, to neglect high order terms (mutation and migration thus must be of the order of $1/2N$ so that lower terms can be neglected without removing the processes of interest ; Kimura, 1962). This is not realistic, but this diffusion approach gives good approximations even under more biological realistic conditions (Rice, 2004).

This population genetic approach, by faithfully describing inheritance, can however become very untractable with more than two loci, and many fitness-related characters are known to be coded by several loci, possibly linked (Futuyma, 1998). The next modelling approach, which has some common points with the previous macroscopic description of microscopic things, will propose a way to overcome this issue.

2.3.2 Quantitative genetics, or dealing with continuous variation of characters

To deal with the previously mentioned limitations, other approaches have been proposed. Quantitative genetics (Falconer, 1996; Rice, 2004), which knew a boom in the 70's and 80's, takes phenotypes rather than genotypes as main focus. A phenotypic trait may be controlled by a large number of loci whose exact description is neglected, as the whole effect is captured by the phenotype value. It is R.A. Fisher in 1918 who first proposed this vision, reconciling Mendelian and biometrical genetics. The latter indeed argued that single loci with large effect governed by the Mendelian principles could not explain the inheritance of continuous traits (Visscher & Goddard, 2019).

Moreover, in quantitative genetics, the phenotypic trait is represented as a continuous rather than a discrete variable. This description is particularly interesting for species traits that do not present sharply demarcated qualitative types (like different colors), but rather a quantitative continuum as many traits of interest (like sizes, life-span, etc.). Despite this difference, inheritance works the same for both qualitative or quantitative traits, and quantitative genetics is thereby an extension of Mendelian genetics, keeping its principle at its foundation. Indeed, the premises of quantitative genetics are (i) that genes are subject to Mendelian laws of transmission, and may have any of the properties known from Mendelian genetics, and (ii) that the expression of the genotype in the phenotype is modifiable by non-genetic causes. The genetic variance indeed comprises various genetic and non-genetic effects as for instance mutations, recombination, epistasis¹, mating success, or also,

¹Epistasis is an effect of the interaction between two or more gene loci on the phenotype or fitness, whereby their joint effect differs from the sum of the loci taken separately.

variations due to the environment. The phenotype is thus divided into two components: the genotype (set of genes possessed by the individual) and the environment (all non genetic circumstances that influence the phenotypic value, or in other words, the environmental deviation from the genotypic value). Moreover, genotype and environment can interact together, modifying the phenotype expected through the addition of genotypic and environmental effects.

Phenotypes, genotypes and environment are represented as continuous variables (called the “phenotypic value”, “genotypic value” and “environmental deviation”), and the population as the statistics (mean and variance usually) of the distribution of phenotypes.

Quantitative genetics has its roots in agriculture, where it has been first proposed to respond to the need to maximize the efficiency of artificial selection for desirable traits (Falconer, 1996; Rice, 2004). The breeder’s equation, whose name reveals its origin, gives the variation of the averaged species trait \bar{x}_i with time:

$$\frac{d\bar{x}_i}{dt} = \beta_{x_i, x^o} S$$

with S the selection differential, which is the change in mean phenotype due to only selection prior to reproduction. It is equivalent to what will be called the selection gradient in the next section. The term β_{x_i, x^o} refers to a linear relationship between x_i (the species trait) and x^o (the parent mean trait), and is the additive genetic variance of the trait (Rice, 2004). This term is also called the heritability and noted h^2 , and represents the genetic part in the phenotypic variation. The mean changes in phenotype per generation is often called R , the response to selection, so that the breeder’s equation is also noted $R = h^2 S$.

This equation appears to be a version of the Price’s theorem, which gives the mean and variance of the phenotypic change in a population as a function of (i) the differences between the mean phenotypes of offspring and parents’ phenotype, and (ii) the covariance between phenotypes and number of descendant (fitness of parents).

In this model, genetic variance has an important role in controlling the rate of evolution. If large enough, it affects the fitness of the offsprings compared to the one of the parents, and doing so, it modifies the magnitude of phenotypic changes from one generation to another.

This model presents some limitations due to the assumptions made. In particular, the contributions of the different loci on the phenotype must add up (no epistasis between loci), and there must not have linkage disequilibrium between the different loci encoding the same trait in the population (Falconer, 1996; Rice, 2004). In practice, these conditions are often unverifiable, but the breeder’s equation has been useful, especially for predicting the short-term response to agronomic selection on crops or livestock.

2.3.3 Adaptive dynamics, or simplify inheritance to more easily consider ecology

Another approach is to consider that phenotypes are fully defined by the average genetic value, with essentially no variance around this mean. In other words, this implies that little genetic variation for the phenotype exists in the population at any given time, and also that environmental variance is averaged out. This is the

approach taken by adaptive dynamics (Metz *et al.*, 1995; Dieckmann & Law, 1996; Geritz *et al.*, 1997, 1998), which has its roots in evolutionary game theory. The latter arose in the mid 20th century, and is designed to deal with situations in which what an individual should do to increase its payoff (modifying its “strategy”) is function of what others are doing. This is interesting for evolutionary biology, where fitnesses are similar to the payoffs and phenotypes to the strategies. Adaptive dynamics specify species traits (as a continuous variable) and a population dynamical model that describes the rules of ecological interactions between the species. From this, one can determine the fitness consequences for a trait to change its value by a very slight amount. This would correspond to the occurrence of a rare mutation with little phenotypic effect within the population of individuals sharing this strategy.

For this we define the invasion fitness F (or selective value, or invasion function), which is the exponential growth rate of a small (mutant) population introduced into a large resident population. A resident at ecological equilibrium has a null invasion fitness. A rare mutant will be able to invade the community and replace the resident species if its invasion fitness is positive. Depending on the slope of the mutant invasion fitness around the resident trait, the species trait will evolve (through successive mutational steps) towards higher or lower values. This is captured by the selection gradient, defined as the first derivative of the invasion fitness F of a rare mutant with respect to the mutant trait. The species trait x_i will then vary the following way as a function of the selection gradient:

$$\frac{dx_i}{dt} = b \left. \frac{\partial F(x_m)}{\partial x_m} \right|_{x_m=x_i}$$

where the proportionality coefficient b is proportional to the mutation rate and the phenotypic variance associated to the mutation. We observe that the species trait varies the same way as in quantitative genetics, proportionally to the selection gradient. Species trait increases if the selection gradient is positive and decreases in the opposite case. The evolutionary equilibrium is reached when the selection gradient cancels, and has reached a singular strategy (Geritz *et al.*, 1997). In that case, where the singular strategy was reachable by successive mutational steps, this strategy is said to be stable by convergence (Christiansen, 1991). Still, singular strategies that are not reachable this way may exist, and are thus unstable by convergence.

In the adaptive dynamics approach, the evolutionary course may not stopped here, at a singular strategy stable by convergence, especially if the selection gradient cancels on a fitness minimum. In that case, the selection is said to be disruptive, the evolutionary equilibrium is unstable and called a branching point (Geritz *et al.*, 1997). Mutants can invade both side of the evolutionary point, and we may assist to diversification and emergence of polymorphism. For such a diversification to occur, the phenotypic variance around the species trait must be null (or to the limit very low). In quantitative genetics, diversification is seen as a strong increase in population variance, but not as a separation into two distinct species. The notions of evolutionary singular strategies (ESS ; in case of a stable evolutionary point ; see Maynard-Smith, 1976) or branching points will be mathematically defined in more details throughout the manuscript when needed, and can be found in some references (e.g. Metz *et al.*, 1995; Geritz *et al.*, 1997). All of this holds also for the co-evolution of several species, with the same mathematical considerations and tools,

so that we are able to derive the co-evolutionary state of an ensemble of population, each defined by their own trait (a community).

The hypotheses of this approach appear rather drastic regarding the reproduction and transmission of characters. Contrarily to population genetics, and in a lesser extent to quantitative genetics, the complexity of character transmission is almost brushed aside. Individuals are considered to have a clonal reproduction and the genetic architecture to have no effect on traits evolution, what questions the realism of some results (branching in particular Dieckmann, 1997; see Barton & Polechová, 2005, for limitations due to the consideration of small mutation effect in the local fitness gradient). This being said, on the one hand, this allows to question the effects of selection alone, without the potential effect of genetic architecture affecting allele transmission. On the other hand, the benefit of such hypothesis also lies in the extreme simplification of the modeling of evolution, that allows to consider more easily the complexity of population dynamics and bring more realism in the ecological interactions between individuals. Also, it is an appropriate approach to consider the long term course of evolution with the possibility of evolutionary diversification (branching).

Those three approaches, even though not covering the entire spectrum of existing methods, represent the three major mathematical formalization of adaptive evolution used in an ecological context. Each of these three approaches emphasizes a particular aspect of the evolutionary process, while making assumptions about the other processes. Population genetics describes precisely the inheritance of genes but it most of the time ignores demography and this approach is limited to one or two loci. Quantitative genetics makes it possible to consider that the traits under selection are determined by many genes, but uses approximations for this purpose that are not always satisfied. Adaptive dynamics makes it possible to consider the long term course of evolution as well as more complex ecological interactions between individuals, but neglects the complications linked to the transmission of genes. In this manuscript, we will investigate different evolutionary questions using either of these approaches as needed, most importantly population genetics and adaptive dynamics.

3 Questions addressed in the thesis

In this thesis, we are interested in the processes and consequences of adaptation under environmental variability. The environment (and a fortiori its variation) impacts both evolution and ecological processes, and this does impact also both ecological and evolutionary outputs in a kind of “eco-evo” feedback loop. The scheme 1 roughly sketches those interactions between ecology, evolution, and the environment, as well as where the question addressed in this thesis will fit into this scheme. All questions will be addressed in a theoretical way, using some of the modeling tools presented in the previous section.

The first chapter is based on the observation that in nature, communities may harbor various levels of co-adaptation. On the one hand, many kinds of environmental variability may disturb communities environment, composition and structure, so that communities (or single populations) are likely to move far from their evolutionary equilibrium ((co-)adapted state). On the other hand, contemporary evolution

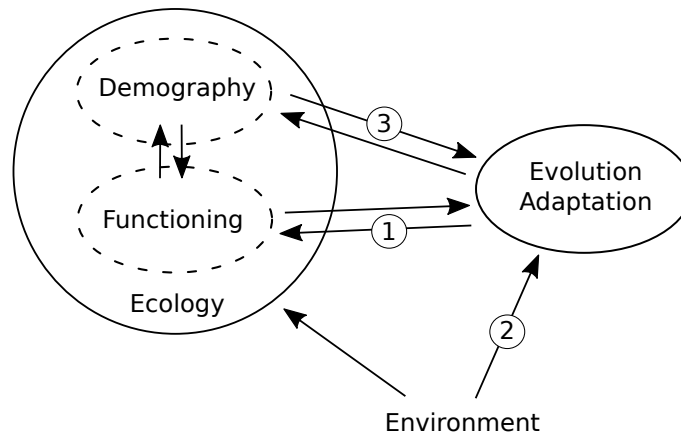


Figure 1: Sketch of the interactions between ecology, evolution and the environment. An arrow between A and B indicates “A impacts B”, so therefore, variability in A impacts B. The numbers indicate the chapters which deal with the corresponding interaction. This sketch does not distinguish between temporal or spatial variability.

may allow a disturbed or newly formed system to rapidly (re)-reach a “more co-adapted” state. Rapid evolution is moreover found to especially occur in context of global variability (see paragraph 2.2.3), what participates in a kind of fluctuating pattern in between different levels of co-adaptation. The first chapter then proposes to ask the question of the ecological impact caused by such differences in community co-adaptation levels. We will regard the impact of community adaptation on some biodiversity–ecosystem functioning (BEF) relationships (see fig. 1), i.e. biodiversity–productivity, biodiversity–stability and biodiversity–invasion relationships (e.g. Tilman *et al.*, 1996; Elton, 1958; Levine, 2000, see Chapter 1 for a more complete description). As evolution affects ecosystems functioning (through trait modification), and as diversity potentially influences evolutionary course (Mazan-court *et al.*, 2008; Jousset *et al.*, 2016; terHorst *et al.*, 2018; van Moorsel *et al.*, 2019; Scheuerl *et al.*, 2020), we expect some non-linear impacts on ecosystem functioning with diversity levels. Several experimental and a few theoretical studies highlighted potential evolution impacts on BEF relationships (van Moorsel *et al.*, 2018; Zuppinger-Dingley *et al.*, 2014; Fiegna *et al.*, 2014, 2015). However, the nature and extent of such impact remains poorly understood. Here, we will not consider the direct impact of fluctuations in between different levels of co-adaptation (that would be a whole other question). Rather, in a simplified way, we will explore the differences brought by two distinct levels of co-adaptation (two extreme cases): using adaptive dynamics methods, we will model both random communities, with no trait evolution, and co-adapted communities, whose traits reached an evolutionary equilibrium (the two extreme cases). The three type of BEF relationships will be compared for both type of communities formed. We will consider various scenarios for trait interaction mechanisms such as niche competition, life-history trade-off or trophic interactions (Doebeli & Dieckmann, 2000; Tilman, 1994; Calcagno *et al.*, 2006; Loeuille & Loreau, 2005). We will demonstrate a clear impact of the co-adaptation level on biodiversity–productivity and biodiversity–response to invasion relationships, and in a lesser extent to biodiversity–stability relationships. Biodiversity–productivity relationships will generally be less positive among co-adapted communities. Invasion resistance will show modest impacts, but the invasion toler-

ance to the contrary will greatly benefit from community co-adaptation, remaining high even at high diversity levels. We will discuss of the potential implication of such a contingency of BEF relationships on the history of ecosystems and their degree of community adaptation.

The first chapter focuses on the consequences of changes in adaptation, and not on the causes of such changes. The second chapter will regard this latter aspect, exploring how different spatial distribution in stress conditions will affect evolution in a specific co-existence model (see fig. 1). Variability will be encountered at two levels: first, in the spatial environmental variability in stress level, with more or less variance. And second, in term of potential temporal change in this stress distribution, which would be likely to affect evolutionary processes. We will focus here on the tolerance-fecundity trade-off (TFT, a model proposed a little bit more than 10 years ago as an alternative to the competition-colonization trade-off, Muller-Landau, 2010; D'Andrea *et al.*, 2013; Haegeman *et al.*, 2014), which has never been considered under an evolutionary perspective. We will study how a given environmental stress distribution may impact the evolutionary outcomes of this co-existence model for one species (see fig. 1), as a function of the TFT intensity. For this, we will first introduce a generalization of the TFT model, that allows the use of adaptive dynamics methods, before investigating evolutionary equilibria, ESS stress tolerance levels, and the possibility of diversification (branching). While the stress distribution will be found to have a minor impact on the evolutionary equilibrium point for stress tolerance, which is mainly driven by the trade-off function slope, it will impact much more its stability (ESS vs. branching point). The stress distribution variance itself will show larger impacts: a loss of variance greatly reduces the probabilities for ecological coexistence and for adaptive radiation. Bimorphic evolutionary equilibrium will not be found in cases the monomorphic equilibrium was stable. Moreover, the possibilities to achieve a bimorphic equilibrium through adaptive radiation will be more restricted than to maintain it. All of this will be discussed in term of ecological restoration.

In the last chapter, we will consider to which extent adaptation may be impacted by temporal variability in demographic processes, and in particular in migration (see fig. 1). As mentioned in this introduction and widely exposed in the third chapter, it is recognized that migration is a process governed by highly variable phenomena, resulting in fluctuating, intermittent or pulsed migration. However, it has rarely been considered as so in theoretical studies (Peniston *et al.*, 2019), and some theoretical results suggest that it may have some impact on evolution (Nagylaki, 1979; Latter & Sved, 1981; Whitlock, 1992; Gaggiotti & Smouse, 1996; Yamaguchi & Iwasa, 2013; Peniston *et al.*, 2019). To extend those results to unexplored cases, we will question the impact that a temporally variable migration may have on allele fixation, using population genetics approaches. We will consider a mainland-island system (Felsenstein, 1976; Bürger, 2014) in which migration will be modeled in a pulsed way, and will translate the impact of migration pulsedness on allele fixation rate in terms of effective migration rate. We will show that migration variability can either decrease or increase the effective migration rate depending on the selection pressure imposed on alleles. More precisely, a beneficial allele fixation will be favored by migration variability while a strongly deleterious allele will benefit from a continuous migration. This difference will be found to result in the homogenization, with migration variability, of fixation rate across loci harboring different selection

values, what may leave a migration variability genomic signature. Those results will be discussed in terms of population management and conservation. We will extend this study, in an appendix of this chapter, to the case of two populations connected by migration, what will allow to question the impact of migration pulsedness on the two populations genetic divergence.

These three chapters will be presented as three self-contained articles, two of which (the first and third) have been published in or submitted to a scientific journal, and one (the second) is still under preparation. The bibliography corresponding to each article will be given at the end of each chapter for easier access. The thesis conclusion will at the end go back to the main results of those three chapters in relation to the problematic of the thesis, and some perspectives will be discussed.

Bibliography

- Ahmadi, N., Baroiller, J.F., Carreras, H.D. & Morillon, R. (2016) Adaptation to salinity. *Climate change and agriculture Worldwide*, pp. 45–58. Springer.
- Alto, B.W., Wasik, B.R., Morales, N.M. & Turner, P.E. (2013) Stochastic temperatures impede RNA virus adaptation. *Evolution: International Journal of Organic Evolution*, **67**, 969–979.
- Arnan, X., Blüthgen, N., Molowny-Horas, R. & Retana, J. (2015) Thermal characterization of European ant communities along thermal gradients and its implications for community resilience to temperature variability. *Frontiers in ecology and evolution*, **3**, 138.
- Bárcenas-Moreno, G., Gómez-Brandón, M., Rousk, J. & Bååth, E. (2009) Adaptation of soil microbial communities to temperature: comparison of fungi and bacteria in a laboratory experiment. *Global Change Biology*, **15**, 2950–2957.
- Barton, K.E., Jones, C., Edwards, K.F., Shiels, A.B. & Knight, T. (2020) Local adaptation constrains drought tolerance in a tropical foundation tree. *Journal of Ecology*, **108**, 1540–1552.
- Barton, N. & Polechová, J. (2005) The limitations of adaptive dynamics as a model of evolution. *Journal of Evolutionary Biology*, **18**.
- Benestan, L., Fietz, K., Loiseau, N., Guerin, P.E., Trofimenko, E., Rühs, S., Schmidt, C., Rath, W., Biastoch, A., Pérez-Ruzafa, A., Baixauli, P., Forcada, A., Arcas, E., Lenfant, P., Mallol, S., Goñi, R., Velez, L., Höppner, M., Kininmonth, S., Mouillot, D., Puebla, O. & Manel, S. (2021) Restricted dispersal in a sea of gene flow. *Proceedings of the Royal Society B: Biological Sciences*, **288**, 20210458.
- Bennett, A.F., Lenski, R.E. & Mittler, J.E. (1992) Evolutionary adaptation to temperature. I. Fitness responses of *Escherichia coli* to changes in its thermal environment. *Evolution*, **46**, 16–30.
- Blanquart, F., Gandon, S. & Nuismer, S. (2012) The effects of migration and drift on local adaptation to a heterogeneous environment. *Journal of evolutionary biology*, **25**, 1351–1363.
- Bürger, R. (2014) A survey of migration-selection models in population genetics. *Discrete & Continuous Dynamical Systems - B*, **19**, 883–959.

- Calcagno, V., Mouquet, N., Jarne, P. & David, P. (2006) Coexistence in a meta-community: the competition–colonization trade-off is not dead. *Ecology letters*, **9**, 897–907.
- Cao, Q., Liu, Y., Georgescu, M. & Wu, J. (2020) Impacts of landscape changes on local and regional climate: a systematic review. *Landscape Ecology*, **35**, 1269–1290.
- Carlton, J.T., Chapman, J.W., Geller, J.B., Miller, J.A., Carlton, D.A., McCuller, M.I., Treneman, N.C., Steves, B.P. & Ruiz, G.M. (2017) Tsunami-Driven Rafting: Transoceanic Species Dispersal and Implications for Marine Biogeography. *Science*, **357**, 1402–1406.
- Carlton, J. & Cohen, A. (2003) Episodic Global Dispersal in Shallow Water Marine Organisms: The Case History of the European Shore Crabs *Carcinus Maenas* and *C-Aestuarius*. *Journal of Biogeography*, **30**, 1809–1820.
- Carroll, S.P., Hendry, A.P., Reznick, D.N. & Fox, C.W. (2007) Evolution on ecological time-scales. *Functional Ecology*, **21**, 387–393.
- Cassidy, C., Grange, L.J., Garcia, C., Bolam, S.G. & Godbold, J.A. (2020) Species interactions and environmental context affect intraspecific behavioural trait variation and ecosystem function. *Proceedings of the Royal Society B*, **287**, 20192143.
- Christiansen, F.B. (1991) On Conditions for Evolutionary Stability for a Continuously Varying Character. *The American Naturalist*, **138**, 37–50.
- Chu, G., Wakelin, S.A., Condron, L. & Stewart, A. (2010) Effect of soil copper on the response of soil fungal communities to the addition of plant residues. *Pedobiologia*, **53**, 353–359.
- Crow, J.F., Kimura, M. *et al.* (1970) *An introduction to population genetics theory*. New York, Evanston and London: Harper & Row, Publishers.
- Czarniecka-Wiera, M., Szymura, T. & Kącki, Z. (2020) Understanding the importance of spatial scale in the patterns of grassland invasions. *Science of The Total Environment*, **727**, 138669.
- Dawson, D.A. (2017) Introductory lectures on stochastic population systems. *arXiv preprint arXiv:1705.03781*.
- DeLong, J.P., Forbes, V.E., Galic, N., Gibert, J.P., Laport, R.G., Phillips, J.S. & Vavra, J.M. (2016) How fast is fast? Eco-evolutionary dynamics and rates of change in populations and phenotypes. *Ecology and Evolution*, **6**, 573–581.
- Dieckmann, U. (1997) Can adaptive dynamics invade? *Trends in Ecology & Evolution*, **12**, 128–131. ISSN 0169-5347.
- Dieckmann, U. & Law, R. (1996) The dynamical theory of coevolution: a derivation from stochastic ecological processes. *Journal of Mathematical Biology*, **34**, 579–612.

- Doebeli, M. & Dieckmann, U. (2000) Evolutionary Branching and Sympatric Speciation Caused by Different Types of Ecological Interactions. *The American Naturalist*, **156**, S77–S101.
- D’Andrea, R., Barabás, G. & Ostling, A. (2013) Revising the Tolerance-Fecundity Trade-Off; or, On the Consequences of Discontinuous Resource Use for Limiting Similarity, Species Diversity, and Trait Dispersion. *The American Naturalist*, **181**, E91–E101.
- Ellner, S.P., Geber, M.A. & Hairston Jr, N.G. (2011) Does rapid evolution matter? Measuring the rate of contemporary evolution and its impacts on ecological dynamics. *Ecology Letters*, **14**, 603–614.
- Elton, C. (1958) *Ecology of invasions by plant and animals*. Chapman and Hall, London.
- Endler, J.A. (2020) *Natural Selection in the Wild. (MPB-21), Volume 21*. Princeton University Press.
- Falconer, D. (1996) *Introduction to Quantitative Genetics*. Always Learning. Pearson Education. ISBN 9788131727409.
- Felsenstein, J. (1976) The theoretical population genetics of variable selection and migration. *Annual Review of Genetics*, **10**, 253–280.
- Fiegna, F., Moreno-Letelier, A., Bell, T. & Barraclough, T.G. (2014) Evolution of species interactions determines microbial community productivity in new environments. *The ISME Journal*, **9**, 1235–1245.
- Fiegna, F., Scheuerl, T., Moreno-Letelier, A., Bell, T. & Barraclough, T.G. (2015) Saturating effects of species diversity on life-history evolution in bacteria. *Proceedings of the Royal Society B-Biological Sciences*, **282**, 20151794.
- Foucault, Q., Wieser, A., Waldvogel, A.M., Feldmeyer, B. & Pfenninger, M. (2018) Rapid adaptation to high temperatures in *Chironomus riparius*. *Ecology and evolution*, **8**, 12780–12789.
- Futuyma, D.J. (1998) *Evolutionary Biology*, Sinauer Associates. Inc. Sunderland, MA.
- Gaggiotti, O. & Smouse, P. (1996) Stochastic Migration and Maintenance of Genetic Variation in Sink Populations. *American Naturalist*, **147**, 919–945.
- Garant, D., Forde, S. & Hendry, A. (2007) The multifarious effects of dispersal and gene flow on contemporary adaptation. *Functional Ecology*, **21**, 434–443.
- Gavrilets, S. & Gibson, N. (2002) Fixation Probabilities in a Spatially Heterogeneous Environment. *Population Ecology*, **44**, 51–58.
- Geritz, S.A.H., Metz, J.A.J., Kisdi, E. & Meszéna, G. (1997) Dynamics of Adaptation and Evolutionary Branching. *Phys. Rev. Lett.*, **78**, 2024–2027.

- Geritz, S.A., Mesze, G., Metz, J.A. *et al.* (1998) Evolutionarily singular strategies and the adaptive growth and branching of the evolutionary tree. *Evolutionary ecology*, **12**, 35–57.
- Ghalambor, C.K., McKay, J.K., Carroll, S.P. & Reznick, D.N. (2007) Adaptive versus non-adaptive phenotypic plasticity and the potential for contemporary adaptation in new environments. *Functional ecology*, **21**, 394–407.
- Gingerich, P.D. (2001) Rates of evolution on the time scale of the evolutionary process. *Microevolution Rate, Pattern, Process*, pp. 127–144.
- Giulia, S., Lea, B.F., Carol, Z.C., Lisa, M., Harper, S.L. & Elizabeth, C.J. (2020) The effect of climatic factors on nutrients in foods: evidence from a systematic map. *Environmental Research Letters*, **15**, 113002.
- Grant, P.R., Grant, B.R., Huey, R.B., Johnson, M.T., Knoll, A.H. & Schmitt, J. (2017) Evolution caused by extreme events. *Philosophical Transactions of the Royal Society B: Biological Sciences*, **372**, 20160146.
- Gratani, L. (2014) Plant Phenotypic Plasticity in Response to Environmental Factors. *Advances in Botany*, **2014**, 208747.
- Green, J. & Bohannan, B.J. (2006) Spatial scaling of microbial biodiversity. *Trends in ecology & evolution*, **21**, 501–507.
- Haegeman, B., Sari, T. & Etienne, R. (2014) Predicting coexistence of plants subject to a tolerance-competition trade-off. *J Math Biol.*, **68**, 1815–47.
- Hart, S.P., Turcotte, M.M. & Levine, J.M. (2019) Effects of rapid evolution on species coexistence. *Proceedings of the National Academy of Sciences*, **116**, 2112–2117.
- Hawkins, N.J., Bass, C., Dixon, A. & Neve, P. (2019) The evolutionary origins of pesticide resistance. *Biological Reviews*, **94**, 135–155.
- Hebert, P.D. (1998) Diversification in Inland Waters. *Advances in molecular ecology*, **306**, 267.
- Hendry, A. (2020) *Eco-evolutionary Dynamics*. Princeton University Press. ISBN 9780691204178.
- Henle, K. & Grobelnik, V. (2014) *Scaling in ecology and biodiversity conservation*. Pensoft Sofia, Bulgaria.
- Hernández-Padilla, J.C., Zetina-Rejón, M.J., Arreguín-Sánchez, F., del Monte-Luna, P., Nieto-Navarro, J.T. & Salcido-Guevara, L.A. (2021) Structure and function of the southeastern Gulf of California ecosystem during low and high sea surface temperature variability. *Regional Studies in Marine Science*, **43**, 101686.
- Hoyos-Santillan, J., Lomax, B.H., Turner, B.L. & Sjögersten, S. (2018) Nutrient limitation or home field advantage: does microbial community adaptation overcome nutrient limitation of litter decomposition in a tropical peatland? *Journal of Ecology*, **106**, 1558–1569.

- Hufbauer, R.A., Facon, B., Ravigne, V., Turgeon, J., Foucaud, J., Lee, C.E., Rey, O. & Estoup, A. (2012) Anthropogenically induced adaptation to invade (AIAI): contemporary adaptation to human-altered habitats within the native range can promote invasions. *Evolutionary applications*, **5**, 89–101.
- Jansen, V.A. & Stumpf, M.P. (2005) Making sense of evolution in an uncertain world. *Science*, **309**.
- Johnson, P.A., Hoppensteadt, F., Smith, J.J. & Bush, G.L. (1996) Conditions for sympatric speciation: a diploid model incorporating habitat fidelity and non-habitat assortative mating. *Evolutionary Ecology*, **10**, 187–205.
- Jones, A.M. & Harrison, R.M. (2004) The effects of meteorological factors on atmospheric bioaerosol concentrations—a review. *Science of the total environment*, **326**, 151–180.
- Jousset, A., Eisenhauer, N., Merker, M., Mouquet, N. & Scheu, S. (2016) High functional diversity stimulates diversification in experimental microbial communities. *Science Advances*, **2**, e1600124.
- Kelley, J.L., Tobler, M., Beck, D., Sadler-Riggelman, I., Quackenbush, C.R., Rodriguez, L.A. & Skinner, M.K. (2021) Epigenetic inheritance of DNA methylation changes in fish living in hydrogen sulfide-rich springs. *Proceedings of the National Academy of Sciences*, **118**.
- Kimura, M. (1962) On the probability of fixation of mutant genes in a population. *Genetics*, **47**, 713–719.
- Kimura, M. (1964) Diffusion models in population genetics. *Journal of Applied Probability*, **1**, 177–232.
- Kimura, M. (1983) *The neutral theory of molecular evolution*. Cambridge University Press.
- Kimura, M. & Crow, J.F. (1964) The number of alleles that can be maintained in a finite population. *Genetics*, **49**, 725.
- Kirkpatrick, M. & Ravigné, V. (2002) Speciation by natural and sexual selection: models and experiments. *the american naturalist*, **159**, S22–S35.
- Latter, B.D.H. & Sved, J.A. (1981) Migration and Mutation in Stochastic Models of Gene Frequency Change. II. Stochastic Migration with a Finite Number of Islands. *J. Math. Biology*, **13**, 95–104.
- Lawson, C.R., Vindenes, Y., Bailey, L. & van de Pol, M. (2015) Environmental variation and population responses to global change. *Ecology Letters*, **18**, 724–736.
- Leal Filho, W., Azeiteiro, U.M., Balogun, A.L., Setti, A.F.F., Mucova, S.A., Ayal, D., Totin, E., Lydia, A.M., Kalaba, F.K. & Oguge, N.O. (2021) The influence of ecosystems services depletion to climate change adaptation efforts in Africa. *Science of The Total Environment*, p. 146414.

- Leimar, O. (2002) Evolutionary change and Darwinian demons. *Selection*, **2**, 65–72.
- Lenormand, T. (2002) Gene Flow and the Limits to Natural Selection. *Trends in Ecology and Evolution*, **17**, 183–189.
- Levine, J.M. (2000) Species diversity and biological invasions: relating local process to community pattern. *Science*, **288**, 852–854.
- Levins, R. (1968) *Evolution in changing environments*. Princeton University Press.
- Loeuille, N. (2010) Consequences of adaptive foraging in diverse communities. *Functional Ecology*, pp. 18–27.
- Loeuille, N. & Loreau, M. (2005) Evolutionary emergence of size-structured food webs. *Proceedings of the National Academy of Sciences USA*, **102**, 5761–5766.
- Losos, J.B. (2017) *The Princeton guide to evolution*. Princeton University Press.
- Lowry, D.B., Hall, M.C., Salt, D.E. & Willis, J.H. (2009) Genetic and physiological basis of adaptive salt tolerance divergence between coastal and inland *Mimulus guttatus*. *New Phytologist*, **183**, 776–788.
- Lynch, M., Ackerman, M.S., Gout, J.F., Long, H., Sung, W., Thomas, W.K. & Foster, P.L. (2016) Genetic drift, selection and the evolution of the mutation rate. *Nature Reviews Genetics*, **17**, 704–714.
- Mahmoud, S.H. & Gan, T.Y. (2018) Impact of anthropogenic climate change and human activities on environment and ecosystem services in arid regions. *Science of the Total Environment*, **633**, 1329–1344.
- Manea, A. & Leishman, M.R. (2018) Soil water content variability drives productivity responses of a model grassland system to extreme rainfall events under elevated CO₂. *Plant Ecology*, **219**, 1413–1421.
- Masson-Delmotte, V., Zhai, P., Pörtner, H.O., Roberts, D., Skea, J., Shukla, P., Pirani, A., Moufouma-Okia, W., Péan, C., Pidcock, R., Connors, S., Matthews, J., Chen, Y., Zhou, X., Gomis, M., Lonnoy, E., Maycock, T., Tignor, M. & Waterfield, T. (2018) *IPCC, 2018: Global Warming of 1.5°C. An IPCC Special Report on the impacts of global warming of 1.5°C above pre-industrial levels and related global greenhouse gas emission pathways, in the context of strengthening the global response to the threat of climate change, sustainable development, and efforts to eradicate poverty*. Working Group I Technical Support Unit, Bern, Switzerland.
- Maynard-Smith, J. (1976) Evolution and the Theory of Games. *American Scientist*, **64**, 41–45.
- Mazancourt, C.D., Johnson, E. & Barraclough, T.G. (2008) Biodiversity inhibits species' evolutionary responses to changing environments. *Ecology Letters*, **11**, 380–388.
- McDonnell, M.J. & Hahs, A.K. (2015) Adaptation and adaptedness of organisms to urban environments. *Annual review of ecology, evolution, and systematics*, **46**, 261–280.

- Metz, J.A.J., Geritz, S.A.H., Meszner, G., Jacobs, F.J.A. & Heerwaarden, J.S.v. (1995) Adaptive dynamics: a geometrical study of the consequences of nearly faithful reproduction. IIASA Working Paper, WP-95-099, IIASA, Laxenburg, Austria.
- Milá, B., Warren, B.H., Heeb, P. & Thébaud, C. (2010) The geographic scale of diversification on islands: genetic and morphological divergence at a very small spatial scale in the Mascarene grey white-eye (Aves: *Zosterops borbonicus*). *BMC Evolutionary Biology*, **10**, 1–13.
- Miles, L.S., Rivkin, L.R., Johnson, M.T., Munshi-South, J. & Verrelli, B.C. (2019) Gene flow and genetic drift in urban environments. *Molecular ecology*, **28**, 4138–4151.
- van Moorsel, S.J., Hahl, T., Wagg, C., De Deyn, G.B., Flynn, D.F., Zuppinge-Dingley, D. & Schmid, B. (2018) Community evolution increases plant productivity at low diversity. *Ecology Letters*, **21**, 128–137.
- van Moorsel, S.J., Schmid, M.W., Wagemaker, N.C., van Gorp, T., Schmid, B. & Vergeer, P. (2019) Evidence for rapid evolution in a grassland biodiversity experiment. *Molecular Ecology*, **28**, 4097–4117.
- Morris-Pocock, J.A., Anderson, D.J. & Friesen, V.L. (2016) Biogeographical barriers to dispersal and rare gene flow shape population genetic structure in red-footed boobies (*Sula sula*). *Journal of Biogeography*, **43**, 2125–2135.
- Muller-Landau, H.C. (2010) The tolerance–fecundity trade-off and the maintenance of diversity in seed size. *Proceedings of the National Academy of Sciences*, **107**, 4242–4247.
- Nagylaki, T. (1979) The Island Model with Stochastic Migration. *Genetics*, **91**, 163–176.
- Olivier, T., Thébaud, E., Elias, M., Fontaine, B. & Fontaine, C. (2020) Urbanization and agricultural intensification destabilize animal communities differently than diversity loss. *Nature communications*, **11**, 1–9.
- Orr, H.A. (2005) The genetic theory of adaptation: a brief history. *Nature Reviews Genetics*, **6**, 119–127.
- Orr, H.A. (2009) Fitness and its role in evolutionary genetics. *Nature Reviews Genetics*, **10**, 531–539.
- Otto, S.P. & Day, T. (2011) *A biologist’s guide to mathematical modeling in ecology and evolution*. Princeton University Press.
- Otto, S.P. & Rosales, A. (2020) Theory in service of narratives in evolution and ecology. *The American Naturalist*, **195**, 290–299.
- Parejko, K. & Dodson, S.I. (1991) The evolutionary ecology of an antipredator reaction norm: *Daphnia pulex* and *Chaoborus americanus*. *Evolution*, **45**, 1665–1674.

- Peniston, J.H., Barfield, M. & Holt, R.D. (2019) Pulsed Immigration Events Can Facilitate Adaptation to Harsh Sink Environments. *The American Naturalist*, **194**, 316–333.
- Pettersson, M. & Bååth, E. (2003) Temperature-dependent changes in the soil bacterial community in limed and unlimed soil. *FEMS Microbiology ecology*, **45**, 13–21.
- Åkesson, A., Curtsdotter, A., Eklöf, A., Ebenman, B., Norberg, J. & Barabás, G. (2021) The importance of species interactions in eco-evolutionary community dynamics under climate change. *Nature Communications*, **12**, 1–12.
- Ravigné, V., Olivieri, I. & Dieckmann, U. (2004) Implications of habitat choice for protected polymorphisms. *Evolutionary Ecology Research*, **6**, 125–145.
- Raymond, M. & Marquine, M. (1994) Evolution of insecticide resistance in *Culex pipiens* populations: the Corsican paradox. *Journal of Evolutionary Biology*, **7**, 315–337.
- Reznick, D.N., Shaw, F.H., Rodd, F.H. & Shaw, R.G. (1997) Evaluation of the rate of evolution in natural populations of guppies (*Poecilia reticulata*). *Science*, **275**, 1934–1937.
- Rice, S. (2004) *Evolutionary Theory: Mathematical and Conceptual Foundations*. Sinauer. ISBN 9780878937028.
- Ricklefs, R.E. (1987) Community diversity: relative roles of local and regional processes. *Science*, **235**, 167–171.
- Rogers, A., Frinault, B., Barnes, D., Bindoff, N., Downie, R., Ducklow, H., Friedlaender, A., Hart, T., Hill, S., Hofmann, E. *et al.* (2020) Antarctic futures: an assessment of climate-driven changes in ecosystem structure, function, and service provisioning in the Southern Ocean. *Annual Review of Marine Science*, **12**, 87–120.
- Ruokolainen, L., Lindén, A., Kaitala, V. & Fowler, M.S. (2009) Ecological and evolutionary dynamics under coloured environmental variation. *Trends in Ecology & Evolution*, **24**, 555–563.
- Rupert, J.L. & Hochachka, P. (2001) Genetic approaches to understanding human adaptation to altitude in the Andes. *Journal of Experimental Biology*, **204**, 3151–3160.
- Sauve, D., Friesen, V.L. & Charmantier, A. (2021) The effects of weather on avian growth and implications for adaptation to climate change. *Frontiers in Ecology and Evolution*, **9**, 5.
- Scheuerl, T., Hopkins, M., Nowell, R.W., Rivett, D.W., Barraclough, T.G. & Bell, T. (2020) Bacterial adaptation is constrained in complex communities. *Nature Communications*, **11**, 754.

- Shama, L.N. (2017) The mean and variance of climate change in the oceans: hidden evolutionary potential under stochastic environmental variability in marine sticklebacks. *Scientific reports*, **7**, 1–14.
- Souther, S. & McGraw, J.B. (2011) Evidence of local adaptation in the demographic response of American ginseng to interannual temperature variation. *Conservation Biology*, **25**, 922–931.
- Sternberg, E.D. & Thomas, M.B. (2014) Local adaptation to temperature and the implications for vector-borne diseases. *Trends in Parasitology*, **30**, 115–122.
- Tanaka, Y., Minggat, E. & Roseli, W. (2021) The impact of tropical land-use change on downstream riverine and estuarine water properties and biogeochemical cycles: a review. *Ecological Processes*, **10**, 1–21.
- terHorst, C.P., Zee, P.C., Heath, K.D., Miller, T.E., Pastore, A.I., Patel, S. & et al. (2018) Evolution in a community context: trait responses to multiple species interactions. *The American Naturalist*, **191**, 368–380.
- Tilman, D. (1994) Competition and Biodiversity in Spatially Structured Habitats. *Ecology*, **75**, 2–16.
- Tilman, D., Wedin, D. & Knops, J. (1996) Productivity and sustainability influenced by biodiversity in grassland ecosystems. *Nature*, **379**, 718–720.
- Tomasini, M. & Peischl, S. (2020) When does gene flow facilitate evolutionary rescue? *Evolution*, **74**, 1640–1653.
- Vanoverbeke, J., Urban, M.C. & De Meester, L. (2016) Community assembly is a race between immigration and adaptation: eco-evolutionary interactions across spatial scales. *Ecography*, **39**, 858–870.
- Vasseur, D.A. & McCann, K.S. (2007) *The impact of environmental variability on ecological systems*, vol. 2. Springer.
- Vermeulen, S.J., Campbell, B.M. & Ingram, J.S. (2012) Climate change and food systems. *Annual review of environment and resources*, **37**, 195–222.
- Visscher, P.M. & Goddard, M.E. (2019) From RA Fisher’s 1918 paper to GWAS a century later. *Genetics*, **211**, 1125–1130.
- Walker, A.S., Ravigné, V., Rieux, A., Ali, S., Carpentier, F. & Fournier, E. (2017) Fungal adaptation to contemporary fungicide applications: the case of *B. otrytis* cinerea populations from Champagne vineyards (France). *Molecular Ecology*, **26**, 1919–1935.
- Whitlock, M.C. (1992) Temporal fluctuations in demographic parameters and the genetic variance among populations. *Evolution*, **46**, 608–615.
- Wiens, J.A. (1989) Spatial scaling in ecology. *Functional ecology*, **3**, 385–397.
- Wilson, D.S. & Yoshimura, J. (1994) On the coexistence of specialists and generalists. *The American Naturalist*, **144**, 692–707.

- Wright, S. (1931) Evolution in Mendelian Populations. *Genetics*, **16**, 97–159.
- Wrona, F.J., Prowse, T.D., Reist, J.D., Hobbie, J.E., Lévesque, L.M. & Vincent, W.F. (2006) Climate change effects on aquatic biota, ecosystem structure and function. *AMBIO: A Journal of the Human Environment*, **35**, 359–369.
- Yamaguchi, R. & Iwasa, Y. (2013) First Passage Time to Allopatric Speciation. *Interface focus*, **3**, 20130026.
- Zari, M.P. (2014) Ecosystem services analysis in response to biodiversity loss caused by the built environment. *SAPI EN. S. Surveys and Perspectives Integrating Environment and Society*.
- Zuppinge-Dingley, D., Schmid, B., Petermann, J.S., Yadav, V., De Deyn, G.B. & Flynn, D.F.B. (2014) Selection for niche differentiation in plant communities increases biodiversity effects. *Nature*, **515**, 108–111.

Chapter 1

How community adaptation impacts biodiversity-functioning relationships

Article published in *Ecology Letters*: <https://doi.org/10.1111/ele.13530>

Flora AUBREE¹, Patrice DAVID², Philippe JARNE², Michel LOREAU³, Nicolas MOUQUET⁴, Vincent CALCAGNO¹.

1. Université Côte d'Azur, INRAE, CNRS, ISA, 06900 Sophia Antipolis, France.
2. Centre d'Ecologie Fonctionnelle et Evolutive, CNRS - Université de Montpellier - Université Paul Valéry Montpellier - IRD - EPHE, 1919 route de Mende, 34293, Montpellier Cedex 5, France.
3. Centre for Biodiversity Theory and Modelling, Theoretical and Experimental Ecology Station, CNRS and Paul Sabatier University, Moulis 09200, France.
4. MARBEC, CNRS-IFREMER-IRD-Univ. of Montpellier, Montpellier 34095, France.

Acknowledgments FA was funded by a PhD fellowship from Université Côte d'Azur (IDEX UCA-JEDI). ML was supported by the TULIP Laboratory of Excellence (ANR-10-LABX-41) and by the BIOTASES Advanced Grant, funded by the European Research Council under the European Union's Horizon 2020 research and innovation program (grant agreement No 666971). PD and PJ were funded by ANR program NGB (ANR 17-CE32-0011-05). VC and PD also thank the CESAB (project COREIDS).

*There is no love of the earth; there
is only usage of the earth.*

Jiddu KRISHNAMURTI

Abstract

Evidence is growing that evolutionary dynamics can impact biodiversity-ecosystem functioning (BEF) relationships. However the nature of such impacts remains poorly understood. Here we use a modelling approach to compare random communities, with no trait evolutionary fine-tuning, and co-adapted communities, where traits have co-evolved, in terms of emerging biodiversity-productivity, biodiversity-stability, and biodiversity-invasion relationships. Community adaptation impacted most BEF relationships, sometimes inverting the slope of the relationship compared to random communities. Biodiversity-productivity relationships were generally less positive among co-adapted communities, with reduced contribution of sampling effects. The effect of community-adaptation, though modest regarding invasion resistance, was striking regarding invasion tolerance: co-adapted communities could remain very tolerant to invasions even at high diversity. BEF relationships are thus contingent on the history of ecosystems and their degree of community adaptation. Short-term experiments and observations following recent changes may not be safely extrapolated into the future, once eco-evolutionary feedbacks have taken place.

Keywords: Adaptive dynamics; Eco-evolutionary dynamics; Species interactions; Species traits; Productivity; Stability; Invasion

1.1 Introduction

Diversity, most classically defined as the number of constituent species in a community, plays an essential role in many aspects of ecosystem functioning (Hooper *et al.*, 2005, 2012; Isbell *et al.*, 2011). Understanding how species composition affects ecosystem properties is a fundamental question in basic and applied ecology, and renewed practical importance given the accelerating biodiversity crisis (Pimm *et al.*, 2014).

Observational data, controlled experiments and theoretical developments have converged in identifying ecosystem properties that exhibit systematic responses to diversity. Three types of so-called biodiversity-ecosystem functioning (BEF) relationships are most commonly described, even though all three are seldom considered in the same study. (i) First, the biodiversity-productivity relationship, historically investigated in grassland communities (Tilman *et al.*, 1996; Loreau & Hector, 2001), has been explored in several other taxa and ecosystems (Abramsky & Rosenzweig, 1984; Naeem *et al.*, 1994; Hooper *et al.*, 2005; Gamfeldt *et al.*, 2015). It is often assumed that more diverse ecosystems are more productive, in agreement with theoretical predictions (Loreau, 1998; Tilman, 1999). (ii) Second, biodiversity-stability relationships have also received a lot of attention (Elton, 1958; Tilman, 1999; McCann, 2000), both theoretically (May, 1973; Loreau & Mazancourt, 2013) and experimentally (Gross *et al.*, 2014; Renard & Tilman, 2019). The intuitive view that diverse ecosystems are more stable in the face of environmental fluctuations appeared contradicted by early theoretical models suggesting the opposite (McCann, 2000). In fact, predictions may differ importantly depending on the type of stability metric, with negative relationships expected at the level of individual species (dynamical stability: May, 1973; Tilman *et al.*, 1996; Ives & Carpenter, 2007), and positive relationships expected for aggregate metrics (ecosystem stability: May, 1973; Tilman *et al.*, 1996; Ives *et al.*, 1999; Barabás & D’Andrea, 2016; Pennekamp *et al.*, 2018). (iii) Last, biodiversity-invasion relationships have also attracted much attention, since native diversity has long been regarded as a key attribute determining the susceptibility of communities to invasions. It is generally considered that more diverse ecosystems should be less susceptible to invasions, and should suffer from fewer adverse impacts (e.g. secondary extinctions) following an invasion (Levine, 2000; Hector *et al.*, 2001; Davis, 2009).

Ecosystem functioning is driven, beyond the sheer number of species, by community composition in terms of key functional trait (Gagic *et al.*, 2015). Communities with the same diversity, but different trait compositions, might possess different functioning characteristics. Communities probably harbor very different traits depending on whether they are recent assemblages drawn from the regional pool, or if species have adapted to the local environment and to the other species, through various mechanisms including plasticity, niche-construction and evolution (Kylafis & Loreau, 2011; Hendry, 2016; Meilhac *et al.*, 2020). In particular, evolutionary changes may be important on ecological timescales (Davis *et al.*, 2005; Hendry, 2016), and there is mounting evidence that species can adapt rapidly to environmental changes and to the presence of competitors or predators (Thompson, 1998; Faillace & Morin, 2016; Kleynhans *et al.*, 2016; Hart *et al.*, 2019; Meilhac *et al.*, 2020). By altering species trait composition, such community adaptation may impact the existence, magnitude and shape of BEF relationships.

Even though BEF studies are traditionally conducted from an ecological perspective, long term grassland experiments (Reich *et al.*, 2012; Meyer *et al.*, 2016) and microbe experiments (Bell *et al.*, 2005) found that biodiversity-yield relationships change through time. The most recent studies have explicitly highlighted a role of evolution in modifying biodiversity-yield relationships: in grasslands (Zuppinge-Dingley *et al.*, 2014; van Moorsel *et al.*, 2018) and with microbes, using experimental evolution (Fiegna *et al.*, 2014, 2015). However, results have proven quite variable, prompting a plea for more theoretical investigations (Fiegna *et al.*, 2015).

Here we propose a theoretical evaluation of the consequences community adaptation may have for BEF relationships. We use a general modeling approach to address the three types of BEF relationships highlighted above (biodiversity-productivity, biodiversity-stability, and biodiversity-invasion). We compare two contrasted types of communities: (i) random communities, in which only ecological processes control species trait composition, with no evolutionary dynamics, and (ii) co-adapted communities, in which species traits composition have further been shaped by microevolution (species adaptation to the environment and to other species). Specifically, species have adjusted their traits and are at (co)evolutionary equilibrium (Christiansen, 1991). Real-life communities would harbour various degrees of co-adaptation in between these two limiting cases. Recently-founded or perturbed ecosystems, such as artificially assembled communities, are probably closer to the random case. In contrast, ecosystems that have long remained in relatively constant conditions, such as primary old-growth forests, may be closer to co-adapted communities.

As species coexistence and eco-evolutionary dynamics depend on the type of ecological interactions (Mouquet *et al.*, 2002; Chave *et al.*, 2002; Calcagno *et al.*, 2017), we model communities governed by four contrasted scenarios of ecological interactions, representative of classical coexistence mechanisms (Doebeli & Dieckmann, 2000; Calcagno *et al.*, 2017): two scenarios based on resource competition (one symmetric, one asymmetric), one life-history trade-off scenario, and a trophic-chain scenario. In each case, several functioning metrics are computed to evaluate BEF relationships. This general approach allows to evaluate the extent to which the consequences of community adaptation are general or depend on particular types of metrics and ecological interactions.

We report clear influences of community adaptation on each of the three BEF relationships investigated, highlighting how co-adaptation impacts species trait distribution and, in turn, functioning properties. Although conclusions may depend importantly on the type of ecological interaction scenario considered, general predictions regarding the consequences of community adaptation are formulated, and discussed in light of available experimental evidence.

1.2 Material and methods

1.2.1 Ecological scenarios and traits

In natural ecosystems species are engaged in various interactions, within the same trophic level (horizontal interactions) and among different trophic levels (vertical interactions), at different spatio-temporal scales. The dominant form of species interaction may differ across communities (Chave *et al.*, 2002), and some studies have

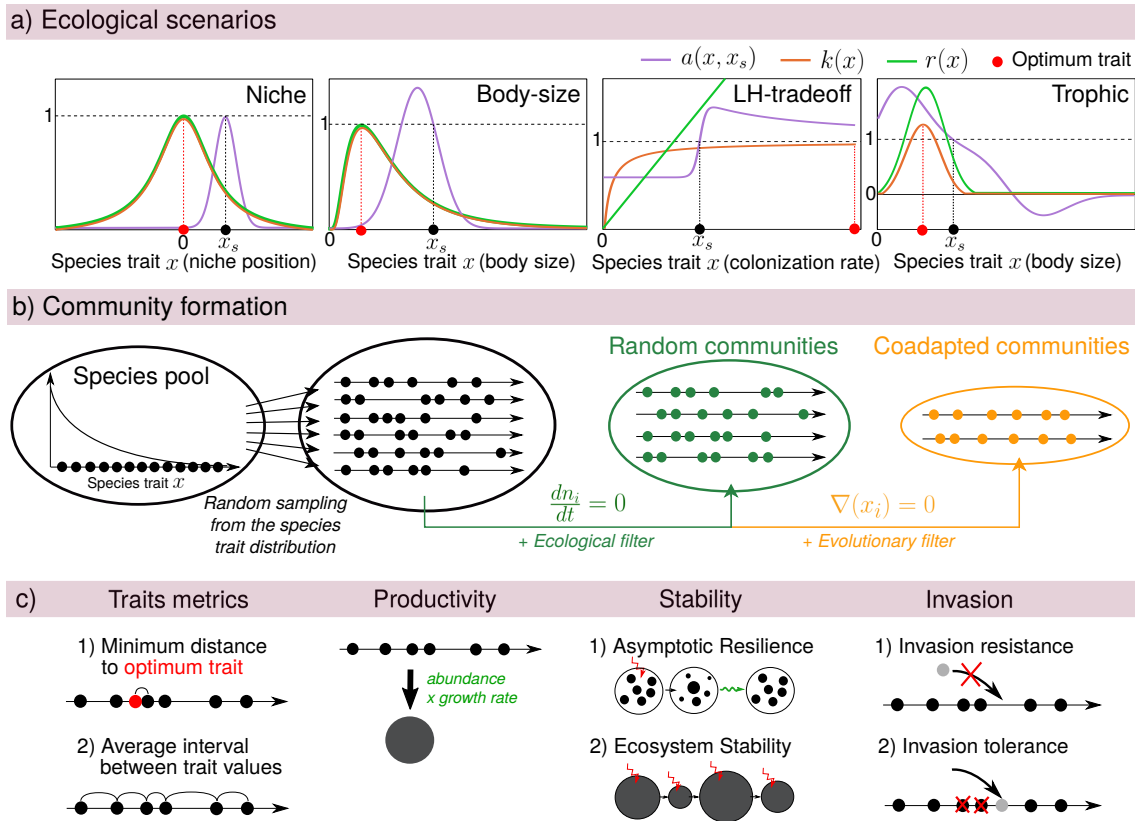


Figure 1.1: (a) Ecological parameters for the four scenarios considered: intrinsic growth rate $r(x)$ (green), mono-specific abundance $k(x)$ (orange) and competitive impact $a(x, x_s)$ (purple) of species x_s over species x as a function of species trait x for the four scenarios. By definition the intra-specific competition is $a(x_s, x_s) = 1$. Red dots indicate the optimum ecological trait, *i.e.* trait that maximizes mono-specific abundances. (b) Community formation. Species are sampled from a species pool within a given distribution. An ecological filter is then applied so that only the ecologically existing communities are kept (with no null abundance), and form the random communities. Then, species evolution towards their evolutionary equilibrium filters out some species, leading to co-adapted communities. (c) For each community (random or co-adapted), we measure two species trait metrics (minimum distance to optimum trait, and average interval between trait values) and the three types of functioning properties: (i) productivity measured by species abundances time species growth rates, (ii) stability, with asymptotic resilience (return rate to equilibrium) and ecosystem stability (reflecting changes in abundances over time), and (iii) response to invasion, with invasion resistance (probability of non-establishment of a foreign species) and tolerance to invasion (probability of non-resident extinction following an invasion).

argued that generalist predation, exploitative competition and simple three-species food chains compose the common backbone of interaction networks (Mora *et al.*, 2018). To reflect this diversity, we here considered a set of four contrasted ecological scenarios (Fig. 1.1a), based on classical species coexistence models, and spanning the range from completely horizontal symmetric interactions to completely vertical asymmetric interactions. The first two scenarios describe competition for resources. The *Niche* scenario is a classical model of symmetric competition along an axis of

niche differentiation (Doebeli & Dieckmann, 2000; Calcagno *et al.*, 2017). The *Body-size* scenario introduces interference and asymmetric competition, based on *e.g.* size differences (Rummel & Roughgarden, 1985; Doebeli & Dieckmann, 2000). The third scenario (*LH-tradeoff*) models a life-history trade-off, describing the strongly asymmetric competition between species good at colonizing empty habitat and species locally dominant, along a competitive hierarchy (Tilman, 1994; Calcagno *et al.*, 2006, 2017). Last, the fourth (*Trophic*) scenario describes a size-structured trophic chain, based on the model introduced by Loeuille & Loreau (2005).

In each interaction scenario, species are characterized by one key trait, denoted x (Fig. 1.1a). In the *Niche* scenario, the trait represents niche position along the continuum of resources, and interspecific competition thus decreases with trait difference (niche differentiation). In the *Body-size* scenario, the trait is body size: species with similar size compete more intensely, and bigger species have a competitive advantage over smaller ones. In the *LH-tradeoff* scenario, species trait is the colonization rate: species with greater trait value are more apt at colonizing empty patches, but also more susceptible to be competitively displaced from occupied patches (Calcagno *et al.*, 2006). Last, in the *Trophic* scenario, species trait is body mass: body mass influences growth and metabolic rates, and species preferentially consume species that are smaller, with some optimal mass difference (Loeuille & Loreau, 2005).

After appropriate reformulations (Supporting information (S.I.) Section A.1), all models can be set in the common Lotka-Volterra form:

$$\frac{dn_i}{dt} = n_i r(x_i) \left(1 - \sum_j \frac{n_j a(x_i, x_j)}{k(x_i)} \right) \quad (1.1)$$

with n_i the abundance of species i , that denotes, depending on scenario, either a number of individuals (*Niche*), a biomass (*Body-size* and *Trophic*) or a fraction of occupied sites (*LH-tradeoff*).

The three functions included in equation (1.1) allow to describe species demography and inter-specific interactions: $r(x_i)$ is the intrinsic growth rate of species i that governs the ecological timescale; $a(x_i, x_j)$ is the impact that a variation in species j abundance has on the per capita growth rate of species i , normalized by the intra-specific interaction (see S.I., Section A.1.1); and $k(x_i)$, usually called the carrying capacity, quantifies the resistance to density dependence of species i . In all scenarios but the *Trophic* one, it is also the equilibrium abundance reached by the species if growing alone in the community, or in other words the mono-culture abundance (Loreau & Hector, 2001). The shape of the functions for each scenario differ in important ways, as represented in Fig. 1.1a. See S.I. Section A.1 for a complete description of each scenario.

Evolution would often favor certain trait values that are better adapted to the current habitat; this is described by the mono-specific abundance function $k(x)$, which defines the optimum trait value, as represented by the red dots in Fig. 1.1a. The relationship between trait value and mono-specific abundance may have an intermediate optimum (*Niche*, *Body-size* and *Trophic*) or be open-ended (*LH-tradeoff*), see red dots positions in Fig.1.1a. Sometimes, inter-individual interactions and competition may counteract evolution towards optimal trait values, in particular in the *LH-tradeoff* scenario, in which evolution effectively results in traits with comparatively low mono-specific abundances (Calcagno *et al.*, 2017).

Species traits, through functions r , k and a , determine species interactions and overall ecosystem and evolutionary dynamics. Note that we consider here species that coexist stably and have distinct ecological traits. For each scenario, one or two parameters controlling the shape of the functions were systematically varied to ensure that conclusions were robust to parameter changes (all details and the parameter ranges explored are provided in S.I., Section A.2).

In the *Niche* scenario, we varied the width of the competition function (Fig. 1.1a) keeping the width of the mono-specific abundance function constant (Doebeli & Dieckmann, 2000). In the *Body-size* scenario, we varied both the width of the competition function and its skew (level of competitive asymmetry; see Rummel & Roughgarden, 1985; Doebeli & Dieckmann, 2000). In the *LH-tradeoff* scenario, we varied the intensity of the tradeoff, and the level of competitive preemption (Calcagno *et al.*, 2006). Finally, in the *Trophic* scenario, we varied the level of interference competition and the width of the consumption function (Loeuille & Loreau, 2005). In the figures, for clarity, only three contrasted and representative parameter sets are presented per scenario.

1.2.2 Random and co-adapted communities

The process of community formation is sketched Fig. 1.1b. For diversity levels (N) between 1 and 10, sets of species were drawn randomly from a regional pool. The ecological equilibrium with N species was computed from equation (1.1), and the community was retained if all species persisted at equilibrium (see S.I. Section A.3 for details). This was repeated until obtaining, for each diversity level, 1,000 such random communities. The distribution of species trait values in the regional pool was chosen to minimize information content (maximum entropy; Jaynes, 1957), while being representative of typical trait values expected for the corresponding ecological scenario and parameter set. This is a generic approach but, of course, there are many ways in which diversity gradients can be generated in nature and experiments. We tried alternative methods to assemble random communities, and conclusions were little affected (see S.I. Section A.3). For some scenarios and parameter sets, no feasible community could be found beyond some diversity level, in which case we stopped at the highest feasible level.

Whereas random communities are only constrained by ecological processes (regional pool and local competitive exclusion), co-adapted communities met the additional constraint that species traits are at (co)evolutionary equilibrium ("evolutionary filter"; Fig. 1b). We computed, for each species in a community, the selection gradient (Christiansen, 1991), defined as

$$\nabla(x_i) = \left. \frac{ds(x_m)}{dx_m} \right|_{x_m=x_i} \quad (1.2)$$

where $s(x_m)$ is the fitness (growth-rate) of a rare phenotype x_m . Note that fitness is density- and frequency-dependent and varies with community composition (species trait and abundances).

If $\nabla(x_i) > 0$, selection acts to increase the trait value, whereas if $\nabla(x_i) < 0$ smaller values are selected for. When all selection gradients are simultaneously cancelled in a community, species have attained an evolutionary attractor and are at equilibrium with respect to first-order selection (Christiansen, 1991). This approach

assumes heritable trait variation and sufficiently small phenotypic variance within each species. We thus generated, for each scenario, parameter set and diversity level, all possible co-adapted communities (most often, only one), in the sense of eq. (1.1) and (1.2). See S.I. Section A.3 for detailed methods.

1.2.3 Biodiversity-functioning relationships

For each generated community, we computed several properties of interest (Fig. 1.1c; full list in S.I. Section A.4) to investigate the three BEF relationships. We present results based on the properties describe hereafter, as conclusions were similar based on the others. First, community productivity (Tilman, 1999; Loreau & Hector, 2001) was measured as the species average rate of production (positive contribution to growth rate) in the community. Second, ecological stability was assessed in two ways. We computed the classical asymptotic resilience (May, 1973; Arnoldi *et al.*, 2016), *i.e.* asymptotic rate of return to equilibrium of the community after a perturbation, and the community stability (May, 1973; Ives *et al.*, 1999), *i.e.* the inverse of the coefficient of variation of total community abundance under sustained environmental noise. Finally, to study the response to invasions, we also used two properties. The first is the resistance to invasion (Elton, 1958; Hector *et al.*, 2001), *i.e.* the probability that a random alien species, introduced at low abundance, fails to establish in the community. The second was the tolerance to invasion (Elton, 1958), *i.e.* the proportion of species that, following a successful invasion, were not driven to extinction. Details on the mathematical computation of each metric are presented in S.I. Section A.4.

For each metric, diversity level, scenario and parameter set, we computed the average value over the 1,000 random communities, and over the few (or, most often, the unique) co-adapted communities. To ensure that average differences represented large effect sizes, we further computed the percentile, in the distribution of values over random communities, corresponding to the value of co-adapted communities. Our results showed that co-adapted communities often lie in the tail of the distribution of random communities, for all metrics (see S.I. Section A.5). Average differences between co-adapted and random communities were thus large relative to the variability of random communities. For this reason we only present average values in the Figures.

The above metrics were correlated to species richness to produce BEF relationships and compare random and co-adapted communities. Since the impacts of co-adaptation are mediated by changes in trait values, we compared the structure of co-adapted and random communities. We then computed the average absolute difference in trait space between the two, as a measure of the strength of the evolutionary filter. We summarized trait compositions using two additional quantities (Fig. 1.1c). The first was the minimum distance to the optimal trait value (red dots in Fig. 1.1a), that reflects how well the better performing species is adapted to the habitat. The second was the average trait interval between species (trait range divided by number of species minus one), that indicates how “packed” species are in trait space. More details are provided in S.I. Section A.4.

1.3 Results

1.3.1 Biodiversity-Productivity

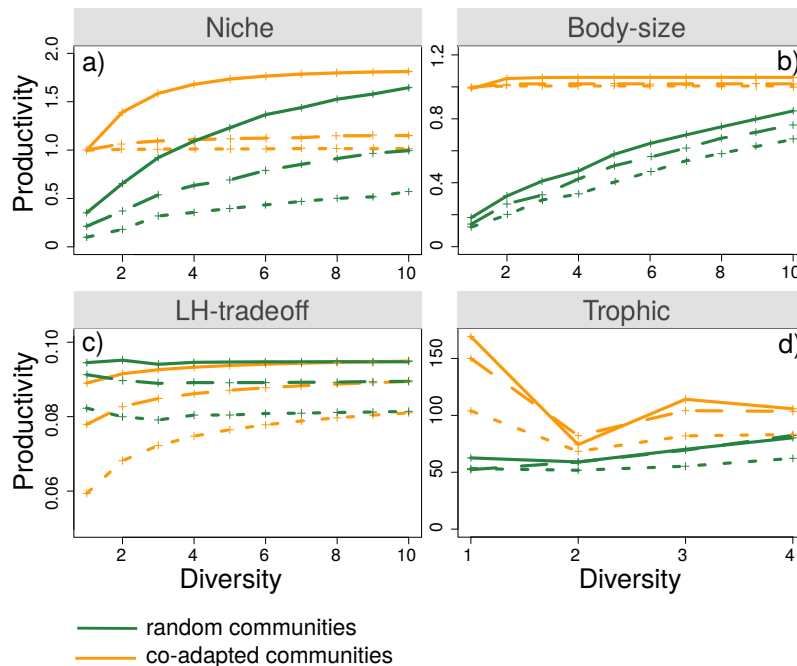


Figure 1.2: Productivity as a function of diversity under the the four scenarios and the two community adaptation levels. Three sets of parameters are used for each scenario, represented by the three different line types. Parameter values are given in S.I. Section A.2 together with other explored parameter sets (not shown for the sake of clarity). Each point represents an average over 1000 random communities or the only or few co-adapted communities.

Random and co-adapted communities differed in productivity at low diversity levels, but at higher diversity levels, differences were more modest (Fig. 1.2). Moreover, in all scenarios except the *LH-tradeoff*, the effect of community adaptation was to increase productivity. Those two observations explain the quantitative differences in biodiversity-productivity relationships between random and co-adapted communities.

Qualitatively, co-adaptation affected the biodiversity-productivity relationship in all four scenarios (Fig. 1.2). The impact could be as spectacular as a slope inversion. For instance, the *LH-tradeoff* scenario, unlike the other scenarios, generated mildly negative biodiversity-productivity relationships in random communities (see also Loreau, 2010), while in co-adapted communities, they switched to markedly positive for all parameter sets (Fig. 1.2c). Conversely, the *Trophic* scenario generated a classical positive biodiversity-productivity relationship in random communities, but the relationships switched to negative in co-adapted communities (with oscillations between odd and even diversity levels, caused by trophic cascades; Fig. 1.2d). The possibility of such inversions of biodiversity-production relationships has, to the best of our knowledge, never been reported so far.

In the remaining scenarios, those based on resource competition, biodiversity-productivity relationships were always positive – at least slightly – irrespective of co-

adaptation (Fig. 1.2a,b). However, the shape of the relationships differed markedly between random and co-adapted communities: the increase in productivity with diversity was close to linear or gradually slowed down with diversity, whereas in co-adapted communities, the relationships saturated very quickly, reaching almost maximum productivity at low diversity levels and then plateauing, especially in the *Body-size* scenario (Fig. 1.2b).

1.3.2 Species trait composition

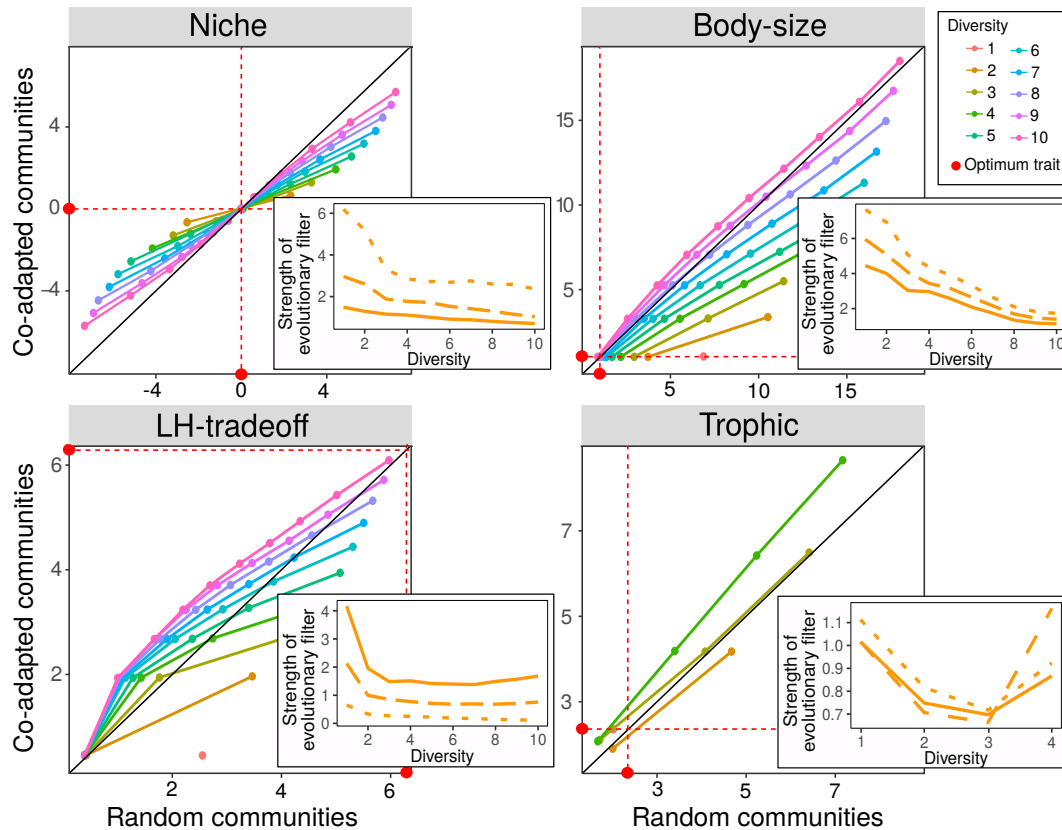


Figure 1.3: Comparative structures of random and co-adapted communities, in the four ecological scenarios. For each diversity level, species were ranked by trait value, and trait values at each species rank were averaged over all communities. The average trait values at each species rank in co-adapted communities was plotted against the corresponding values in random communities, and connected with colored lines for each diversity level (see legend). As a consequence, lines close to the first diagonal indicate very similar trait compositions in the two community types. Slopes smaller than one indicate greater trait dispersion in random than in co-adapted communities, while slopes greater than one indicate the opposite. Only one parameter set was showed in each scenario (the one corresponding to the wide dotted lines in other figures), for clarity, as patterns are similar in other parameter sets. Optimal trait values (see Fig. 1.1) are also shown on both axes (red dots). In inserts, we represented the strength of the evolutionary filter as a function of diversity, for all three parameter sets (each with a different line type). This was computed as the absolute trait difference between random and co-adapted communities, per species rank, averaged over all ranks and all communities.

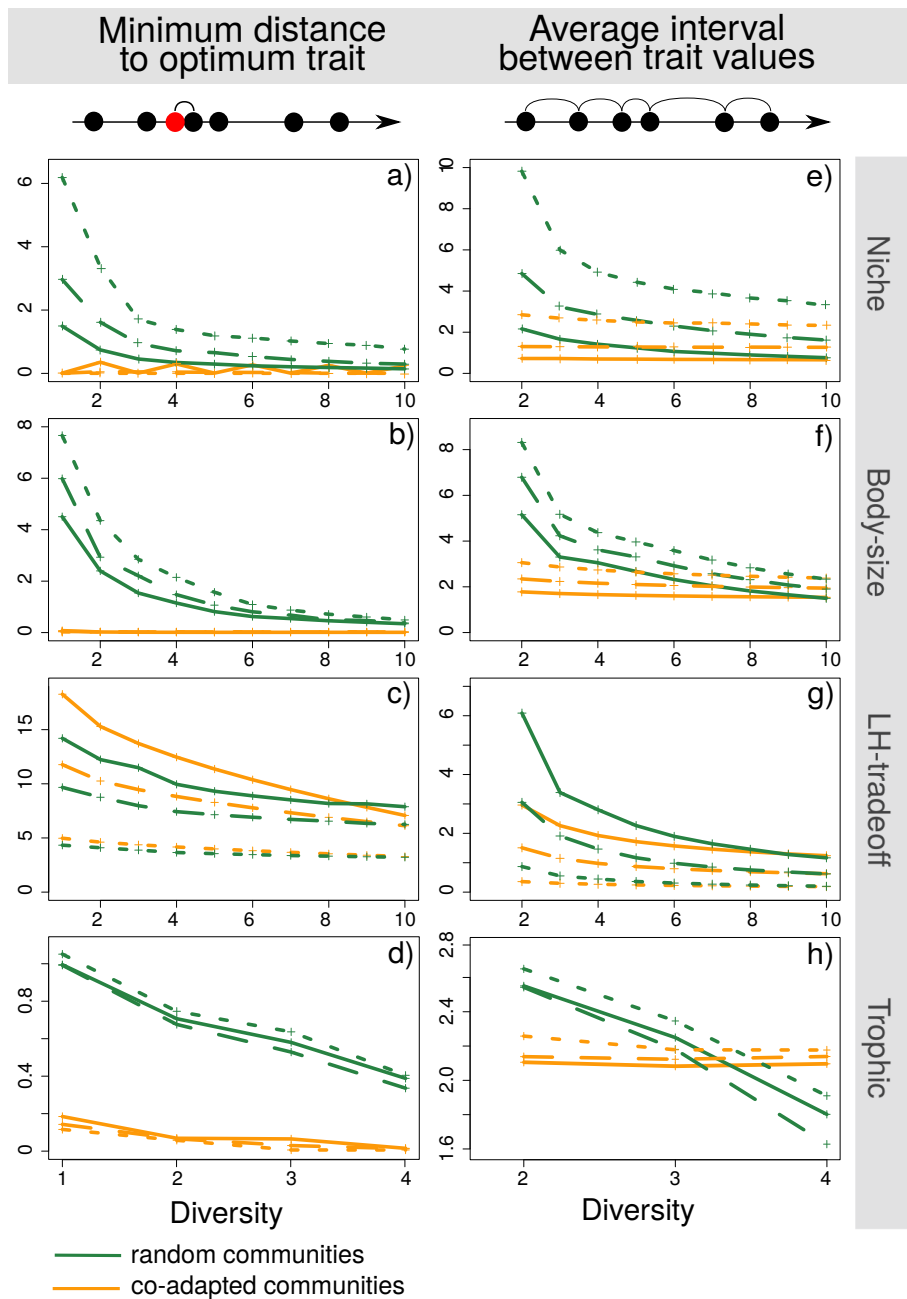


Figure 1.4: Minimum distance to optimum trait (a-d) and average interval between trait values (e-h) as a function of diversity under the four scenarios and the two types of communities. Three sets of parameters are used for each scenario, represented by the three different line types. Parameter values are given in S.I. Section A.2 together with other explored parameter sets (not shown for the sake of clarity). Each point represents an average over 1000 random communities or the only or few co-adapted communities.

As shown in Fig. 1.3, random and co-adapted communities exhibited systematic differences in their trait composition and structure. The specifics differed across ecological scenarios, but general trends can be identified. First, random communities are generally less packed than co-adapted ones, as can be seen by the slopes lower than one in Fig. 1.3), indicative of broader trait ranges in random communities. Second, the difference was maximal at low diversity and tended to vanish as diversity

increases. Increasing diversity made random and co-adapted communities converge to similar trait distributions on average (aligning on line $x = y$ in Fig. 1.3), with one exception in the *Trophic* scenario. As a result, the impact of community adaptation on community structure, i.e. the strength of the evolutionary filter, globally declined with the number of species (insert panels in Fig. 1.3).

More specifically, in random communities, the chance to find a highly performing species inevitably increased with the number of species, so that the minimum trait distance to the optimum decreased with diversity in all scenarios (Fig. 1.4a-d). Concomitantly, the average distance between species decreased sharply with species richness (Fig. 1.4e-h), reflecting the greater species packing. In contrast, a close-to-optimal species was always present in co-adapted communities (constant minimum distance to optimum trait Fig. 1.4a,b,d), except for the *LH-tradeoff* scenario in which evolution did not drive species to the optimum trait (Fig. 1.4c). Community adaptation also made the level of species packing virtually constant irrespective of species number (Fig. 1.4e-h; see also Fig. 1.3).

1.3.3 Biodiversity-Stability

Asymptotic resilience, in all four ecological scenarios, declined with diversity (Fig. 1.5a-d). Moreover, the biodiversity-stability relationships were similarly negative, regardless of community adaptation, even though co-adapted communities were generally more stable than random ones.

Ecosystem stability, was also higher overall in co-adapted than in random communities (Fig. 1.5e-h). However, unlike asymptotic resilience, it had different responses to diversity depending on ecological scenario. It increased with species richness in the two scenarios based on resource competition (*Niche* and *Body-size*), but decreased with species richness in the *LH-tradeoff* and *Trophic* scenarios. In all cases, unlike asymptotic resilience, the variation of ecosystem stability with species richness was strongly affected by co-adaptation, and the patterns were quite consistent with those observed for total productivity (Fig. 1.2), except for the *LH-tradeoff*.

1.3.4 Biodiversity-Invasion

Resistance to invasion (Fig. 1.6a-d) presented consistent trends in the four ecological scenarios. First, it increased with species richness, reflecting classical expectations. Second, co-adapted communities were generally more resistant to invasion than random ones, at any species richness level, reflecting the concentration of species around trait optima, which leaves only more peripheral niches available for potential invasive species. This difference was also quite in line with common expectations, but it could vanish, or even reverse for some parameter values, in the *LH-tradeoff* scenario (Fig. 1.6c). Overall, the biodiversity-invasion relationships were thus similar regardless of co-adaptation.

The effects of co-adaptation were much more dramatic and consistent when looking at tolerance to invasion (Fig. 1.6e-g), with a pronounced interaction between the effects of diversity and community adaptation. In random communities tolerance to invasion steeply declined with species richness, meaning that successful invasions were more and more harmful (in terms of diversity loss) as diversity increased (Fig. 1.6e-g). In contrast, co-adapted communities were in all cases more tolerant

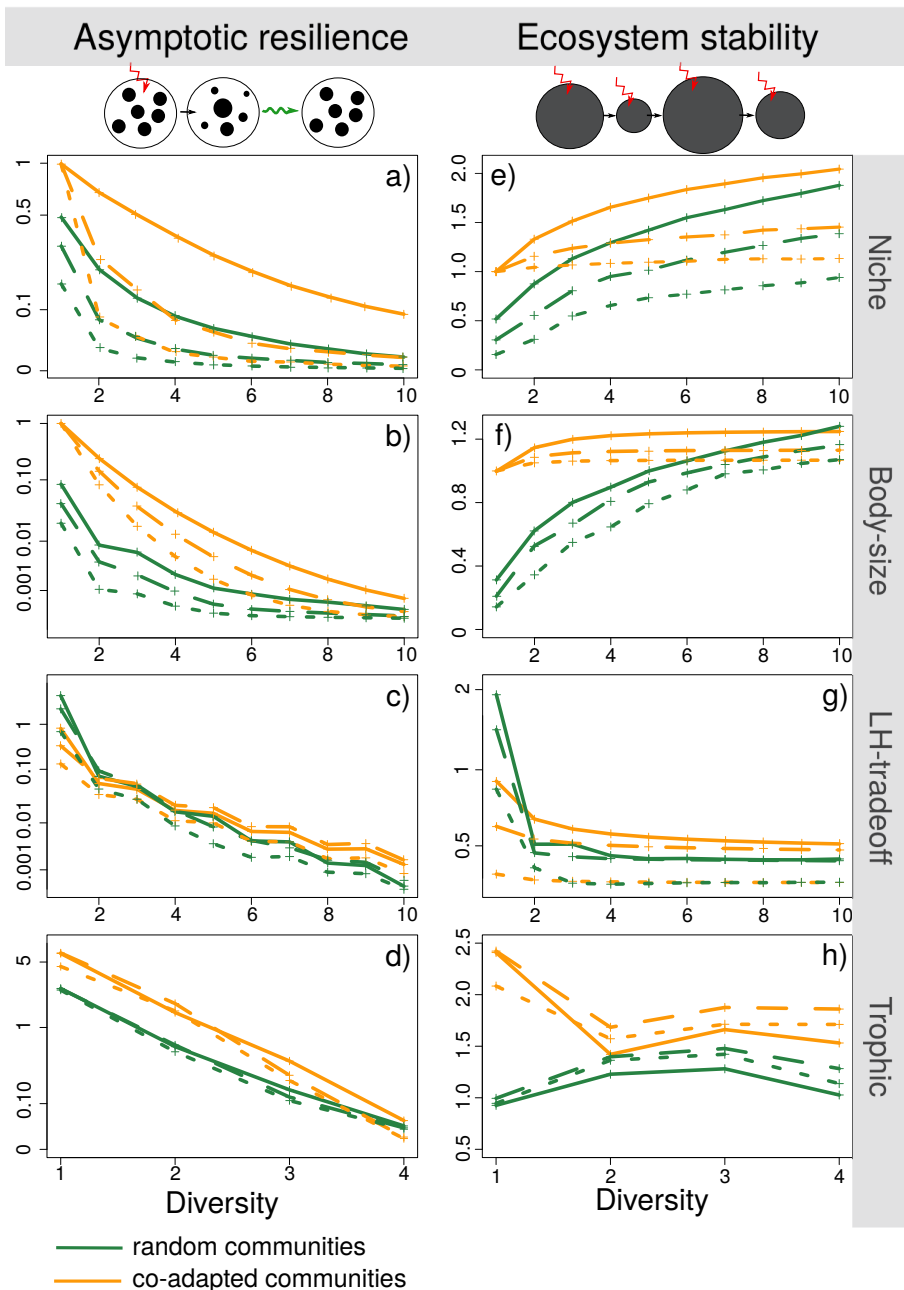


Figure 1.5: Asymptotic resilience (a-d) and ecosystem stability (e-h) as a function of diversity under the four scenarios and the two community adaptation levels. Asymptotic resilience is represented in log-scale, which does not modify the interpretation on co-adaptation effect and allows to better visualize the consequences of co-adaptation. Three sets of parameters are used for each scenario, represented by the three different line types. Parameter values are given in S.I. Section A.2 together with other explored parameter sets (not shown for the sake of clarity). Each point represents an average over 1000 random communities or the only or few co-adapted communities.

to invasion than random communities: they retained their almost perfect tolerance to invasion as diversity increases, the biodiversity-invasion relationship being essentially flat.

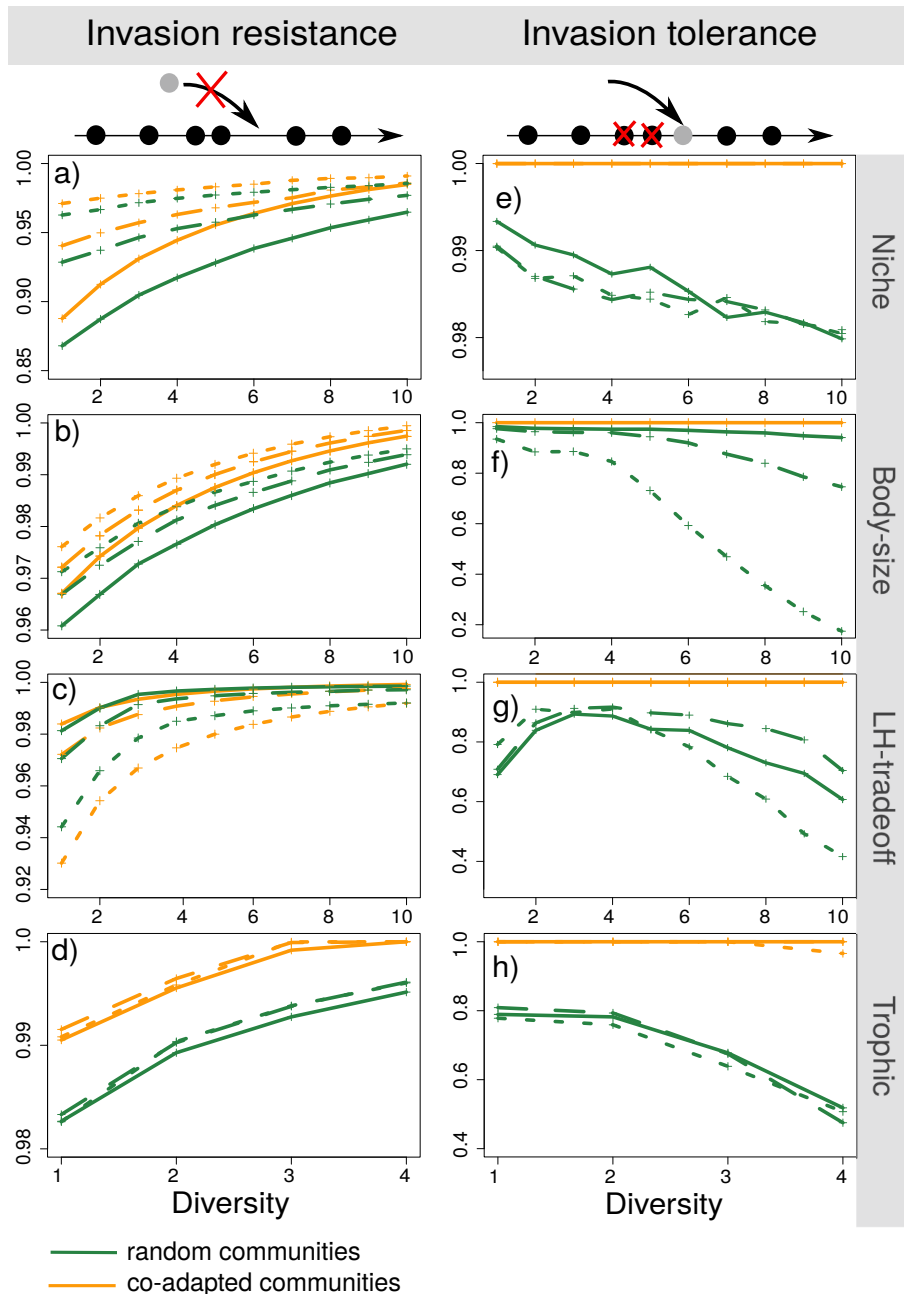


Figure 1.6: Probability that a foreign species does not get installed into a community, i.e. resistance to invasion (a-e), and proportion of resident species that do not undergo a secondary extinction, i.e. tolerance to invasion (f-j), as a function of diversity, under the four scenarios and the two community adaptation levels. Three sets of parameters are used for each scenario, represented by the three different line types. Parameter values are given in S.I. Section A.2 together with other explored parameter sets (not shown for the sake of clarity). Each point represents an average over 1000 random communities or the only or few co-adapted communities.

1.4 Discussion

Natural and anthropized ecosystems present tremendous variation in their diversity and composition (species richness and trait values), and also in the degree to which component species are adapted to the local environmental conditions and to one

another, here referred to as community adaptation. While it is clear that diversity is an important determinant of ecosystem functioning, we still know little about how the level of community adaptation might impact BEF relationships (Fiegna *et al.*, 2015; Hendry, 2016). In this study we addressed this question with a general modelling approach, systematically comparing random and co-adapted communities with respect to three BEF relationships (biodiversity-productivity, biodiversity-stability and biodiversity-invasion) and across four classical scenarios of ecological interactions.

We found that community adaptation had an impact on all BEF relationships, but that the nature and extent of the impact depend on both the metrics and the scenarios considered for species interactions. Overall, the biodiversity-productivity and biodiversity-invasion relationships were strongly impacted by community adaptation, while the biodiversity-stability relationships were much less so. Indeed, co-adapted communities, at any species richness, tended to be more dynamically stable in terms of asymptotic resilience than random ones, but there was little interaction with diversity: BEF relationships looked qualitatively very similar in random and co-adapted communities. This suggests that the connection between diversity and dynamical stability is a rather universal property in such systems of interacting species, largely insensitive to the details of species interactions and to community adaptation. Co-adapted communities were more dynamically stable, which likely reflects the fact that co-adaptation brings traits closer to optimal values (Fig. 1.4a-d), entailing faster returns to equilibrium (see also Loeuille, 2010). Consistent with this interpretation, the only case where co-adapted communities were on average less dynamically stable than random ones occurred at low diversity in the *LH-tradeoff* (Fig. 1.5c), a case where co-adaptation pushes traits away from the optimum (Fig. 1.1a and 1.3). When looking at ecosystem stability (May, 1973; Ives *et al.*, 1999; Arnoldi *et al.*, 2016), BEF relationships differed more importantly between co-adapted and random communities, but these differences closely mirrored those observed for biodiversity-productivity relationships (Fig. 1.5e-h). This suggests that variation in ecosystem stability were linked to variation in total productivity and the total biomass of species, but, beyond that, were little impacted by community adaptation in a direct manner (see Ives *et al.*, 1999), especially for the *Niche*, *Body-size* and *Trophic* scenarios. Consistent with this interpretation, overall Spearman correlation coefficients between productivity and ecosystem stability were, across all communities, 0.97, 0.97, 0.65 and 0.79 for the *Niche*, *Body-size*, *LH-tradeoff*, *Trophic* scenarios, respectively.

Biodiversity-productivity relationships were both quite variable across ecological scenarios and strongly impacted by community adaptation. The impact could be as pronounced as a slope inversion between random and co-adapted communities, with switches from positive to negative (*Trophic* scenario; Fig. 1.2d) or from negative to positive (*LH-tradeoff* scenario; Fig. 1.2c). In all cases, changes in the shape of biodiversity-productivity relationships were mostly driven by low diversity levels, at which co-adapted communities differed importantly for random ones, while at higher diversity levels community adaptation had modest impact on average (Fig. 1.2). Theoretical (Mazancourt *et al.*, 2008) and experimental (terHorst *et al.*, 2018; Scheuerl *et al.*, 2020) studies have found that biodiversity inhibits the evolution of species traits (but see Jousset *et al.* (2016), and our *Trophic* scenario; Fig. 1.3d). This can be attributed to the strong constraints on species trait distri-

butions in rich communities, due to species interactions and persistence conditions (ecological filter), which leaves adaptive evolution much less room to alter species traits. As a result, co-adapted and random communities are more and more similar as the number of species increases, i.e. the strength of the evolutionary filter decreases (see Fig. 1.3: its presence makes less and less of a difference for ecosystem functioning).

In most ecological scenarios (*Niche*, *Body-size* and *Trophic*), co-adapted communities at low diversity levels were more productive than random ones on average (Fig. 1.2a,b,d). Therefore, community adaptation weakened the positive biodiversity-productivity relationships observed in random communities, making those shallower, or even reversing them to negative (*Trophic*). In the *LH-tradeoff* scenario, low diversity co-adapted communities were on the contrary less productive than random ones, so that the effect of community adaptation was opposite: co-adapted communities exhibited a positive biodiversity-functioning relationships, whereas a slightly negative relationship is predicted in random communities (see also Loreau, 2010).

The qualitative effect of community adaptation on biodiversity-productivity relationships could thus be determined, to a large extent, from the overall direction of selection in isolated species (monocultures), either towards higher productivity (*Niche*, *Body-size*, *Trophic* scenarios), weakening positive relationships or switching them to negative, or towards lower productivity (*LH-tradeoff* scenario), switching negative relationships to positive.

Community adaptation also affected the mechanisms underlying biodiversity-productivity relationships. In the two scenarios describing competition for resources (*Niche* and *Body-size*) and in the *Trophic* scenario, low diversity co-adapted communities were more productive because adaptive evolution favoured traits that were close to the optimum (Fig. 1.4a,b,d). At higher diversity levels, more and more species were kept farther away from the optimal trait value, and thus intrinsically less productive. Such a change in the intrinsic productivity of species as diversity increases is often called a “selection effect” (Loreau & Hector, 2001), but here, following Zuppinger-Dingley *et al.* (2014), we will call it a “sampling effect” to avoid confusion. In random communities, this sampling effect was positive, as usually expected, and contributed importantly to the positive biodiversity-productivity relationship: richer communities were more likely, by chance, to harbor species that were intrinsically more productive in the habitat (Fig. 1.4a,b,d, blue curves). In co-adapted communities, the sampling effect was much reduced or entirely absent, owing to the effect of co-adaptation explained above. In contrast, the average trait distance between adjacent species (the level of niche packing) declined sharply with diversity in random communities, but much less so in co-adapted communities (Fig. 1.4e-h). Therefore, the level of species trait complementarity was less sensitive to diversity with community adaptation. Altogether, this suggests positive biodiversity-productivity relationships should be more driven by complementarity effects, and less by sampling effects, in co-adapted communities compared to random communities.

There is good experimental evidence that biodiversity-productivity relationships do change over time. In grassland experiments, the positive biodiversity-productivity relationships were reported to become steeper (Reich *et al.*, 2012), or sometimes flatter (Meyer *et al.*, 2016, for most of its biomass-related metrics), over several years.

A study of decomposing microbial communities observed a decline in productivity and a flattening of the biodiversity-productivity relationship over several days (Bell *et al.*, 2005). Several of these studies (Bell *et al.*, 2005; Reich *et al.*, 2012; Meyer *et al.*, 2016) deal with short timescales and are not directly relevant to address community adaptation, since observed changes are generally attributed to transient ecological mechanisms, such as below-ground feedbacks or resource depletion. Direct comparison with our results, in which transient dynamics have been sorted out, is thus difficult. Fortunately, more recent analyses of the longest grassland experiments have looked for, and found, evidence of character displacement and evolution of niche differentiation, even on relatively short timescales (Zuppingen-Dingley *et al.*, 2014; van Moorsel *et al.*, 2018). This suggests that the evolutionary effects analyzed in this work might have begun to play a role. Interestingly, it was observed that biodiversity-productivity relationships assembled from co-selected species were higher at low diversity, but saturated faster with diversity, thus being more concave (van Moorsel *et al.*, 2018). This is strikingly reminiscent of our predictions in the standard “resource competition” scenarios (*Niche* and *Body-size*; see Fig. 1.2a,b). Furthermore, it was found that species evolving in mixed assemblages (thus approaching a state of community adaptation) elicited more complementarity effects, and less sampling effects, than assemblages of non-co-adapted species (Zuppingen-Dingley *et al.*, 2014). This too is quite consistent with our findings. In a more direct approach, Fiegna *et al.* (2014, 2015) used experimental evolution to demonstrate that biodiversity-productivity relationships are impacted by co-adaptation in bacteria. They further showed that these changes involved an evolutionary component in species interactions, not just of individual species performances, even though the overall impact on biodiversity-productivity relationships was quite variable among experiments. These studies thus clearly support a role for community adaptation in the dynamics of BEF relationships as highlighted here.

Regarding the biodiversity-invasion relationships (Fig. 1.6), the effects of community adaptation were much more consistent across ecological scenarios than for biodiversity-productivity relationships. Resistance to invasion increased, and tolerance to invasion decreased, with diversity under all scenarios, which conforms well to general expectations (Levine, 2000; Hector *et al.*, 2001; Davis, 2009). The impact of community adaptation was moderate for resistance to invasion (probability of establishment) but spectacular for tolerance to invasion (number of secondary extinctions) (Fig. 1.6e-h), highlighting that different invasion properties can behave quite differently. Indeed, resistance to invasion was only slightly impacted by community adaptation, the latter generally increasing invasion resistance, but with almost no interaction with diversity. In contrast, biodiversity-tolerance relationships markedly differed with community adaptation (Fig. 1.6e-h): while tolerance to invasion gradually decreased with species diversity in random communities, it remained virtually constant with community adaptation.

This can be understood in terms of changes in species trait distributions. In co-adapted communities, species traits were more concentrated around the optimal trait (Fig. 1.3 and Fig. 1.4e-h orange curves) and more evenly spaced (see S.I. Section A.6 Fig. A.2), so that successful invaders tended to occupy peripheral niches at either tail of the trait distribution, which did not cause resident extinctions. However, this is not the case in random communities in which an invader might find vacant niche space anywhere along the trait spectrum, possibly very close to a resident species,

thus potentially excluding the latter and triggering further secondary extinctions.

Beyond BEF relationships, these results have interesting implications for community assembly dynamics. With the possibility of species (co)evolution, invasion resistance and tolerance would both increase in between species colonization events. In other words, successful invasions would be rarer, but also more constructive in terms of community assembly: invaders would more often add to the community without driving many resident species extinct. With trait co-evolution, assembly trajectories should therefore be less eventful (fewer invasions and fewer extinctions), and more steadily progressing or "efficient", compared to pure invasion-assembly. Although this prediction deserves further exploration, it nicely complements some earlier studies of community assembly (Rummel & Roughgarden, 1985).

Unfortunately, empirical evidence is even scarcer regarding the role of community adaptation for invasion properties than for productivity. Most studies focus on documenting the impact of invasions on the evolutionary dynamics of communities, not the other way round; yet, evolutionarily immature (e.g. insular) communities or recently assembled ecosystems such as anthropized habitats are known to be more sensitive to invasions than old species assemblages. Although this is suggestive of a protective role of co-evolution, the diversity-invasion relationship is difficult to relate to evolutionary history, as most long-co-evolved communities are highly diverse while recently assembled ones are usually species-poor (David *et al.*, 2017).

Our approach was a first attempt at combining eco-evolutionary theory and BEF-relationships. It could be extended and improved in several ways. One important simplification was the assumption of one single trait that structures communities and is subject to evolution. It would be interesting to describe species interactions as governed by multiple traits, which is probably more realistic and might result in more complex eco-evolutionary dynamics (Vasconcelos & Rueffler, 2020). Similarly, we assumed no upper limit on the amount of phenotypic change a species can undergo. Trait changes between random and co-adapted communities may sometimes be quite large, especially at low diversity levels (Fig. 1.3). However, since genetic variation is usually not infinite, species responses to selection can be constrained. Such limits on evolution would probably weaken some of the reported effects, even though preliminary analyses suggest that results are quite robust to this (see S.I. Fig. A3 Section A.7).

Overall our work highlights some potentially important consequences of evolutionary dynamics for biodiversity-functioning relationships. Through its action on species trait values, community adaptation can profoundly change the expected relationship between diversity and various ecosystem functioning properties, even in qualitative terms. This occurs because of the differential magnitude and direction of species trait evolution in poor versus rich communities, so that the ecological impact of species number interacts with the evolutionary history of communities. Therefore, BEF relationships derived from short-term experiments or observed following recent habitat perturbations might not be safely extrapolated into the future, once eco-evolutionary feed-backs have played out. This may have consequences for our understanding and prediction of the way ecosystems respond to species loss and environmental perturbations, and for ecosystem management and restoration. Eco-evolutionary theory definitely calls for more long-term and evolution-oriented studies of BEF relationships.

Bibliography

- Abramsky, Z. & Rosenzweig, M.L. (1984) Tilman's predicted productivity–diversity relationship shown by desert rodents. *Nature*, **309**, 150–151.
- Arnoldi, J.F., Loreau, M. & Haegeman, B. (2016) Resilience, reactivity and variability: A mathematical comparison of ecological stability measures. *Journal of Theoretical Biology*, **389**, 47–59.
- Barabás, G. & D'Andrea, R. (2016) The effect of intraspecific variation and heritability on community pattern and robustness. *Ecology Letters*, **19**, 977–986.
- Bell, T., Newman, J.A., Silverman, B.W., Turner, S.L. & Lilley, A.K. (2005) The contribution of species richness and composition to bacterial services. *Nature*, **436**, 1157–1160.
- Calcagno, V., Mouquet, N., Jarne, P. & David, P. (2006) Coexistence in a meta-community: the competition–colonization trade-off is not dead. *Ecology Letters*, **9**, 897–907.
- Calcagno, V., Jarne, P., Loreau, M., Mouquet, N. & David, P. (2017) Diversity spurs diversification in ecological communities. *Nature Communications*, **8**, 15810.
- Chave, J., Muller-Landau, H.C. & Levin, S.A. (2002) Comparing classical community models: theoretical consequences for patterns of diversity. *The American Naturalist*, **159**, 1–23.
- Christiansen, F.B. (1991) On Conditions for Evolutionary Stability for a Continuously Varying Character. *The American Naturalist*, **138**, 37–50.
- David, P., Thébault, E., Anneville, O., Duyck, P.F., Chapuis, E. & Loeuille, N. (2017) Chapter one - Impacts of invasive species on food webs: a review of empirical data. *Networks of Invasion: A Synthesis of Concepts* (eds. D.A. Bohan, A.J. Dumbrell & F. Massol), vol. 56 of *Advances in Ecological Research*, pp. 1 – 60. Academic Press.
- Davis, M.B., Shaw, R.G. & Etterson, J.R. (2005) Evolutionary responses to changing climate. *Ecology*, **86**, 1704–1714.
- Davis, M.A. (2009) *Invasion Biology*. OUP Oxford.
- Doebeli, M. & Dieckmann, U. (2000) Evolutionary Branching and Sympatric Speciation Caused by Different Types of Ecological Interactions. *The American Naturalist*, **156**, S77–S101.

- Elton, C. (1958) *Ecology of invasions by plant and animals*. Chapman and Hall, London.
- Faillace, C.A. & Morin, P.J. (2016) Evolution alters the consequences of invasions in experimental communities. *Nature Ecology & Evolution*, **1**, 0013.
- Fiegna, F., Moreno-Letelier, A., Bell, T. & Barraclough, T.G. (2014) Evolution of species interactions determines microbial community productivity in new environments. *The ISME Journal*, **9**, 1235–1245.
- Fiegna, F., Scheuerl, T., Moreno-Letelier, A., Bell, T. & Barraclough, T.G. (2015) Saturating effects of species diversity on life-history evolution in bacteria. *Proceedings of the Royal Society B-Biological Sciences*, **282**, 20151794.
- Gagic, V., Bartomeus, I., Jonsson, T., Taylor, A., Winqvist, C., Fischer, C. & et al. (2015) Functional identity and diversity of animals predict ecosystem functioning better than species-based indices. *Proceedings of the Royal Society B: Biological Sciences*, **282**, 20142620.
- Gamfeldt, L., Lefcheck, J.S., Byrnes, J.E.K., Cardinale, B.J., Duffy, J.E. & Griffin, J.N. (2015) Marine biodiversity and ecosystem functioning: what's known and what's next? *Oikos*, **124**, 252–265.
- Gross, K., Cardinale, B.J., Fox, J.W., Gonzalez, A., Loreau, M., Wayne Polley, H. & et al. (2014) Species richness and the temporal stability of biomass production: a new analysis of recent biodiversity experiments. *The American Naturalist*, **183**, 1–12.
- Hart, S.P., Turcotte, M.M. & Levine, J.M. (2019) Effects of rapid evolution on species coexistence. *Proceedings of the National Academy of Sciences USA*, **116**, 2112–2117.
- Hector, A., Dobson, K., Minns, A., Bazeley-White, E. & Hartley Lawton, J. (2001) Community diversity and invasion resistance: an experimental test in a grassland ecosystem and a review of comparable studies. *Ecological Research*, **16**, 819–831.
- Hendry, A.P. (2016) *Eco-evolutionary Dynamics*. Princeton University Press.
- Hooper, D.U., Chapin III, F.S., Ewel, J.J., Hector, A., Inchausti, P., Lavorel, S. & et al. (2005) Effects of biodiversity on ecosystem functioning: a consensus of current knowledge. *Ecological Monographs*, **75**, 3–35.
- Hooper, D.U., Adair, E.C., Cardinale, B.J., Byrnes, J.E.K., Hungate, B.A., Matulich, K.L. & et al. (2012) A global synthesis reveals biodiversity loss as a major driver of ecosystem change. *Nature*, **486**, 105–108.
- Isbell, F., Calcagno, V., Hector, A., Connolly, J., Harpole, W.S., Reich, P.B. & et al. (2011) High plant diversity is needed to maintain ecosystem services. *Nature*, **477**, 199–202.
- Ives, A.R., Gross, K. & Klug, J.L. (1999) Stability and variability in competitive communities. *Science*, **286**, 542–544.

- Ives, A.R. & Carpenter, S.R. (2007) Stability and diversity of ecosystems. *Science*, **317**, 58–62.
- Jaynes, E.T. (1957) Information theory and statistical mechanics. *Phys. Rev.*, **106**, 620–630.
- Jousset, A., Eisenhauer, N., Merker, M., Mouquet, N. & Scheu, S. (2016) High functional diversity stimulates diversification in experimental microbial communities. *Science Advances*, **2**, e1600124.
- Kleynhans, E.J., Otto, S.P., Reich, P.B. & Vellend, M. (2016) Adaptation to elevated CO₂ in different biodiversity contexts. *Nature Communications*, **7**, 12358.
- Kylafis, G. & Loreau, M. (2011) Niche construction in the light of niche theory. *Ecology Letters*, **14**, 82–90.
- Levine, J.M. (2000) Species diversity and biological invasions: relating local process to community pattern. *Science*, **288**, 852–854.
- Loeuille, N. (2010) Influence of evolution on the stability of ecological communities. *Ecology Letters*, **13**, 1536–1545.
- Loeuille, N. & Loreau, M. (2005) Evolutionary emergence of size-structured food webs. *Proceedings of the National Academy of Sciences USA*, **102**, 5761–5766.
- Loreau, M. (1998) Biodiversity and ecosystem functioning: a mechanistic model. *Proceedings of the National Academy of Sciences USA*, **95**, 5632–5636.
- Loreau, M. (2010) *From populations to ecosystems*. Princeton University Press. ISBN 978-0-691-12269-4.
- Loreau, M. & Hector, A. (2001) Partitioning selection and complementarity in biodiversity experiments. *Nature*, **412**, 72–76.
- Loreau, M. & Mazancourt, C.d. (2013) Biodiversity and ecosystem stability: a synthesis of underlying mechanisms. *Ecology Letters*, **16**, 106–115.
- May, R.M. (1973) Stability in randomly fluctuating versus deterministic environments. *The American Naturalist*, **107**, 621–650.
- Mazancourt, C.D., Johnson, E. & Barraclough, T.G. (2008) Biodiversity inhibits species' evolutionary responses to changing environments. *Ecology Letters*, **11**, 380–388.
- McCann, K.S. (2000) The diversity-stability debate. *Nature*, **405**, 228–233.
- Meilhac, J., Deschamps, L., Maire, V., Flajoulot, S. & Litrico, I. (2020) Both selection and plasticity drive niche differentiation in experimental grasslands. *Nature Plants*, **6**, 28–33.
- Meyer, S.T., Anne, E., Nico, E., Lionel, H., Helmut, H., Alexandru, M. & et al. (2016) Effects of biodiversity strengthen over time as ecosystem functioning declines at low and increases at high biodiversity. *Ecosphere*, **7**, e01619.

- van Moorsel, S.J., Hahl, T., Wagg, C., De Deyn, G.B., Flynn, D.F.B., Zuppinger-Dingley, D. & Schmid, B. (2018) Community evolution increases plant productivity at low diversity. *Ecology Letters*, **21**, 128–137.
- Mora, B.B., Gravel, D., Gilarranz, L.J., Poisot, T. & Stouffer, D.B. (2018) Identifying a common backbone of interactions underlying food webs from different ecosystems. *Nature Communications*, **9**, 2603.
- Mouquet, N., Moore, J.L. & Loreau, M. (2002) Plant species richness and community productivity: why the mechanism that promotes coexistence matters. *Ecology Letters*, **5**, 56–65.
- Naeem, S., Thompson, L.J., Lawler, S.P., Lawton, J.H. & Woodfin, R.M. (1994) Declining biodiversity can alter the performance of ecosystems. *Nature*, **368**, 734–737.
- Pennekamp, F., Pontarp, M., Tabi, A., Altermatt, F., Alther, R., Choffat, Y. & et al. (2018) Biodiversity increases and decreases ecosystem stability. *Nature*, **563**, 109–112.
- Pimm, S.L., Jenkins, C.N., Abell, R., Brooks, T.M., Gittleman, J.L., Joppa, L.N. & et al. (2014) The biodiversity of species and their rates of extinction, distribution, and protection. *Science*, **344**, 1246752.
- Reich, P.B., Tilman, D., Isbell, F., Mueller, K., Hobbie, S.E., Flynn, D.F.B. & et al. (2012) Impacts of biodiversity loss escalate through time as redundancy fades. *Science*, **336**, 589–592.
- Renard, D. & Tilman, D. (2019) National food production stabilized by crop diversity. *Nature*, **571**, 257–260.
- Rummel, J.D. & Roughgarden, J. (1985) A theory of faunal buildup for competition communities. *Evolution*, **39**, 1009–1033.
- Scheuerl, T., Hopkins, M., Nowell, R.W., Rivett, D.W., Barraclough, T.G. & Bell, T. (2020) Bacterial adaptation is constrained in complex communities. *Nature Communications*, **11**, 754.
- terHorst, C.P., Zee, P.C., Heath, K.D., Miller, T.E., Pastore, A.I., Patel, S. & et al. (2018) Evolution in a community context: trait responses to multiple species interactions. *The American Naturalist*, **191**, 368–380.
- Thompson, J.N. (1998) Rapid evolution as an ecological process. *Trends in Ecology & Evolution*, **13**, 329–332.
- Tilman, D. (1994) Competition and Biodiversity in Spatially Structured Habitats. *Ecology*, **75**, 2–16.
- Tilman, D. (1999) The ecological consequences of changes in biodiversity: a search for general principles. *Ecology*, **80**, 1455–1474.
- Tilman, D., Wedin, D. & Knops, J. (1996) Productivity and sustainability influenced by biodiversity in grassland ecosystems. *Nature*, **379**, 718–720.

- Vasconcelos, P. & Rueffler, C. (2020) How Does Joint Evolution of Consumer Traits Affect Resource Specialization? *The American Naturalist*, **195**, 331–348.
- Zupinger-Dingley, D., Schmid, B., Petermann, J.S., Yadav, V., De Deyn, G.B. & Flynn, D.F.B. (2014) Selection for niche differentiation in plant communities increases biodiversity effects. *Nature*, **515**, 108–111.

Chapter 2

Evolution of stress tolerance under a tolerance-fecundity trade-off

Article in preparation.

Flora AUBREE¹, Ludovic MAILLERET^{1,2}, Vincent CALCAGNO¹.

1. Université Côte d'Azur, INRAE, CNRS, ISA, 06900 Sophia Antipolis, France.
2. Université Côte d'Azur, INRIA, INRAE, CNRS, Sorbonne Université, BIOCORE, Sophia Antipolis, France

Acknowledgments FA was funded by a PhD fellowship from Université Côte d'Azur (IDEX “Investissements d’Avenir UCAJEDI”, project reference n°ANR-15-IDEX-01). The authors thank the GDR TheoMoDive for interesting discussions.

*Everyone is right from their own point of view,
but it is not impossible that everyone is wrong.*

GANDHI

Abstract

The tolerance-fecundity trade-off (TFT) model describes a trade-off between the number of seeds produced (plant fecundity) and their tolerance to stress. This model has received significant theoretical interest in the past 10 years, as a general alternative to competition-colonization trade-offs. However, it has only been studied from an ecological perspective, and no attention has been yet given to the evolutionary dynamics of stress tolerance under a TFT. Here we introduce a generalization of the TFT model, that incorporates explicit stress-tolerance traits, an explicit relation between fecundity and stress tolerance, and a dose-response curve commonly used in empirical studies. On top of facilitating parametrization, this allows the use of adaptive dynamics methods. We study the evolution of stress tolerance as a function of trade-off intensity parameters and of the distribution of stress level across patches. We investigate the value of evolutionary equilibria and their evolutionary stability (with in particular the possibility of diversification or branching). Stress tolerance is found to evolve to a single evolutionary attractor, whose value is mainly determined by the steepness and height of the fecundity function. Evolutionary stability, in contrast, is mostly determined by the dose-response function. The evolutionary attractor turns from ESS to branching point when the later becomes steep enough. Branching is also more frequent when the advantage of very tolerant species over less tolerant but more fecund ones is higher, which occurs when the dose-response function is asymmetrical. The probability of coexistence is found to be maximized for some intermediate trade-off intensity, characterized by an intermediate-to-high dose-response steepness and a shallow fecundity function. Greater spatial heterogeneity in stress levels promotes branching, whereas intermediate heterogeneity maximizes coexistence. Further diversification can occur, but requires more stringent conditions than for one species, and can be asymmetric or symmetric.

Keywords: Adaptive dynamics, ESS, Branching point, Coexistence, Stress level distributions, Dose-response curves

2.1 Introduction

The stable coexistence of a diversity of species is not always straightforward, because of possible competitive exclusion (Levin, 1970). In this context, several coexistence mechanisms have been proposed (Chesson, 2000), and many involve trade-offs. The competition-colonization trade-off (CCT; Calcagno *et al.*, 2006) is one of them, and has often been proposed as an explanation for plant species coexistence in particular (Tilman, 1994) and also used to explore species coexistence in general (Thompson *et al.*, 2020). However, the CCT involves a competitive hierarchy that often seems too strong in the light of empirical observations of plant communities (Coomes & Grubb, 2003; Muller-Landau, 2010). This has thus motivated the search of other possible general trade-off mechanisms in plant communities. The tolerance-fecundity trade-off (TFT) model has first been proposed by Muller-Landau (2010) as an alternative to the CCT. Muller-Landau (2010) replaced competitive dominance (ability of a species to displace another locally) with the maximum stress level, at the site of germination, that a species can survive or resist to (stress tolerance). The trade-off is described by the fact that the more tolerant species are also the less fecund, so that the number of seeds they actually send in the environment is lower. The coexistence of species that possess different stress tolerance levels is allowed in this model by the heterogeneity of stress levels in the environment. If there is no heterogeneity (i.e. the same stress conditions everywhere), the one species with the lowest tolerance acceptable would exclude all other due to its higher fecundity (D'Andrea & O'Dwyer, 2021). Muller-Landau (2010) proposed that tolerance might be driven by seed size (the larger a seed the more stress tolerant), but this can be generalized to other tolerance-mediating traits that can yield a cost in terms of fecundity (such as various quantitative trait loci for seed tolerance during germination, see for instance Sayama *et al.*, 2009; Thabet *et al.*, 2018).

The appropriateness of this coexistence mechanism has been experimentally assessed several times. Ben-Hur *et al.* (2012) designed an experiment to specifically test the impact of a negative correlation between seed size and seed number on species richness. They found that the results were coherent with theory (i.e. that coexistence is favored by this negative correlation) and that it could not be attributed to a CCT, but possibly to a TFT. Their result is, according to them, the first experimental evidence for this mechanism to promote coexistence. Villellas & García (2013) experimentally tested an intraspecific version of this model, and some of their results suggest the existence of a TFT interaction. More recently, Maron *et al.* (2021) experimentally showed that large seeds are more tolerant than small ones. Exploring the interaction between tolerance and fecundity, they evidenced that a tolerance-fecundity trade-off may contribute to the observed coexistence. Even if not considering TFTs as their main topic, several other studies have also invoked this model as a possible mechanism to explain their observations (de la Riva *et al.*, 2016; Lebrija-Trejos *et al.*, 2016; Alstad *et al.*, 2018).

Theoretically, Muller-Landau (2010) found that the TFT model allows for the coexistence of a large number of species, even in the presence of seed limitation. Subsequently, theoretical studies proposed some modification of Muller-Landau's model, in order to improve its realism and test the robustness of the conclusions. In the initial model (Muller-Landau, 2010), the probability that a seed survives is either 0 or 1 depending on species tolerance, resulting in an infinitely sharp probability func-

tion. However, in addition to being very unlikely in nature (Muller-Landau, 2010; Barabás *et al.*, 2013; D’Andrea *et al.*, 2013), such infinitely sharp thresholds are shown to have a strong impact on species coexistence predictions (Barabás *et al.*, 2013). D’Andrea *et al.* (2013) thus proposed a modification of the TFT model, enabling the probability to survive a given stress level to be smooth. While the discontinuous transition from Muller-Landau’s model allowed for a robust continuous coexistence (possibility of an infinite number of species over a continuum of traits), they found that removing this discontinuity suppressed the continuous coexistence itself. Species coexistence was then led by the classical limiting similarity conditions (proposed by MacArthur & Levins, 1967, and largely used as a thinking tool to understand coexistence since then). Haegeman *et al.* (2014) gave a generalization of the TFT model of Muller-Landau (2010), allowing low site recruitment (namely the existence of empty sites). They provided a graphical tool to assess the necessity for coexistence of a trade-off between the two life-history parameters, and proposed a derivation of the model in both discrete and continuous time. Later on, with the same idea of increasing this model realism, D’Andrea & O’Dwyer (2021) introduced space explicitly in the model simulations. They questioned the impact of spatial homogeneity and seed limitation on coexistence. They showed that coexistence depends both on dispersal limitation and environmental variations, evidencing that coexistence in a patchy landscape is higher under short dispersal scales relative to the scale of environmental variation.

The TFT model is an interesting mechanism that has been mostly – if not only – used to explain ecological patterns of coexistence, but there has been no consideration of the evolutionary behavior of this model. It is clear that evolution has a role in shaping ecological communities, determining the type and number of species that coexist (Lankau, 2011; Hart *et al.*, 2019), and thus a role in determining ecological properties of ecosystems (Loeuille, 2010; Gagic *et al.*, 2015; van Moorsel *et al.*, 2018; Aubree *et al.*, 2020). Moreover, evolution appears to be relevant even on ecological timescales (Carroll *et al.*, 2007; Ellner *et al.*, 2011; Hart *et al.*, 2019), making this process important to consider from an ecological perspective, and almost inseparable from ecological studies. Among others, trade-offs in general are of particular interest in understanding evolutionary outcomes, like evolutionary rescue (Liukkonen *et al.*, 2021), ecological limiting similarity in co-adapted communities (Bonsall *et al.*, 2004), emergence and maintenance of specialist-generalist coexistence (Egas *et al.*, 2004; Ravigné *et al.*, 2009), or also patterns of diversity in a meta-community (Laroche *et al.*, 2016). In the CCT model in particular, trait evolution has been theoretically considered to question the evolution of viruses virulence (Ojosnegros *et al.*, 2010) or diversification (Calcagno *et al.*, 2017). It would thus seem relevant to analyze the evolutionary behavior of the TFT model, and the present study is a first step in that direction.

This paper aims at studying the evolutionary behavior of an ecological model that builds a community starting from one species, using the framework of adaptive dynamics (Metz *et al.*, 1995; Geritz *et al.*, 1997; Dieckmann & Doebeli, 1999; Geritz *et al.*, 1999). To this end, we need to extend the model in a way that allows the use of adaptive dynamics. In particular, we must explicitly describe the evolving phenotypes (species traits) and express fecundity and stress tolerance as smooth functions of the traits. Previous studies on the TFT model have only considered a negative correlation between stress tolerance and fecundity, without specifying a

mathematical expression linking the two (Muller-Landau, 2010; D’Andrea *et al.*, 2013; Haegeman *et al.*, 2014). This prevents modelling the continuous evolutionary change of stress tolerance as a quantitative trait. Our model formulation makes this possible, enabling us to determine the evolutionary equilibrium, the type of evolutionary point (ESS, branching point) and the coexistence zones. Furthermore, it is more explicit in how it relates to measurable quantities such as fecundity costs and dose-response curves.

Using this model, we explore then how the fecundity and the survival probability (the two components that shape the trade-off) influence the evolution of stress tolerance. The survival probability as a function of species stress tolerance is described using a dose-response curve that is commonly used in experimental studies. We use a flexible function that allows to take response asymmetry (about the stress level in the environment) into account (Liao & Liu, 2009). Such kind of asymmetry is poorly considered in the literature, despite its potentially high relevance (Van der Graaf & Schoemaker, 1999). Furthermore, a special attention is given to the seed germination conditions, that are described by a distribution of the stress levels present on each micro-site (i.e. the different micro-site do not carry the same level of stress, so that the environment is spatially heterogeneous regarding the stress conditions). Many sites can present some heterogeneity in various properties and composition such as in soil moisture (Moran *et al.*, 2004; Wilson *et al.*, 2004; Liang & Wei, 2021), nitrogen (Austin *et al.*, 2004; Wang *et al.*, 2021), carbon (Wang *et al.*, 2019; Cao *et al.*, 2020) and water availability (Austin *et al.*, 2004) or also in soil organisms, and in many kind of pollutant as various types of metals (Ginocchio *et al.*, 2004). Depending on their level, these various components may present a stress or a toxicity that impedes germination or development, and the heterogeneities are found to impact for instance seed germination, fitness and species richness (Jordan *et al.*, 2020; Kaur *et al.*, 2021). There are plenty of ways to distribute those stress levels across patches. The type (e.g. Gaussian or not, heavy tail or not, etc.), the variance and the mean of stress distribution themselves may possibly have an impact on the results. This has not yet been studied under the TFT model, even within an ecological perspective. In the present study, we question the impact that the environment – represented by the stress distribution – may have on both coexistence and evolutionary behavior. Quite obviously, we expect the variance to impact the coexistence possibilities, because the limit of the null variance is the limit of an homogeneous environment in which no coexistence is possible.

To sum up, we will explore the impact that the trade-off intensity, the environmental conditions (led by the stress distribution function), and the dose-response curve asymmetry may have on the evolutionary behavior of the TFT model. To do so, because of the large amount of parameters to consider, we will first perform a sensitivity analysis to get a first general overview of the evolutionary behavior of this model, before focusing on particular points to understand it in greater detail. We end by exploring the possibility of branching in a two-species community.

The slope of both the fecundity function and the survival probability function with respect to species tolerance (the two parameters that shape the trade-off) are found to play an essential role in determining the evolutionary behavior of this model, but does not have the same qualitative and quantitative effects. The evolution of stress tolerance (evolutionary equilibrium point) is found to be mainly driven by the fecundity function. Branching points are found to arise for steep sur-

vival probability functions, but mostly occur for low-to-intermediate values of the fecundity function slope. We also show that the coexistence surface is maximized by a given trade-off intensity, characterized by an intermediate-to-high survival probability slope and a smooth fecundity function. Concerning spatial conditions, the variance of the stress distribution contributed more than the mean, favoring branching when broader, and the averaged coexistence surface when intermediate. Finally, we show that a bimorphic evolutionary equilibrium is impossible when the monomorphic one was stable (ESS). Bimorphic evolutionary equilibrium can present evolutionary instabilities (branching points), but this occurs under even more restricted conditions than for monomorphic equilibrium.

2.2 Model and Method

2.2.1 Model definition

Our model is based on the model described by Muller-Landau (2010), which was also studied by D’Andrea *et al.* (2013); Haegeman *et al.* (2014); D’Andrea & O’Dwyer (2021). Here, we modify it in order to make it suitable for the study of adaptive dynamics. The model is of patch-occupancy type, in which patches are local microsites in which one plant at most can germinate and establish as an adult. Patches harbor different stress levels. Stress level is spatially distributed according to a stationary continuous probability distribution $p(y)$ of possible stress levels y , so that $p(y)$ is the probability density of patches with stress level y . Adults cannot be displaced by incoming seeds until they die. This occurs at rate m : when an adult dies its patch becomes vacant and incoming seeds immediately engage in a competitive lottery for settlement in that patch. For simplicity, a patch does not retain a fixed stress level over consecutive adult replacements, but instead has it drawn from the stationary probability distribution $p(y)$. In other words, there are continuous (and rapid relative to m) spatio-temporal fluctuations of the stress level across patches. It is only at the time of germination that this stress level matters (since adults are otherwise immune to the stress), so that over consecutive recolonization of a given patch, the stress levels are effectively sampled from the stationary distribution. Making patches have a fixed stress level through time would increase the number of equations needed to describe the dynamics. Following previous models, the mortality rate m is supposed to be the same for all patches, i.e. once an adult has installed into a patch, its death does not depend on the patch stress-level it has experienced or on the species tolerance level. This model is here described in continuous time. As we consider an implicit spatial distribution (as often the case; Muller-Landau, 2010; D’Andrea *et al.*, 2013; Haegeman *et al.*, 2014), it would remain the same to consider an discrete time version. This would not be the case with an explicit spatial distribution.

We assume that a species is characterized by some tolerance level x , which is the evolving phenotype of interest. Contrary to previous tolerance-fecundity trade-off models, we give an explicit form to the trade-off, describing the fecundity as a decreasing function $c(x)$ of stress tolerance x (species are thus characterized by only one trait). This modification allows the use of adaptive dynamics methods to track continuous changes in species traits. According to their fecundity level, each adult produces seeds that will compete for the free patches. Seed production is supposed

to be proportional to the occupancy fraction n_i (the proportion of sites occupied by species i whose stress tolerance is x_i) and to species i fecundity. Conversely, a species with trait x landing in a patch with stress level y has a probability to survive the stress given by some increasing function $b(x - y)$. Finally, among all the surviving seeds, a competitive lottery is then engaged to determine which seed will germinate (see also Muller-Landau, 2010; D’Andrea *et al.*, 2013; Haegeman *et al.*, 2014; D’Andrea & O’Dwyer, 2021). In a patch with stress level y , the effective number of seeds engaged in the competitive lottery from species i will be:

$$f(x_i - y) = c(x_i)b(x_i - y)$$

The proportion n_i of species i in the environment thus varies with time as:

$$\frac{1}{n_i} \frac{dn_i}{dt} = m \left(\int_{-\infty}^{+\infty} p(y) \frac{f(x_i, y)}{\sum_j f(x_j, y)n_j + \epsilon} dy - 1 \right) \quad (2.1)$$

The ratio $\frac{f(x_i, y)n_i}{\sum_j f(x_j, y)n_j + \epsilon}$ represents the competitive lottery in between surviving seeds in a patch with stress level y (Muller-Landau, 2010). The ϵ term represents a background level of competition that all seeds are experiencing in all patches. This may represent, for instance, other species not considered in the guild of interest. This background level is considered small, and thus it will typically not affect the competitive lottery in an important manner. But when a species is the only one able to exploit a patch, and is very poor at using this patch, the background level of competition prevents the species from acquiring the patch with probability one, regardless of the number of seeds sent. This unpleasant property was absent in the Muller-Landau’s model, because of her step survival probability function, set to 0 below a given tolerance level. We integrate this ratio over all stress levels y whose distribution is $p(y)$. The mortality rate m scales the unit time and the turnover speed of species occupancy.

2.2.2 Analysis

2.2.2.1 Invasion fitness

The fitness $F(x_m)$ of a mutant trying to invade a community writes:

$$F(x_m) = \lim_{n_m \rightarrow 0} \left(\frac{1}{n_m} \frac{dn_m}{dt} \right) = \lim_{n_m \rightarrow 0} m \left(\int_{-\infty}^{+\infty} p(y) \frac{f(x_m, y)}{\sum_j (f(x_j, y)n_j) + \epsilon} dy - 1 \right) \quad (2.2)$$

where all species are at their respective equilibrium abundance (Metz *et al.*, 1995; Geritz *et al.*, 1997).

In the following, we will only consider the case of one resident species invaded by a rare mutant, so that the sum over j in the integral only contains two terms. The probability to survive a given stress may cancel for high stress levels. Let’s imagine that $b(x_i - y)$ (and therefore $f(x_i, y)$) cancels for $y > y_1$ for the resident species, and that $b(x_m - y)$ (and therefore $f(x_m, y)$) cancels for $y > y_2$. If $y_2 > y_1$ then:

$$\begin{aligned}
 F(x_m) &= \lim_{n_m \rightarrow 0} m \left(\int_{-\infty}^{y_1} p(y) \frac{f(x_m, y)}{f(x_i, y)n_i + f(x_m, y)n_m + \epsilon} dy \right. \\
 &\quad \left. + \int_{y_1}^{y_2} p(y) \frac{f(x_m, y)}{f(x_m, y)n_m + \epsilon} dy + 0 - 1 \right) \\
 &= m \int_{-\infty}^{y_1} p(y) \frac{f(x_m, y)}{f(x_i, y)n_i + \epsilon} dy + m \int_{y_1}^{y_2} p(y) \frac{f(x_m, y)}{\epsilon} dy - m
 \end{aligned}$$

If $y_2 \rightarrow y_1$ (i.e. the mutant is close to the resident, as the case in the following) it simplifies as

$$F(x_m) = m \int_{-\infty}^{y_1} p(y) \frac{f(x_m, y)}{f(x_i, y)n_i + \epsilon} dy - m$$

If $y_1 > y_2$ it is directly:

$$\begin{aligned}
 F(x_m) &= \lim_{n_m \rightarrow 0} m \left(\int_{-\infty}^{y_2} p(y) \frac{f(x_m, y)}{f(x_i, y)n_i + f(x_m, y)n_m + \epsilon} dy \right. \\
 &\quad \left. + \int_{y_2}^{y_1} p(y) \frac{0}{f(x_i, y)n_i + \epsilon} dy + 0 - 1 \right) \\
 &= m \int_{-\infty}^{y_2} p(y) \frac{f(x_m, y)}{f(x_i, y)n_i + \epsilon} dy - m
 \end{aligned}$$

In the end, we only have to calculate the integral from $-\infty$ to $y_m = \min(y_1, y_2)$. In case b cancels for some stress levels, this would allow to simplify the numerical integration of the model.

2.2.2.2 Viability condition

For the first species trying to invade an empty environment (with no species from the guild of interest), the fitness simply writes:

$$F(x_m) = \lim_{n_m \rightarrow 0} m \left(\int_{-\infty}^{y_m} p(y) \frac{f(x_m, y)}{f(x_m, y)n_m + \epsilon} dy - 1 \right)$$

with y_m the stress level from which the probability to survive cancels (it can be finite or infinite). Taking the limit we obtain:

$$F(x_m) = m \left(\frac{1}{\epsilon} \int_{-\infty}^{y_m} p(y) f(x_m, y) dy - 1 \right)$$

in which we recognize the average over all possible stress levels of the number of seeds (from species with trait x_m) engaged in the competitive lottery: $\langle f(x_m, y) \rangle = \int_{-\infty}^{y_m} p(y) f(x_m, y) dy$. The fitness $F(x_m)$ has to be positive for the x_m trait individual to invade. Then, the viability condition writes:

$$\langle f(x_m, y) \rangle > \epsilon \tag{2.3}$$

This condition allows us to determine the viable traits located in the interval $[x_{min}, x_{max}]$, and to carry out the analysis only within this range. In the following, we will consider that $c(x)$ tends to zero when $x \rightarrow +\infty$, that $b(x - y)$ tends to zero when

$x \rightarrow -\infty$, and that they are both bounded by a finite value. Thus, $f(x, y)$ tends to zero both when $x \rightarrow -\infty$ and when $x \rightarrow +\infty$, so that x_{min} and x_{max} will always take finite values.

2.2.2.3 Adaptive dynamics and types of evolutionary equilibria

The ecological abundance at equilibrium n_{eq} is simply obtained searching for the equilibrium point of equation (2.1). Here, we only have one species and thus only one equation to solve. Then, the evolutionary equilibrium is characterized by the trait value at equilibrium x^* , the abundance at equilibrium n_{eq} and the type of evolutionary point. The trait value at equilibrium is obtained using the selection gradient. x_m being a rare phenotype, the selection gradient writes (Geritz *et al.*, 1997):

$$\nabla(x_i) = \left. \frac{\partial F(x_m)}{\partial x_m} \right|_{x_m=x_i} = \left. \frac{\partial}{\partial x_m} \left(m \int_{-\infty}^{y_m} p(y) \frac{f(x_m, y)}{f(x_i, y)n_i + \epsilon} dy - m \right) \right|_{x_m=x_i}$$

Putting the derivative inside the integral we simply get:

$$\begin{aligned} \nabla(x_i) &= m \int_{-\infty}^{y_m} \left(p(y) \frac{\left. \frac{\partial f(x_m, y)}{\partial x_m} \right|_{x_m=x_i}}{f(x_i, y)n_i + \epsilon} \right) dy \\ &= m \int_{-\infty}^{y_m} \left(p(y) \frac{c(x_i)b'(x_i - y) + c'(x_i)b(x_i - y)}{b(x_i - y)c(x_i)n_i + \epsilon} \right) dy \end{aligned} \quad (2.4)$$

with b' and c' the first derivative of b and c with respect to x . When the selection gradient is positive (resp. negative), selection tends to increase (resp. decrease) the trait value. It cancels when the trait value reaches an equilibrium value x^* . For every evolutionary point we calculate, we verify that it is stable by convergence, what means that it may be reachable in practice. The condition for convergence stability is (Geritz *et al.*, 1997):

$$\left(\frac{\partial^2 F}{\partial x_m^2} - \frac{\partial^2 F}{\partial x_i^2} \right) \Big|_{x_m=x_i=x^*} < 0$$

The evolutionary stability is determined using the curvature of the fitness:

$$\nabla^2(x_i) = \left. \frac{\partial^2 F(x_m)}{\partial x_m^2} \right|_{x_m=x_i}$$

Similarly to the gradient, the curvature writes:

$$\nabla^2(x_i) = m \int_{-\infty}^{+\infty} \left(p(y) \frac{c(x_i)b''(x_i - y) + c''(x_i)b(x_i - y) + 2c'(x_i)b'(x_i - y)}{b(x_i - y)c(x_i)n_i + \epsilon} \right) dy \quad (2.5)$$

When $\nabla^2(x^*) > 0$ (resp. < 0), the evolutionary point is unstable (resp. stable). In the case of convergence stability (namely that the point is reachable, see above), the evolutionary point is called a branching point when unstable (fitness minimum). It

means that a resident can coexist with a similar mutant under disruptive selection. This cannot occur when the evolutionary point is stable (fitness maximum), in which case the evolutionary point is called an evolutionary singular strategy (ESS).

We also calculate the mutual invasibility, which informs whether a pair of neighboring phenotypes on either side of the evolutionary equilibrium can invade each other or not. A set of two species characterized by their trait x and y are said to be able to invade mutually if $F(x) > 0$ knowing that the resident is y and $F(y) > 0$ knowing that the resident is x . The condition for mutual invasibility is (Geritz *et al.*, 1997):

$$\left(\frac{\partial^2 F}{\partial x_m^2} + \frac{\partial^2 F}{\partial x_i^2} \right) \Big|_{x_m=x_i=x^*} > 0$$

We define $M_{inv} = \left(\frac{\partial^2 F}{\partial x_m^2} + \frac{\partial^2 F}{\partial x_i^2} \right) \Big|_{x_m=x_i=x^*}$. If the equilibrium is a branching point, M_{inv} is always positive. At an ESS, it can have any sign.

In order to get an idea of the average performance (in term of tolerance) a species has at the evolutionary equilibrium, we also compute the mean survival probability at x^* , over all patches, that we call the species performance:

$$b_{x^*} = \int_y p(y)b(x^*, y)dy \quad (2.6)$$

This informs on the ability of that species to tolerate stress in the environment, independently of its fecundity. This quantity is easy to evaluate experimentally from seed survival experiments.

2.2.2.4 Pairwise Invasibility Plots

The above evolutionary characteristics can also be visualized on a pairwise invasibility plot (PIP; Geritz *et al.*, 1997). To obtain the PIP we first determined the viability zone (x_{min} and x_{max}) by numerically solving relation (2.3). Then, for 100 resident traits contained in $[x_{min}; x_{max}]$, we numerically search the abundance equilibrium solving equation $\frac{dn_i}{dt} = 0$. This enables us to integrate the invader fitness for each of the 100x100 pair of traits (resident-invader) of a grid whose minimum is x_{min} and maximum x_{max} . The sign of the fitness were reported on the grid (in black when positive in all the PIP encountered in this manuscript).

From the PIP, we graphically derived a coexistence plot (sometimes called a mutual invasibility plot). This consists in mirroring the PIP over the main diagonal, and then, overlapping the region from the PIP and its mirrored version. The resulting positive zone corresponds to the coexistence region (in dark in all the next coexistence plot encountered). The latter informs on the pairs of species trait that can coexist together, and allows us to calculate the relative surface of coexistence S_{coex} (i.e. the proportion of pair of species that can coexist over all possible pairs of viable species).

We derived the PIP and different metrics using either Mathematica 11.3 or Java. The differential equation (2.1), which is the basis of all subsequent mathematical derivations, involves an integral that renders the calculation more difficult to handle. Mathematica allows very accurate integral computations (through the use of the *NIntegrate* function) but is rather slow. We use it to calculate the PIP, evolutionary equilibria and the other metrics used in the sensitivity analysis (see next paragraph).

For the rest of the analyses, we used custom Java and R codes. We coded in Java a trapezoidal integration algorithm to evaluate the integrals, that is much faster than Mathematica, at the cost of a loss in precision. To search for the evolutionary equilibrium, we then used function *runsteady* from R to compute the equilibria. The same methods in R and Java were used to compute the evolutionary equilibrium and other metrics with two species (last part of this study).

2.2.2.5 Sensitivity analysis

The evolutionary analysis of the model gives several output variables: the trait at equilibrium x^* , the boundaries of the viability zone (x_{min} and x_{max}), the equilibrium abundance n^* at x^* , the relative coexistence surface S_{coex} , the curvature ∇^2 at x^* , the mutual invasibility M_{inv} , and the performance b_{x^*} at x^* . There may have many input parameters that will depend on the definitions of functions c , b , p . In order to get a first general idea of the relative impact and importance of each of the input parameters on the output values, we first realize a sensitivity analysis on the vector containing all the output variables mentioned above. We then further analyse in more details some of the relationships and interactions highlighted by the sensitivity analysis.

The sensitivity analysis was done using R version 3.4.4, with the package *multisensi* and the eponymous function, that allows to calculate the Sobol indices (here referred to as the sensitivity indices or SI). The sensitivity indice gives the percentage of the variation in the output variable that is explained by a given input variable. This function also provides the total sensitivity indices (tSI) that account for the interactions between the given input variable and all the other up to 95% of the variance (Bidot *et al.*, 2018).

In addition to the analysis provided by the function *multisensi*, whenever the percentage of the variance explained by a given variable exceeds 5%, we reported the direction of the effect (positive or negative impact) with colors added on the sensitivity analysis plot.

2.2.3 Specific definition and functions for numerical analyses

2.2.3.1 Stress tolerance

We will characterize here the seed tolerance level as the level (or dose) of stress at which the species has 50% of chance to survive. This level of stress is typically described as a concentration. It is also called the LD50, for Lethal Dose at 50%, and is a metric of usually practical interest (Liao & Liu, 2009). Following the notation of dose-response studies, we will express the LD50, as well as the stress concentration, in log scales. We will use the following notation: y (refereed as stress level) refers to the logarithm $\log(Y)$ of a toxic substance(stress) concentration Y . Species tolerance trait x corresponds to the LD50 in log scales.

2.2.3.2 The distribution of stress levels in the environment

On a log scale, the stress level is distributed over $] -\infty, +\infty[$. We choose two contrasted forms: a Normal distribution, very often considered in the literature,

and a Gumbel distribution, which allows to consider heavy tails scenarios for some parameters (fig. 2.1a):

$$p_1(y) = \frac{1}{\sigma\sqrt{2\pi}} \exp\left(-\frac{(y-\mu)^2}{2\sigma^2}\right)$$

$$p_2(y) = \frac{e^z}{\beta} z \text{ with } z = \exp\left(-\frac{x-\alpha}{\beta}\right)$$

The Normal distribution is the equivalent of a Log-Normal distribution on the scale of concentration, while the Gumbel is equivalent either to an exponential (for $\beta = 1$) or a Weibull distribution (for $\beta \neq 1$). If the scale parameter β of the Gumbel distribution is greater than one, it refers to a heavy-tailed distribution on the scale of concentration (in the sense that it exhibits a large skewness relative to that of the exponential distribution ; Rolski *et al.*, 2009). Parameter β is related to the variance of the Gumbel distribution: $\beta = \sigma^2 \frac{6}{\pi^2}$. We will vary the variance σ of those distributions, and keep its mean $\mu = 1$. The averaged stress level felt by a species will be varied thanks to another parameter (see next paragraph).

2.2.3.3 Fecundity function

The fecundity function $c(x)$ is the trade-off function. It decreases with species tolerance x . We chose a function whose height and slope can be varied independently one from another (fig. 2.1b):

$$c(x) = c_0 e^{-c_a(e^x)^{c_b}}$$

with c_0 the maximal fecundity (obtained in case $x \rightarrow -\infty$, or in other words, for a null stress concentration $X = e^x = 0$). c_a and c_b are two parameters that scale the slope and height of this function. When parameter $c_b = 1$, it corresponds to an exponential function in concentration scales (instead of log concentration scales). It is steeper (resp. less steep) when $c_b > 1$ (resp. $c_b < 1$).

In addition, we define c_s as the slope of the fecundity function at the point $x_{1/2}$ such that $c(x_{1/2}) = \frac{1}{2}c_0$. In term of the function parameters it is equal to $c_s = -\frac{1}{2}c_b c_0 \log(2)$ (see the supplementary information (S.I.) section B.1). In the following, we will call c_s the slope of the fecundity function, without mentioning every time that it refers to the slope at the point $x_{1/2}$. We also define $c_\mu = \frac{c(\mu)}{c_0}$, which is the relative fecundity at μ (i.e. the relative height of the function). Varying c_μ (keeping c_s constant) is equivalent to vary μ itself. Indeed, varying c_μ , we translate the whole fecundity values toward larger or lower tolerance values. This is equivalent to shifting the whole stress distribution toward larger or lower stress values.

2.2.3.4 Survival function

The logistic function is often used in the literature to describe tolerance to stress. We used a generalized function described by (Liao & Liu, 2009) to fit dose-response curves in bioassay experiments. It has been proposed to address the lack of flexibility imposed by the symmetrical logistic curve usually used, that often appears to be limiting to catch the entirety of the process (Van der Graaf & Schoemaker, 1999). It allows to adjust the asymmetry level of the function, and thus to explore broader scenarios than the simple symmetric logistic curve (fig. 2.1c):

$$b(x, y) = 1 - \frac{1}{(1 + (2^{1/g} - 1) e^{(y-x) \cdot B})^g}$$

with x the species LD50, y the log concentration of the toxic substance, and B and g two parameters each controlling both the slope and the asymmetry of the function. When $g = 1$, we get the symmetric logistic curve.

We define β_s as the slope of $b(x, y)$ at the inflexion point $x = y$ in the symmetric case. It simply writes $\beta_s = \frac{B}{4}$ (see S.I. section B.1). We want to construct two asymmetric versions of the logistic function for each value of β_s : one for which the survival probability of low-tolerance species ($x < y$) is decreased compared to the symmetric case (asymmetry to the left case; see fig. 2.1c) and one for which the survival probability of high-tolerance species ($x > y$) is increased compared to the symmetric case (asymmetry to the right case; see fig. 2.1c). For this, we skew the symmetric function either to the left or to the right, through both B and g parameters (see S.I. section B.2 for more details). We reference the kind of asymmetry that results from this manipulation using a single qualitative parameter called γ_{as} . As we only explore one level of asymmetry to the left and one level of asymmetry to the right per β_s value, we say that γ_{as} is 1 in the asymmetry to the right case, -1 in the asymmetry to the left case, and 0 in the symmetric case. Of course, changing the asymmetry modifies the slope at the point $x = y$. To help qualitatively categorize the nine different functions formed (3 symmetric forms and two asymmetric deviations per symmetric form), we keep parameter β_s to characterize the asymmetric forms formed from a specific symmetric case (e.g. with a given β_s). We thus define β_s as being also the ‘‘slope’’ of those asymmetric cases as well, even if the real slope at the inflexion point in the asymmetric case would rigorously be slightly different.

2.2.3.5 Parameter values considered

Table 2.1 describes the parameters used and their range of variation when needed. For each of the two stress distributions, we explore three different variances σ^2 such that $\sigma_1 = \sigma_2/2$ and $\sigma_3 = 2\sigma_2$ (fig. 2.1a). The variance $\sigma_2^2 = \frac{\pi^2}{6}$ is chosen such that the Gumbel distribution refers to the exponential distribution in concentration scales.

The mean of the stress distribution is kept constant, as the average level of stress felt by species is governed by the fecundity function: we adjust the fecundity function parameters in order to get cases in which species are rather either very tolerant in average (corresponding to low stress environment, $c_\mu = 0.95$), mildly tolerant in average ($c_\mu = 0.5$), or very few tolerant to stress (corresponding to high stress environment, $c_\mu = 0.1$). We also vary the slope c_s of the fecundity function (see fig. 2.1c) that we chose to be either -0.1 , -0.3 or -0.75 . This slope will be later varied continuously on a range that incorporates those values (see table 2.1). Parameter c_0 is chosen relatively to ϵ , as they are exclusively linked through the ratio $\frac{c_0}{c_0 + \epsilon}$. This ratio corresponds to the probability that a species get installed in a patch where the stress level is $-\infty$ in log scales. We fixate $\epsilon = 0.001$, and we chose $c_0 = 1$ and 0.3 .

The survival probability function parameters are chosen relatively to environment. For the symmetric logistic case (when $g = 1$), we choose the slopes β_s such that the survival probability increases by a given percentage ξ ($1e^{-5}$, 0.05 or 0.3) of

Parameter	Description	Values
x	species tolerance trait (the logarithm of the LD50)	within the viability zone
x^*	stress tolerance evolutionary equilibrium value	
y	the logarithm of the stress concentration Y	
$c(x)$	the fecundity function	
c_s	the fecundity function slope (one of the two parameter shaping the trade-off intensity)	$[-0.75, -0.01]$
c_0	the fecundity function height	$\{0.3, 1\}$
c_μ	fecundity for a theoretical species whose trait would be $x = \mu$. It represents the average stress level in the environment.	$\{0.1, 0.5, 0.95\}$
$b(x - y)$	the dose-response curve (probability for a species with trait x to survive a stress y)	
β_s	the dose-response curve slope (one of the two parameter shaping the trade-off intensity)	$[0.01, 2.7]$
γ_{as}	dose-response asymmetry level	$\{-1, 0, 1\}$
$p_i(y)$	the stress distribution (Normal for $i = 1$ and Gumbel for $i = 2$)	
σ	variance of the stress distribution	$\{\frac{\pi}{2\sqrt{6}}, \frac{\pi}{\sqrt{6}}, \frac{2\pi}{\sqrt{6}}\}$
x_{min}	lower boundary of the viability zone	
x_{max}	upper boundary of the viability zone	
S_{coex}	the relative coexistence surface	
b_{x^*}	the mean survival probability at the evolutionary equilibrium point x^*	
∇^2	the curvature at the evolutionary equilibrium point	
ϵ	background competition level	0.001

Table 2.1: Description of model parameters, and range of values explored in numerical simulations.

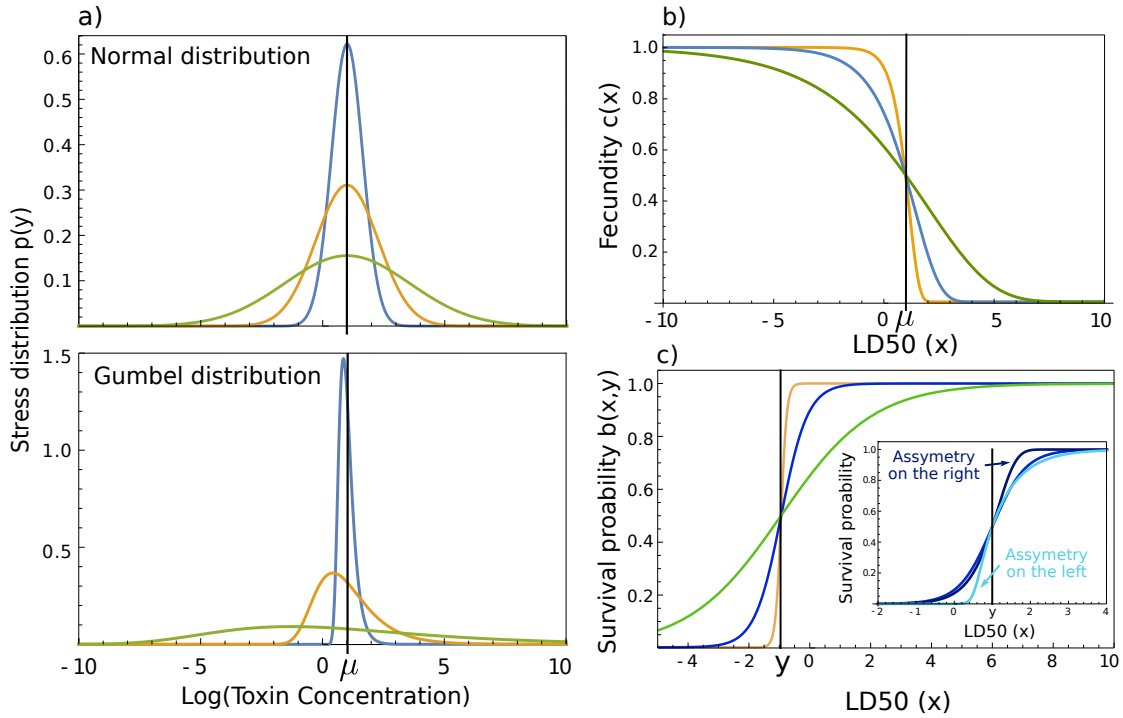


Figure 2.1: (a) The two stress distribution form considered (Normal and Gumbel). y denotes the stress level in log scale concentration. μ is the average stress level in the environment. (b) The fecundity function as a function of the species trait x (the LD50), for the different slopes considered. For each slope, $c(\mu)$ is widely varied in order to represent environment in which species are more or less tolerant in average. (c) The survival probability as a function of x , shown for the symmetric case (symmetric about y) and three slopes considered. The sub-panel illustrates the asymmetric version of this function: an asymmetry to the right and another one to the left. Such asymmetric versions are considered for all three slopes represented.

the maximum when, for a given species with tolerance x , the stress level goes from $x + \sigma_2$ to $x - \sigma_2$. In term of slopes this gives $\beta_s = 2.7, 0.6$ or 0.2 . This slope is later varied on a continuous range (see table 2.1).

In fine, the input variables used in the sensitivity analysis are p_i (2 levels), c_0 (2 levels), σ (3 levels), c_μ (3 levels), c_s (3 levels), β_s (3 levels) and γ_s (3 levels). They form a complete plan for the sensitivity analysis.

2.3 Results

2.3.1 Overview of model behavior through sensitivity analysis

The sensitivity analysis made on the nine output variables represented figure 2.2 gives a first idea of the model behavior. In the following, we will briefly expose the results obtained with this sensitivity analysis, before exploring in more details some of the points raised.

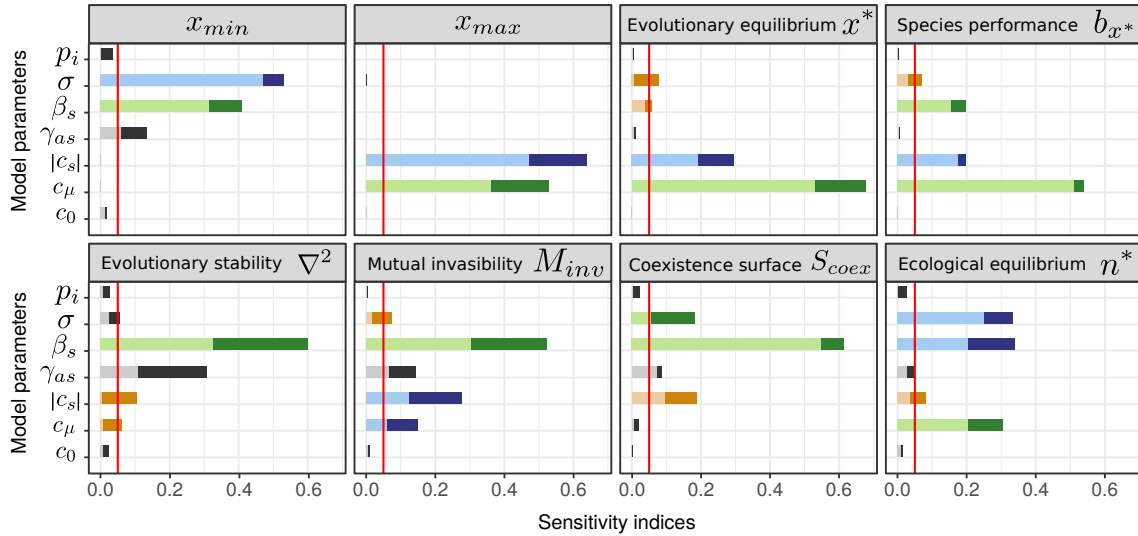


Figure 2.2: Sensitivity indices. Light colored or light grey bars stand for the sensitivity indices without interaction, and dark (colored or grey) bars stands for the total sensitivity indices (with interactions). The difference between the two indicates to what extent the input variable influences the output variable in interaction with other input parameters. Green (resp. blue) bars stand for a positive (resp. negative) impact of the input variable on the output variable. Orange bars stand for input variable that can have both a positive or a negative impact on the output variable depending on other parameters. Bars are kept grey when the input/output variables are qualitative, or when the impact is less than 5%.

Viability zone The two variables delimiting the viability zone (x_{min} and x_{max}) are not impacted by the same parameters (fig. 2.2, x_{min} and x_{max}). The upper limit of the viability zone is affected by the fecundity, while the lower limit is affected by the dose-response curve and the stress distribution variance. This is coherent with the fact that x_{min} and x_{max} are determined with condition (2.3). Fecundity c regulates x_{max} , because it becomes small at large values of x . And survival probability b regulates x_{min} , because it becomes small at small values of x (see figure 2.1). More precisely, with a shallower fecundity function (c_s decreases) or a higher fecundity at μ (c_μ increases), the fecundity of larger traits becomes large enough, what renders them viable. Thus, x_{max} increases. And for lower traits, it is the tolerance to stress that becomes critical: at some point, it is simply too small for species to survive the given stress. This is controlled by both the the dose-response curve and the stress distribution. The shallower the dose-response, the more traits available, and thus, the lower limit is pushed toward smaller values. Similarly, the broader the stress distribution, the more site available for low tolerance species, and the lower x_{min} .

Evolutionary equilibrium Similarly to x_{max} , the evolutionary equilibrium x^* is mainly driven by the fecundity (fig. 2.2, x^*). A species trait tends to evolve toward the highest tolerance it can achieve as long as fecundity remains at an acceptable value. An increase in the fecundity of the larger traits thus displaces the evolutionary equilibrium toward higher trait values (more tolerant).

Species performance at the evolutionary equilibrium Because species performance b_{x^*} monotonically increases with x^* and does not explicitly depend on fecundity, it varies the same way as x^* with fecundity (fig. 2.2, b_{x^*}). On the contrary, the steepness β_s of the dose-response does not impact x^* and b_{x^*} in the same direction. This point is later explored.

Species abundance As the performance, species abundance (fig. 2.2, n^*) is found to increase with c_μ , which is a proxy for the inverse of the average stress level in the environment. On the contrary, species abundance is negatively impacted by both the slope of the dose-response and the variance of the stress distribution. In any case, the abundance of a single species is relatively little impacted and is almost always close to 1. The background competition level ϵ introduced is the only parameter that prevents a single species to occupy the whole environment (and get abundance 1). As ϵ is very small, a more tolerant species will not gain much abundance compared to a lower tolerant species.

Evolutionary stability and mutual invasibility The relative impact of model parameters on the two metrics that characterise the type of evolutionary point (the curvature ∇^2 and the mutual invasibility M_{inv}) is almost the same (see fig. 2.2). They both are mostly determined by the slope β_s of the dose-response curve (fig. 2.2). Dose-response asymmetry also impacts both metrics, and this can be at first sight explained by the fact that asymmetry also slightly modifies the dose-response slope. This is explored in more details in the following. Fecundity slope (c_s) and height at μ (c_μ) have a negative impact on the mutual invasibility, while its effect on the curvature depends on other parameters. This is also later explored.

Relative coexistence surface The relative coexistence surface (S_{coex}) is also led by β_s (fig. 2.2). The steeper the dose-response, the larger the coexistence zone. Indeed, a steep slope of the dose-response functions allows a niche differentiation conducive to coexistence (D'Andrea *et al.*, 2013). As expected, the coexistence zone surface is also positively impacted by the variance of stress distribution, which controls the level of heterogeneity into the environment. Less intuitive but not negligible, the steepness of the fecundity function is also found to impact the coexistence zone surface, but in a direction that depends on other parameters.

Parameters with small impact The type of stress distribution function p_i has, comparatively to other parameters, a very small influence on the metrics considered (fig. 2.2). However, its variance σ and the average stress level in the environment (lead by c_μ) both have some impact. It is interesting to note that they each impact their own metrics, and rarely the same. The maximum height of the fecundity function c_0 has also very small influences, as it mainly acts as a scaling factor.

In the following, we will explore in more details some of the parameter impacts. We will focus on the impact of the two parameters shaping the trade-off intensity (c_s and β_s), on the impact of the mean and variance of the stress distribution function, and on the role of the dose-response asymmetry. And we will finish with the study of two species communities.

2.3.2 Evolutionary equilibrium of stress tolerance x^*

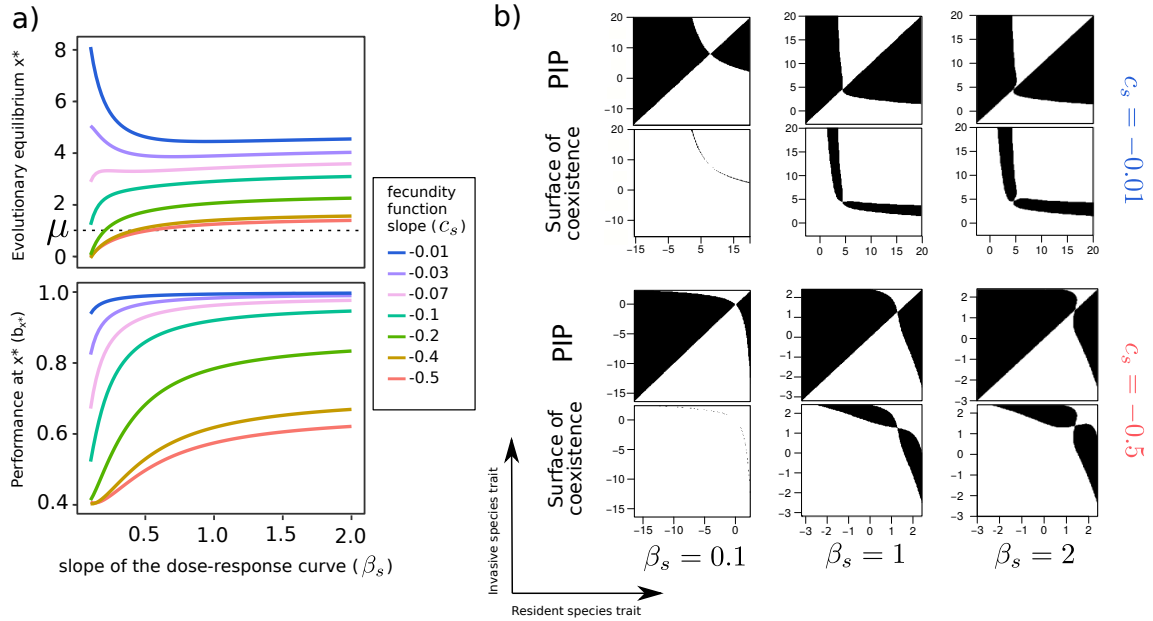


Figure 2.3: (a) The evolutionary equilibrium (x^*) and the mean survival probability at evolutionary equilibrium (b_{x^*}) as a function of the slope β_s of the dose-reponse curve. The relation is plotted for different slopes c_s of the fecundity function. (b) The PIP and surface of coexistence plot corresponding to two slopes fecundity c_s and three survival probability slopes β_s . Parameters: $p_i = p_1$ (Normal distribution), $\sigma = \pi/\sqrt{6}$, $c_\mu = 0.5$, $c_0 = 1$, $\gamma_s = 0$.

Consistent with the sensitivity analysis, the tolerance level at evolutionary equilibrium x^* is almost constant with β_s , except for low β_s (fig.2.3a). In those cases of shallow dose-response curve (low β_s), x^* is found to either decrease or increase with β_s : it increases for steep fecundity functions, but decreases for shallow enough fecundity functions (low c_s ; fig.2.3a). For steep dose-response curve (large β_s), x^* is mainly driven by the fecundity slope c_s . In any case of β_s , the shallower the fecundity function, the higher x^* .

Similarly, for large β_s , the species performance (the mean survival probability over all patches at the evolutionary equilibrium b_{x^*}) is almost constant with β_s . It thus mainly depends on the fecundity steepness c_s and the shallower the fecundity function, the higher b_{x^*} . For low β_s , contrary to x^* , b_{x^*} does always increase with β_s . The evolutionary equilibrium (x^*) and the species performance (b_{x^*}) do not vary the same way with β_s for shallow fecundity functions (low c_s).

Unless the fecundity function is very shallow (low $|c_\mu|$), the stress distribution variance (σ , i.e. the level of heterogeneity in the environment) has relatively few impacts on the tolerance level at the evolutionary equilibrium (fig. 2.4a). On the contrary, the average level of stress (proportional to the inverse of c_μ) impacts the tolerance level at the evolutionary equilibrium (fig. 2.4b). The lower the stress level, the greater x^* . Unless the dose-response curve is very shallow (low β_s), the absolute value of this impact hardly depends on the two trade-off intensity parameters (c_μ and β_s).

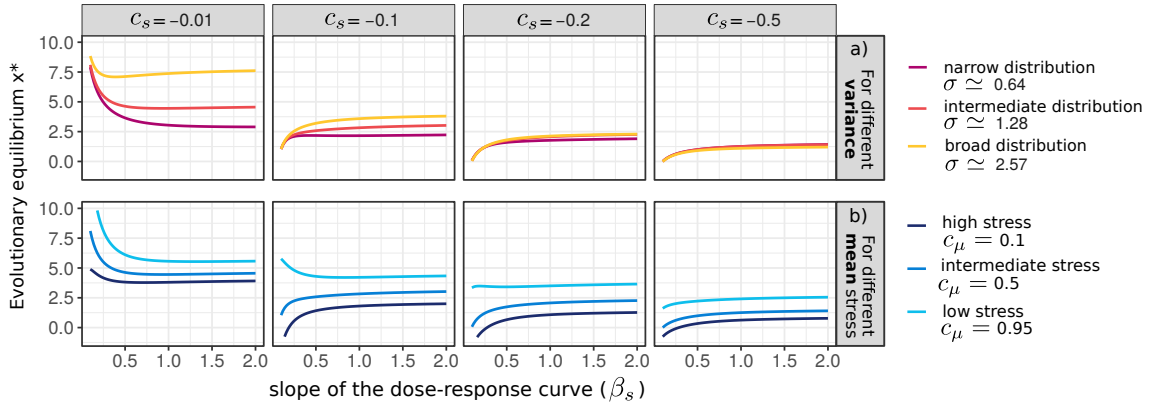


Figure 2.4: The evolutionary equilibrium (x^*) as a function of the slope β_s of the dose-response curve, (a) for three different variance of the stress distribution σ , and (b) for three different level of stress in the environment (proportional to the inverse of c_μ). The relations are plotted for different slopes c_s of the fecundity function. Parameters for (a): $p_i = p_1$ (Normal distribution), $c_\mu = 0.5$, $c_0 = 1$, $\gamma_s = 0$. Parameters for (b): $p_i = p_1$ (Normal distribution), $\sigma = \pi/\sqrt{6}$, $c_0 = 1$, $\gamma_s = 0$.

2.3.3 The evolutionary stability

Figure 2.3b gives contrasted examples of the PIP and coexistence surface plots that have been obtained. For low β_s (shallow dose-response) the PIP presents an ESS, which turns progressively into a branching point as β_s increases (PIP fig.2.3b). While c_s has a large impact on the evolutionary equilibrium, it has less impact on the stability of the evolutionary point (PIP fig.2.3b). Nonetheless, the PIP presents different shape depending on the steepness of the fecundity function. This is even more visible on the relative surface coexistence plot (fig.2.3b). They look like a swallow going to the bottom left in case of a shallow fecundity function ($c_s = -0.01$), and a swallow going to the top right in case of a steep fecundity function ($c_s = -0.5$).

To better understand the role of the two trade-off intensity parameters (c_s and β_s) in the evolutionary stability and their interactions with germination condition distribution (stress distribution), we summarized information on figure 2.5. We find the not surprising property that a steeper survival probability function favors evolutionary branching. Increasing β_s , we move from an ESS point with no mutual invasibility (small green zone) to an ESS with mutual invasibility, then to a branching point (fig. 2.5).

We also observe that, consistently with the sensitivity analysis and figure 2.3, c_s (fecundity function steepness) has less impact than β_s (dose-response steepness) on the evolutionary stability. However, the impact of c_s is not null, and it is particularly interesting to note that the change in evolutionary stability is monotonic with β_s , but not with c_s . Branching is more likely to occur for low-to-intermediate steepness of the fecundity function. This evidences that those two trade-off intensity parameters (c_s and β_s) do not play the same role in the evolution of stress tolerance, and could not easily be aggregated in a single trade-off metric.

The observed patterns for the evolutionary stability depend on the stress distribution (see the nine different panels figure 2.5): there are more branching when (i) the stress distribution is broader (more heterogeneous environment) and (ii) the average stress level is lower (see the values for the branching surface zone S_{br} indicated

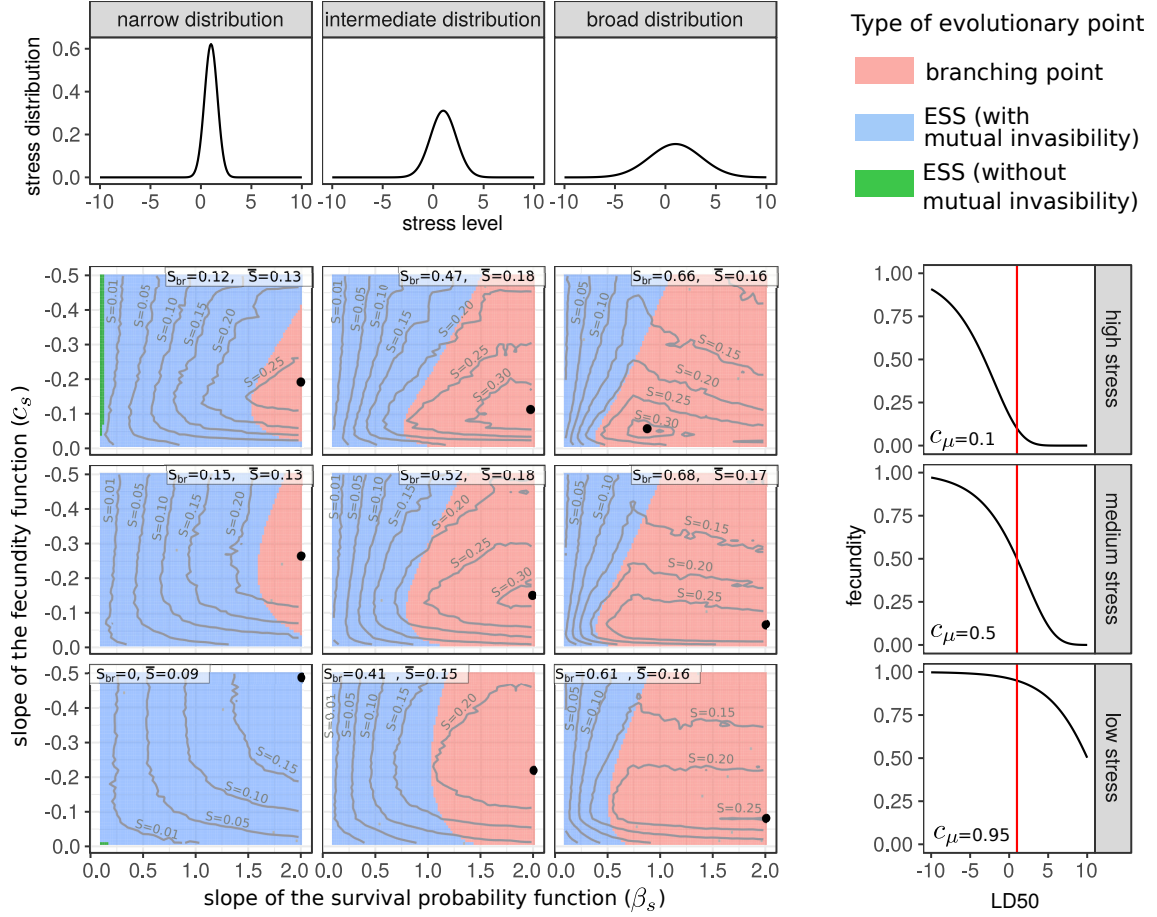


Figure 2.5: Type of evolutionary point as a function of the trade-off parameters (c_s and β_s) and of the environmental conditions (the mean stress level, reflected by c_μ , and the stress distribution variance σ). The contour lines indicate the relative surface of coexistence and the black points indicate where its maximum stands. This figure is made with a symmetric survival probability function. The environmental conditions are described by the variance of the stress distribution (σ is respectively equal to σ_1 , σ_2 and σ_3 for the narrow, intermediate and broad distributions), and by the averaged stress level which is inversely proportional to c_μ (c_μ is respectively equal to 0.1, 0.5 and 0.95 for the high, medium and low stress). S_{br} stands for the relative surface in which branching is possible (within the trade-off parameter zone explored), and \bar{S} stands for the averaged coexistence surface over the trade-off parameter zone explored. The panel in the center (middle column, middle row) is the one that corresponds to the plots in figure 2.3.

in the sub panels). We also note that the average stress level has less impact than the stress variance on the branching zone surface. However, a change in the stress distribution seems to solely shift the patterns, and to not qualitatively change their forms. The higher c_μ and narrower the stress distribution, the more zoomed is the pattern. What we get for a low stress with low variance (large c_μ and low σ , bottom left panel) is a zoom of the lower left part of the pattern we obtain for a high stress with large variance (low c_μ and large σ , top right panel).

2.3.4 The relative coexistence surface for two species

We could have expected the relative coexistence surface (grey lines fig. 2.5) to follow the evolutionary point type zones. This is not as simple, even if the coexistence surface is almost null for low β_s , and increases while moving toward the branching point pattern (fig. 2.5). Inside the branching point zone, the coexistence surface presents a maximum (indicated by a black point) for an intermediate-to-large value of β_s and a low value of c_s (at least when the stress distribution is broad enough). The coexistence surface is thus maximized by a given trade-off intensity characterized by a shallow fecundity function and a rather steep dose-response curve.

Note here that the coexistence surface is a global metric derived from the whole PIP, while the mutual invasibility exposed in the method is a local metric, at the equilibrium point. Thus, an ESS with mutual invasibility always imply that coexistence is possible (at least on a small zone), but the reverse is not always true.

The coexistence surface is impacted by the stress distribution: both c_μ and σ are found to influence the coexistence surface (see the values for the average surface coexistence \bar{S} over all possible trade-off combination indicated in the sub panels figure 2.5). However, \bar{S} is not maximized by the broader stress distribution, as was the branching surface S_{br} , but by an intermediate stress variance.

2.3.5 Impact of the dose-response curve asymmetry

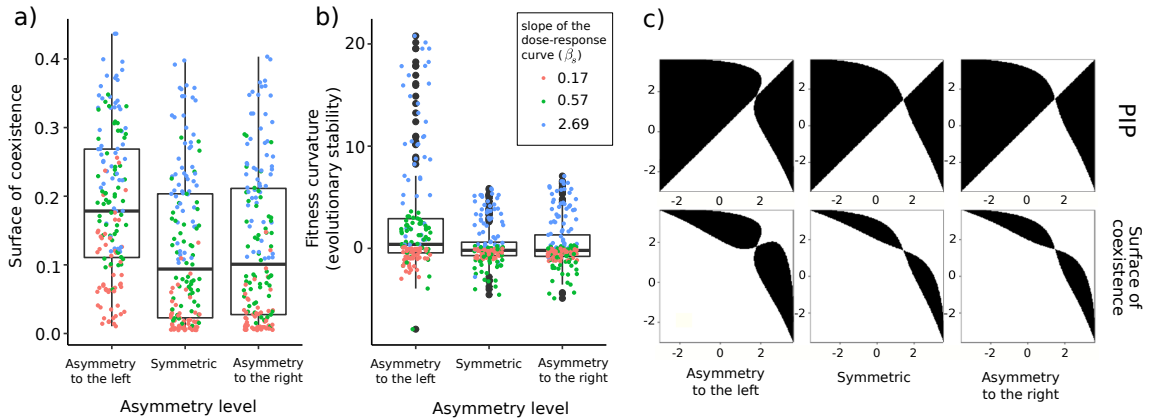


Figure 2.6: Impact of the dose-response curve asymmetry level (γ_{as}) on (a) the relative coexistence surface and (b) the curvature at the evolutionary equilibrium. All the parameters varied to obtain (a) and (b) are those used for the sensitivity analysis in figure 2.2. (c) PIP and coexistence surface plot for the case $\beta_s = 0.57$ and for the three asymmetry levels considered. Parameters for (c): $p_i = p_1$ (Normal distribution), $\sigma = \pi/\sqrt{6}$, $c_\mu = 0.5$, $c_0 = 1$.

The sensitivity analysis showed that dose-response asymmetry does impact the evolutionary point stability (∇^2) and the surface of coexistence (see fig. 2.2). Adding an asymmetry to the function indeed increases its slope (in both asymmetry cases considered), and we furthermore found that the slope of the survival probability function greatly impact the evolutionary stability and the coexistence surface (see previous paragraphs). Introducing an asymmetry to the left however has more impacts than introducing a comparable asymmetry to the right (fig. 2.6a,b), even if in both cases, the slope remains the same: the coexistence surface is greater

and the chance of having an unstable evolutionary equilibrium is larger. This is also visible on the PIP (fig. 2.6c) where the relative surface of coexistence in the asymmetry to the left case is larger. On the other hand, this asymmetry to the left case presents a branching pattern where the two other not, which is consistent with the fact that branching occurs when the coexistence surface is larger. All else being equal, adding an asymmetry to the left makes branching occur for lower β_s (i.e. for shallower dose-response curves).

2.3.6 Evolutionary dynamics with more than one species

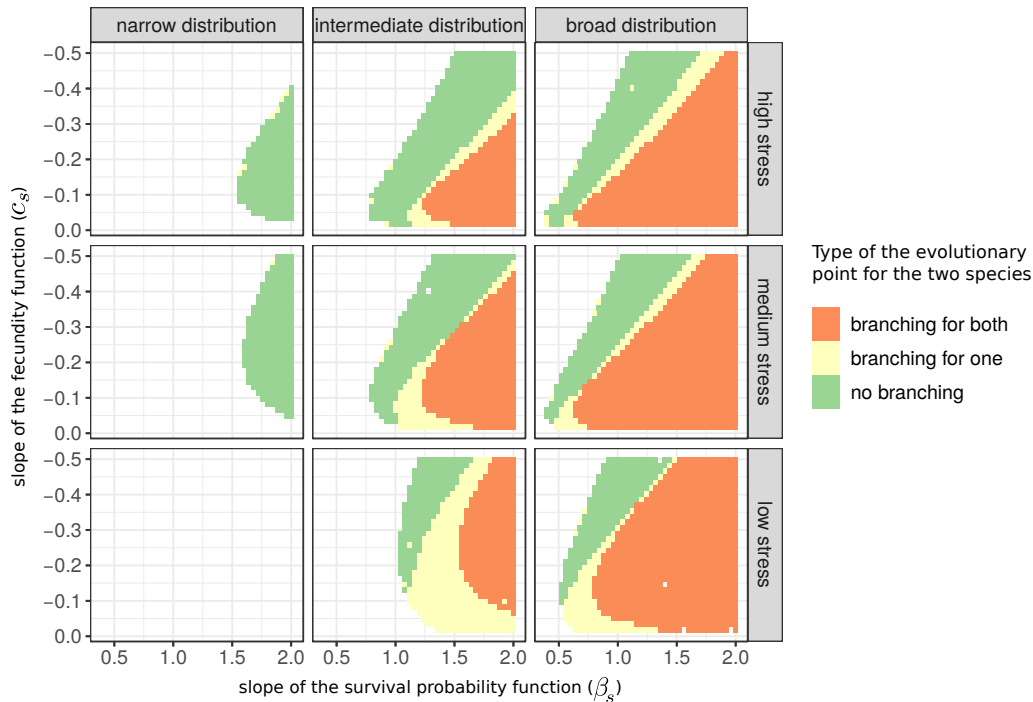


Figure 2.7: Evolutionary stability for two species. The colored zones correspond to the cases where the monomorphic evolutionary equilibrium was unstable (branching). With two species, the evolutionary equilibrium can present a branching point for either the two, only one or no species. The white area corresponds to the stable monomorphic evolutionary equilibrium. In this area, we verified that no dimorphic evolutionary equilibrium can exist. The nine panels stand for the same parameters as figure 2.5.

In case of a branching point, a resident species and a rare mutant similar to the resident can coexist under disruptive selection. This means that both can coexist and evolve separately, possibly settling at a joint co-evolutionary equilibrium (Metz *et al.*, 1995; Geritz *et al.*, 1997). Alternatively, we saw that even in the case of an ESS, pairs of strategies could coexist (fig. 2.3 and 2.5). A dimorphic state could thus also be brought up by large-effect mutations or invasions from outside the focal community. In either case, one can ask whether further diversification could occur.

For all the parameter sets that presented an unstable monomorphic evolutionary equilibrium (branching point for one species), we searched for the evolutionary equilibrium traits for two species using the selection gradient. We then looked at the evolutionary stability of those two species communities, and discriminated cases

in which both species were at branching points, only one was at a branching point, and none of them was at a branching point (see colored zone figure 2.7). Results show that bimorphic unstable evolutionary equilibria occur for even more restricted conditions than for monomorphic ones (fig. 2.7).

When the monomorphic evolutionary equilibrium was stable (ESS), we plotted some flowfields and nullclines which indicate the direction of the selection gradient and their cancellation points. We found no existence of a bimorphic evolutionary equilibrium (stable or unstable) in cases of a stable monomorphic evolutionary equilibrium (white zone figure 2.7).

2.4 Discussion

This paper is a first attempt at characterizing the adaptive dynamics under a TFT model (Muller-Landau, 2010; D’Andrea *et al.*, 2013; Haegeman *et al.*, 2014; D’Andrea & O’Dwyer, 2021). We studied the evolution of stress tolerance of a single species, the possibility of diversification (branching), and then explored the possibility of further diversification. To that purpose, we proposed a new formulation of the model that is amenable to adaptive dynamics, and is based on explicit traits and continuous trade-off functions that can be more easily related to real-world measurements. We investigated the impact of trade-off parameters, and of the distribution of stress levels across patches, on evolutionary equilibria and diversification. We will discuss here the main results obtained.

How the evolutionary equilibrium depends on the steepness of the fecundity and dose-response functions. Within the viability zone, the model presents a single evolutionary attractor, and the stress tolerance at evolutionary equilibrium is mainly driven by the fecundity cost of tolerance (the shallower the fecundity function, the more tolerance traits can be high). The dose-response curve has comparatively less impact, unless it becomes quite shallow: when the steepness of the transition from low to high survival (steepness of the dose-response curve) exceeds a given threshold (around $\beta_s = 0.5 - 0.6$; see fig. 2.3a), it does not impact stress tolerance evolutionary equilibrium any more. Indeed, in that case (β_s higher than the threshold), the survival probability tends to be either 0 or 1. A change in β_s has almost no impact on this pattern, and the fecundity is then the only driver of evolution. Below the threshold however, the dose-response is shallower, and two cases are encountered depending on fecundity steepness. They are both illustrated in the S.I. figure B.1, and explained bellow. If fecundity (which is a decreasing function of stress tolerance) is steep enough, the stress tolerance equilibrium can reach lower values while maintaining a high fecundity. In addition, because the dose-response is shallow (i.e. relatively high for a large proportion of possible stress tolerance), the stress tolerance can be even lower while maintaining a relatively high survival probability for a large proportion of sites. Thus, the shallower the dose-response curve, the lower x^* , giving a positive relationship between β_s and x^* . On the contrary, if fecundity slope is very shallow, the sign of this relationship switches to negative. This is surprising at first sight (the same explanation as above could hold), but is understandable. In those cases, the fecundity function is so shallow that it seems almost constant for all traits. The trade-off is very weak. Thus, the species trait has the freedom to evolve to very high values and reach the point where it achieves

maximal survival probability (close to one) over all patches. Then, when β_s increases (but still bellow the threshold), the dose-response curve becomes steeper, and the species trait does not have to go as far to achieve this maximal response, which explains the observed negative relationship between x^* and β_s .

What is a steep dose-response curve? The dose-response slope threshold, found around $\beta_s = 0.5 - 0.6$, separates the β_s values for which a variation in β_s does impact the tolerance level at evolutionary equilibrium from those for which it does not. It corresponds to the blue curve figure 2.1c. This curve was not considered to represent a very sharp transition in a previous study (D’Andrea *et al.*, 2013). The shallowest slope considered by D’Andrea *et al.* (2013) is 2.8 (their $\nu = 5$), while this value corresponds to our steepest slope. The threshold we found around 0.6 suggests that some transitions may occur at even lower slopes, and the fact that we already have branching at 2.8 (implied, for higher values as well) tells that $\beta_s = 2.8$ may still fall in the “steep functions category” regarding evolutionary behavior. Nevertheless, D’Andrea *et al.* (2013) found ecological differences (in terms of coexistence) brought by their “steep” function (with 2.8). All of this suggests that a “steep” function may not have the same meaning from an ecological or an evolutionary perspective. It would seem that ecological predictions are more sensitive than evolutionary ones with respect to the steepness of the dose-response curve, but this would be an hypothesis that would need further investigations.

Species performance versus species tolerance. It is interesting to note that the performance of a species at an evolutionary equilibrium (b_{x^*}) is not always increasing with x^* (fig. 2.3a, comparison between the two panels), as we could have expected at first sight. Indeed, all else being equal, b_{x^*} is a priori an increasing function of x^* . But the steepness of the dose-response curve (β_s) is not constant across the different situations compared. Let us explain what occurs. To obtain b_{x^*} , we perform the integral (over all patches) of $b(x^*, y)$ that is weighted by the stress distribution whose mean is μ . This means that the larger values of the weighting coefficient $p(y)$ are found around μ (at least for the Normal distribution). The survival probability $b(x^*, y)$, as for it, is a decreasing function of y , and is equal to 0.5 for $y = x^*$. Thus, if x^* is higher than μ , the steeper the dose-response, the more the high survival values are weighted by large coefficients, and thus the higher b_{x^*} . On the contrary, if x^* is lower than μ , the steeper the dose-response, the less the high survival values are weighted by large coefficients, and thus the lower b_{x^*} . We provide an illustration of those two cases in the S.I. figure B.2. We can thus distinguish three patterns in the presented results. First, in cases where x^* is higher than μ and increases with β_s , both effects go in the same direction: b_{x^*} increases with β_s and x^* increasing also with β_s , participating to this increase. In that case, x^* and b_{x^*} are de facto positively correlated. Second, in cases where x^* is higher than μ and decreases with β_s (for very shallow fecundity functions), the increase in b_{x^*} with β_s is slowed down by the fact that x^* decreases with β_s . In that case, x^* and b_{x^*} are negatively correlated. In the limit of completely flat fecundity function (no trade-off), $b_{x^*} \rightarrow 1$ for all β_s so that b_{x^*} will never be found to decrease with β_s . And third, in cases where x^* is lower than μ and increases with β_s , the a priori decrease in b_{x^*} with β_s is compensated by the fact that x^* increases with β_s , resulting in a low-increasing relationship between b_{x^*} and β_s . In

that case, x^* and b_{x^*} are positively correlated. What is interesting to remember from all those considerations is that the absolute value of x^* , as long as with β_s , is crucial in determining the correlation between x^* and the performance. x^* being mostly determined by the fecundity function steepness c_s , we can say that there exists a strong interaction between the two parameters shaping the trade-off intensity (c_s and β_s), one determining the consequences of varying the other one.

The dose-response curve steepness impacts evolutionary stability...

Changes in the steepness of the two functions that determine the trade-off intensity (c and b) can modify the evolutionary stability from ESS to branching points. It is interesting to note that even when a change in the dose-response steepness β_s does not impact the position of the evolutionary attractor x^* any more (β_s higher than the above mentioned threshold), it does impact its stability (fig. 2.5). A steeper dose-response curve has more chance to result in an unstable evolutionary attractor (branching point). Such a steep transition indeed favors disruptive selection because close individuals (in trait value) may harbor very different responses to stress: an increase in dose-response steepness is nothing else than an increase in the survival advantage of high-tolerance seeds over closely lower-tolerance seeds (around the inflection point). We can note that such an adaptive radiation pattern from a single species is not always predicted. For instance, it was not predicted in a competition-colonization trade-off model, which required at least two species for diversification to be possible (Calcagno *et al.*, 2017).

... because of the advantage of tolerant species over less tolerant species.

The relative increase in survival advantage is illustrated by the study of the dose-response asymmetry consequences (fig. 2.6 ; Liao & Liu, 2009). We have observed that introducing an asymmetry to the left (i.e. decreasing the survival probability of low-tolerance seeds) has more impacts on the coexistence surface and evolutionary stability than adding an asymmetry to the right (i.e. increasing the survival probability of already high-tolerance seeds). Yet, in both cases, the dose-response slope is modified the same way. But the advantage of high-tolerance seeds over low-tolerance seeds increases more in the case where the survival probability of low-tolerance seeds is decreased (all else being equal; i.e. asymmetry to the left), rather than in the case where the survival probability of high-tolerance seeds is increased (i.e. asymmetry to the right). Indeed, in that case (low-tolerance seeds survival probability decreased), the relative difference in survival between low and high tolerance seeds is larger. Geritz *et al.* (1999) observed a similar effect of the survival advantage of high-tolerance seeds over low-tolerance seeds on evolutionary stability in a trade-off between seed size and seedling competitive ability.

The role of the dose-response slope in evolutionary stability is also consistent with the work of Egas *et al.* (2004) who studied adaptive dynamics in a general trade-off model. They found that branching occurs when the probability to enter habitat (similar to our dose-response function) presents a sharp transition. They also showed that the efficiency in an habitat (the trade-off function, similar to our fecundity function) has no impact on the possibility of branching. This is consistent with our finding that the trade-off function (fecundity) has much less impact than the dose-response steepness.

The small, but non-zero, role of fecundity function for evolutionary stability. Still, this impact of the fecundity function steepness is not null in our study (fig. 2.5), and fecundity has also a – smaller but still existing – role in shaping selection. In general, a shallow fecundity function favors branching, except when too smooth. This is rather counter intuitive at first sight, as we could have expected a steep fecundity function (strong trade-off) to favor niche differentiation. But actually, the species that can survive are the ones whose fecundity is not too small. In the case of a steep fecundity function, those “surviving” species all arbor almost the same large fecundity. On the contrary, in the case of a shallow fecundity function, the species that can survive arbor a broader range of possible fecundity values. Thus, the shallowness of the fecundity function allows for niche differentiation, and the possibility of coexistence. This observation was here made possible by the explicit mathematical expression of the trade-off relationship between fecundity and stress tolerance.

The probability that two random species coexist. Evolutionary stability zones were found to be relatively well aligned with the relative coexisting surface level lines (fig. 2.5). Our metric of coexistence surface describes the probability for two species randomly chosen to coexist, and is thereby different from the coexistence metric explored in the TFT model literature (Muller-Landau, 2010; D’Andrea *et al.*, 2013; D’Andrea & O’Dwyer, 2021). The latter questioned the maximum number of species that are able to ecologically coexist. We thus cannot directly link our metric to previous results about coexistence. Indeed, that the probability of having two species is greater for an intermediate level of β_s is interesting to note, but does not necessarily correlate with the probability of coexistence of more species. This would be interesting to explore, such as Calcagno *et al.* (2006) did for the competition-colonization trade-off model. Ecological coexistence (maximum number of species) has been found to be greatly impacted by the dose-response slope β_s (D’Andrea *et al.*, 2013; D’Andrea & O’Dwyer, 2021). The steeper their dose-response, the more species coexistence (i.e. a higher number of species can coexist). This is interpreted in term of niche occupancy and limiting similarity among competing species. The fact that the higher β_s , the highest species diversity is consistent with our results that the higher β_s the more branching (and globally the more coexistence surface), because branching would generally promote the formation of more diverse communities through adaptive radiation (Geritz *et al.*, 1997).

Further adaptive diversification. While possibly any trade-off intensity allows a two (and potentially more) species polymorphisms (coexistence surface not null), the conditions to form communities through gradual evolution are rather restricted. The slope of the dose-response must be steep enough, and the stress distribution must be rather broad. And the more species, the strongest those conditions. This reminds us the results from Ravigné *et al.* (2009). In a trade-off on local adaptation, they demonstrated that stronger trade-offs (convex trade-off function) restrict the conditions under which a polymorphism can emerge through gradual evolution, though it does not restrict the maintenance of polymorphism.

The role of spatial heterogeneity and its consequences for site regeneration. Since evolutionary dynamics can often occur even on ecological timescales

(Carroll *et al.*, 2007; Hendry, 2020; Hart *et al.*, 2019), our results can have potential consequences for site regeneration. Indeed, we found that a decrease in spatial heterogeneity can first minimize the probability that two species randomly chosen can coexist, and second, minimize the probability for species to evolve through adaptive radiation and form new communities this way. Third, it also reduces the possibility for two (or potentially more) species to reach a dimorphic evolutionary attractor through evolutionary processes, and to not collapse to a single monomorphic equilibrium. Thus, site formation or regeneration might be easiest in case of high stress heterogeneity. Yet, spatial heterogeneity is for instance found to decrease after a fire (Wang *et al.*, 2021), what may reduce the chance of site regeneration based only on this TFT coexistence mechanism.

Conclusion. To summarize our main findings, this study demonstrates that the evolution of stress tolerance and its stability are not driven by the same parameters. The evolution of stress tolerance is mainly driven by the fecundity function and the average stress level in the environment, but barely affected by the spatial heterogeneity level. On the other hand, the possibility of evolutionary diversification (the evolutionary stability of the equilibrium) mostly depends on the survival function, and is more affected by the spatial heterogeneity level than by the average stress level: the highest the advantage of high-tolerance seeds over low-tolerance and the broader the stress distribution, the more possibility of evolutionary diversification. Then, dimorphic evolutionary equilibrium is only possible when the monomorphic equilibrium was unstable (i.e. resulting in a possible diversification). Further evolutionary diversification occurs in even more restricted conditions.

Our results suggest that the patterns of species coexistence obtained from an ecological perspective (Muller-Landau, 2010; D'Andrea *et al.*, 2013; D'Andrea & O'Dwyer, 2021) are likely to be modified if one also considers the evolutionary dynamics of communities. Most of those results would not be easy to be directly tested experimentally, because they are mostly based on differences between trade-off intensities. This would require the use of different systems (i) who are governed by a TFT, and (ii) who present various steepness for their dose-response and fecundity functions. Both conditions are not easily identifiable in nature or in specific organisms. Nevertheless, testing whether and how species tolerance and performance are affected by evolution should remain more feasible, and could be a first logical step. This study calls for future consideration of the evolution of communities governed by a TFT, and more generally, of evolution in any coexistence mechanism scenario.

Bibliography

- Alstad, A.O., Damschen, E.I. & Ladwig, L.M. (2018) Fire as a Site Preparation Tool in Grassland Restoration: Seed Size Effects on Recruitment Success. *Ecological Restoration*, **36**, 219–225.
- Aubree, F., David, P., Jarne, P., Loreau, M., Mouquet, N. & Calcagno, V. (2020) How community adaptation affects biodiversity–ecosystem functioning relationships. *Ecology Letters*, **23**, 1263–1275.
- Austin, A.T., Yahdjian, L., Stark, J.M., Belnap, J., Porporato, A., Norton, U., Ravetta, D.A. & Schaeffer, S.M. (2004) Water pulses and biogeochemical cycles in arid and semiarid ecosystems. *Oecologia*, **141**, 221–235.
- Barabás, G., D’Andrea, R. & Ostling, A.M. (2013) Species packing in nonsmooth competition models. *Theoretical Ecology*, **6**, 1–19.
- Ben-Hur, E., Fragman-Sapir, O., Hadas, R., Singer, A. & Kadmon, R. (2012) Functional trade-offs increase species diversity in experimental plant communities. *Ecology Letters*, **15**, 1276–1282.
- Bidot, C., Monod, H. & Taupin, M.L. (2018) A quick guide to multisensi, an R package for multivariate sensitivity analyses.
- Bonsall, M.B., Jansen, V.A.A. & Hassell, M.P. (2004) Life History Trade-Offs Assemble Ecological Guilds. *Science*, **306**, 111–114.
- Calcagno, V., Jarne, P., Loreau, M., Mouquet, N. & David, P. (2017) Diversity spurs diversification in ecological communities. *Nature Communications*, **8**, 15810.
- Calcagno, V., Mouquet, N., Jarne, P. & David, P. (2006) Coexistence in a meta-community: the competition–colonization trade-off is not dead. *Ecology letters*, **9**, 897–907.
- Cao, Q., Liu, Y., Georgescu, M. & Wu, J. (2020) Impacts of landscape changes on local and regional climate: a systematic review. *Landscape Ecology*, **35**, 1269–1290.
- Carroll, S.P., Hendry, A.P., Reznick, D.N. & Fox, C.W. (2007) Evolution on ecological time-scales. *Functional Ecology*, **21**, 387–393.
- Chesson, P. (2000) Mechanisms of maintenance of species diversity. *Annual review of Ecology and Systematics*, **31**, 343–366.

- Coomes, D.A. & Grubb, P.J. (2003) Colonization, tolerance, competition and seed-size variation within functional groups. *Trends in Ecology & Evolution*, **18**, 283–291.
- Dieckmann, U. & Doebeli, M. (1999) On the origin of species by sympatric speciation. *Nature*, **400**, 354–357.
- D’Andrea, R., Barabás, G. & Ostling, A. (2013) Revising the Tolerance-Fecundity Trade-Off; or, On the Consequences of Discontinuous Resource Use for Limiting Similarity, Species Diversity, and Trait Dispersion. *The American Naturalist*, **181**, E91–E101.
- D’Andrea, R. & O’Dwyer, J.P. (2021) Competition for space in a structured landscape: The effect of seed limitation on coexistence under a tolerance-fecundity trade-off. *Journal of Ecology*, **109**, 1886–1897.
- Egas, M., Dieckmann, U. & Sabelis, M. (2004) Evolution Restricts the Coexistence of Specialists and Generalists: The Role of Trade-off Structure. *The American Naturalist*, **163**, 518–531.
- Ellner, S.P., Geber, M.A. & Hairston Jr, N.G. (2011) Does rapid evolution matter? Measuring the rate of contemporary evolution and its impacts on ecological dynamics. *Ecology Letters*, **14**, 603–614.
- Gagic, V., Bartomeus, I., Jonsson, T., Taylor, A., Winqvist, C., Fischer, C. & et al. (2015) Functional identity and diversity of animals predict ecosystem functioning better than species-based indices. *Proceedings of the Royal Society B: Biological Sciences*, **282**, 20142620.
- Geritz, S.A.H., Metz, J.A.J., Kisdi, E. & Meszéna, G. (1997) Dynamics of Adaptation and Evolutionary Branching. *Phys. Rev. Lett.*, **78**, 2024–2027.
- Geritz, S.A., van der Meijden, E. & Metz, J.A. (1999) Evolutionary Dynamics of Seed Size and Seedling Competitive Ability. *Theoretical Population Biology*, **55**, 324–343.
- Ginocchio, R., Carvallo, G., Toro, I., Bustamante, E., Silva, Y. & Sepúlveda, N. (2004) Micro-spatial variation of soil metal pollution and plant recruitment near a copper smelter in Central Chile. *Environmental Pollution*, **127**, 343–352.
- Van der Graaf, P. & Schoemaker, R. (1999) Analysis of asymmetry of agonist concentration–effect curves. *Journal of pharmacological and toxicological methods*, **41**, 107–115.
- Haegeman, B., Sari, T. & Etienne, R. (2014) Predicting coexistence of plants subject to a tolerance-competition trade-off. *J Math Biol.*, **68**, 1815–47.
- Hart, S.P., Turcotte, M.M. & Levine, J.M. (2019) Effects of rapid evolution on species coexistence. *Proceedings of the National Academy of Sciences*, **116**, 2112–2117.
- Hendry, A. (2020) *Eco-evolutionary Dynamics*. Princeton University Press. ISBN 9780691204178.

- Jordan, S.E., Palmquist, K.A., Bradford, J.B. & Lauenroth, W.K. (2020) Soil water availability shapes species richness in mid-latitude shrub steppe plant communities. *Journal of Vegetation Science*, **31**, 646–657.
- Kaur, J., Schwilk, D. & Sharma, J. (2021) Seed germination and plant fitness response of a narrowly endemic, rare winter annual to spatial heterogeneity in microenvironment. *Plant Species Biology*, **36**, 36–51.
- Lankau, R.A. (2011) Rapid Evolutionary Change and the Coexistence of Species. *Annual Review of Ecology, Evolution, and Systematics*, **42**, 335–354.
- Laroche, F., Jarne, P., Perrot, T. & Massol, F. (2016) The evolution of the competition–dispersal trade-off affects α - and β -diversity in a heterogeneous meta-community. *Proceedings of the Royal Society B: Biological Sciences*, **283**, 20160548.
- Lebrija-Trejos, E., Reich, P.B., Hernández, A. & Wright, S.J. (2016) Species with greater seed mass are more tolerant of conspecific neighbours: a key driver of early survival and future abundances in a tropical forest. *Ecology Letters*, **19**, 1071–1080.
- Levin, S.A. (1970) Community equilibria and stability, and an extension of the competitive exclusion principle. *The American Naturalist*, **104**, 413–423.
- Liang, W. & Wei, X. (2021) Spatial heterogeneity of topsoil moisture and impact of vegetation factors on its distribution under pure and mixed black locust (*Robinia Pseudoacacia* L.) and chinese red pine (*Pinus Tabulaeformis* Carr.) forests on the loess plateau in China. *Applied Ecology and Environmental Research*, **19**, 795–815.
- Liao, J.J.Z. & Liu, R. (2009) Re-parameterization of five-parameter logistic function. *Journal of Chemometrics*, **23**, 248–253.
- Liukkonen, M., Kronholm, I. & Ketola, T. (2021) Evolutionary rescue at different rates of environmental change is affected by trade-offs between short-term performance and long-term survival. *Journal of Evolutionary Biology*, **n/a**, 1–8.
- Loeuille, N. (2010) Influence of evolution on the stability of ecological communities. *Ecology Letters*, **13**, 1536–1545.
- MacArthur, R. & Levins, R. (1967) The Limiting Similarity, Convergence, and Divergence of Coexisting Species. *The American Naturalist*, **101**, 377–385.
- Maron, J.L., Hahn, P.G., Hajek, K.L. & Pearson, D.E. (2021) Trade-offs between seed size and biotic interactions contribute to coexistence of co-occurring species that vary in fecundity. *Journal of Ecology*, **109**, 626–638.
- Metz, J.A.J., Geritz, S.A.H., Meszner, G., Jacobs, F.J.A. & Heerwaarden, J.S.v. (1995) Adaptive dynamics: a geometrical study of the consequences of nearly faithful reproduction. IIASA Working Paper, WP-95-099, IIASA, Laxenburg, Austria.

- van Moorsel, S.J., Hahl, T., Wagg, C., De Deyn, G.B., Flynn, D.F.B., Zuppinger-Dingley, D. & Schmid, B. (2018) Community evolution increases plant productivity at low diversity. *Ecology Letters*, **21**, 128–137.
- Moran, M.S., Peters-Lidard, C.D., Watts, J.M. & McElroy, S. (2004) Estimating soil moisture at the watershed scale with satellite-based radar and land surface models. *Canadian Journal of Remote Sensing*, **30**, 805–826.
- Muller-Landau, H.C. (2010) The tolerance–fecundity trade-off and the maintenance of diversity in seed size. *Proceedings of the National Academy of Sciences*, **107**, 4242–4247.
- Ojosnegros, S., Beerenwinkel, N., Antal, T., Nowak, M.A., Escarmís, C. & Domingo, E. (2010) Competition-colonization dynamics in an RNA virus. *Proceedings of the National Academy of Sciences*, **107**, 2108–2112.
- Ravigné, V., Dieckmann, U. & Olivieri, I. (2009) Live where you thrive: joint evolution of habitat choice and local adaptation facilitates specialization and promotes diversity. *The American Naturalist*, **174**, E141–E169.
- de la Riva, E.G., Tosto, A., Pérez-Ramos, I.M., Navarro-Fernández, C.M., Olmo, M., Anten, N.P., Marañón, T. & Villar, R. (2016) A plant economics spectrum in Mediterranean forests along environmental gradients: is there coordination among leaf, stem and root traits? *Journal of Vegetation Science*, **27**, 187–199.
- Rolski, T., Schmidli, H., Schmidt, V. & Teugels, J.L. (2009) *Stochastic processes for insurance and finance*, vol. 505. John Wiley & Sons.
- Sayama, T., Nakazaki, T., Ishikawa, G., Yagasaki, K., Yamada, N., Hirota, N., Hirata, K., Yoshikawa, T., Saito, H., Teraishi, M., Okumoto, Y., Tsukiyama, T. & Tanisaka, T. (2009) QTL analysis of seed-flooding tolerance in soybean (*Glycine max* [L.] Merr.). *Plant Science*, **176**, 514–521.
- Thabet, S.G., Moursi, Y.S., Karam, M.A., Graner, A. & Alqudah, A.M. (2018) Genetic basis of drought tolerance during seed germination in barley. *PloS one*, **13**, e0206682.
- Thompson, P.L., Guzman, L.M., De Meester, L., Horváth, Z., Ptacnik, R., Vanschotenwinkel, B., Viana, D.S. & Chase, J.M. (2020) A process-based metacommunity framework linking local and regional scale community ecology. *Ecology Letters*, **23**, 1314–1329.
- Tilman, D. (1994) Competition and Biodiversity in Spatially Structured Habitats. *Ecology*, **75**, 2–16.
- Villellas, J. & García, M. (2013) The role of the tolerance-fecundity trade-off in maintaining intraspecific seed trait variation in a widespread dimorphic herb. *Plant Biol (Stuttg)*, **15**, 899–909.
- Wang, G., Li, J., Ravi, S., Theiling, B. & Burger, W. (2021) Fire changes the spatial pattern and dynamics of soil nitrogen (N) and $\delta^{15}\text{N}$ at a grassland-shrubland ecotone. *Journal of Arid Environments*, **186**, 104422.

- Wang, G., Li, J., Ravi, S., Theiling, B.P. & Sankey, J.B. (2019) Fire changes the spatial distribution and sources of soil organic carbon in a grassland-shrubland transition zone. *Plant and Soil*, **435**, 309–321.
- Wilson, D.J., Western, A.W. & Grayson, R.B. (2004) Identifying and quantifying sources of variability in temporal and spatial soil moisture observations. *Water Resources Research*, **40**.

Chapter 3

Migration pulsedness alters patterns of allele fixation and local adaptation in a mainland-island model

Article published on BioRxiv: <https://doi.org/10.1101/2021.06.24.449762>
Submitted to *Evolution*.

**Flora AUBREE¹, Baptiste LAC¹, Ludovic MAILLERET^{1,2},
Vincent CALCAGNO¹.**

1. Université Côte d'Azur, INRAE, CNRS, ISA, 06900 Sophia Antipolis, France.
2. Université Côte d'Azur, INRIA, INRAE, CNRS, Sorbonne Université, BIOCORE, Sophia Antipolis, France

Acknowledgments The authors are grateful to the OPAL infrastructure from Université Côte d'Azur for providing resources and support to run stochastic simulations. They thank in particular the computation cluster NEF (Inria Sophia-Antipolis Méditerranée) and the cluster 'BPI' of ISA, Sophia-Antipolis. The authors thank Thomas Guillemaud for regular discussions and comments on the manuscript. FA was funded by a PhD fellowship from Université Côte d'Azur (IDEX "Investissements d'Avenir UCAJEDI", project reference n° ANR-15-IDEX-01).

Great things are not done by impulse, but by a series of small things brought together.

Vincent VAN GOGH

Abstract

Gene flow, through allele migration and spread, is critical in determining patterns of population genetic structure, divergence and local adaptation. While evolutionary theory has typically envisioned gene flow as a continuous connection among populations, many processes can render it fluctuating and intermittent. We analyze mathematically a stochastic mainland-island model in continuous time, in which migration occurs as recurrent “pulses”. We derive simple analytical approximations regarding how migration pulsedness affects the effective migration rates across a range of selection and dominance scenarios. Predictions are validated with stochastic simulations and summarized with graphical interpretations in terms of fixation probabilities. We show that migration pulsedness can decrease or increase gene flow, respectively above or below a selection threshold that is $s \simeq -\frac{1}{N}$ for additive alleles and lower for recessive deleterious alleles. We propose that pulsedness may leave a genomic detectable signature, by differentially affecting the fixation rates of loci subjected to different selection regimes. The additional migration created by pulsedness is called a “pulsedness” load. Our results indicate that migration pulsedness, and more broadly temporally variable migration, is important to consider for evolutionary and population genetics predictions. Specifically, it would overall be detrimental to local adaptation and persistence of small peripheral populations.

Keywords: Temporally variable migration, Effective migration rate, Stochastic simulations, Gene flow, Genomic signature, Migration load

3.1 Introduction

Gene flow between populations, as a major determinant of evolutionary dynamics, has received a large interest since almost a century. Depending on its intensity and interactions with other evolutionary forces, gene flow has a range of contrasting effects (e.g. Felsenstein, 1976; Lenormand, 2002; Bürger, 2014; Tigano & Friesen, 2016). In a focal population, it can enhance genetic diversity, prevent inbreeding, or on the contrary hamper local adaptation (Gomulkiewicz *et al.*, 1999; Garant *et al.*, 2007; Bürger & Akerman, 2011). Across populations, it controls the spatial spread of novel mutations, the maintenance of polymorphisms, the level of population divergence and, eventually, the possibility of speciation (e.g. Maynard-Smith, 1966; Johnson *et al.*, 2000; Yeaman & Otto, 2011; Mailund *et al.*, 2012; Rousset, 2013; Feder *et al.*, 2019). These effects have been studied in a range of spatial configurations, such as simply two interconnected populations (Maynard-Smith, 1966; Yeaman & Otto, 2011), mainland-island systems (Johnson *et al.*, 2000; Bürger & Akerman, 2011) or metapopulations (Slatkin, 1981; Rousset, 2013; Feder *et al.*, 2019).

However, temporal variability in the flows of propagules is rarely investigated in theoretical studies (Peniston *et al.*, 2019): the process of migration (here used in the sense of dispersal) is usually considered as constant, even though it is governed by time-fluctuating and potentially highly variable phenomena. As causes of temporal variability of migration rates, the most frequently cited phenomena can be classified in three categories. A first category relates to environmental variations. Geographical barriers can change depending on land bridges (Morris-Pocock *et al.*, 2016; Keyse *et al.*, 2018), sea levels fluctuations (Hewitt, 2000) or habitat fragmentation (Peacock & Smith, 1997).

Dispersal can also be affected by variation in oceanic and atmospheric (Renner, 2004; White *et al.*, 2010; Smith *et al.*, 2018; Benestan *et al.*, 2021; see also Catalano *et al.*, 2020 for a recent attempt to quantify dispersal variability). Last, but not least, dispersal is also affected by extreme meteorological or climatic events such as floods and storms (Reed *et al.*, 1988; Boedeltje *et al.*, 2004) that can provoke rafting events (Garden *et al.*, 2014; Carlton *et al.*, 2017). These extreme phenomena are bound to become more prevalent with climate change (Masson-Delmotte *et al.*, 2018). A second category includes variations caused by behavioral processes, such as ballooning (Bishop, 1990) or various forms of group or clump dispersal (Soubeyrand *et al.*, 2015). And finally, a third category encompasses variation related to dispersal by animal vectors (Yamazaki *et al.*, 2016; Martin & Turner, 2018) or human activities (through ballast waters for instance, see Carlton & Cohen, 2003). All three categories are known to result in variable dispersal rates, in the form of random fluctuations (Yamazaki *et al.*, 2016), intermittent flows (Hewitt, 2000; Keyse *et al.*, 2018) or episodic bursts of migration (Peacock & Smith, 1997; Reed *et al.*, 1988; Carlton & Cohen, 2003; Reiniers & Driese, 2004; Morris-Pocock *et al.*, 2016). The latter form is particularly common and is often referred to as “pulsed migration” (Boedeltje *et al.*, 2004; Bobadilla & Santelices, 2005; Folinsbee & Brooks, 2007; Smith *et al.*, 2018; Martin & Turner, 2018).

Despite the strong evidence for temporally variable migration patterns, comparatively little has been done theoretically to explore their consequences for population genetics and adaptation. Nagylaki (1979), Latter & Sved (1981) and Whit-

lock (1992) have all used discrete-time island models and considered neutral genetic variation only (infinite alleles model). All three concur in predicting that temporal variability in migration rates should decrease effective gene flow, and thus increase differentiation among populations (see also Rousset, 2013). In a two-population model, Yamaguchi & Iwasa (2013), and following papers, studied the fixation of incompatible mutations and the progress to allopatric speciation, and found that speciation occurred faster with variable migration. Some studies have investigated non-neutral cases in spatially heterogeneous environments, in particular in the context of source-sink population systems. Gaggiotti & Smouse (1996) found that spacing out migration events, while keeping the mean number of migrants constant, decreases the level of genetic variation in the sink population. Rice & Papadopoulos (2009) studied a mainland-island model and suggested that neglecting migration stochasticity would generally lead to overestimating the impacts of migration on adaptation. More recently, Peniston *et al.* (2019) extended the results of Gaggiotti & Smouse (1996), investigating the impact of temporally pulsed migration on the level of local adaptation in the sink population. They found that spacing out migration events (with a constant mean number of migrants) can either hamper or facilitate adaptation in a harsh sink environment, depending on genetic scenarios. In a different context, Matias *et al.* (2013) studied specific diversity in a metacommunity model, and found that with randomly fluctuating migration rates, larger mean dispersal values were needed to produce the same local species richness. Overall, these studies seemingly converge on a negative impact of dispersal variability on effective migration rate. However they remain few and limited in their scope. Most of them underline the need for more attention being given to the consequences of migration variability.

The present study aims at providing a more comprehensive appraisal of the consequences of temporal variability in migration, considering both neutral, beneficial and deleterious alleles, under various forms of selection and levels of dominance. We will consider a mainland-island system where a small island population receives migrants from a large mainland population (Wright, 1931; Felsenstein, 1976; Bürger, 2014). In the island population, we will model the dynamics of allele fixation in continuous time, at one locus, in diploid individuals. We will focus on the case of “pulsed” migration patterns, i.e. gene flow from the mainland occurs as bursts of migration of variable size and frequency (Rice & Papadopoulos, 2009; Peniston *et al.*, 2019, e.g.). We explore the range of migration “pulsedness” from continuous migration (independent migration of individuals) to very pulsed migration (rare migration of groups of individuals).

A simplified mathematical model using a low-migration limit is introduced and analyzed. We derive a simple graphical criterion that allows to predict how the level of migration pulsedness affects the effective migration rate. Predictions are validated with Monte-Carlo simulations that relax timescale separations and explicitly describe the stochastic demography of the island population.

We show that in the neutral case, migration pulsedness reduces the effective migration rate (negative impact), decreasing the rate of allele fixation. However, with selection, this conclusion can change quantitatively and even reverse. When the selection coefficient falls below some threshold value, we show that the qualitative impact of migration pulsedness can switch sign, so that the effective migration rate increases for deleterious alleles. This threshold is approximated as $s = -\frac{1}{N}$

for co-dominant alleles, and becomes lower for recessive deleterious alleles. Moreover, for sufficiently recessive deleterious alleles, migration pulsedness can have a non monotonous effect on the effective migration rate. The interplay of selection, dominance and drift is thus found to play an essential role in determining the effect of migration variability on effective migration rate.

Our results indicate that the effect of migration pulsedness is not uniform across loci subject to different selection regimes and dominance levels. The predictions obtained generalize several earlier theoretical results derived for specific contexts. More practically, we show migration pulsedness effectively homogenizes the fixation rate across the genome. This impacts the dynamics of genetic load and creates an additional migration load that we call the “pulsedness” load. Migration pulsedness thus leaves a characteristic signature across the genome, which could be detected using available genomic data. Overall, our results highlight migration variability as an important aspect of gene flow to be taken into account. Specifically, pulsed migration patterns would overall be less conducive to local adaptation and persistence of small peripheral populations.

3.2 Methods

3.2.1 Mainland-island model

A very large mainland population is supposed to send migrant individuals into a small island population of finite size N . Individuals are diploid (so that we consider $2N$ alleles) and mate randomly within the island population. We consider an arbitrary locus at which some allele A is fixed in the mainland whereas some other allele a is fixed, initially, in the island population. The three possible genotypes AA , Aa and aa have fitness values $1 + s$, $1 + hs$ and 1 in the island population, with $h \in [0, 1]$ the degree of dominance as usually defined (Thurman & Barrett, 2016). Note that our results also apply to haploids if one considers genic selection ($h = 0.5$) and takes the number of genes to be N rather than $2N$. For simplicity, mutation is neglected. The system is modelled in continuous time (overlapping generations, Moran, 1962), with a stochastic logistic demography that is assumed to bring populations back to their carrying capacity following a migration event.

Migration occurs as discrete migration events (pulses of migrants) corresponding to the arrival of n individuals into the island population, which (transiently) takes the total population size to $N + n$ (see Yamaguchi & Iwasa, 2013, for a similar description of migration). The overall intensity of migration is controlled by the migration rate m , the mean number of migrants per unit of time. We impose that the more individuals arrive per migration event (the larger n), the less frequent are migration events, such that the mean number of migrants per unit of time m stays constant. The frequency of migration events is thus m/n . For a given migration rate m , we consider increasing migration pulsedness levels, from $n = 1$ to larger and less frequent packs of migrants reaching the island ($n > 1$). The case $n = 1$, corresponding to the steady and independent migration of individuals (“continuous migration”), is taken as a reference against which the consequences of migration pulsedness will be evaluated.

The degree of migration pulsedness is thus quantified by parameter n . The number of migration events occurring over a period of time T_e is assumed to follow

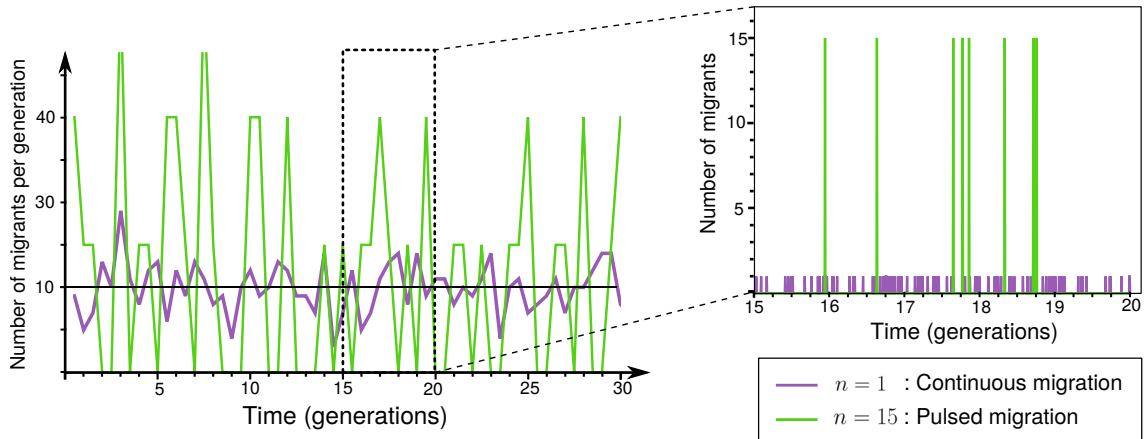


Figure 3.1: Number of migrants as a function of time in the continuous case ($n = 1$, independent migration of individuals) and in a pulsed migration case ($n = 15$). The left panel averages the number of migrants over 1 generation. The right panel is a close-up over 5 generations, showing the arrival of individual migrants at each migration event.

a Poisson distribution with rate m/n so that a mean of mT_e/n migration events occur per unit time, with variance also equal to mT_e/n . The variance in the number of migrants ($n \times mT_e/n$) over that period is then $n^2 mT_e/n = nmT_e$. Parameter n thus quantifies the degree of overdispersion (variance inflation) in the number of migrants per unit of time, relative to the continuous case. Under this model, migration events thus range from very frequent and of small intensity, with minimal temporal variance in the number of migrants per generation (low n), to very infrequent and intense, with large temporal variance in the number of migrants per generation (large n ; see Fig. 3.1b).

To reflect the isolation of the island population and avoid regimes in which its dynamics is entirely overtaken by migration (in which case genetic homogenization is a trivial matter), the migration rate m should have small enough values. More precisely, if the average generation time (here intended as the average time for N selective deaths to occur, see Moran, 1962) is T , then mT should be no greater than roughly 1–10. This corresponds to the “one migrant per generation rule” (Mills & Allendorf, 1996, see also Blanquart *et al.*, 2013).

We are interested in how the fixation of mainland alleles on the island varies with the pulsedness level n , across population sizes (N) and selection parameters (s and h). In both the following mathematical analysis and stochastic simulations, we will derive and calculate this fixation rate. Then, to facilitate comparisons across parameter values, we will compute, in both methods too, the effective migration rate m_e , defined as the migration rate that would produce exactly the same allele fixation rate if migration were continuous (i.e. $n = 1$). This definition is a variant of other definitions (Wang & Whitlock, 2003; Kobayashi *et al.*, 2008; Rice & Papadopoulos, 2009) adapted to our study of migration pulsedness. The value of m_e is m when $n = 1$, and deviates from m for larger n . If, for some level of migration pulsedness, m_e is larger (resp. lower) than m , we will say that the effect of pulsedness is positive (resp. negative).

The next two paragraphs describe (i) the deterministic mathematical model with its related assumptions, and (ii) the stochastic simulation model, in which some of

these assumptions can be relaxed.

3.2.2 Mathematical analysis

To render the model analytically tractable, we make the usual assumption that demography (population regulation) is relatively fast, so that population size is effectively constant at N in the island. However we cannot employ, as is also usual in population genetics, a diffusion approximation. The latter would imply making n very small relative to N , *de facto* preventing the investigation of pulsed migration patterns (see Kimura, 1962; Yamaguchi & Iwasa, 2013). Instead, we use another approximation, by assuming that migration events are sufficiently rare (m/n is small enough), so that genetic drift and selection would typically result in fixation or loss before the next migration event occurs. Formally, this time scale separation holds if the average time between two migration events (n/m) is much larger than the average time to fixation after one migration event. From classical population genetics theory (Kimura & Ohta, 1969; Whitlock, 2003; Otto & Whitlock, 2013), we can show that, in the case of $n = 1$ and $s = 0$ (the most unfavorable case in terms of fixation time), this holds if $m \ll \frac{1}{4NT}$ (see S.I. section C.1.1). This condition is conservative: the time scale separation is more easily satisfied when $s \neq 0$ or $n > 1$. We can see that this mathematical constraint is smaller than the “one migrant per generation rule” constraint introduced above ($mT < 1-10$) by a factor $4N$ (i.e. by 2–3 orders of magnitude for the N values we will consider).

Under these assumptions, at each migration event, n homozygous AA individuals arrive into the island population containing N aa individuals. The initial frequency of the incoming allele is $f = \frac{2n}{2n+2N} = \frac{n}{N+n}$ and the fast population regulation quickly takes population size back to N . There are two possible outcomes after such a migration event: either the mainland allele goes to fixation (the migration event is said to be a success), or it disappears and we revert to the initial state (failure) (see also Yamaguchi & Iwasa, 2013). The mainland allele ultimately gets fixed in the island population, as soon as the first successful migration event occurs. The probability that the mainland allele has not yet gotten fixed decreases exponentially in time depending on the rate of migration events (m/n) and on the probability of success of each particular event. The latter is well described by the fixation probability of an allele with initial frequency f in an isolated population of size N , written $u(f, N, s, h)$. Expressions of u can be readily obtained from classical diffusion approximations (Kimura, 1962; Whitlock, 2003). To simplify notations, we write interchangeably $u(f)$ or $u(f, N, s, h)$.

3.2.3 Simulations

In addition to the analysis of the mathematical model presented above, we also performed simulations to validate predictions. We simulated an island population receiving migrants from the mainland as a continuous time birth-death-immigration process, using a Gillespie algorithm. The population dynamics of the island population follows a stochastic logistic model with carrying capacity K (Goel & Richter-Dyn, 1974). Each diploid individual has some basal death rate d , birth rate $b = d$, and density dependence acts through a larger increase in death rate than in birth rate with population density (the death rate is equal to $d\frac{N^2}{K}$ while the birth rate

is equal to bN). Selection occurs at reproduction (fertility selection). See S.I. section C.1.2 for a detailed description of the model.

The island is initially fixed for allele a and at carrying capacity $N = K$. At the beginning of a simulation it starts receiving AA migrants from the mainland under the stochastic migration process described above. A simulation ends when allele A gets fixed in the island. We conducted 10,000 replicates per parameter set to capture the stochasticity in migration times, population size, and genetic drift. To speed up simulations, we optimized the Gillespie algorithm as explained in the S.I. section C.1.2. Effective migration rates were calculated from the realized fixation times using a pre-calculated abacus that returns m_e as a function of fixation time (see S.I. section C.4 for details and examples).

We systematically varied selection parameters h (from 0 to 1) and s (from -0.05 to 0.05 , see Thurman & Barrett, 2016), the carrying capacity N (from 50 to 200, see Palstra & Ruzzante, 2008; Peniston *et al.*, 2019), and migration rate m . Having chosen that the duration T of a generation is 1 (with $d = N$, see Moran, 1962), we vary m from 0.001 (which fits the mathematical assumptions), to 10 (which deviates from it by three orders of magnitude).

3.3 Results

3.3.1 A general criterion to predict the impact of migration pulsedness

Under our simplifying mathematical assumptions, the fixation rate of the mainland allele equals the product of the migration event rate (m/n) and the probability of success $u\left(\frac{n}{N+n}\right)$ of a particular migration event. By definition of the effective migration rate, we thus have $\frac{m_e}{1}u\left(\frac{1}{N+1}\right) = \frac{m}{n}u\left(\frac{n}{N+n}\right)$. It follows that $m_e > m$ (i.e. pulsedness has a positive effect) if and only if:

$$u\left(\frac{n}{N+n}\right) > nu\left(\frac{1}{N+1}\right) \quad (3.1)$$

This amounts to comparing $u\left(\frac{n}{N+n}\right)$ (the probability of fixation of $2n$ allele copies immigrating in a single migration event) to n times $u\left(\frac{1}{N+1}\right)$ (the mean number of copies that would have fixed had they arrived as n independent events). In other words, the criterion determines whether the probability of fixation (through genetic drift and selection) from a group of migrants is sufficiently greater than that from a single migrant to compensate for the reduced frequency of migration events.

The fixation probability u is a monotonically increasing function from zero to one as $n \rightarrow \infty$ (Kimura, 1962). Compared to the linearly increasing term $nu\left(\frac{1}{N+1}\right)$ (eq. 3.1), it is inevitably lower for large enough values of n , i.e. there is some n_1 value beyond which pulsedness will always have a negative effect.

If function u is strictly concave, there is no other crossing point. This is true for frequency-independent selection and non-additive allelic effects in diploids (Kimura, 1962; Whitlock, 2003). Therefore there are only two possibilities: either $u\left(\frac{n}{N+n}\right)$ is always below $nu\left(\frac{1}{N+1}\right)$, and migration pulsedness always has a negative effect, i.e. it reduces the effective migration rate (case A, see fig. 3.2), or it can be initially greater than $nu\left(\frac{1}{N+1}\right)$, and falls below at $n = n_1$ (case B, see fig. 3.2). In that

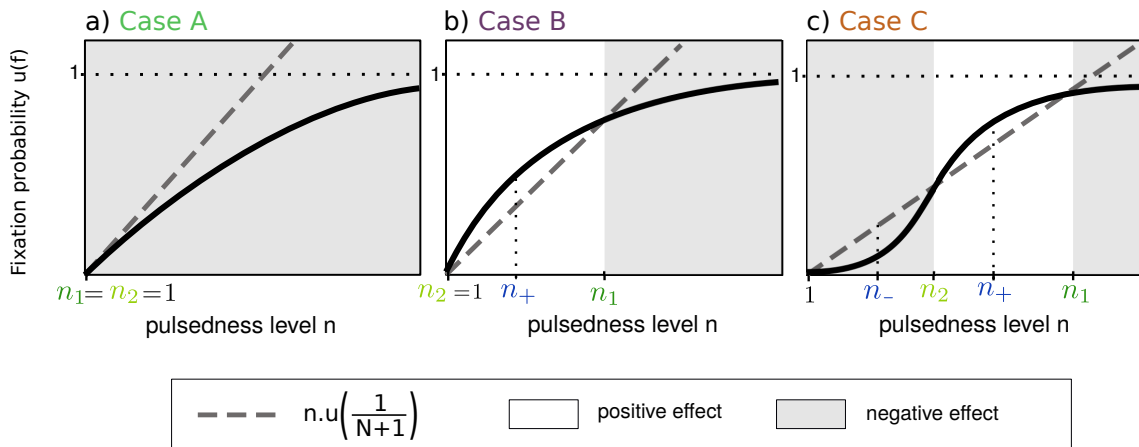


Figure 3.2: Graphical criterion to predict the effect of migration pulsedness (positive or negative) on the effective migration rate. The three panels represent the three possible situations. The effect is either always negative (case A) or depends on the value of n (cases B and C). n_1 and n_2 corresponds to the pulsedness values which have the same impact on fixation rate as a continuous migration. n_+ (resp. n_-) corresponds to the pulsedness value which maximizes resp (minimizes) the effective migration rate. $f = \frac{n}{N+n}$.

case, migration pulsedness on the contrary has a positive effect, i.e. it increases the effective migration rate, on $(1, n_1)$. The bifurcation from case A to case B occurs when the initial slope of $u(f)$ with respect to n becomes greater than $u\left(\frac{1}{N+1}\right)$.

More generally, function u can have an inflexion point and switch from convex to concave. This can occur when there is negative frequency-dependent selection, e.g. for recessive deleterious mutations in diploids (Kimura, 1962). In that case (case C, fig. 3.2), a second crossing point n_2 can exist, so that migration pulsedness can have a positive effect (increase the effective migration rate) for an intermediate range of pulsedness levels ($n_2 < n < n_1$). Bifurcations may occur from case C to case B (n_2 collapses into $n = 1$) or from C to A (n_1 and n_2 annihilate each other). This is the entire set of possibilities.

In addition to the threshold values n_1 and n_2 , one value of interest is n_+ , the pulsedness level that maximizes the effective migration rate m_e compared to m (or mathematically, which maximizes the positive difference between $u\left(\frac{n}{N+n}\right)$ and $nu\left(\frac{1}{N+1}\right)$). It is different from 1 only in cases B and C (fig. 3.2). Similarly, we can define n_- , a value that minimizes m_e compared to m , which is different from $+\infty$ in case C only.

This general criterion allows to determine the consequences of migration pulsedness for any type of genetic variation, using simple graphical arguments. We will apply it to specific cases just below.

3.3.2 Neutral alleles

The fixation probability for neutral alleles is known to be (Otto & Whitlock, 2013):

$$u(f) = f$$

In that case, it is clear that $\frac{n}{N+n} < n\frac{1}{N+1}$ for all $n > 1$. Thus, migration pulsedness should invariably decrease the effective migration rate (case A, fig. 3.2a). Simulations

(blue points fig. 3.3a) confirm this mathematical prediction (for $m = 0.001 < \frac{1}{4NT}$), which continues to hold when moving out of the mathematical limits (for $m = 0.1$).

Intuitively, this result can be explained by greater competition among A alleles in the case of pulsed migration. The rate of migration events is inversely proportional to n , but the initial frequency of migrant alleles (and thus the fixation probability) increases less than linearly with n . As a result, the former effect dominates and the effective gene flow drops as n increases. The less-than-linear increase of probability of success is caused by n in the denominator of f : it represents the fact that with pulsed migration, packs of immigrant alleles do not only compete with resident alleles, but also among themselves, and more and more so as pulsedness increases. It is therefore less efficient, per capita, for alleles to arrive in a clustered way, rather than being more temporally interspersed.

3.3.3 Alleles under selection with co-dominance

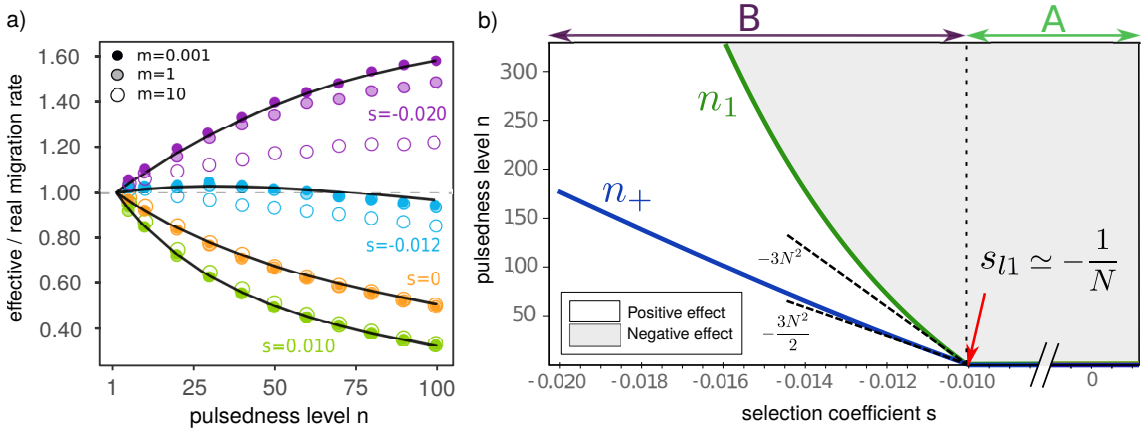


Figure 3.3: Neutral and co-dominance cases. (a) Effective migration rate (relative to real migration rate m) as a function of n , for different selection coefficients s and three migration rates. Solid lines are mathematical predictions and dots are simulated values. Here, $N = 100$. The dashed line at 1 corresponds to case in which the effective migration rate is equal to the real migration rate. Above this line, the effect of migration pulsedness is positive, below it is negative. (b) Summary of curves for any s . The green solid line represents the theoretically expected n_1 curve as a function of s , and the blue one shows n_+ . Dashed lines indicate the slopes of n_1 and n_+ at $s = s_{l1}$. Note that the slopes are pretty high (this figure zooms around $s = -1/N$), to the order of 100,000. Here, $N = 100$.

With co-dominance ($h = 1/2$), or frequency-independent selection in haploids, the probability of fixation can be expressed as

$$u(f) = \frac{1 - \exp(2Nsf)}{1 - \exp(2Ns)}$$

This expression is derived from a diffusion approximation that requires large enough population sizes (Kimura, 1962; Maruyama, 1970; Whitlock, 2003).

In this case, function u is concave, and criterion (3.1) thus follows either case A (fig. 3.2a) or case B (fig. 3.2b), depending on the selection coefficient s . The switch from case A (as for neutral alleles) to case B occurs for some negative value

of s called s_{l1} . Alleles that are sufficiently selected against ($s < s_{l1}$) fall into case B: migration pulsedness increases the effective migration rate, at least for small levels of pulsedness (i.e. if $n < n_1$). All other cases (slightly deleterious or beneficial alleles) yield case A and the same qualitative predictions as for neutral alleles. Overall, migration pulsedness favors the fixation of deleterious alleles and it disfavors the fixation of beneficial alleles. Doing so, alleles least likely to establish (deleterious) are favored, while alleles most likely to establish (beneficial) are disfavored. This results in a homogenisation of responses across alleles which carry different selection coefficients.

Through a local approximation around $n = 1$ and $s = 0$ (see S.I. section C.3 for details), we can show that $s_{l1} \approx -\frac{1}{N}$ (fig. 3.3b). This indicates that counter selection must be strong enough relative to drift for a positive effect of migration pulsedness to arise (see also Wright, 1931; Lande, 1994). Furthermore, close to s_{l1} , $n_1 \approx 2n_+$ (see S.I. section C.3) and both slopes are pretty steep, of the order of N^2 (fig. 3.3b). The transition is very sharp, and the value of n_1 quickly becomes very high. This means that case B will in practice correspond to a positive effect of migration pulsedness for alleles with $s < s_{l1}$, since the values of pulsedness required for the effect to revert to negative are most of the time unrealistically elevated ($n = 100$ or more; see fig. 3.3b).

These predictions were verified in stochastic simulations (fig. 3.3a). Simulations made close to the mathematical limit ($m = 0.001$) show very good quantitative agreement (see also S.I. section C.6.2), which remains rather good even 3 orders of magnitude away from it ($m = 1$). It is only when reaching the “one migrant per generation” limit ($m = 10$) that quantitative deviations appear, especially for negative s values. As m increases beyond our mathematical assumptions, positive effects of pulsedness are weakened or shifted to more negative s values (fig. 3.3a). In all cases, mathematical predictions are qualitatively well supported.

An increase in population size influences the above predictions in two ways: by making s_{l1} closer to zero, and by increasing the slopes of n_1 and n_+ (fig. 3.3b). Therefore, larger population sizes make positive effects of migration pulsedness more likely, all else being equal. Approximately, figure 3.3 becomes almost invariant to population size if rescaling both axes by N , i.e. in terms of n/N and Ns (see S.I. fig. C.4). This indicates that predictions are largely controlled by the relative level of migration pulsedness n/N and the balance between selection and drift (Ns ; Wright, 1931; Lande, 1994).

3.3.4 Introducing dominant and recessive alleles

An expression for function u in the general case of any dominance is

$$u(f) = \frac{\int_0^f G(x)dx}{\int_0^1 G(x)dx}$$

with $G(x) = \exp[2Ns((2h - 1)x^2 - 2hx)]$ (Kimura, 1962).

As long as the level of dominance h is higher than a threshold value h_c (fig. 3.4), whose value is numerically found to be $h_c \simeq 0.326$, predictions are qualitatively identical to the case of co-dominance (i.e. a pattern involving cases A and B). The main quantitative difference is that the value of s_{l1} gets closer to 0 as h increases (s_{l1} depends on h): it is therefore slightly more likely to have a positive effect of

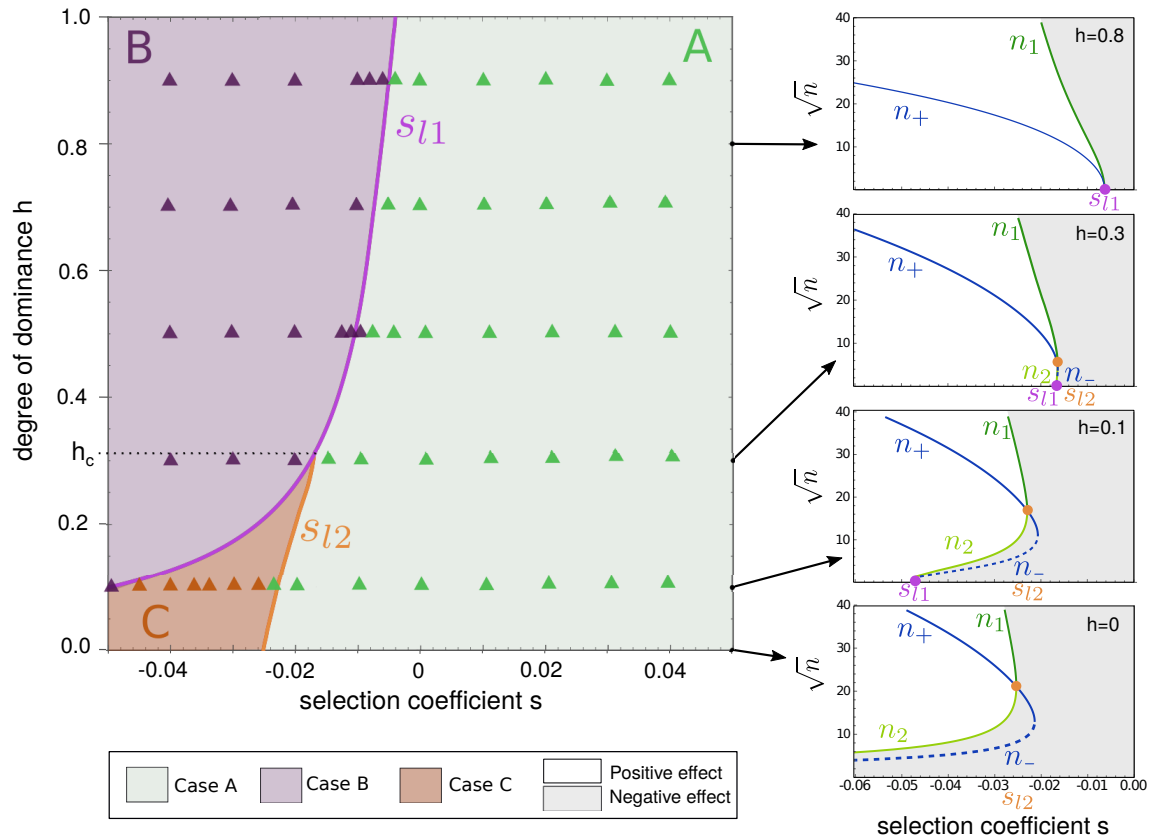


Figure 3.4: The effect of migration pulsedness as a function of selection coefficient s and dominance h . The plane is partitioned according to the pattern (case A, B or C) predicted by the mathematical model. Details can be found in S.I. section C.2. Simulation results are shown as triangles whose color corresponds to the observed pattern. Subpanels are cross-sections of the left panel for four specific values of dominance ($h = 0.8$, $h = 0.3$, $h = 0.1$ and $h = 0$), similar to figure 3.3b. Note the square-root y-scale in the subpanels.

migration pulsedness for dominant deleterious alleles than for recessive deleterious alleles.

In contrast, predictions differ qualitatively if h moves below h_c : moving from positive to negative s values, we first have a bifurcation from case A to case C (at another threshold value s_{l2} , that also depends on h), and then a bifurcation from case C to case B (at s_{l1}). The positive effect of migration pulsedness first appears (at s_{l2}) for intermediate values of n (A \rightarrow C bifurcation; orange line in fig.3.4) instead of low n , i.e. it requires a minimal level of pulsedness to occur. When $s < s_{l1}$ however (after the C \rightarrow B bifurcation; purple line in fig.3.4), the positive effect occurs for any n , as was the case for less recessive alleles. For deleterious mutations that are fully recessive ($h = 0$), case C is the rule (when $s < s_{l2}$). However, as the minimal level of pulsedness required to get a positive effect is quite large ($n_2 = 40$ – 100) in most cases, the effect would always be negative in any practical sense. Overall, when alleles are more recessive, positive effects occur under more restricted conditions (greater pulsedness levels and/or stronger counter-selection).

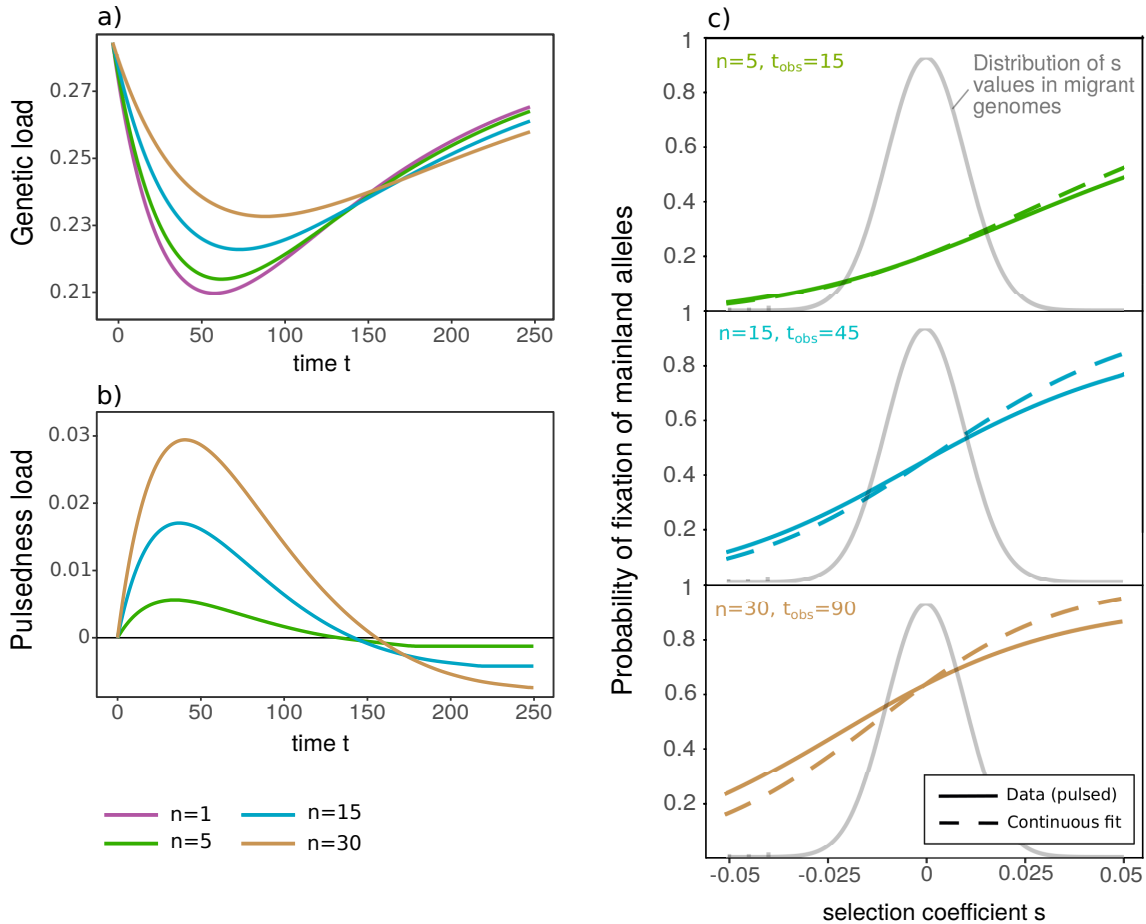


Figure 3.5: Genetic load (a) and pulsedness load (b) in the island population, as a function of time after onset of migration, for different levels of migration pulsedness (n). A large amount of unlinked loci were considered throughout the genome, with a distribution of s values normal, centered on 0, and with standard deviation 0.01 (grey curve in (c)). Pulsedness load is first positive, when mostly non maladapted alleles fixate, then negative, when mostly maladapted alleles are left to fixate, and eventually tends to zero when all mainland alleles have fixed. (c) Genomic signature of pulsedness. Continuous fits (assuming $n = 1$; dashed lines) of synthetic datasets (probabilities of fixation of mainland alleles), as a function of s . Synthetic datasets were generated from the mathematical model (i.e. in the limit $m \rightarrow 0$), for the same distribution of s values (grey curve) as used in (a) and (b), and for three pulsedness levels (5, 15 and 90). Population size was $N = 60$ and the time of observation t_{obs} was set so that three migration events or more have occurred on average in each case. More (or less) dramatic differences can be observed for other choices of t_{obs} . Population size N and elapsed time t_{obs} were treated as unknown and estimated by maximum likelihood (see S.I. section C.8 for details). The best continuous fits returned estimated parameters $N' = 60$ and $t'_{obs} = 14.2$ (for $n = 5$), $N' = 59$ and $t'_{obs} = 35.7$ (for $n = 15$), and $N' = 57$ and $t'_{obs} = 58.2$ (for $n = 30$). The best continuous fit

3.3.5 Mean fitness and pulsedness load

An overarching result is that migration pulsedness homogenises fixation over loci subjected to different types of selection (see previous section), and this has important

consequences at the level of entire genomes. In particular, it impacts the dynamics of genetic load. Genetic load at time t is defined as the relative difference in between the maximum fitness value theoretically reachable and the mean absolute fitness actually obtained at this time (see S.I. section C.7.2 for more details). Once an island population is subjected to gene flow from the mainland, beneficial alleles establish first (increasing the fitness), followed by neutral alleles, and eventually deleterious alleles. To illustrate this, we consider a large number of independent (unlinked) loci in the genome, whose selection coefficients follow a normal distribution centered on $s = 0$. As expected, we observe that the genetic load initially declines and eventually goes up again (fig. 3.5a). This dynamics will differ depending on the level of migration pulsedness, because the latter affects allele fixation rate in different ways depending on s . As migration is more pulsed, the initial decline of genetic load is slower, the minimal load value is larger and its occurrence is delayed in time, and the eventual increase is also slower (fig. 3.5a).

As a consequence, the level of genetic load at any time depends on the level of migration pulsedness. This results in a “pulsedness load” (fig. 3.5b), i.e. an additional component of genetic load brought about by the pulsed nature of migration (the difference in between the genetic load in the pulsed and in the continuous cases). This pulsedness load may account for a non negligible part of the total load ($> 10\%$ in the example of figure 3.5). Variations of the pulsedness load will of course depend on the distribution of allelic effects among migrants (see fig. C.6 in S.I.). The positive part of pulsedness load will be most important if migrants carry a large proportion of either beneficial (for which n decreases m_e , see fig.3.4) or relatively strongly deleterious mutations (for which n increases m_e , see fig.3.4). Thus, in most cases, migration pulsedness would promote maladaptation and counteract local adaptation (see fig. C.6 in S.I.). Note that in the example presented in figure 3.5, the pulsedness load becomes negative, reflecting the point at which deleterious but still pulse-disadvantaged alleles ($s_{l1} < s < 0$) fix. See figure C.6 in S.I. for other examples with a different distribution of selection coefficients for mainland alleles.

3.3.6 The genomic signature of pulsedness

As migration pulsedness has a negative effect on the effective migration rate for all neutral and beneficial alleles (fig. 3.4), it would typically lower the overall genomic migration rate. Obviously, if one had independent estimates of the migration rate (m), it would be rather straightforward to detect migration pulsedness by comparing observed fixation rates with those predicted under continuous migration. However, it is notoriously difficult to estimate average migration intensity, and such information is most often lacking (Wang & Whitlock, 2003). Even so, the inhomogeneous impact of migration pulsedness across loci might leave a distinctive fingerprint in the genome (a genomic signature), compared to continuous migration regimes. To detect this, one would need genomic data to assess the fixation status (or frequency) of mainland alleles in the island population, at many independent loci, at some point in time. In addition, one should know, or have an indication of, the type of selection that those loci experience (ideally, a range of h and s values). One could then compare the fixation rates across loci in order to detect the homogenizing effect that migration pulsedness introduces. This can be achieved by fitting the observed frequencies with

a model that assumes continuous migration, and test whether the data deviate from the model in the predicted direction.

The principle of this approach is illustrated in Figure 3.5c. We assumed a Gaussian distribution of selection coefficients of mainland alleles, centered on $s = 0$, across a large amount of independent biallelic loci in the genome. For simplicity, all alleles were assumed co-dominant ($h = 0.5$). Using the mathematical model, we generated artificial datasets (probabilities of fixation at each locus; see S.I. section C.7.1) under different levels of migration pulsedness, and fitted these data with the continuous ($n = 1$) model by maximum likelihood (see S.I. section C.8). Unknown parameters were: population size N , migration rate m , and time since onset of migration t_{obs} (see S.I. section C.8 for details).

As shown in Figure 3.5c, for low levels of migration pulsedness ($n = 5$), simulated datasets can be fitted quite well with a continuous migration model. However, as migration gets more pulsed ($n = 15$ or 30), the best continuous fit obviously deviates from the simulated data (in addition to yielding biased parameter estimates for migration rate and time since onset of migration; Figure 3.5). Specifically, it overestimates the fixation of beneficial alleles and underestimates the fixation of deleterious alleles, as predicted (fig. 3.5). It might therefore be possible to construct an operational statistical test that exploits this signal to detect migration pulsedness from genomic snapshots.

3.4 Discussion

Temporal variability in migration is likely pervasive in nature. Plants, fungi, seashells, birds and marine invertebrates are most represented in the literature about variable dispersal, but there is no reason that other taxa would not be concerned, including hominoids (Folinsbee & Brooks, 2007). Yet classical evolutionary theory largely rests on the assumption of constant migration rates (Johnson *et al.*, 2000; Yeaman & Otto, 2011; Mailund *et al.*, 2012; Rousset, 2013; Peniston *et al.*, 2019, e.g.). Considering the growing evidence for non-constant migration processes, it is important to gain a general theoretical understanding of their evolutionary consequences.

We here focused on pulsed migration patterns (Yamaguchi & Iwasa, 2013; Peniston *et al.*, 2019). Albeit a specific form of migration variability, it is arguably quite common, and it allowed us to make significant analytical progress. Furthermore, given our stochastic modelling framework, which makes migration pulses randomly distributed in time, and based on our mathematical results, we can reasonably expect our predictions to apply more broadly to other forms of “variable” migration patterns, intended as a temporal overdispersion in the number of migrants per generation.

Confirming this, our predictions for neutral alleles are consistent with the few earlier population genetics analyses, which used modelling approaches entirely different from ours (Nagylaki, 1979; Latter & Sved, 1981; Whitlock, 1992; Rousset, 2013). Indeed, for neutral variation, we found higher levels of migration pulsedness to decrease the effective migration rate, all else being equal. In our model, the interpretation is that a larger initial frequency of immigrant alleles less than compensates for the accompanying lower frequency of migration events, so that the overall effect of pulsedness on fixation rate is negative. This is because migrant alleles arriving clustered in time compete more among themselves, compared to when arriving more

evenly spaced out in time.

Unlike earlier analyses though, our approach is able to address arbitrary forms of selection, not just neutral alleles. Importantly, predictions were found to depend quantitatively, but also qualitatively, on the type of selection. The qualitative prediction that migration pulsedness negatively impacts gene-flow remains true for beneficial alleles, even though the effect size increases with selection, and for slightly deleterious alleles. This means that, for those selection scenarios, we overestimate the consequences of migration if we omit to consider its variability (see also Rice & Papadopoulos, 2009). However, for deleterious alleles, the effect weakens and at some point switches sign. For sufficiently strong counter-selection (below $s \approx -1/N$ for additive alleles, a value reminiscent of the selection-drift balance; Wright, 1931), the effect of migration pulsedness switches to positive: pulsedness now increases the effective gene flow. This prediction radically differs from predictions based on neutral alleles.

Results with selection can be understood by the contribution of migrant alleles to the mean fitness at their locus. Compared to neutral alleles, beneficial alleles arriving in a more clustered way increase the mean fitness, thereby reducing their per-capita advantage, which further reduces the effective gene-flow. In contrast, deleterious alleles arriving in a pulsed manner lower the mean fitness, thereby alleviating their per-capita selective disadvantage. For sufficiently counter-selected alleles, this positive effect of lowering the mean fitness exceeds the negative effect of competing with identical alleles, switching the overall effect of the fixation probability to positive.

Selection was not the only genetic factor determining the impact of migration pulsedness. The dominance level (h) was also found to impact the results, in qualitative terms. Results are qualitatively similar for dominant alleles, with a slight tendency of positive effects of pulsedness to be more prevalent as h increases. In contrast, results for recessive alleles, especially below $h = 0.3$, differ significantly. In quantitative terms, stronger selection values are required to obtain the same results as for co-dominant alleles, presumably due to the fact that recessive alleles are 'hidden' in heterozygotes at low frequencies. Moreover, there is a qualitative difference for recessive deleterious alleles: positive effects of migration pulsedness may also require migration to be sufficiently pulsed. In other words, migration pulsedness has a non-monotonous effect on gene-flow for those alleles, and there exists a minimum level of pulsedness above which the effect switches from negative to positive. This result echoes those of Peniston *et al.* (2019), who found that pulsedness levels were favorable to local adaptation in some intermediate pulsedness scenarios, in particular when considering density-dependent selection. It is interesting to note that the threshold value of dominance we found ($h = 0.3$) is close to the average value of dominance for mildly deleterious mutations in data and theory, as reported by Manna *et al.* (2011).

Our mathematical results were derived from a low-migration limit and with constant population size, but were found to hold in stochastic simulations with not-so-low migration and population size fluctuations. In general, increasing the overall migration rate shifted the predictions toward a negative effect of migration pulsedness on gene-flow (Fig. 3.3). This is presumably caused by the direct contribution of migration to fixation in those cases (a "mass effect"), which increases the relative importance of selection/drift, and is unaffected by pulsedness. This mass effect, i.e. the fact that migrant alleles persist and accumulate over consecutive migration

events, can indeed explain the observed shift towards larger values of Ns . Mathematically speaking, an increase in initial frequency of migrant alleles due to the mass effect is equivalent to a decrease in population size (see S.I. section C.6.1). It thus requires higher values of N (or s) to get the same effects of migration pulsedness (see S.I fig. S4).

From a whole-genome perspective, the overarching result is that migration variability homogenizes the effective migration rate across alleles with different selection coefficients: it increases it for counter-selected alleles, and reduces it for positively selected alleles. As a consequence, throughout the genome, the fixation of beneficial variation will be slowed down, while the fixation of deleterious and maladaptive variation will be promoted. Obviously, the net impact on average population fitness will generally be negative, with higher levels of genetic load. We call this additional component of genetic load brought-up by the pulsed nature of migration the “pulsedness load”. More pragmatically, the differential impact of migration pulsedness on different loci might be used as a detectable signature in genomic data. One can distinguish loci with different selection pressures in the focal population. With a single snapshot of allelic frequencies (or fixation probabilities) at those many different loci across the genome provided, it may be possible to fit a continuous-migration model, and detect the homogenization of fixation rates caused by migration pulsedness, as exemplified in figure 3.5. Of course, building such a statistical test and evaluating its power and applicability is beyond the scope of this article. Still, the approach has the advantage of requiring allele frequency data only, e.g. pool-seq data and Site Frequency Spectrums (SFSs), that are increasingly available for a broad range of organisms. Existing methods to infer migration pulses would typically use individual genome sequences or haplotypes to detect repeated admixture events, and exploit neutral variation only (Marchi *et al.*, 2021). The approach we sketched out here could thus provide a way to improve our methodological arsenal to infer the occurrence of pulsed migration from genomic data.

Our results have direct implications for biological conservation, population management and island biology. For instance, population reinforcement usually takes the form of periodic releases of groups of individuals, whose frequency and intensity must both be optimized. Our results suggest that rare introductions of relatively large numbers of individuals, i.e. pulsed introduction patterns, would favor the spread into the focal population of deleterious mutations, and disfavor the establishment of favorable mutations. In short, it is detrimental to population fitness and local adaptation, relative to more continuous fluxes of individuals, possibly compromising population viability and persistence. Of course, this impact would combine with other effects, in particular demographical effects. It has been shown for instance that in small populations subject to Allee effects, pulsed migration patterns can be favourable to population establishment and persistence (Rajakaruna *et al.*, 2013; Bajeux *et al.*, 2019). Similarly, Peniston *et al.* (2019) analyzed the impact of migration pulsedness for small peripheral populations that are demographic sinks. In the case most similar to our assumptions, Peniston *et al.* (2019) observed that migration pulsedness could promote local adaptation, in superficial contradiction with our results for strongly deleterious alleles. However, to our results the population was small but viable, whereas in theirs, the sink population was sustained through gene-flow only. This implies that the overall migration rate, i.e. the “mass effect”, had to be strong. Since for large values of m , we showed that predictions are shifted

towards negative effects of pulsedness, the results of Peniston *et al.* (2019) are in fact consistent with our predictions. These examples underline how complex it is to determine an optimal management policy when demo-genetics effects are taken into account.

Our conclusions extend to broader scenarios as well. For instance, it is relatively easy to apply our approach to the case of two diverging populations, connected by bi-directional migration, and undergoing mutation (not shown in this article). The main conclusions are similar: more pulsed migration patterns would reduce the level of local adaptation and hamper adaptive divergence, while promoting neutral genetic divergence reducing the spread of commonly beneficial mutations. This shows how migration variability may have important consequences for population divergence (e.g. Mailund *et al.*, 2012), and ultimately for the process of speciation (see also Yamaguchi & Iwasa, 2013). Extending our reasoning to island communities (Cowie & Holland, 2006), this also suggests that sporadic but potentially intense bouts of immigration, as brought about by rafting and human-driven invasions, could favour the establishment of relatively maladapted mainland species within communities competing for similar resources.

We conclude by joining Peniston *et al.* (2019) in saying that it is time to test existing predictions on migration pulsedness in empirical systems with well designed experimental set-ups. We add that available data on migration flows, e.g. from monitoring of oceanic rafting, individual tracking of dispersal routes, or marine and aerial current models (Ser-Giacomi *et al.*, 2015; Lagomarsino Oneto *et al.*, 2020), combined with genomics data, may also provide opportunities for testing such predictions. Understanding the consequences of ecological variability is increasingly important in the present context of climate and biodiversity change, and the spatio-temporal variability in migration flows probably deserves to receive more attention.

Bibliography

- Bajeux, N., Grognaud, F. & Mailleret, L. (2019) Influence of the components of propagule pressure, Allee effects, and stochasticity on the time to establish introduced populations. *Journal of Theoretical Biology*, **471**, 91 – 107.
- Benestan, L., Fietz, K., Loiseau, N., Guerin, P.E., Trofimenko, E., Rühls, S., Schmidt, C., Rath, W., Biastoch, A., Pérez-Ruzafa, A., Baixauli, P., Forcada, A., Arcas, E., Lenfant, P., Mallol, S., Goñi, R., Velez, L., Höppner, M., Kininmonth, S., Mouillot, D., Puebla, O. & Manel, S. (2021) Restricted dispersal in a sea of gene flow. *Proceedings of the Royal Society B: Biological Sciences*, **288**, 20210458.
- Bishop, L. (1990) Meteorological Aspects of Spider Ballooning. *Environmental Entomology*, **19**, 1381–1387.
- Blanquart, F., Kaltz, O., Nuismer, S.L. & Gandon, S. (2013) A practical guide to measuring local adaptation. *Ecology Letters*, **16**, 1195–1205.
- Bobadilla, M. & Santelices, B. (2005) Variations in the dispersal curves of macroalgal propagules from a source. *Journal of Experimental Marine Biology and Ecology*, **327**, 47–57.
- Boedeltje, G., Bakker, J.P., Ten Brinke, A., Van Groenendael, J.M. & Soesbergen, M. (2004) Dispersal phenology of hydrochorous plants in relation to discharge, seed release time and buoyancy of seeds: the flood pulse concept supported. *Journal of Ecology*, **92**, 786–796.
- Bürger, R. (2014) A survey of migration-selection models in population genetics. *Discrete & Continuous Dynamical Systems - B*, **19**, 883–959.
- Bürger, R. & Akerman, A. (2011) The effects of linkage and gene flow on local adaptation: A two-locus continent–island model. *Theoretical Population Biology*, **80**, 272–288.
- Carlton, J.T., Chapman, J.W., Geller, J.B., Miller, J.A., Carlton, D.A., McCuller, M.I., Treneman, N.C., Steves, B.P. & Ruiz, G.M. (2017) Tsunami-Driven Rafting: Transoceanic Species Dispersal and Implications for Marine Biogeography. *Science*, **357**, 1402–1406.
- Carlton, J. & Cohen, A. (2003) Episodic Global Dispersal in Shallow Water Marine Organisms: The Case History of the European Shore Crabs *Carcinus Maenas* and *C-Aestuarius*. *Journal of Biogeography*, **30**, 1809–1820.

- Catalano, K.A., Dedrick, A.G., Stuart, M.R., Puritz, J.B., Montes Jr., H.R. & Pinsky, M.L. (2020) Quantifying dispersal variability among nearshore marine populations. *Molecular Ecology*, **n/a**.
- Cowie, R.H. & Holland, B.S. (2006) Dispersal is fundamental to biogeography and the evolution of biodiversity on oceanic islands. *Journal of Biogeography*, **33**, 193–198.
- Feder, A.F., Pennings, P.S., Hermisson, J. & Petrov, D.A. (2019) Evolutionary Dynamics in Structured Populations Under Strong Population Genetic Forces. *G3: Genes, Genomes, Genetics*, **9**, 3395–3407.
- Felsenstein, J. (1976) The theoretical population genetics of variable selection and migration. *Annual Review of Genetics*, **10**, 253–280. PMID: 797310.
- Folinsbee, K.E. & Brooks, D.R. (2007) Miocene hominoid biogeography: pulses of dispersal and differentiation. *Journal of Biogeography*, **34**, 383–397.
- Gaggiotti, O. & Smouse, P. (1996) Stochastic Migration and Maintenance of Genetic Variation in Sink Populations. *American Naturalist*, **147**, 919–945.
- Garant, D., Forde, S. & Hendry, A. (2007) The multifarious effects of dispersal and gene flow on contemporary adaptation. *Functional Ecology*, **21**, 434–443.
- Garden, C., Currie, K., Fraser, C. & Waters, J. (2014) Rafting dispersal constrained by an oceanographic boundary. *Marine Ecology Progress Series*, **501**, 297–302.
- Goel, N.S. & Richter-Dyn, N. (1974) *Stochastic models in biology*. Academic Press., New York, San Francisco, London.
- Gomulkiewicz, R., Holt, R.D. & Barfield, M. (1999) The Effects of Density Dependence and Immigration on Local Adaptation and Niche Evolution in a Black-Hole Sink Environment. *Theoretical Population Biology*, **55**, 283–296.
- Hewitt, G. (2000) The Genetic Legacy of the Quaternary Ice Ages. *Nature*, **405**, 907–913.
- Johnson, K.P., Adler, F.R. & Cherry, J.L. (2000) Genetic and phylogenetic consequences of island biogeography. *Evolution*, **54**, 387–396.
- Keyse, J., Treml, E.A., Huelsken, T., Barber, P.H., DeBoer, T., Kochzius, M., Nuryanto, A., Gardner, J.P.A., Liu, L.L., Penny, S. & Riginos, C. (2018) Historical divergences associated with intermittent land bridges overshadow isolation by larval dispersal in co-distributed species of *Tridacna* giant clams. *Journal of Biogeography*, **45**, 848–858.
- Kimura, M. (1962) On the probability of fixation of mutant genes in a population. *Genetics*, **47**, 713–719.
- Kimura, M. & Ohta, T. (1969) The average number of generations until fixation of a mutant gene in a finite population. *Genetics*, **61**, 763–771.

- Kobayashi, Y., Hammerstein, P. & Telschow, A. (2008) The neutral effective migration rate in a mainland-island context. *Theoretical Population Biology*, **74**, 84–92.
- Lagomarsino Oneto, D., Golan, J., Mazzino, A., Pringle, A. & Seminara, A. (2020) Timing of fungal spore release dictates survival during atmospheric transport. *Proceedings of the National Academy of Sciences*, **117**, 5134–5143.
- Lande, R. (1994) Risk of population extinction from fixation of new deleterious mutations. *Evolution*, **48**, 1460–1469.
- Latter, B.D.H. & Sved, J.A. (1981) Migration and Mutation in Stochastic Models of Gene Frequency Change. II. Stochastic Migration with a Finite Number of Islands. *J. Math. Biology*, **13**, 95–104.
- Lenormand, T. (2002) Gene Flow and the Limits to Natural Selection. *Trends in Ecology and Evolution*, **17**, 183–189.
- Mailund, T., Halager, A.E., Westergaard, M., Dutheil, J.Y., Munch, K., Andersen, L.N., Lunter, G., Prüfer, K., Scally, A., Hobolth, A. & Schierup, M.H. (2012) A New Isolation with Migration Model along Complete Genomes Infers Very Different Divergence Processes among Closely Related Great Ape Species. *PLOS Genetics*, **8**, 1–19.
- Manna, F., Martin, G. & Lenormand, T. (2011) Fitness Landscapes: An Alternative Theory for the Dominance of Mutation. *Genetics*, **189**, 923–937.
- Marchi, N., Schlichta, F. & Excoffier, L. (2021) Demographic inference. *Current Biology*, **31**, R276–R279.
- Martin, C.H. & Turner, B.J. (2018) Long-distance dispersal over land by fishes: extremely rare ecological events become probable over millennial timescales. *Proceedings of the Royal Society B: Biological Sciences*, **285**, 20172436.
- Maruyama, T. (1970) Effective number of alleles in a subdivided population. *Theoretical Population Biology*, **1**, 273–306.
- Masson-Delmotte, V., Zhai, P., Pörtner, H.O., Roberts, D., Skea, J., Shukla, P., Pirani, A., Moufouma-Okia, W., Péan, C., Pidcock, R., Connors, S., Matthews, J., Chen, Y., Zhou, X., Gomis, M., Lonnoy, E., Maycock, T., Tignor, M. & Waterfield, T. (2018) *IPCC, 2018: Global Warming of 1.5°C. An IPCC Special Report on the impacts of global warming of 1.5°C above pre-industrial levels and related global greenhouse gas emission pathways, in the context of strengthening the global response to the threat of climate change, sustainable development, and efforts to eradicate poverty*. Working Group I Technical Support Unit, Bern, Switzerland.
- Matias, M.G., Mouquet, N. & Chase, J.M. (2013) Dispersal stochasticity mediates species richness in sourcesink metacommunities. *OIKOS*, **122**, 395–402.
- Maynard-Smith, J. (1966) Sympatric Speciation. *The American Naturalist*, **100**, 637–650.

- Mills, L.S. & Allendorf, F.W. (1996) The One-Migrant-per-Generation Rule in Conservation and Management. *Conservation Biology*, **10**, 1509–1518.
- Moran, P.A.P. (1962) *The statistical processes of evolutionary theory*. Clarendon Press; Oxford University Press.
- Morris-Pocock, J.A., Anderson, D.J. & Friesen, V.L. (2016) Biogeographical barriers to dispersal and rare gene flow shape population genetic structure in red-footed boobies (*Sula sula*). *Journal of Biogeography*, **43**, 2125–2135.
- Nagylaki, T. (1979) The Island Model with Stochastic Migration. *Genetics*, **91**, 163–176.
- Otto, S.P. & Whitlock, M.C. (2013) Fixation probabilities and times. *eLS*. American Cancer Society. ISBN 978-0-470-01590-2.
- Palstra, F.P. & Ruzzante, D.E. (2008) Genetic estimates of contemporary effective population size: what can they tell us about the importance of genetic stochasticity for wild population persistence? *Molecular Ecology*, **17**, 3428–3447.
- Peacock, M.M. & Smith, A.T. (1997) The effect of habitat fragmentation on dispersal patterns, mating behavior, and genetic variation in a pika (*Ochotona princeps*) metapopulation. *Oecologia*, **112**, 524–533.
- Peniston, J.H., Barfield, M. & Holt, R.D. (2019) Pulsed Immigration Events Can Facilitate Adaptation to Harsh Sink Environments. *The American Naturalist*, **194**, 316–333.
- Rajakaruna, H., Potapov, A. & Lewis, M. (2013) Impact of stochasticity in immigration and reintroduction on colonizing and extirpating populations. *Theoretical Population Biology*, **85**, 38–48.
- Reed, D.C., Laur, D.R. & Ebeling, A.W. (1988) Variation in Algal Dispersal and Recruitment: The Importance of Episodic Events. *Ecological Monographs*, **58**, 321–335.
- Reiners, W.A. & Driese, K.L. (2004) *Transport Processes in Nature: Propagation of Ecological Influences Through Environmental Space*, vol. 2. Cambridge University Press.
- Renner, S. (2004) Plant Dispersal across the Tropical Atlantic by Wind and Sea Currents. *International Journal of Plant Sciences*, **165**, S23–S33.
- Rice, S.H. & Papadopoulos, A. (2009) Evolution with Stochastic Fitness and Stochastic Migration. *PLOS ONE*, **4**, 1–12.
- Rousset, F. (2013) *Genetic structure and selection in subdivided populations (MPB-40)*, vol. 40. Princeton University Press.
- Ser-Giacomi, E., Rossi, V., López, C. & Hernández-García, E. (2015) Flow networks: A characterization of geophysical fluid transport. *Chaos: An Interdisciplinary Journal of Nonlinear Science*, **25**, 036404.

- Slatkin, M. (1981) Fixation Probabilities and Fixation Times in a Subdivided Population. *Evolution*, **35**, 477–488.
- Smith, T.M., York, P.H., Broitman, B.R., Thiel, M., Hays, G.C., van Sebille, E., Putman, N.F., Macreadie, P.I. & Sherman, C.D.H. (2018) Rare long-distance dispersal of a marine angiosperm across the Pacific Ocean. *Global Ecology and Biogeography*, **27**, 487–496.
- Soubeyrand, S., Sache, I., Hamelin, F. & Klein, E.K. (2015) Evolution of dispersal in asexual populations: to be independent, clumped or grouped? *Evolutionary Ecology*, **29**, 947–963.
- Thurman, T.J. & Barrett, R.D.H. (2016) The genetic consequences of selection in natural populations. *Molecular Ecology*, **25**, 1429–1448.
- Tigano, A. & Friesen, V.L. (2016) Genomics of local adaptation with gene flow. *Molecular Ecology*, **25**, 2144–2164.
- Wang, J. & Whitlock, M.C. (2003) Estimating Effective Population Size and Migration Rates From Genetic Samples Over Space and Time. *Genetics*, **163**, 429–446.
- White, C., Selkoe, K.A., Watson, J., Siegel, D.A., Zacherl, D.C. & Toonen, R.J. (2010) Ocean currents help explain population genetic structure. *Proceedings of the Royal Society B: Biological Sciences*, **277**, 1685–1694.
- Whitlock, M.C. (1992) Temporal fluctuations in demographic parameters and the genetic variance among populations. *Evolution*, **46**, 608–615.
- Whitlock, M.C. (2003) Fixation Probability and Time in Subdivided Populations. *Genetics*, **164**, 767–779.
- Wright, S. (1931) Evolution in Mendelian Populations. *Genetics*, **16**, 97–159.
- Yamaguchi, R. & Iwasa, Y. (2013) First Passage Time to Allopatric Speciation. *Interface focus*, **3**, 20130026.
- Yamazaki, Y., Naoe, S., Masaki, T. & Isagi, Y. (2016) Temporal variations in seed dispersal patterns of a bird-dispersed tree, *Swida controversa* (Cornaceae), in a temperate forest. *Ecological Research*, **31**, 165–176.
- Yeaman, S. & Otto, S.P. (2011) Establishment and Maintenance of Adaptive Genetic Divergence under Migration, Selection, and Drift. *Evolution*, **65**, 2123–2129.

Conclusions & Perspectives

The highest function of ecology is the understanding of consequences.

Remembering the words of Pardot KYNES
– *Dune* (Frank HERBERT)

All along this manuscript, we have explored several questions related to ecosystem adaptation and variability, using different scales and modeling approaches. It is good at this point to remember the guideline of this thesis. Some environmental variability may impact evolution and ecological/demographic processes. In return, modifications in those processes are likely to impact both ecological and evolutionary outcomes in a kind of “eco-evo” feedback loop (Hendry, 2020). In this manuscript, we focused on questions related to both branches of this loop, at biological scales from the community to the population.

Community adaptation and biodiversity-ecosystem functioning relationships

The first chapter of this thesis considered the fact that communities in nature may harbor various levels of co-adaptation, either because of the many environmental variations that may disturb the existing co-adapted state, or because of contemporary evolution that may allow a disturbed or newly formed system to rapidly (re)-reach a more co-adapted state. Based on those facts, we decided to question whether changes in the co-adaptation level of communities would have consequences for some ecological properties, and in particular for some biodiversity-ecosystem functioning (BEF) relationships. We have found a clear impact of the co-adaptation level on biodiversity-productivity and biodiversity-response to invasion relationships, and in a lesser extent to biodiversity-stability relationships. The ecological impact of species number interacts with the evolutionary history because of a differential magnitude and direction of species trait evolution in poor versus rich communities. This may have implications for the way we consider and manage ecosystems facing environmental perturbations and species loss/gain. In addition to illustrating that evolution can have large consequences for BEF relationships, this chapter is one more example that the study of ecological properties and behavior of ecosystems would greatly benefit from the consideration of shorter term evolutionary processes.

A few studies written since the publication of this chapter confirm, illustrate or soften certain assertions of our present work. First, because species loss is likely

to be trait mediated and not purely random in nature, Wolf *et al.* (2021) studied the impact of a realistic species loss, i.e. based on species trait, on some ecosystem functioning (productivity and resistance to invasion). They found that such a realistic loss leads to higher invasion resistance than expected with random loss, but also to more productivity decline. Even if we didn't explicitly study the impact of biodiversity loss (random communities were not formed from losses of species from larger communities), we still can intuit what would be the consequences of such realistic loss on our results. In term of biodiversity-productivity relationships, Wolf *et al.* (2021)'s results are likely to reinforce the differences between poorly adapted (random) and completely co-adapted communities we highlighted in this chapter. In term of biodiversity-resistance to invasion relationship, reducing the difference in between random and co-adapted communities at low diversity level, it may even create a difference where none was observed.

Second, in our eco-evolutionary dynamics modeling process, we kind of separated evolutionary processes from ecological processes, applying first selection on species traits, and then looking for the ecological equilibrium. If we would have liked to form co-adapted communities that would have resulted from purely gradual evolutionary processes (adaptive radiation), this method could have artificially formed some communities that, at some point, would have not been ecologically suitable. Nevertheless, an interesting study made by Cortez *et al.* (2020) showed that most of the time, considering ecological and evolutionary processes alone does not change the stability of the system compared to considering eco-evolutionary feedback together. This implies that our modelling assumptions regarding the separation of ecological and evolutionary processes is somehow less restrictive than we could have thought.

Third, new experimental studies continued to highlight the effect of what is called the community history (past historical co-occurrence of species). van Moorsel *et al.* (2021) recently showed, with a long term grassland experiment, that communities having a past of co-occurrence (resulting in short term evolution) had temporally more stable biomass than naive (random) communities, especially at low species richness. This is coherent with our finding that low-diverse communities are more sensitive to gain or loss in co-adaptation levels than high-diverse communities. In the same idea they said "A history of co-occurrence can in part compensate for species loss, as can high plant diversity in part compensate for the missing opportunity of such adaptive adjustments".

Finally, in this study, as for many ecological interaction models and experiments, we modeled communities using well defined traits (what is useful to make them evolve), only one type of ecological interaction at once, and a relatively low diversity level. If we would like to consider higher diversity levels, it might be needed to consider higher phenotype dimensions (Doebeli & Ispolatov, 2017). Doing so, of course, would complexify the approach (increased number of equations). Barbier *et al.* (2021) proposed an elegant approach based on statistical physics, looking for some aggregated statistical metrics that would describe species interactions with a minimum of constraints. Considering evolution in such a framework would be a whole different approach from the trait based one, and would be interesting to explore. In particular, it would be interesting to see if the minimal statistical structure that can describe coexisting species in communities would depend on the constraints imposed on species interactions or on species past-history.

Spatial heterogeneity and the evolution of stress tolerance

While the first chapter addressed the consequences of a change in the community co-adaptation level on some ecological properties, the second chapter looked into the adaptive process itself. It gave an example of how different environmental spatial heterogeneities (stress level distribution) can impact the evolutionary outcomes of a co-existence model (the tolerance-fecundity trade-off ; TFT). We found that the stress tolerance evolutionary equilibrium is mainly impacted by the trade-off function slope, and only little affected by the distribution of stress conditions in the environment. However, its evolutionary stability showed greater sensitivity to the stress distribution (ESS vs. branching point). The variance – more than the mean – of the stress distribution had a large role: a loss of variance greatly reduced the probabilities for ecological coexistence and for adaptive radiation. This can have great impacts for site regeneration, which may be impeded or slowed down by a loss in environmental stress variance due to any kind of perturbations as discussed in the corresponding chapter.

This first exploration of the evolution of stress tolerance within this coexistence model opens the way for the exploration of the impact of (co)-evolutionary processes driven by a tolerance-fecundity trade-off. As in the first chapter, we could for instance compare random (naive) versus co-adapted communities governed by the TFT model. It would be interesting to compare those results with the first chapter results, especially concerning the competition-colonization trade-off (CCT). Indeed, the CCT had patterns that notably differed from the other three scenarios, and it would be interesting to see if this was due to the presence of a trade-off, or to some specificity of the CCT. Of course, the application does not restrict to biodiversity-ecosystem functioning relationships but to any kind of ecological properties in communities governed by such a coexistence mechanism. Moreover, considering evolutionary processes governed by this coexistence mechanism could also help in determining whether some coexistence observations can be explained by the TFT or not.

Pulsed migration patterns and local adaptation

Contrarily to the two first chapters, which applied to average changes in environmental conditions, the third chapter directly questioned the consequences of fluctuations on evolution. It regarded the impact of a temporally variable migration between sub-populations from the same species on allele fixation and genetic divergence (namely on evolution). Another difference with the first two chapters, which tackled the questions within a mean phenotype perspective, is that we used here a population genetics approach. We have shown that migration variability can either decrease or increase the effective migration rate depending on the selection pressure imposed on alleles. More precisely, a beneficial allele fixation will be favored by migration variability while a strongly deleterious allele will benefit from a less variable migration pattern. This difference results in the homogenization, with migration variability, of fixation rates across loci harboring different selection values, what may leave a migration variability genomic signature. This study showed that considering the temporal variability of migration is likely to have consequences for population management and conservation. The latter indeed needs to know which is the best migration rate to impose in order to maintain sufficient genetic variation

within a population.

All the above results are restricted to unlinked loci. As soon as two or more loci are linked, linkage disequilibrium may modify the theoretical prediction as it changes the expected ratio between the different possible genotypes (Losos, 2017). Mathematically, we would have to consider more possible transition and fixation probabilities: either the fixation of both loci, or only one, with a correlation that depends on the recombination rate. With no recombination (i.e. fully linked loci) we obviously expect the same as with only one locus. When recombination is allowed, is migration pulsedness acting the same way on the mainland allele fixation? Preliminary studies made with neutral alleles highlighted that, where we would expected the effective migration rate to decrease with migration pulsedness within a single locus scenario, it can actually increase within a two partially linked loci scenario. This would be an interesting point to explore as it may modify the present expectations, in a way that seems to reinforce the positive effect of migration pulsedness encountered in this study.

In population genetics literature, the migration rate is often considered as a proportion of migrants rather than as a number of migrants as we did (see for instance Whitlock, 1992). In our study, we decided to consider a number instead of a proportion, so that the intensity of migration is independent of the size of the host population. Yet, we can wonder what would be the consequences of considering the migration rate as a proportion. This would impact the frequency of migration events. In our case, it is inversely proportional to n , the number of migrant per migration event. In the case we consider the proportion of migrant being constant within time, it would be inversely proportional to the proportion of migrant in the host population $\frac{n}{N+n}$. This would modify some of our expectations: mathematically, two terms cancel each other so that the pulse has no longer an impact on a neutral allele fixation rate, and the selection threshold found to $s = -\frac{1}{N}$ becomes $s = 0$. In other words, this would strengthen the positive effects of migration pulsedness on effective migration rate we highlighted in this study.

We obtained several theoretical expectations in our study that it would be nice to verify experimentally. For that, we would have to chose an organism with sexual reproduction and with a relatively short life cycle. A relatively large knowledge about this organism genome would also be needed, in order to consider loci or SNPs for which we know the behavior in given environments and the potential interactions with other genes. For that, well studied and documented organisms as *Drosophila* could be suitable. The first and easiest step would be to test prediction about the introduction of neutral alleles. We could verify for instance whether a pulsed introduction reduces the frequency of the introduced allele in the focal population or not with respect to less pulsed introduction. This frequency should be measured at a time interval that should not be correlated to the migration events (otherwise it would be automatically biased). These are first thoughts about possible experimental studies, which it would be interesting to not limit to simple tests of predictions in controlled environments, but to apply to concrete cases.

This leads us to two other main perspectives of this work that are intended to prepare the ground for testing predictions on real data from the field. First, efforts are needed to estimate the minimal data set that it would be necessary to get in order to have a chance to detect a pulsedness genomic signature. How many loci are needed, and distributed over how many selection coefficient? Indeed, the Chapter 3's

mathematical model allowed us to make a fit on an infinite number of loci distributed over an infinite number of different selection coefficients. These are ideal conditions to detect a signal, but in reality, we will never have such precision in the genetic data. Our stochastic simulation could be helpful to answer the question of the minimal genetic data set required. To fit simulation data points (and real genomic data) we would also need a mathematical model that can represent those data. Indeed, the model in Chapter 3, in addition to imposing strong constraints on migration rates, only allows access to a probability of fixation at time t , not to the probability of having a given proportion of a given mainland allele on the island. In Appendix D, we propose such a model, which describes the change in mainland allele proportion in the island with time. We consider that the system changes through a Markov process that we represent with a Master equation. We compare this model with both the mathematical model and the stochastic simulations described Chapter 3, before proposing ideas for a protocol to estimate the minimal genomic data set needed to detect a pulsedness signature. The latter would be interesting to determine before looking at a real genomic data set from which we would like to infer the migration pattern.

Second, to test those model predictions on real data sets and verify whether we really can estimate migration variability, it would be interesting to actually know the level of migration variability. Thus, we could compare our estimations to the real migration patterns. Estimating the level of migration variability between some distant sub-populations would then be a first step in that direction. Such patterns are not often described in the literature, and studies mainly focus on spatial connectivity patterns rather than on temporal connectivity patterns (conversations with researchers from the field - J.O. Irisson and E. Ser-Giacomi). There are still few quantitative evaluations of the temporal variability of gene flows and individual flows between populations, and of the type of dynamics that this variability may follow. Currents (oceanographic or atmospheric currents for instance) are useful to get an idea of the potential biological routes in case of passive transportation (e.g. for larvae). We had the chance to get at our disposal two datasets from Lagrangian geophysical fluid mechanics simulation models: (i) simulations of marine currents that could describe the passive dispersion of larvae of coastal species at the Mediterranean scale (Ser-Giacomi *et al.*, 2015), and (ii) simulations of atmospheric currents modeling the dispersion of fungus spores at the North American continent scale (Lagomarsino Oneto *et al.*, 2020). The idea with those datasets would be to quantify the temporal variations of connectivity patterns and exchanges of individuals between populations, and to classify the variability profiles according to different scenarios (constant, periodic, stochastic, pulsed, etc.). Preliminary analysis have been done with the oceanographic currents dataset (see fig. 3.6), and let us think that both continuous and pulsed patterns could be detected between different places. In figure 3.6, we highlight the existence of both continuous and pulsed migration patterns, either bilateral (from place A to place B and the other way around) or unilateral. Further analyses would be needed to estimate in more details the patterns of temporal variability between various places and their frequency of occurrence.

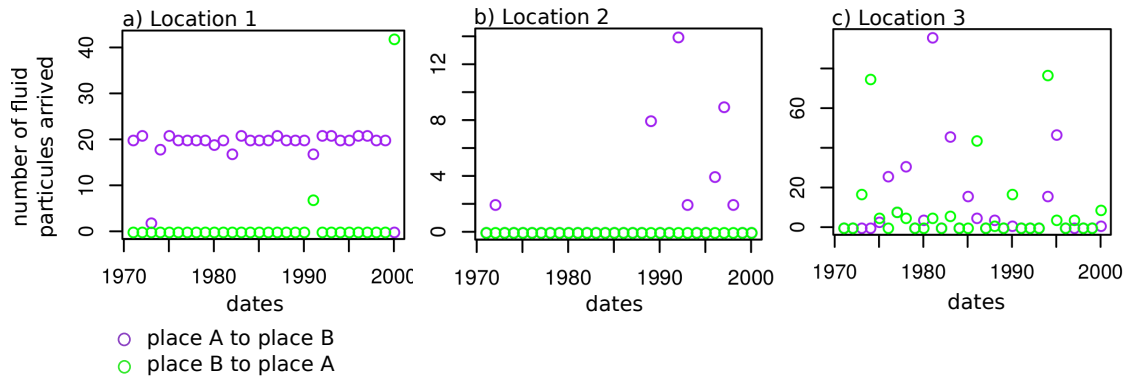


Figure 3.6: Temporal connectivity between different places along the Mediterranean coast (from Lagrangian current data simulated by E. Ser-Giacomi). Places denoted A and B are not the same for the three panels. (a) Example of a continuous unilateral connection, (b) example of a pulsed unilateral connection, and (c) example of a pulsed bilateral connection.

Concluding words

Throughout this manuscript, we have addressed questions at different biological scales, explored different types of variability, and used different evolutionary modeling methods. A question that could arise is whether each of the questions could have been addressed with a different model of evolution, and whether one model of evolution would ultimately be more useful than the others. The simple answer to this question is that each model focuses on a particular aspect of evolution, or even a particular biological scale. They each have their strengths and weaknesses, and they complement rather than replace each other. Population genetics is mainly concerned with the scale of populations or the scale of a set of population belonging to the same species. It focuses mainly on inheritance. On the other hand, adaptive dynamics is concerned with the scale of either a single population/species or a community. While one of the strength of population genetics lies in inheritance, the adaptive dynamics strength lies in the possibility to take into account ecological interactions between these different populations (as well as within the same population). Thus, the consequences of variabilities that affect the transmission of traits are rather addressed by population genetics, while those affecting ecological interactions are rather addressed by adaptive dynamics.

That said, the same initial disturbance may well impact either mating opportunities or ecological interactions, or both at the same time. It would then also be relevant, for example, to ask the question of the impact of the migration temporal variability on ecological interactions between individuals and between populations belonging to different species. This is likely to complement the predictions we have obtained by considering only the inheritance part of the question (see for instance Matias *et al.*, 2013; Rajakaruna *et al.*, 2013).

I see the different modeling approaches used in this manuscript as parallel layers that are superimposed on top of the same general scheme. Each of them participates in their own way to the understanding of evolutionary processes and consequences. Discoveries and findings made with a specific approach will feed the intuitions and questionings at the level of the whole picture. And these new questions could be addressed with any appropriate method, independently of the origin of the intuition.

At this time when science may have to answer more and more practical questions about climate, ecology and social issues, no approach (among those existing) is a priori to be favored. What must guide the choice of a particular method is obviously the questions of interest, which need to be clearly identified, and the type of answer we need.

Let me conclude highlighting that, as illustrated by the introductory scheme presented in this manuscript introduction, the three studies presented here, despite seeming relatively disparate, are just different bricks from the same pyramid. This pyramid aims at understanding the complex interactions between living things and the environment, from which many kind of temporal and spatial variabilities cannot be separated. The latter comes to complexify those interactions, but also enrich, put in movement, and in evolution. Around 500 years ago, Leonardo da Vinci poetically illustrated part of this by leaving us his famous sentence "*Movement is the principle of all life*".

Bibliography

- Barbier, M., de Mazancourt, C., Loreau, M. & Bunin, G. (2021) Fingerprints of high-dimensional coexistence in complex ecosystems. *Physical Review X*, **11**, 011009.
- Cortez, M.H., Patel, S. & Schreiber, S.J. (2020) Destabilizing evolutionary and eco-evolutionary feedbacks drive empirical eco-evolutionary cycles. *Proceedings of the Royal Society B*, **287**, 20192298.
- Doebeli, M. & Ispolatov, I. (2017) Diversity and coevolutionary dynamics in high-dimensional phenotype spaces. *The American Naturalist*, **189**, 105–120.
- Hendry, A. (2020) *Eco-evolutionary Dynamics*. Princeton University Press. ISBN 9780691204178.
- Lagomarsino Oneto, D., Golan, J., Mazzino, A., Pringle, A. & Seminara, A. (2020) Timing of fungal spore release dictates survival during atmospheric transport. *Proceedings of the National Academy of Sciences*, **117**, 5134–5143.
- Losos, J.B. (2017) *The Princeton guide to evolution*. Princeton University Press.
- Matias, M.G., Mouquet, N. & Chase, J.M. (2013) Dispersal stochasticity mediates species richness in sourcesink metacommunities. *OIKOS*, **122**, 395–402.
- van Moorsel, S.J., Hahl, T., Petchey, O.L., Ebeling, A., Eisenhauer, N., Schmid, B. & Wagg, C. (2021) Co-occurrence history increases ecosystem stability and resilience in experimental plant communities. *Ecology*, **102**, e03205.
- Rajakaruna, H., Potapov, A. & Lewis, M. (2013) Impact of stochasticity in immigration and reintroduction on colonizing and extirpating populations. *Theoretical Population Biology*, **85**, 38–48.
- Ser-Giacomi, E., Rossi, V., López, C. & Hernández-García, E. (2015) Flow networks: A characterization of geophysical fluid transport. *Chaos: An Interdisciplinary Journal of Nonlinear Science*, **25**, 036404.
- Whitlock, M.C. (1992) Temporal fluctuations in demographic parameters and the genetic variance among populations. *Evolution*, **46**, 608–615.
- Wolf, A.A., Funk, J.L., Selmants, P.C., Morozumi, C.N., Hernández, D.L., Pasari, J.R. & Zavaleta, E.S. (2021) Trait-based filtering mediates the effects of realistic biodiversity losses on ecosystem functioning. *Proceedings of the National Academy of Sciences*, **118**.

Appendix

Appendix A

Supplementary information for Chapter 1

A.1 Modelling of the four ecological scenarios

Preliminary remark: the first three ecological scenarios are models that have already been used and presented in several earlier works, such as Calcagno *et al.* (2017). More information on these can thus be found in the latter reference; only the main elements will be provided here, for easier reading. The fourth scenario is a new model derived from, and almost identical to, the size-structured trophic chain model introduced by and studied by simulation methods in Loeuille & Loreau (2005). Therefore we will provide here its mathematical derivation.

A.1.1 Niche scenario

This scenario represents the tendency of species to exploit different parts of a resource spectrum (Dieckmann & Doebeli, 1999; Calcagno *et al.*, 2017). It models a symmetric competition along a continuum of resources, such as a range of seed sizes for granivorous birds. Trait x here represents the average position of a species along that gradient, *i.e.* mean niche position (*e.g.* mean beak size). The model is usually directly formulated under a Lotka-Volterra form represented by equation (A.1):

$$\frac{dn_i}{dt} = r_i n_i f_i = r_i n_i \left(1 - \sum_j \frac{n_j a_{i,j}}{k_i} \right) \quad (\text{A.1})$$

where $a_{i,j} = a(x_i, x_j)$ is the impact that a variation in species j abundance has on the per capita growth rate of species i ($\frac{1}{n_i} \frac{dn_i}{dt}$), normalized by the intra-specific interaction (so that $a_{i,i} = 1$). The closer species traits (*i.e.* the more similar resources species consume), the stronger competitive impact between them. It results that the competition is a decreasing function of the trait difference between two species, taking maximum value 1 when the two species have identical niche position. Function $a(x_i, x_j)$ is following general practice taken to be Gaussian with width s_a .

$$a(x_i, x_j) = \exp \left(\frac{-(x_i - x_j)^2}{s_a^2} \right) \quad (\text{A.2})$$

The carrying capacity function $k_i = k(x_i)$ describes the distribution of resources available along the resource gradient, and is classically supposed to have a symmetric dome-shaped distribution centered on some optimal trait value (0 for convenience). Following Calcagno *et al.* (2017), in order to avoid some degenerate mathematical properties we use a Lorentzian function of width s_k

$$k(x) = \frac{1}{1 + x^2/s_k^2} \quad (\text{A.3})$$

Last, $r_i = r(x_i)$ is the intrinsic growth rate of species i that governs the ecological timescale, and is taken to be proportional to the mono-specific abundance $r(x) = k(x)$. The shape of the three functions presented above are represented in Fig. 1a in the main article.

Parameter s_a is varied in the simulation, over the range presented in section A.2, while parameter s_k has been kept constant equal to 1.

A.1.2 Body-size scenario

This second scenario (Rummel & Roughgarden, 1985) is an extension of the *niche* model in which asymmetric competition between species is used instead of symmetric competition. In this case, species trait can represent for instance species body size. It is represented by the same equation (A.1), with different competitive, carrying capacity and intrinsic growth rate functions. As in Calcagno *et al.* (2017), we use a log-normal carrying capacity function:

$$k(x) = \exp(-\log(x)^2) \quad (\text{A.4})$$

and an asymmetric Gaussian competitive function:

$$a(x_i, x_j) = \exp(d^2/s_a^2) \exp\left(\frac{-(x_i - x_j + d)^2}{s_a^2}\right) \quad (\text{A.5})$$

with s_a controlling the competitive function width, and d the level of asymmetry. The intrinsic growth rate is also taken proportional to function k : $r(x) = k(x)$. The form of those functions are represented in Fig. 1a in the main article.

Parameters s_a and d are varied in the simulation, over the range presented in section A.2.

A.1.3 Life History Trade-off scenario

This scenario rests on a patch-occupancy model describing the competition between species in a meta-community, arranged in a competitive hierarchy. There is a trade-off between colonization ability at the regional scale and competitive dominance at a local scale (Calcagno *et al.*, 2006, 2017).

The patch-occupancy equation given in Calcagno *et al.* (2006) can easily be rewritten under the same Lotka-Volterra form as in the two first scenarios (eq. A.1) as detailed in Calcagno *et al.* (2017). The corresponding three functions $a(x_i, x_j)$, $k(x)$ and $r(x)$ are represented Fig. 1a of the main article and are defined as:

$$a(x_i, x_j) = 1 + x_j \frac{\eta(x_j - x_i)}{x_i - \eta(x_i - x_j)} \quad (\text{A.6})$$

$$k(x_i) = N - \mu/x_i \quad (\text{A.7})$$

$$r(x_i) = x_i N - \mu \quad (\text{A.8})$$

with η a logistic function relating the probability to win competition for a patch and the difference in colonization abilities; see Calcagno *et al.* (2017) for the full derivation.

Parameters α (trade-off intensity, *i.e.* the steepness of the logistic function η) and γ (the preemption level, *i.e.* the maximum value of function η) were both varied, over the range presented in section A.2. Parameters N (total amount of patches in the metacommunity) and μ (patch extinction rate) were kept fixed to $N = 1$ and $\mu = 0.1$.

A.1.4 Trophic scenario: derivation of the Lotka-Volterra form

This scenario presents a vertical trophic interaction, with species arranged in a trophic chain structured by body mass. Body mass is thus the species trait x . This model is taken from Loeuille & Loreau (2005) and reads:

$$\frac{1}{n_i} \frac{dn_i}{dt} = f(x_i) \sum_{j=0} \gamma(x_i - x_j) n_j - m(x_i) - \sum_{j=1} \beta(x_i - x_j) n_j - \sum_{j=1} \gamma(x_j - x_i) n_j \quad (\text{A.9})$$

with n_i the biomass of species i . Index $i = 0$ corresponds to the basal resource, and its trait x_0 does not evolve. The first term in the right-hand side corresponds to the consumption by species i of species lower into the trophic chain, and fourth term of the consumption of species i by species higher in the chain. The consumption rate function $\gamma(x_i - x_j)$ is a Gaussian of width (standard deviation) s , and taking maximum value when species biomasses differ by some interval d .

$$\gamma(x_i - x_j) = \frac{\gamma_0}{s\sqrt{2\pi}} \exp\left(\frac{-(x_i - x_j - d)^2}{s^2}\right)$$

for $x_i > x_j$. Birth function f depends on species size. The second term of equation (A.9) is mortality rate, also depending on species size. Following Loeuille & Loreau (2005), the size dependence of the birth and mortality rates reads $f(x_i) = f_0 x_i^{-0.25}$ and $m(x_i) = m_0 x_i^{-0.25}$. Finally, the third term corresponds to competition by interference between species of similar size. Function β is the competition by interference rate. It is a gaussian of width s_a and height b (competition intensity):

$$\beta(x_i - x_j) = b \exp\left(-\frac{(x_i - x_j)^2}{s_a^2}\right)$$

This model is a consumer-resource model with an abiotic compartment, but using a mass balance hypothesis, *i.e.* $\sum_{j=0} n_j = N_{tot}$, (mass conservation: Leibold, 1996), it can be, as the previous scenarios, reformulated under the Lotka-Volterra form (equation A.1). Starting from the original equation (A.9):

$$\frac{1}{n_i} \frac{dn_i}{dt} = f(x_i) \sum_{j=0} \gamma(x_i - x_j) n_j - m(x_i) - \sum_{j=1} \beta(x_i - x_j) n_j - \sum_{j=1} \gamma(x_j - x_i) n_j$$

in the first sum, we separate the first term ($j=0$) from the other ones ($j \neq 0$):

$$\frac{1}{n_i} \frac{dn_i}{dt} = f(x_i) (\gamma(x_i - x_0) n_0 + \sum_{j=1} \gamma(x_i - x_j) n_j) - m(x_i) - \sum_{j=1} \beta(x_i - x_j) n_j - \sum_{j=1} \gamma(x_j - x_i) n_j$$

we then introduce the mass-balance constraint $n_0 = N_{tot} - \sum_{j=1} n_j$ and get, after a few rearrangements:

$$\begin{aligned} \frac{1}{n_i} \frac{dn_i}{dt} = & f(x_i) \gamma(x_i - x_0) (N_{tot} - \sum_{j=1} n_j) \\ & + f(x_i) \sum_{j=1} n_j \gamma(x_i - x_j) - m(x_i) - \sum_{j=1} \beta(x_i - x_j) n_j - \sum_{j=1} \gamma(x_j - x_i) n_j \end{aligned}$$

we rearrange to get all the term summing over j together:

$$\begin{aligned} \frac{1}{n_i} \frac{dn_i}{dt} = & f(x_i) \gamma(x_i - x_0) N_{tot} - m(x_i) \\ & + \sum_{j=1} n_j [f(x_i) (\gamma(x_i - x_j) - \gamma(x_i - x_0)) - \beta(x_i - x_j) - \gamma(x_j - x_i)] \end{aligned}$$

and finally we factorize by $f(x_i) \gamma(x_i - x_0) N_{tot} - m(x_i)$ and get:

$$\begin{aligned} \frac{1}{n_i} \frac{dn_i}{dt} = & (f(x_i) \gamma(x_i - x_0) N_{tot} - m(x_i)) * \\ & \left(1 - \frac{\sum_{j=1} n_j [f(x_i) (\gamma(x_i - x_0) - \gamma(x_i - x_j)) + \beta(x_i - x_j) + \gamma(x_j - x_i)]}{f(x_i) \gamma(x_i - x_0) N_{tot} - m(x_i)} \right) \end{aligned}$$

which can be recognized as a Lotka-Volterra form with

$$r(x_i) = f(x_i) \gamma(x_i - x_0) N_{tot} - m(x_i) \tag{A.10}$$

so that:

$$\frac{1}{n_i} \frac{dn_i}{dt} = r(x_i) \left(1 - \frac{\sum_{j=1} n_j [f(x_i) (\gamma(x_i - x_0) - \gamma(x_i - x_j)) + \beta(x_i - x_j) + \gamma(x_j - x_i)]}{r(x_i)} \right)$$

and using the hypothesis that $a_{i,i} = 1$, we have:

$$\frac{a(x_i, x_i)}{k(x_i)} = \frac{1}{k(x_i)} = \frac{f(x_i) (\gamma(x_i - x_0) - \gamma(0)) + \beta(0) + \gamma(0)}{r(x_i)}$$

so that:

$$k(x_i) = \frac{r(x_i)}{f(x_i)(\gamma(x_i - x_0) - \gamma(0)) + \beta(0) + \gamma(0)} \quad (\text{A.11})$$

Equation (A.9) now writes:

$$\frac{1}{n_i} \frac{dn_i}{dt} = r(x_i) \left(1 - \frac{\sum_{j=1} n_j [f(x_i)(\gamma(x_i - x_0) - \gamma(x_i - x_j)) + \beta(x_i - x_j) + \gamma(x_j - x_i)]}{k(x_i) (f(x_i)(\gamma(x_i - x_0) - \gamma(0)) + \beta(0) + \gamma(0))} \right)$$

so that function $a(x_i, x_j)$ writes:

$$a(x_i, x_j) = \frac{f(x_i)(\gamma(x_i - x_0) - \gamma(x_i - x_j)) + \beta(x_i - x_j) + \gamma(x_i - x_j)}{f(x_i)(\gamma(x_i - x_0) - \gamma(0)) + \beta(0) + \gamma(0)} \quad (\text{A.12})$$

Those three functions are represented Fig. 1a in the main article. In this scenario, following Loeuille & Loreau (2005), we set $m_0 = 0.1$, $s_a = 1.5$, $\gamma_0 = 1$, $f_0 = 0.3$, $d = 2$, $x_0 = 0$ and we varied b (interference intensity) and s (consumption function width). Parameter values explored are given in section A.2 below.

A.2 Parameter sets explored and those plotted in the main article figures

In each scenario, key parameters were varied in order to ensure that conclusions are robust to parameters changes.

- In the *Niche* scenario, the width s_a of the symmetric competition function $a(x_i, x_j)$ was varied from 0.5 to 1.5. In this scenario what matters is only the ratio of s_a over s_k , hence the two parameters need not be both varied. A value $s_a = 1$ thus means that the widths of the competition kernel and of the carrying capacity functions are identical ($s_a = s_k$).
- In the *Body-size* scenario, the width of the competition function (s_a) and the level of competitive asymmetry (d) were varied respectively from 1.2 to 2.4 and from 0.1 to 0.3.
- In the *LH-tradeoff* scenario, the preemption level (γ) and the trade-off intensity (α) were respectively varied from 0.3 to 0.7 and from 2 to 12.
- In the *Trophic* scenario, the level of competition by interference (b) and the width of the consumption function (s) were varied respectively from 0.10 to 0.19 and from 1.0 to 1.6.

The parameter ranges presented above have been explored from the minimum to the maximum value. For clarity, in the main article, only three curves corresponding to parameter combinations yielding representative and contrasted patterns were selected and shown in figures. The parameter combinations corresponding to each curve in Figures 2-5 are provided in table A.1.

Legend	Niche	Body-size	LH-tradeoff	Trophic
—	$s_a = 0.5$	$s_a = 1.2, d = 0.1$	$\alpha = 2, \gamma = 0.3$	$s = 1.0, b = 0.10$
- - -	$s_a = 0.9$	$s_a = 1.5, d = 0.1$	$\alpha = 4, \gamma = 0.7$	$s = 1.0, b = 0.13$
- - - - -	$s_a = 1.5$	$s_a = 1.8, d = 0.1$	$\alpha = 12, \gamma = 0.7$	$s = 1.2, b = 0.10$

Table A.1: Parameter sets used in the main text for the four scenarios. Legend line types refers to the line types used in the figures.

A.3 Algorithm of community formation

Co-adapted communities We assume that each species is characterized by its mean trait value x and possesses some (small) heritable variance around the latter. In these conditions, the direction and intensity of natural selection on the species trait can be determined by the selection gradient around the species trait value (Christiansen, 1991). The selection gradient is computed at the first derivative of the fitness (exponential rate of increase) of a rare variant with respect to its trait value, evaluated at the trait value of the focal species. The fitness of a rare variant with trait value x_m is defined as, from equation (A.1):

$$F(x_m) = \lim_{n_m \rightarrow 0} \left(\frac{1}{n_m} \frac{dn_m}{dt} \right) = r(x_m) \left(1 - \sum_j \frac{n_j a(x_m, x_j)}{k(x_m)} \right), \quad (\text{A.13})$$

where all species are at their respective equilibrium abundance (Christiansen, 1991; Metz *et al.*, 1995). The selection gradient for the i -th species in the community is thus:

$$\nabla(x_i) = \left. \frac{dF(x_m)}{dx_m} \right|_{x_m=x_i} \quad (\text{A.14})$$

If the selection gradient is positive, adaptive evolution pushes the trait value towards higher values, and if the gradient is negative, the trait moves to lower values, at a speed approximately proportional to the value of the gradient. Fitness and selection gradient are frequency- and density-dependent and change with the composition of the entire community. If the system reaches a state where the selection gradient cancels for all species, then directional evolution ceases and the community has reached a (co)evolutionary equilibrium (Christiansen, 1991; Abrams *et al.*, 1993). Note that at such an equilibrium individual species may be at an evolutionary maximum or at an evolutionary minimum. Evolutionary minima may under appropriate circumstances and inheritance modes favor the splitting of a species into two novel lineages (evolutionary branching) and thus an increase in the number of evolving lineages (Metz *et al.*, 1995; Dieckmann & Doebeli, 1999; Calcagno *et al.*, 2017). Since in this work we systematically consider all diversity levels, we can remain agnostic to second-order selection and to the specific history of transitions among diversity levels (that might involve branchings, invasions and extinctions). We just need to identify, for every diversity level, all feasible co-evolutionary equilibria, characterized by:

$$\nabla(x_i) = 0 \quad i \in [1, \dots, s] \quad (\text{A.15})$$

For computational efficiency, for each ecological scenario and diversity level, we first identify the different coevolutionary equilibria that are attractors by iterating the adaptive dynamics of traits (defined by the selection gradient (A.14)) forward in time, starting from 100 random species trait values. From these we identify the one or several coevolutionary equilibria. Then, by continuation, we track these equilibria continuously through the range of parameter values, together with potential bifurcations (changes in the number or nature of equilibria). This provides an exhaustive list of coevolutionary equilibria for all parameter combinations.

Random communities To assemble random communities, we randomly drew each species trait value, independently, from a common probability distribution. The latter distribution can be regarded as characterizing the available regional pool of species and trait values. This species pool distribution was chosen in order to allow all feasible trait values and to be as “random” as possible: specifically, it was chosen to minimize information content, using the maximum entropy principle (Jaynes, 1957). For each scenario, we first specified the support of the distribution, *i.e.* the range of possible values for species traits. We then specified only one additional constraint, for each parameter set: the mean trait value, that had to be representative of the species typically expected for the given parameter set. Specifically, it was taken to be equal to the mean trait value λ that would be observed in the full (saturated) community. In practice, the co-adapted communities with maximum diversity levels were used as good approximations of the saturated communities. This constraint ensured that there is no systematic (average) difference between the random species trait values and the traits that are expected in the current environment, and thus to generate communities that remain of similar nature across parameter sets. This also allows to perform comparisons between co-adapted and random communities that are not biased by the fact that species in random communities would be, intrinsically, ill-adapted. Of course, with only one constraint on the mean value, max-entropy random distributions were quite broad and all trait values had a fair chance to be picked.

In the *Body-size*, *LH-tradeoff* and *Trophic* scenarios, species trait values x could take values in $]0, +\infty[$, and the entropy-maximizing distributions were thus exponential distributions of mean λ defined as explained above. In the *Niche* scenario, trait values can spread over $] -\infty, +\infty[$ and the model is by construction symmetric around $x = 0$. Thus the random trait distribution was a double exponential, centered on zero, and with width defined by the average deviation from zero observed in the saturated community. Values for λ are given in table A.2. Remark that we also used a much more classical and simpler approach consisting in using uniform distributions for random traits, between some arbitrary defined minimum and maximum values. Results were similar, and are thus not qualitatively dependent on the precise random distributions used.

In practice, for each parameter set and diversity level (N), random communities were formed by picking N traits from the species pool defined in the previous paragraphs. The ecological equilibrium obtained from equation (A.1) was computed,

Legend	Niche	Body-size	LH-tradeoff	Trophic
—	1.52	7.63	7.35	5.10
- - -	3.35	9.65	3.71	5.15
-----	6.48	11.9	1.17	5.33

Table A.2: Mean trait values λ of the saturated communities, taken to define the entropy-maximising distributions. See table A.1 for the correspondence between legend line types and the parameter sets used in the main text.

and the community was retained (ecological filter) if all N species persisted at equilibrium with a positive abundance (*i.e.* had abundance above a threshold value of 10^{-5}). The process was repeated until 1,000 such communities were obtained. Remark that co-adapted communities (as defined in the previous section) are always a specific subset of random communities, characterized by the additional constraint (A.15), as illustrated in Fig. 1 of the main article.

A.4 Metrics used to quantify diversity-functioning relationships

For each BEF relationship, we computed several alternative metrics that may be used to quantify the corresponding ecosystem function. Several metrics gave identical or similar conclusions, and for clarity we retained only one or two metrics per BEF relationship that are more commonly used. A summary of all metrics can be found in Table A.3 to inform the reader that no different conclusion could be drawn from those various metrics. Then, in the following, for each BEF relationships, we describe the metric(s) effectively used for the results presented in the main text.

A.4.1 Productivity

Community productivity is the summed productivity of each of the N component species.

$$\Pi = \sum_{i=1}^N n_i g_i \quad (\text{A.16})$$

with g_i the per capita production rate of species i in its community whose expression depends on the ecological interaction and community composition.

For the *Niche* and *Body-size* scenarios, there is no explicit production rate since the models are directly formulated in Lotka-Volterra form. We made the simple choice of using the intrinsic growth-rate r_i as the metric per capita productivity so that :

$$\Pi_{Niche} = \sum_i n_i r_i$$

BEF relationship	Metrics	References
Production	Total abundance	(1)
	Productivity*	(1)
Stability	Asymptotic resilience*	(2) (3)
	Stochastic invariability	(3)
	Initial Resilience	(3)
	Ecosystem stability*	(4) (5)
	Robustness	(6)
	Robustness heterogeneity	(6)
Invasion	Deterministic invasion probability	(7) (8)
	Stochastic invasion probability*	(7) (8)
	Proportion of the invader	(7)
	Mean impact of an invader on abundances	(7)
	Proportion of species non extinct*	(7)

* Metrics retained in the main article

Table A.3: Metrics measured on the two types of communities for different parameter sets. Metrics in bold types are the one plotted and analyzed in the main article. Each are representative of their categories of relationships. (1) Tilman *et al.* (1996) ; (2) May (1973a) ; (3) Arnoldi *et al.* (2016) ; (4) May (1973b) ; (5) Ives *et al.* (1999) ; (6) Barabás & D’Andrea (2016) ; (7) Elton (1958) ; (8) Hector *et al.* (2001)

$$\Pi_{Body} = \sum_i n_i r_i$$

For the *LH-tradeoff* scenario, we consider the colonization of empty sites ($N - \sum_j n_j$) as a contributions to productivity. This leads to the per capita productivity:

$$g_{i,LH} = n_i x_i (N - \sum_j n_j)$$

and the total productivity is the sum over all species i :

$$\Pi_{LH} = \sum_i n_i g_{i,LH} = \sum_i n_i x_i (N - \sum_j n_j)$$

Finally for the *Trophic* scenario, the net growth rate is straightforward, simply referring to consumption by specie i of lower size species.

$$\Pi_{chain} = \sum_i n_i \left(f(x_i) \sum_{j=0} \gamma(x_i - x_j) n_j \right)$$

A.4.2 Stability

Asymptotic resilience is taken as a measure of species stability (May, 1973a; Arnoldi *et al.*, 2016). It refers to the asymptotic return speed of the slowest species to equilibrium after an external abundance perturbation.

$$R_\infty = -\Re(\lambda_m(J)) \quad (\text{A.17})$$

with $\lambda_m(J)$ the highest eigen value of the Jacobian matrix J of the ecological system whose coefficient are given by (A.18).

$$J_{i,j} = \frac{\partial}{\partial n_j} \left(\frac{dn_i}{dt} \right)^* \quad (\text{A.18})$$

To get a measure of the all community stability, we consider the community variance, namely in the variance of the sum of abundances. This measure differs from individual direction stability metrics such as the asymptotic resilience. The sum of abundances can return faster to its equilibrium value after a perturbation, even if species abundances are still fluctuating into the community. It is commonly expected (even if not general and depending on metrics) that species stability has more often a negative relationship with diversity while community stability tends to get a positive one. Mathematically,

$$var(N_T) = \sum_i var(n_i) + \sum_{i,j,j \neq i} cov(n_i, n_j)$$

with $N_T = \sum_{i=1}^S n_i$ the sum of each species abundance for a community with S species. The variance-covariance matrix B is involved into the equilibrium distribution for population fluctuation in a stochastic environment (May, 1973b) and is the solution of the Lyapunov matrix equation (A.19) (see also Wang *et al.* (2015) for a similar derivation):

$$D = 1/2(BA + A^T B) \quad (\text{A.19})$$

with $A = N^{-1} J N$ and N the diagonal matrix containing the equilibrium abundances of each species whose coefficients are $N_{i,i} = n_i^*$. A^T is A transpose, and D the matrix containing $D_{i,j}$ coefficient which are the overall covariance between white-noise fluctuations in the stochastic differential equation of species i and the one of species j :

$$\frac{dn_i}{dt} = r_i n_i \left(1 - \sum_j \frac{n_j a_{i,j}}{k_i} \right) + \sum_k \rho_{i,k} \gamma_k(t) n_k \quad (\text{A.20})$$

with $\rho_{i,k}$ measuring the covariance between the environmental fluctuation for species i and for species j , and $\gamma_k(t)$ is environmental stochasticity in the growth rate of population k at time t , taken as a white noise random fluctuation with variance σ^2 . $D_{i,j}$ coefficients are the diffusion coefficient involved in the Fokker-Planck equation, which is the differential equation for the probability of transition in between two states of the system. In our case, we choose to put a perturbation in a white-noise form that has no inter-species dependence: $\rho_{i,i} = 1$ ($\forall i$) and $\rho_{i,k} = 0$ ($\forall i \neq k$), and D is a diagonal matrix. All individuals get the same amount of perturbation, so that each species is perturbed with an intensity that depends on its abundance. More precisely, the variance imposed on a given species is proportional to the squared of its abundance: $D_{i,i} = \sigma^2 n_i^2$. This derivation assumes sufficiently small perturbations around the equilibrium to get a local linearization of the system. To solve the continuous Lyapunov matrix equation (A.19), we use the *lyap()* function from Scilab. We then sum all the elements from the variance-covariance matrix B , and divide this sum by σ^2 (the variance of perturbation received by each individual, *e.g.* we normalize by the per individual perturbation). The coefficient of variation CV is defined by:

$$CV = \frac{\sqrt{\frac{\sum_{i,j} B_{i,j}}{\sigma^2}}}{N_T} \quad (\text{A.21})$$

And the community stability metrics is defined by the inverse of CV . Actually, in the calculation, the value of sigma has no importance because we finally divide by the same quantity. We take it equal to 1.

A.4.3 Response to invasion

Two aspects of ecological invasion are considered: (i) the resistance to invasion and (ii) the tolerance to invasion. Resistance to invasion is defined as the probability that an alien species (randomly drawn from the regional pool and introduced at low initial abundance) does not successfully establishes in the community. The probability P_{instal} that this alien species establishes is:

$$P_{instal} = \int_{x_{min}}^{x_{max}} p_x(x_e) H_{st}(x_e) dx_e \quad (\text{A.22})$$

with $p_x(x_e)$ the trait distribution probability, $H_{st}(x_e) = \begin{cases} \frac{s(x_e)}{b(x_e)} & \text{if } s(x_e) > 0 \\ 0 & \text{if not} \end{cases}$, x_e

the trait of the foreign species which is trying to invade, $b(\cdot)$ the growth rate and $s(\cdot)$ the fitness function. The trait distribution probability is the same used to form the random communities (see section A.3). Resistance to invasion is then defined by

$$R_{inv} = 1 - P_{instal}$$

Tolerance to invasion T_{inv} (eq. A.23) is defined by the proportion of species, following a successful invasion, that are not driven to extinction by the invader:

$$T_{inv} = \frac{N_{final}}{N_{init}} \quad (\text{A.23})$$

with N_{init} the number of species into the community right after the invasion, thus including the invasive species, and N_{final} the number of species into the community once ecological equilibrium has been recovered.

A.4.4 Metrics for trait composition

A.4.4.1 Trait composition representation

We sort communities by trait values, and calculate the average trait per rank over the 1000 random communities (or few co-adapted communities when needed). For each diversity level with N specie, we thus obtain N random averaged trait, and N co-adapted averaged trait. Values obtained for co-adapted and random traits are plotted one against the other in Fig. 3 of the main article.

A.4.4.2 Strength of evolutionary filter

The strength of evolutionary filter is defined with trait difference in between random and co-adapted communities. We sort communities by trait values. Then, for each random community with N species, we calculated the trait difference between random and co-adapted trait per rank, and we made the average over all N species ranks

$$\frac{1}{N} \sum_{i=1}^N |x_{i,coadapt} - x_{i,random}|$$

where i denotes the rank and $x_{i,coadapt}$ (resp. $x_{i,random}$) is the trait value for the i^{th} co-adapted (resp.random) species. In the case of multiple co-adapted communities (*Niche* scenario), we calculated the difference to the closest co-adapted community (which is likely to be the evolutionary attractor corresponding to this random community).

A.4.4.3 Minimum distance to the optimum trait

In the *Niche*, *Body-size*, *TF-tradeoff* scenarios, the optimum trait value x_o is defined as the trait corresponding to the maximum of function $k(x)$. In the *TF trade-off* scenario, the trait value maximizing function $k(x)$ is infinite. We thus take as optimal value x_o the 95th percentile of the species pool distribution defined for the community formation. The minimum trait distance to the optimum is defined as:

$$\min_{i=1}^{N-1} (|x_i - x_o|)$$

A.4.4.4 Average interval between species trait values

The average interval between species traits is the average two-by-two trait distance:

$$\sum_{i=1}^{N-1} \frac{|x_{i+1} - x_i|}{N-1}$$

with x_i the trait of species i and N the number of species into the community.

A.5 Magnitude of the difference between random and co-adapted communities

In order to ascertain that co-adapted communities can be considered as different from random communities, we measured the percentile of the metric for random communities in which the mean value of the metric for co-adapted communities is (Fig. A.1). In all cases, co-adapted values stand above the 8th decile or below the 2nd decile of the random values distribution, for at least part of the BEF relationship. This indicates that co-adapted communities are quite atypical, relative the variability within random communities.

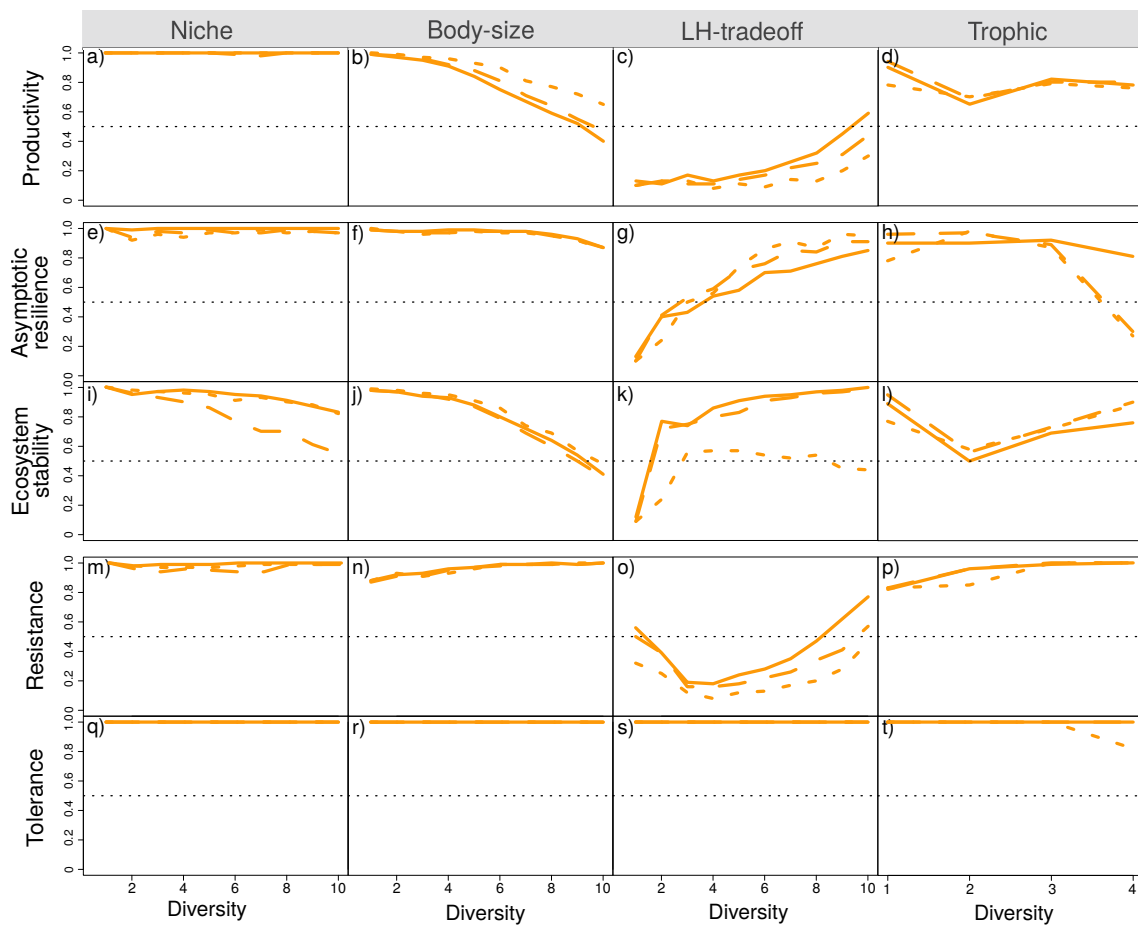


Figure A.1: Quantile Q_c of the metric for random communities in which the mean value of the metric for co-adapted communities is. It is measured for the four scenarios and 5 metrics explored (productivity a-d, asymptotic resilience e-h, ecosystem stability i-l, resistance m-p and tolerance q-t). The closest Q_c to 0.5, the more similar co-adapted and random communities regarding this metric. When Q_c is larger (resp. lower) than 0.5, the metric for co-adapted communities is larger (resp. lower) than for random communities. Ecological interaction parameters set are varied in each scenario (three different line types). Parameters values are given paragraph A.2, together with other explored parameters sets (not shown for readability reasons).

A.6 Coefficient of variation of the average interval between trait values

In the main article, the average interval between trait values is plotted against diversity (Fig. 4e-h), but it does not give information about how evenly might be distributed traits among a particular community. To get this information, we plotted the coefficient of variation of the average interval between trait values (Fig. A.2). Species traits in co-adapted communities are found more evenly distributed (lower coefficient of variation at any single diversity level) than in random communities.

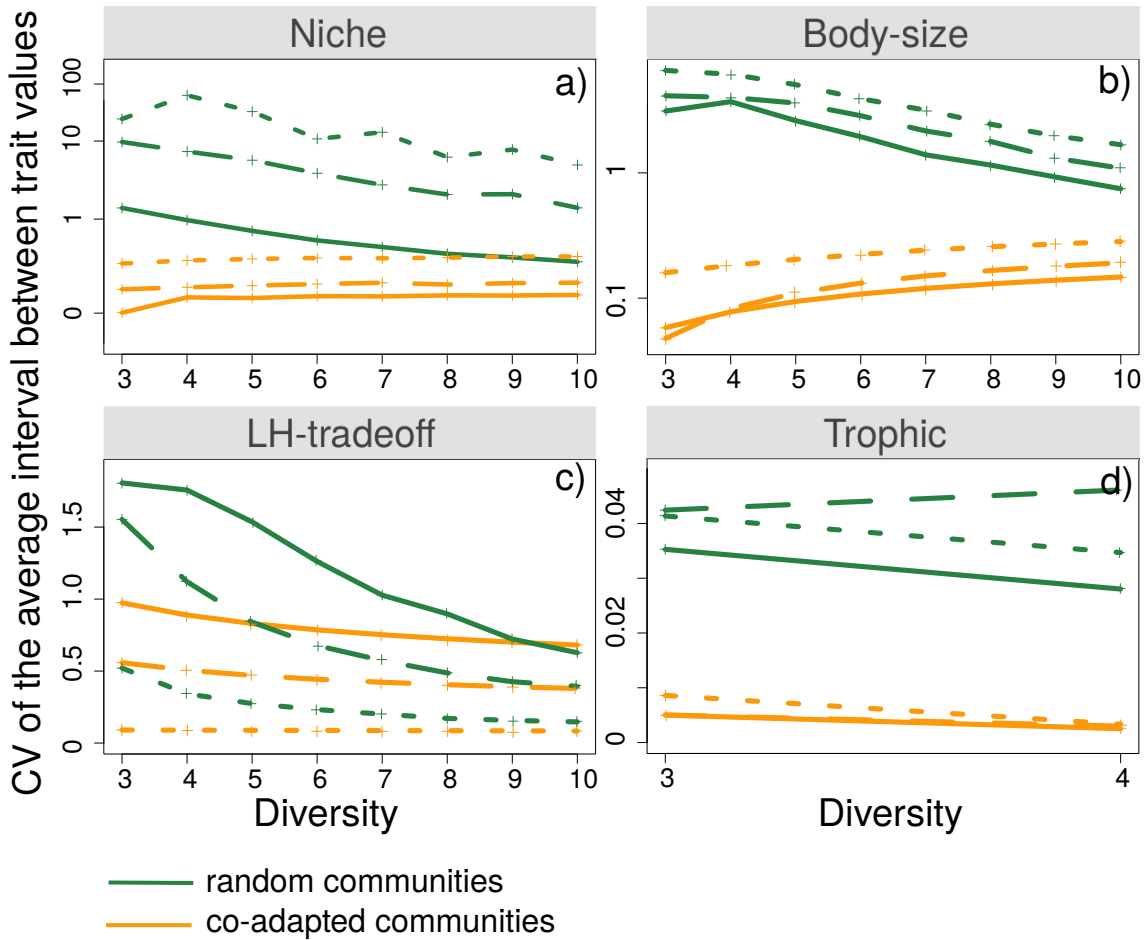


Figure A.2: Coefficient of variation of the average interval between trait values in the four ecological scenarios. The smaller the value, the more evenly distributed are species traits. Ecological interaction parameter sets are varied in each scenario (three different line types). Parameters values are given paragraph A.2, together with other explored parameters sets (not shown for readability reasons).

A.7 Results with a limit on possible trait change

The model assumes possible unbounded changes of species traits, implying either sufficient mutational supply or some kind of infinitely additive alleles. However, genetic variation is usually not infinite, and the response to selection could at some point slow down or stop. To investigate this point, we have sub-sampled the random communities, excluding the ones where at least one species would have to undergo too much trait change to reach the co-adapted state. More precisely, we have defined a maximum trait displacement x_{max} , which corresponds to the amount of change such that the interaction strength of evolved individuals with ancestral individuals would fall to 1%. In other words, this means that traits can only undergo changes that keep individuals in a similar ‘niche’ as their ancestors, in the sense that they retain non-negligible interaction strength. In practice, this also prevents a species from evolving more than the typical trait interval existing between coexisting species, in species-rich communities. Having retained only the communities with no species further from x_{max} , we recomputed all the metrics for the *Niche* scenario, with the new set of communities (Fig. A.3).

As expected, the difference between co-adapted and random communities tends to erode. Low diversity levels are more impacted as random species were more likely to stand far from the evolutionary point (see also Fig. 3 in the main text). It follows that, for instance, the patterns for biodiversity-production relationships is less pronounced (Fig. A.3f compared to Fig. A.3a). Interestingly, the pattern for invasion tolerance (Fig. A.3j) is not affected at all, presumably because the largest differences are observed at high diversity, where a restriction on evolutionary change has little importance. In all cases, we still observe the general trends and differences that sustain our conclusions. Even though a limit on the amount of evolutionary change allowed would weaken the reported effects, it appears that the general messages are rather robust to this.

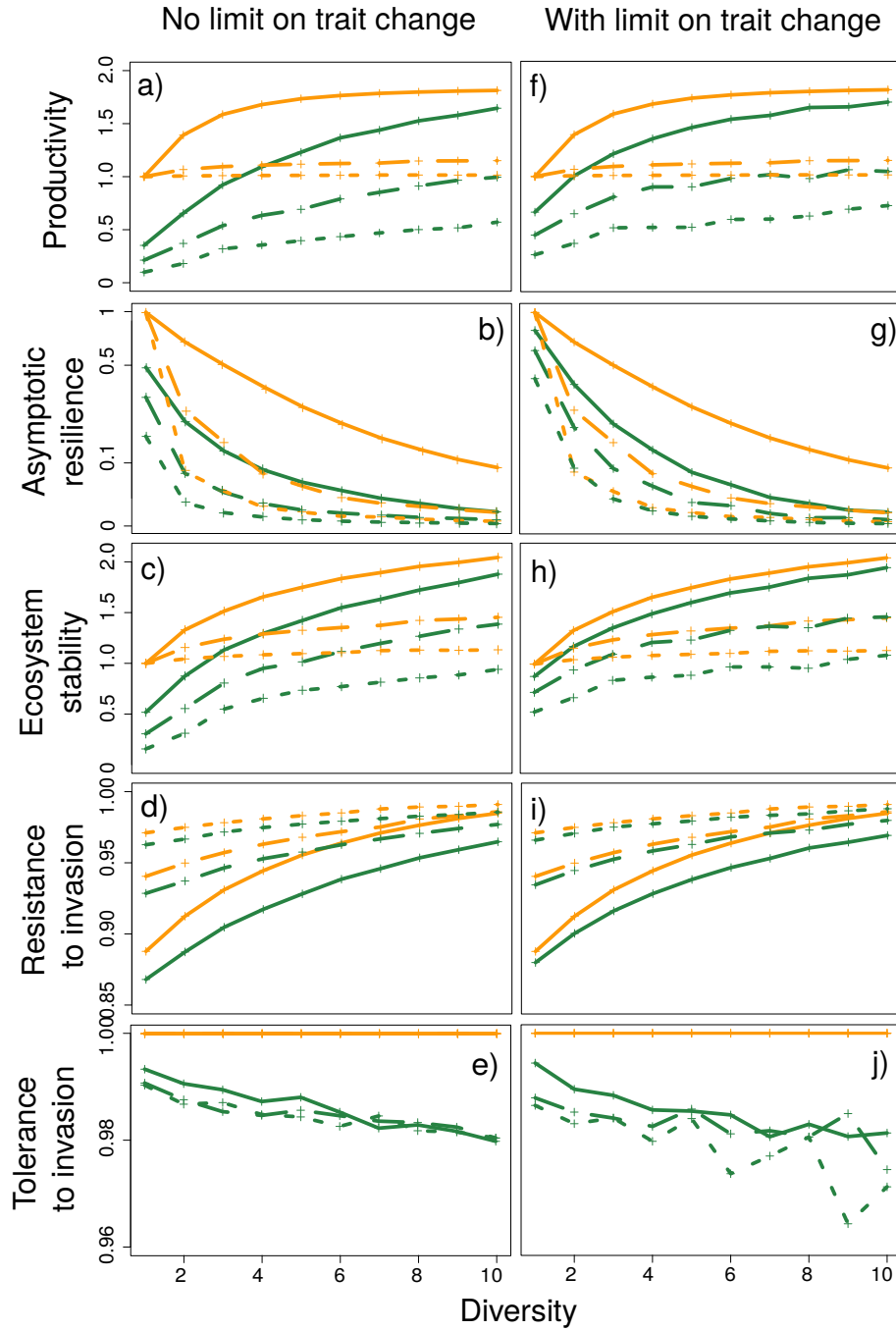


Figure A.3: The five explored metrics for *Niche* scenario, (a-e) when all random communities are considered, and (f-j) when restricting random communities to be not too far in trait space to co-adapted ones. Parameters values (different lines type) are given paragraph A.2.

Bibliography

- Abrams, P.A., Matsuda, H. & Harada, Y. (1993) Evolutionarily unstable fitness maxima and stable fitness minima of continuous traits. *Evolutionary Ecology*, **7**, 465–487. ISSN 1573-8477.
- Arnoldi, J.F., Loreau, M. & Haegeman, B. (2016) Resilience, reactivity and variability: A mathematical comparison of ecological stability measures. *Journal of Theoretical Biology*, **389**, 47–59.
- Barabás, G. & D’Andrea, R. (2016) The effect of intraspecific variation and heritability on community pattern and robustness. *Ecology Letters*, **19**, 977–986.
- Calcagno, V., Mouquet, N., Jarne, P. & David, P. (2006) Coexistence in a meta-community: the competition–colonization trade-off is not dead. *Ecology Letters*, **9**, 897–907.
- Calcagno, V., Jarne, P., Loreau, M., Mouquet, N. & David, P. (2017) Diversity spurs diversification in ecological communities. *Nature Communications*, **8**, 15810.
- Christiansen, F.B. (1991) On Conditions for Evolutionary Stability for a Continuously Varying Character. *The American Naturalist*, **138**, 37–50.
- Dieckmann, U. & Doebeli, M. (1999) On the origin of species by sympatric speciation. *Nature*, **400**, 354–357.
- Elton, C. (1958) *Ecology of invasions by plant and animals*. Chapman and Hall, London.
- Hector, A., Dobson, K., Minns, A., Bazeley-White, E. & Hartley Lawton, J. (2001) Community diversity and invasion resistance: an experimental test in a grassland ecosystem and a review of comparable studies. *Ecological Research*, **16**, 819–831.
- Ives, A.R., Gross, K. & Klug, J.L. (1999) Stability and variability in competitive communities. *Science*, **286**, 542–544.
- Jaynes, E.T. (1957) Information theory and statistical mechanics. *Phys. Rev.*, **106**, 620–630.
- Leibold, M.A. (1996) A Graphical Model of Keystone Predators in Food Webs: Trophic Regulation of Abundance, Incidence, and Diversity Patterns in Communities. *The American Naturalist*, **147**, 784–812.
- Loeuille, N. & Loreau, M. (2005) Evolutionary emergence of size-structured food webs. *Proceedings of the National Academy of Sciences USA*, **102**, 5761–5766.

- May, R.M. (1973a) Qualitative stability in model ecosystems. *Ecology*, **54**, 638–641.
- May, R.M. (1973b) Stability in randomly fluctuating versus deterministic environments. *The American Naturalist*, **107**, 621–650.
- Metz, J.A.J., Geritz, S.A.H., Meszner, G., Jacobs, F.J.A. & Heerwaarden, J.S.v. (1995) Adaptive dynamics: a geometrical study of the consequences of nearly faithful reproduction. IIASA Working Paper, WP-95-099, IIASA, Laxenburg, Austria.
- Rummel, J.D. & Roughgarden, J. (1985) A theory of faunal buildup for competition communities. *Evolution*, **39**, 1009–1033.
- Tilman, D., Wedin, D. & Knops, J. (1996) Productivity and sustainability influenced by biodiversity in grassland ecosystems. *Nature*, **379**, 718–720.
- Wang, S., Haegeman, B. & Loreau, M. (2015) Dispersal and metapopulation stability. *PeerJ*, **3**, e1295.

Appendix B

Supplementary information for Chapter 2

B.1 Equivalence between parameters

B.1.1 The fecundity steepness c_s

The stress tolerance $x_{1/2}$ such that $c(x_{1/2}) = c_0/2$ can be derived the following way:

$$\frac{c_0}{2} = c_0 e^{-c_a(e^{x_{1/2}})^{c_b}}$$

so that

$$x_{1/2} = \log \left[\left(-\frac{\log(2)}{c_a} \right)^{-\frac{1}{c_b}} \right]$$

Then, we derive $c(x)$ with respect to x :

$$\begin{aligned} \frac{dc(x)}{dx} &= -c_0 c_a c_b (e^x)^{c_b-1} (e^x) e^{-c_a(e^x)^{c_b}} \\ &= -c_0 c_a c_b (e^x)^{c_b} e^{-c_a(e^x)^{c_b}} \end{aligned}$$

and we replace x by the above expression of $x_{1/2}$, what leaves us with:

$$c_s = \left. \frac{dc(x)}{dx} \right|_{x=x_{1/2}} = -\frac{1}{2} c_b c_0 \log(2)$$

B.1.2 The dose-response steepness β_s

The derivative of $b(x, y)$ with respect to x , taken at the point $y = x$ gives

$$\left. \frac{db(x, y)}{dx} \right|_{y=x} = - (2^{1/g})^{-1-g} (-1 + 2^{1/g}) Bg$$

This steepness being expressed with respect to the the symmetric case ($g = 1$), we simply obtain:

$$\beta_s = \frac{B}{4}$$

B.2 Complements for the dose-response parameter choices

B.2.1 Symmetric versions

The parameters choice of the dose-response curve is based on the environmental stress distribution. We decided to base parameters choice on the distribution with intermediate variance: σ_2^2 .

We first look for symmetric logistic functions (when $g = 1$). We want the probability to survive to increase by a given percentage of the maximum when the stress level goes from $x - \sigma_2$ to $x + \sigma_2$ (x being the LD50). In other words, we want the probability to survive to increase by a percentage $\xi/2$ of the maximum when the stress tolerance increases from x to $x + \sigma_2$. Solving the following equation:

$$b(x, x - \sigma_2) = 0.5 - \xi/2$$

leaves us with a simple expression for parameter B :

$$B = \frac{\log\left(-1 + \frac{1}{1-\xi/2}\right)}{\sigma_2}$$

We take three different B for ξ to be 10^{-6} , 0.90 and 0.4, and we end up with the three values of $\beta_s = B/4$ described in the main document.

B.2.2 Asymmetric versions

We then construct the asymmetric versions of the dose-response. For each of the three symmetric version constructed above, we construct an asymmetric version to the left and an asymmetric version to the right, so that we end up with 9 different dose-response curve. The deviation to the right is made in order that the probability to survive bellow y (the stress level experienced) remains the same as in the symmetric case, and that the probability to survive above y increases. We manually adjust parameters B and g so that the stress tolerance x_1 such that $b(x_1, y) = 0.8$ in the symmetric case gives approximately $b(x_1, y) = 0.95$ in the asymmetric to the right case. The deviation to the left is made similarly. The probability above y remains the same and the probability bellow y decreases. We manually similarly adjust parameters B and g so that the stress tolerance x_1 such that $b(x_1, y) = 0.2$ in the symmetric case gives approximately $b(x_1, y) = 0.05$ in the asymmetric to the left case.

B.3 Changes in x^* with the steepness of the fecundity and dose-response functions

The steepness of the fecundity and dose-response functions (respectively c_s and β_s) are the two parameters controlling the intensity of the trade-off. Depending on their values, different patterns occur. Figure B.1 illustrates what's occurring in case of low (or very low) β_s (namely a shallow dose-response curve).

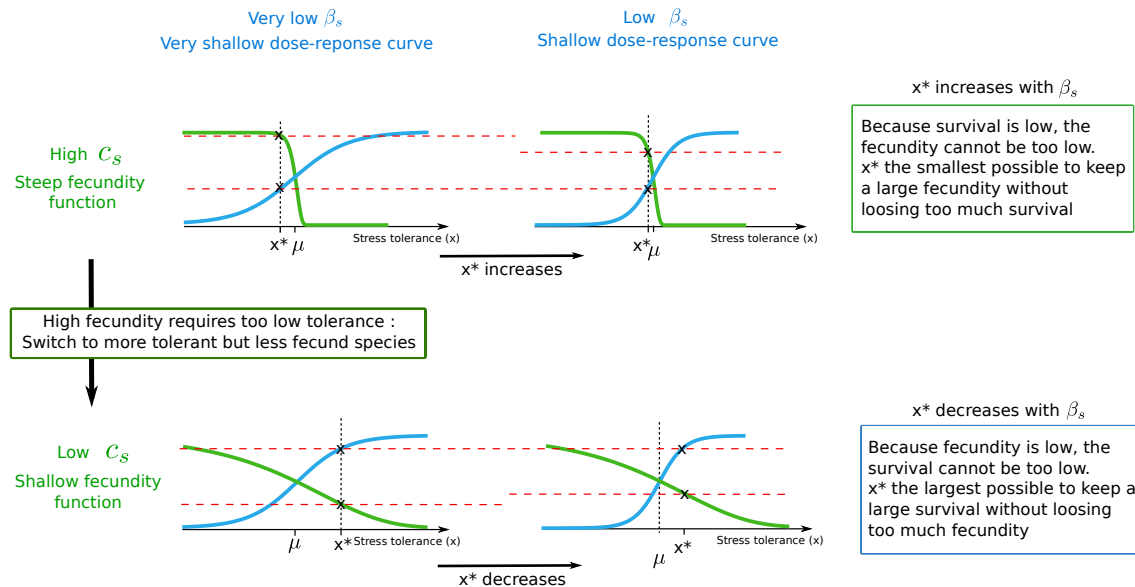


Figure B.1: Changes in x^* with the steepness of the fecundity and dose-response functions in case of a shallow dose-response curve (β_s below the threshold).

B.4 Performance of the species at the evolutionary equilibrium

Depending on the values of the dose-response curve function steepness β_s , the species performance is not always increasing with species tolerance x^* . Figure B.2 illustrates what's occurring.

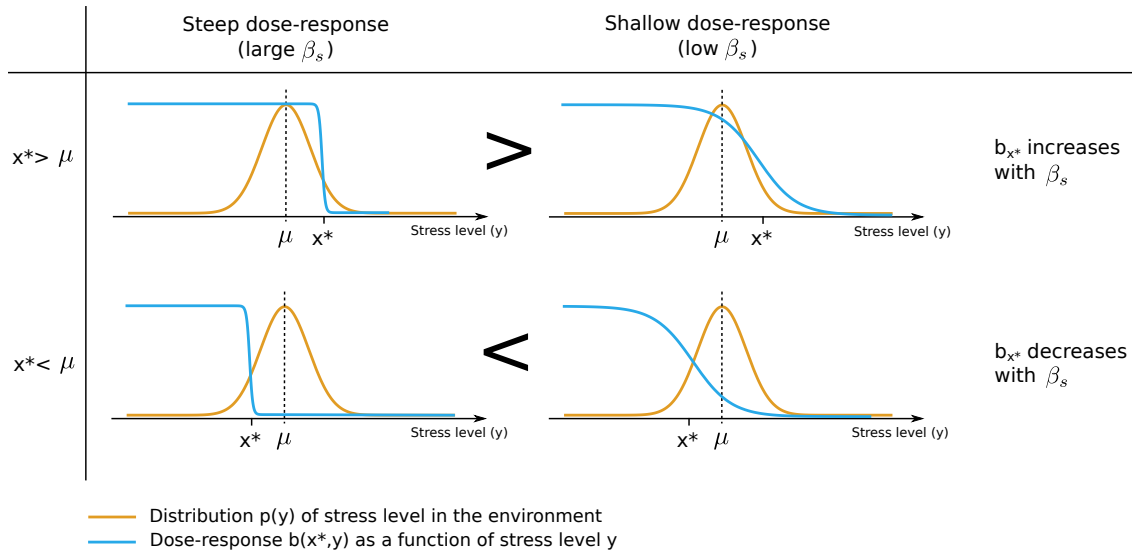


Figure B.2: Comparison of the four cases encountered in the calculation of species performance $b_{x^*} = \int_y p(y)b(x^*, y)dy$. In case $x^* > \mu$ (and x^* remains constant), b_{x^*} increases with the dose-response steepness β_s . In case $x^* < \mu$ (and x^* remains constant), b_{x^*} decreases with the dose-response steepness β_s . Of course, x^* does not remain constant with β_s . It is x^* variation as long as with the above effect of the performance with β_s which gives the observed pattern figure 3a of the main document.

Appendix C

Supplementary information for Chapter 3

C.1 Complements to the method

C.1.1 Time scale separation for the mathematical analysis

The time scale separation needed for the mathematical analysis is respected if the averaged time between two migration events $t_m = \frac{n}{m}$ is large enough so that $t_m \gg t_{c,fix}$, with $t_{c,fix}$ the averaged fixation time before fixation (after a unique initial introduction of an allele into a population). According to Otto & Whitlock (2013), this time is largest for neutral alleles. The general expression of fixation time for any initial allele frequency f and any selection or dominance coefficient can be found in Kimura & Ohta (1969); Whitlock (2003).

At most, $t_{c,fix}$ is the fixation time of one initial copy of the allele of interest in a large population ($f \ll 1$). In that case, $t_{c,fix} \approx 4N$ generations (see also Kimura & Ohta, 1969). On the other hand, the smallest value of t_m is $1/m$. Thus, the time scale separation is respected if $1/m \gg 4NT$, namely for $mT \ll \frac{1}{4N}$, with T the duration of one generation.

C.1.2 Gillespie algorithm for the simulations

We perform fully stochastic simulations of the island population partially connected to a mainland population, using a Gillespie algorithm to model a logistic demography of the island population with migration (Goel & Richter-Dyn, 1974).

There are three possible events: birth, death, and migration from mainland to island (rate m/n), whose rates are reevaluated at every iteration step and are used to weight the random choice of the next occurring event. To avoid too frequent population extinctions during the simulations, birth rate is taken proportional to the population size N_t at time t while death rate is taken proportional to $\frac{N_t^2}{N}$ (logistic demography). The factor of proportionality d scales the time unit to a given number of generation. A generation lasts $\frac{N}{d}$ units time in average, and d is taken equal to N . When death occurs, an individual is randomly drawn and removed from the population. At birth, two random individuals are drawn with replacement, with a

probability that depends on their fitness (fertility selection), and one allele of each is randomly chosen to form the newborn. Because our approach only models selection at birth and not at death and to make our selection coefficient comparable to the one classically used (Kimura, 1962), we multiplied by 2 the effect of selection felt by individuals at birth. When a migration event occurs, $2n$ A alleles immigrate into the island. After event application, time is incremented by a quantity drawn from a Poisson distribution, whose rate is the sum of the three event rates ($N_t + \frac{N_t^2}{N} + \frac{m}{n}$).

The first migration event occurs on average $\frac{n}{m}$ generations after the simulation starts. This models the case when populations are physically connected, but where stochasticity may not yet have allowed individuals to move from one to another. We chose not to start time at the first migration event, because this would diminish the effect of large pulses occurring less often (see Bajeux *et al.*, 2019 for a similar simulation start, or also Peniston *et al.*, 2019).

C.1.3 Simulation time optimization

When migration is very rare compared to demographic events, simulations can take a very long time to end (waiting for fixation). To reduce simulation time, we do not simulate demographic events if the island population becomes monomorphic (namely when stochastic birth or death will no longer impact genetic drift). In order not to distort time, we must take into account the time that would have elapsed if we had let the demography unfold.

For this, we increment time by a value drawn from the distribution of migration event times ($\tau_m e^{-\tau_m x}$, with $\tau_m = \frac{m}{n}$ the migration event rate), which is truncated from Δ_t to infinity. Δ_t is the elapsed time between the last migration event and the point at which we stopped the simulation of demography.

C.2 Selection values at transitions (figure 4 from the main article)

To determine the boundaries for figure 4 in the main article, we use the mathematical criterion. If $\alpha = \frac{u(\frac{n}{n+N})}{n}$ is larger (resp. smaller) with $n > 1$ than for $n = 1$, it means that migration pulsedness positively (resp. negatively) impacts allele fixation. So if $\frac{u(\frac{n}{n+N})}{n} > \frac{u(\frac{1}{1+N})}{1}$, namely if $u(\frac{n}{n+N}) > nu(\frac{1}{1+N})$, the impact of migration pulsedness is positive. Figure 2 in the main article illustrates this criterion.

The transition from A to B and from C to B is found with the following equation, which is given by the equality between the tangent to the fixation probability function at $n = 1$ and the tangent of the comparison line $nu(\frac{1}{1+N})$ at $n = 1$:

$$\left. \frac{\partial u(\frac{n}{n+N})}{\partial n} \right|_{n=1} = u\left(\frac{1}{1+N}\right)$$

For a given h and N , we solve this equality for s with Mathematica (function *FindRoot*) which leaves us with the selection value at the boundary.

The transition from A to C corresponds to the values of s and n such that two conditions are respected:

$$u\left(\frac{n}{n+N}\right) = nu\left(\frac{1}{1+N}\right)$$

and

$$\left. \frac{\partial u(\frac{n}{n+N})}{\partial n} \right|_n = 0$$

We use Mathematica to solve those equation for s and n , using the *FindRoot* function. In the limit of $n \rightarrow 1$, we come close to the A to B transition (purple).

C.3 Finding s_{l1} and slopes of n_l and n_+ around it

C.3.1 Finding s_{l1} in frequency-independent selection case

To simplify the notation, in the following we write $u(s, n) = u(\frac{n}{n+N}, N, s, h)$. The limiting value of selection above which the effect is always negative, and below which the effect can be positive depending on the value of n , is defined by:

$$u(s_{l1}, 1) = \left. \frac{\partial u}{\partial n} \right|_{(s_{l1}, n=1)}$$

In the case of frequency independent selection (genic selection),

$$u\left(s, \frac{n}{n+N}\right) = \frac{1 - e^{-2Ns \frac{n}{n+N}}}{1 - e^{-2Ns}}$$

and

$$\frac{\partial u}{\partial n} = \frac{e^{-2Ns} \frac{n}{n+N} \left(\frac{n2Ns}{(n+N)^2} - \frac{2Ns}{n+N} \right)}{e^{-2Ns} - 1}$$

so that when we evaluate those quantities at $n = 1$ and equalize them we get:

$$e^{\frac{-2Ns}{1+N}} - 1 = e^{\frac{-2Ns}{1+N}} \left(\frac{2Ns}{(1+N)^2} - \frac{2Ns}{1+N} \right)$$

Multiplying by $e^{\frac{2Ns}{N+1}}$ both side of the equation leaves us with:

$$\begin{aligned} 1 - e^{\frac{2Ns}{1+N}} &= \left(\frac{2Ns}{(1+N)^2} - \frac{2Ns}{1+N} \right) \\ &= \frac{2Ns}{1+N} \left(\frac{1}{N+1} - 1 \right) \\ &= \frac{2Ns}{1+N} \left(\frac{-N}{N+1} \right) \end{aligned}$$

We denote $z = \frac{2Ns}{1+N}$ so that the above equation becomes $1 - e^z = z \frac{-N}{N+1}$. Assuming that $s \ll 1$, we have that $z \ll 1$ and we can write the Taylor series $e^z = 1 + z + \frac{1}{2}z^2 + \mathcal{O}(z^3)$. Thus,

$$\begin{aligned} 1 - \left(1 + z + \frac{1}{2}z^2 \right) &= z \frac{-N}{N+1} \\ \frac{1}{2}z^2 + z \left(1 - \frac{N}{N+1} \right) &= 0 \\ z \left(\frac{1}{2}z + \frac{1}{N+1} \right) &= 0 \end{aligned}$$

which yields $z = 0$ or $z = \frac{-2}{N+1}$. The biologically relevant solution is $z = \frac{-2}{N+1}$, which leaves us with $\frac{2Ns}{N+1} = \frac{-2}{N+1}$, and we finally get

$$s_{l1} = -\frac{1}{N}$$

C.3.2 Finding the slope of n_+ around s_{l1} as a function of s

There exists a value n_+ of n that maximises the difference in fixation rate between the continuous case and the pulsed case. Owing to the fact that fixation rate is proportional to the ratio $\frac{u(s,n)}{n}$, we can study the latter to find n_+ . Along a curve $(s, n_+(s))$ the following condition is verified:

$$\left. \frac{\partial}{\partial n} \frac{u(s,n)}{n} \right|_{(s, n_+(s))} = 0 \quad (\text{C.1})$$

Similarly to the previous paragraph, we differentiate equation (C.1) with respect to s . We use the notation used in the previous paragraph.

$$\frac{d}{ds} \left(\left. \frac{\partial}{\partial n} \frac{u(s,n)}{n} \right|_{(s, n_+(s))} \right) (s, n_+(s)) = 0$$

with

$$\begin{aligned} \frac{d}{ds} \left(\frac{\partial}{\partial n} \frac{u(s, n)}{n} \Big|_{(s, n_+(s))} \right) (s, n_+(s)) &= \frac{2u(s, n_+(s)) \frac{dn_+}{ds}}{n_+^3(s)} \\ &\quad - \frac{2 \frac{dn_+}{ds} u^n(s, n_+(s)) + u^s(s, n_+(s))}{n_+^2(s)} \\ &\quad + \frac{\frac{dn_+}{ds} u^{n^2}(s, n_+(s)) + u^{s, n}(s, n_+(s))}{n_+(s)} \end{aligned}$$

Then we isolate the slope $\frac{dn_+}{ds}$ and find:

$$\frac{dn_+}{ds} = \frac{n_+(s) (n_+(s) u^{s, n}(s, n_+(s)) - u^s(s, n_+(s)))}{2u(s, n_+(s)) - 2n_+(s) u^n(s, n_+(s)) + n_+^2(s) u^{n^2}(s, n_+(s))}$$

As in the previous case, at this stage, the expression of the slope $\frac{dn_+}{ds}$ is valid for any shape of u . We can express this slope in the particular case of frequency independent selection where $u = \frac{1 - e^{-2Ns \frac{n}{n+N}}}{1 - e^{-2Ns}}$. In that case, we know that $(s_{l1}, n_+(s_{l1})) \simeq (-1/N, 1)$, so we can know the slope around s_{l1} . Using Mathematica, a Taylor expansion for large N ($N \gg 1$) gives that

$$\left. \frac{dn_+}{ds} \right|_{s=s_{l1}} \simeq -\frac{3}{2} N^2 \quad (\text{C.2})$$

Using the same method as in the previous case, we verify this result numerically (see fig. C.1). We find that the slope of n_+ as a function of s close to the limit s_{l1} is well approximated by $-\frac{3}{2} N^2$. We can notice that is is half the slope of n_l as a function of s .

C.3.3 Finding the slope of n_l , knowing the slope of n_+

Along a curve $(s, n_l(s))$ the following condition is verified:

$$u(s, n_l(s)) = n_l(s) u(s, 1) \quad (\text{C.3})$$

Solving this condition, we can observe numerically that the slope of n_l close to s_l is approximated by $-\frac{3}{2} N^2$ (see fig. C.1). It is twice the slope found for n_+ : $\left. \frac{dn_+}{ds} \right|_{s=s_{l1}} \simeq -\frac{3}{4} N^2$ (see the previous paragraph). This means that, for a given s close to s_{l1} , the pulsedness value $n = 2n_+$ should verify the condition for the effect of pulsedness, i.e.

$$u(s, 2 * n_+(s)) = 2 * n_+(s) u(s, 1) \quad (\text{C.4})$$

Let's verify this relationship. We note $\Delta_c(s) = u(s, 2 * n_+(s)) - 2 * n_+(s) u(s, 1)$, and we want to verify whether or not it cancels close to s_{l1} . We know that $(s_{l1}, n_+(s_{l1})) \simeq (-2/N, 1)$. Thus, close to s_{l1} , the equation of function $n_+(s)$ is

$$n_+(s) = -\frac{3N^4}{2} s - \frac{3N}{2}$$

Plugging this equation into Δ_c gives:

$$\Delta_c(s) = \left(1 + \frac{1}{-1 + e^{Ns}}\right) \left(1 - e^{-\frac{3Ns(2+Ns)}{4+3Ns}} + 3N + \frac{3}{2}N \left(Ns - e^{-\frac{Ns}{1+N}}(2 + Ns)\right)\right)$$

We then evaluate Δ_c in $s = s_{l1} + ds = -\frac{2}{N} + ds$, and look for the Taylor expansion for $ds \ll 1$ and large $N \gg 1$. Neglecting the term of order $\mathcal{O}(ds^2)$ we obtain that

$$\Delta_c(s_{l1} + ds) \simeq \frac{2}{(e^2 - 1)N} ds$$

Then

$$\lim_{ds \rightarrow 0} \Delta_c(s_{l1} + ds) = 0$$

Note that this limit was already true without the Taylor expansion for small ds . This limit means that close to s_{l1} , the condition (C.4) is verified. Thus we have

$$n_l = 2n_+$$

close to s_{l1} , and the slope of n_l as a function of s is twice the slope of n_+ (see fig. C.1):

$$\left. \frac{dn_l}{ds} \right|_{s=s_{l1}} \simeq -2 \frac{3}{2} N^2 \simeq -3N^2 \quad (\text{C.5})$$

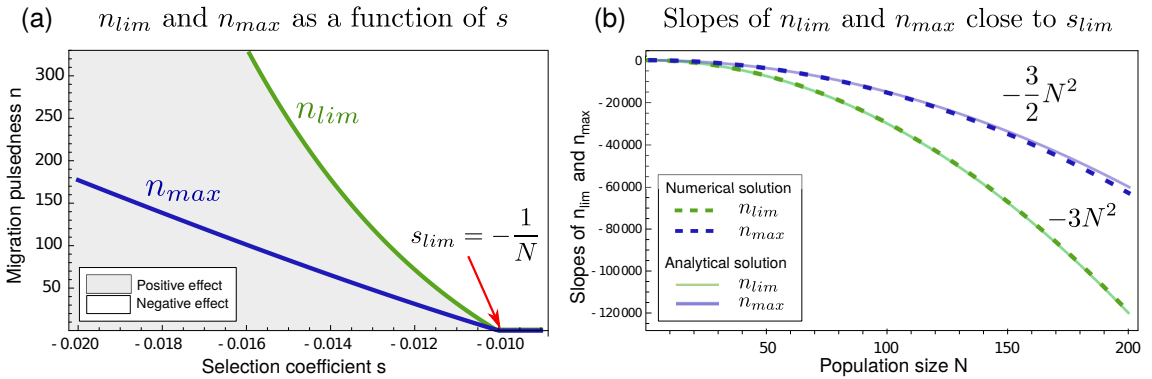


Figure C.1: (a) n_l and n_+ as a function of s , found numerically solving equation (C.3) for n_l and equation (C.1) for n_+ . The limit value s_{l1} of selection below which the qualitative effect of migration pulsedness depends on the value of n is indicated with a red arrow. It has been analytically estimated to be equal to $s_{l1} = -\frac{1}{N}$. Here $N = 100$. (b) Close to this selection limit value, the slopes of n_l and n_+ are estimated both numerically (dotted lines) and analytically (solid lines).

C.4 Effective migration rate from simulation

Effective migration rates are calculated from fixation time using an abacus which gives m_e as a function of fixation time.

To get the abacus, we record fixation times t_f in simulations for $n = 1$ (constant migration) and a large range of migration rates m . We then fit the relation between $\log(m)$ and $\log(t_f)$ by a polynomial order 3 function, which allows to make the correspondence between any measured fixation time (for any n and m) and an effective migration rate. Figure C.2 gives an example of such an abacus.

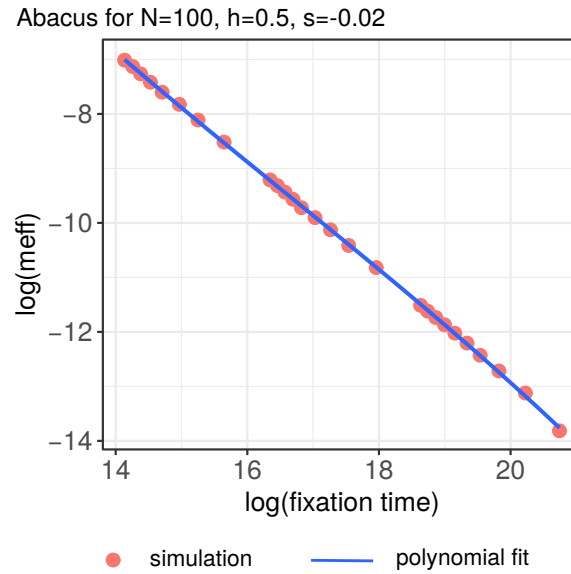


Figure C.2: Example of abacus with a polynomial order 3 function fit. For any fixation time obtained in a simulation with the same parameters N , s and h , we can derive the corresponding effective migration rate.

C.5 Mean number of migration events before fixation

To verify that a minimum of three migration events occur before fixation, we recorded the mean number of migration events before fixation (fig. C.3).

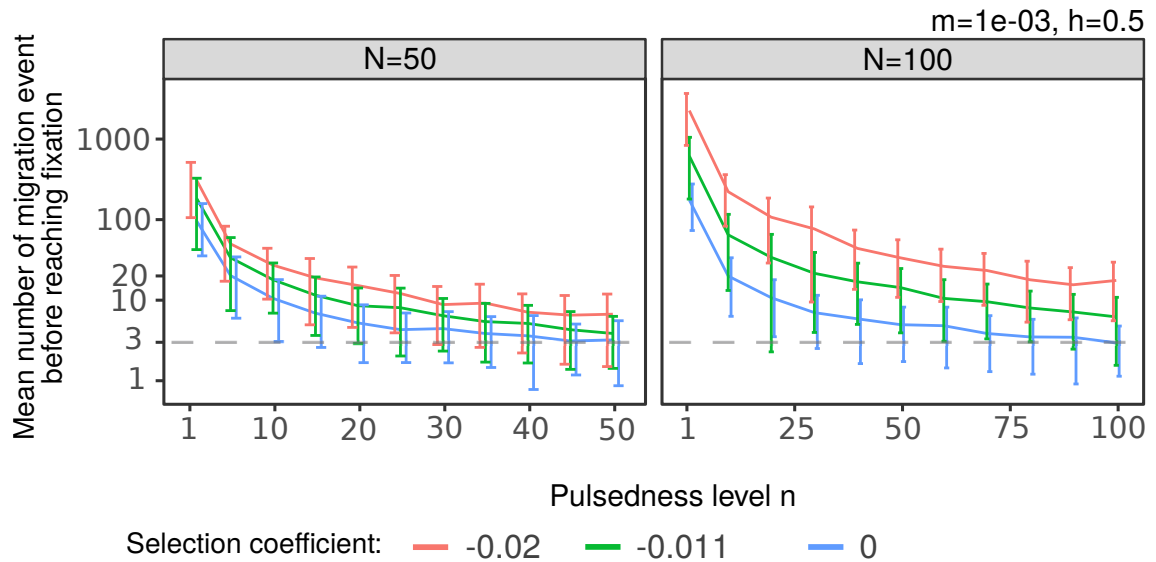


Figure C.3: Mean number of migration event before reaching fixation of the mainland allele into the island in log scale, as a function of pulsedness level. Error bar stands for standard deviation.

C.6 Simulations without time-scale separation and for different population sizes

C.6.1 Large m cases: the “mass” effect

If migration rate is large enough (such that the timescale separation is not respected), mainland alleles might already be present on the island when a new migration event occurs. We can see this “mass” effect as an artificial reduction of island population size. Instead of frequency $\frac{n}{n+N}$ mainland alleles that remain are at frequency $\frac{n+pN}{n+N}$ with p the proportion of mainland allele that remains in the island at the beginning of a new migration event. We have $\frac{n}{n+N} < \frac{n+pN}{n+N}$ so that it is equivalent to a larger propagule size. Also, looking for the mathematically equivalent population size N_a such that $\frac{n}{n+N_a} = \frac{n+pN}{n+N}$, we find $N_a = \frac{nN-nNp}{n+Np}$ and we can show that $N_a < N$ for any n or p . Thus, mathematically, an increase in initial frequency of the mainland island due to residual individuals in the island is equivalent to a decrease in population size. This can explain the observed shift towards higher values of Ns : we would need highest values of N to get the same effects of migration pulsedness.

C.6.2 Simulations for various m and N

Figure C.4 shows the observed effect of pulsedness (positive or negative) as a function of n and N for different m and N .

More precisely, the curves are plotted against Ns , and for n up to N . This highlights the fact that results are qualitatively almost invariant to population size if rescaling both axes by N , i.e. in terms of n/N and Ns .

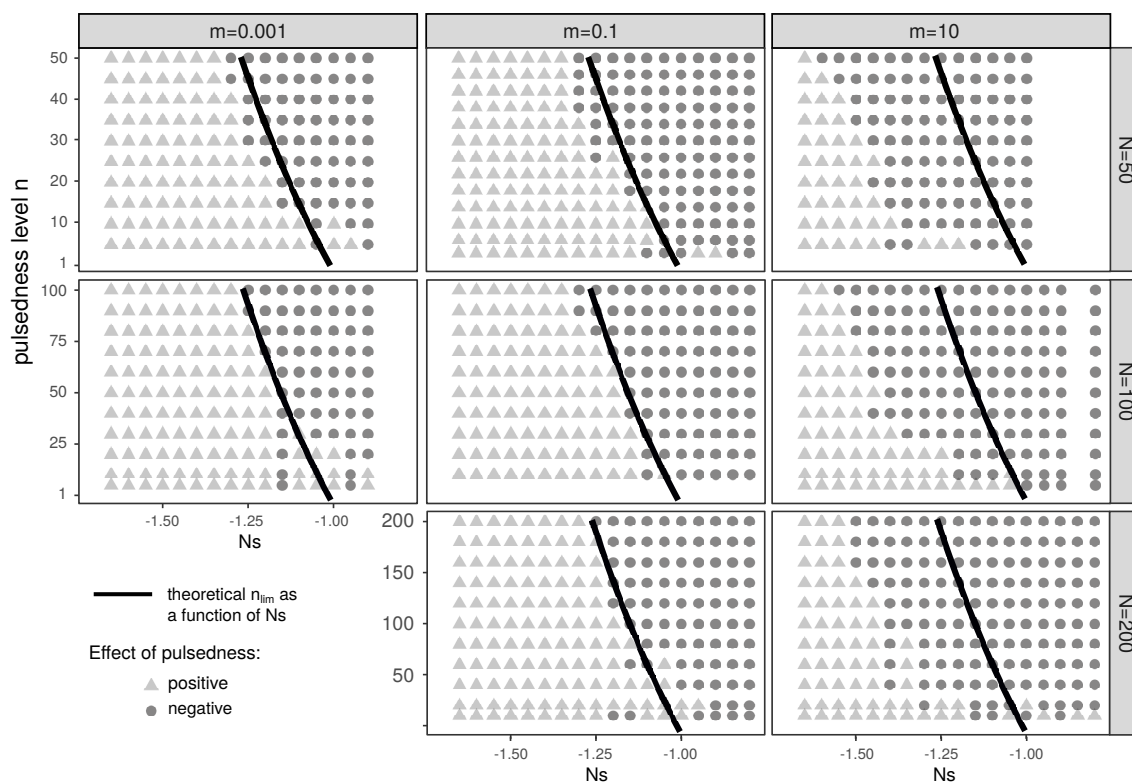


Figure C.4: The impact (found in simulations), either positive or negative, of migration pulsedness n as a function of the product Ns , for different values of population size N and migration rate m . We are here in a frequency-independent scenario ($h = 0.5$).

C.7 Probability that a mainland allele gets fixed, mean fitness in the island and pulsedness load

C.7.1 Probability f_1 that a mainland allele gets fixed

At a given selection value s and dominance degree h , the proportion of alleles $f_1(n, N, mt, s, h, t)$ in the island that comes from the mainland follows:

$$\frac{\partial f_1}{\partial t} = \beta(1 - f_1)$$

with $\beta = \frac{m}{n}u(f, N, s, h)$ and $u(f, N, s, h)$ the fixation probability of an allele arriving in frequency $f = \frac{n}{n+N}$. Solving this differential equation leaves us with

$$\begin{aligned} f_1(n, N, m, t, s, h) &= 1 - (1 - f_1(0)) \exp(-\beta t) \\ &= 1 - (1 - f_1(0)) \exp \left[-\frac{m}{n} u \left(\frac{n}{n+N}, N, s, h \right) t \right] \end{aligned}$$

The proportion $f_1(n, N, m, t, s, h)$ can be seen as the probability that an allele from the mainland with selection parameters s and h gets fixed in the island at a given time t . To simplify the notation, $f_1(n, N, m, t, s, h) = f_1$ in the main article.

C.7.2 Genetic load and pulsedness load

We suppose that migrant pools from the mainland follow an allelic distribution $p_m(s)$, so that an allele with a selection coefficient s has a probability $p_m(s)$ to be found in the migrant pool. Mean fitness $\bar{w}(n, t)$ is thus defined at each time t and each pulsedness level n by:

$$\bar{w}(n, t) = 1 + \sum_s s f_1(n, N, m, t, s, h) p_m(s)$$

Genetic load $L_g(n, t)$ is defined below (Wallace, 1970), with w_{max} the maximum fitness that can be reached in the island (corresponding to the hypothetical case of the fixation of all mainland beneficial alleles, and the absence of all the mainland deleterious alleles). It has been represented in the main article figure 5b.

$$L_g(n, t) = \frac{w_{max} - \bar{w}(n, t)}{w_{max}}$$

Pulsedness load $L_p(n, t)$ is defined as the difference in between the genetic load in a pulsed case and the genetic load in a continuous case. It corresponds to the additional load brought about by the pulse, and can be either positive (a pulsed migration provokes more genetic load than a continuous one) or negative (a pulsed migration provokes less genetic load than a continuous one).

$$L_p(n, t) = L_g(n, t) - L_g(1, t)$$

C.8 Likelihood and fitting the continuous model on pulsed data

C.8.1 Methodology

To fit the continuous model on pulsed data, we look at the parameters N' , m' and t' which maximize the likelihood of a data set. In our case, a data set corresponds to continuous values of $f_1 = f_1(n, N_i, m_i, t_i, s, h)$ over s . Every s corresponds to a locus, and loci are supposed to be independent of each other. In our examples, we suppose h to be constant and equal to $1/2$ (frequency independent selection case), but it could be set to other value, too. Parameters n , N_i , m_i and t_i are the “real” demographic parameters used to obtain the data set, and are supposed to be unknown.

Given some parameters N , m and t , the logarithm of the likelihood of a pulsed data point $f_{1,d}(s)$ for one given locus writes

$$L_h(f_{1,d}(s), N, m, t) = f_{1,d}(s) \log(f_{1,f}(s)) + (1 - f_{1,d}(s)) \log(1 - f_{1,f}(s))$$

with $f_{1,d}(s) = f_1(n, N_i, m_i, t_i, s, 1/2)$ the observed f_1 in pulsed data for a given locus (characterized by its selection s value), and $f_{1,f}(s) = f_1(1, N, m, t, s, 1/2)$ the model evaluated for this locus in a continuous case ($n = 1$) and at the given parameters N , m and t .

Every locus being independent, the total likelihood for the whole data set is the integral over s of the logarithm of the individual likelihood:

$$\int_s L_h(f_{1,d}(s), N, m, t)$$

In practice, we chose to give different weight to the different loci, specifying a migrant pool distribution of allelic frequency $p_m(s)$. Indeed, we can easily imagine that neutral loci are more frequent than very highly counter selected or very highly positively selected loci. In the main article, we give an example of a distribution of allelic frequencies centered around neutral loci, and in the following section, we illustrate the case of an allelic frequency centered on a weakly counter-selected locus. With this distribution, the total likelihood of the data set reads

$$L_{h,tot} = \int_s L_h(f_{1,d}(s), N, m, t) p_m(s)$$

As m and t are not identifiable under the mathematical model, however we simply fix $m = 1$ and estimate t . In practice, we use *Mathematica 11.3* to evaluate $L_{h,tot}$ for a grid of N and t values. We then interpolate this grid (using function *Interpolation*) which allows us to find the parameters N' and t' which maximize the interpolated function (using function *FindMaximum*).

C.8.2 The case of a migrant pool distribution centered on a negative value of s

In this example (fig. C.5), we considered an allelic distribution of the migrant pool centered on $s = -0.01$ with standard deviation 0.010.

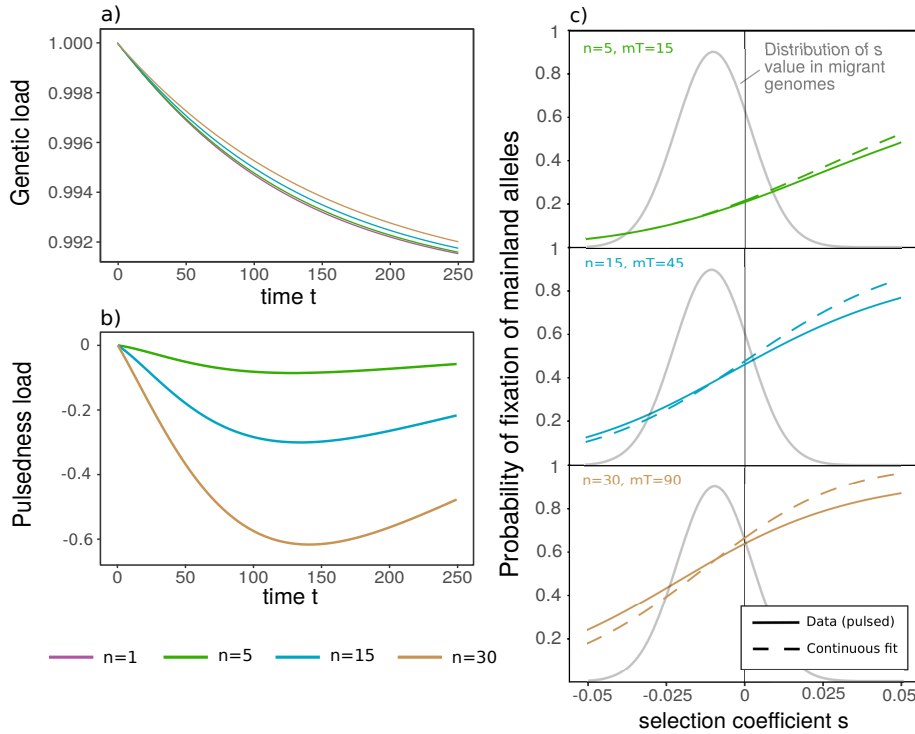


Figure C.5: (a) and (b) Genetic load and pulsedness load in the island as a function of time t in a continuous ($n = 1$) and in pulsed cases. (c) Continuous fit of pulsed data, made on the probability of fixation f_1 of a mainland allele as a function of s . The fit is made on data weighted by the allelic distribution of the migrant pool (here a normal distribution centered on $s = -0.01$ with 0.01 standard deviation). Data correspond to pulsed migration with $N = 60$ and $t = T = 3 * n$, so that at least 3 migration events have had time to occur in average. The best continuous fit gives $N' = 60$ and $T' = 14.4$ for $n = 5$, $N' = 59$ and $T' = 37.4$ for $n = 15$ and $N' = 57$ and $T' = 62.2$ for $n = 30$.

C.8.3 Pulsedness load depending on the allelic distribution of the migrant pool

Figure C.6 shows the genetic load and pulsedness load for various distributions of the migrant pool. We observe that pulsedness load is either positive or negative. It is positive when the allelic distribution of the migrant pool is centered around beneficial alleles, or around strongly deleterious alleles. Pulsedness load turns to negative (namely pulse has a positive impact on genetic load) in cases where the allelic distribution of the migrant pool is centered around a value between $s = -1/N$ and $s = 0$.

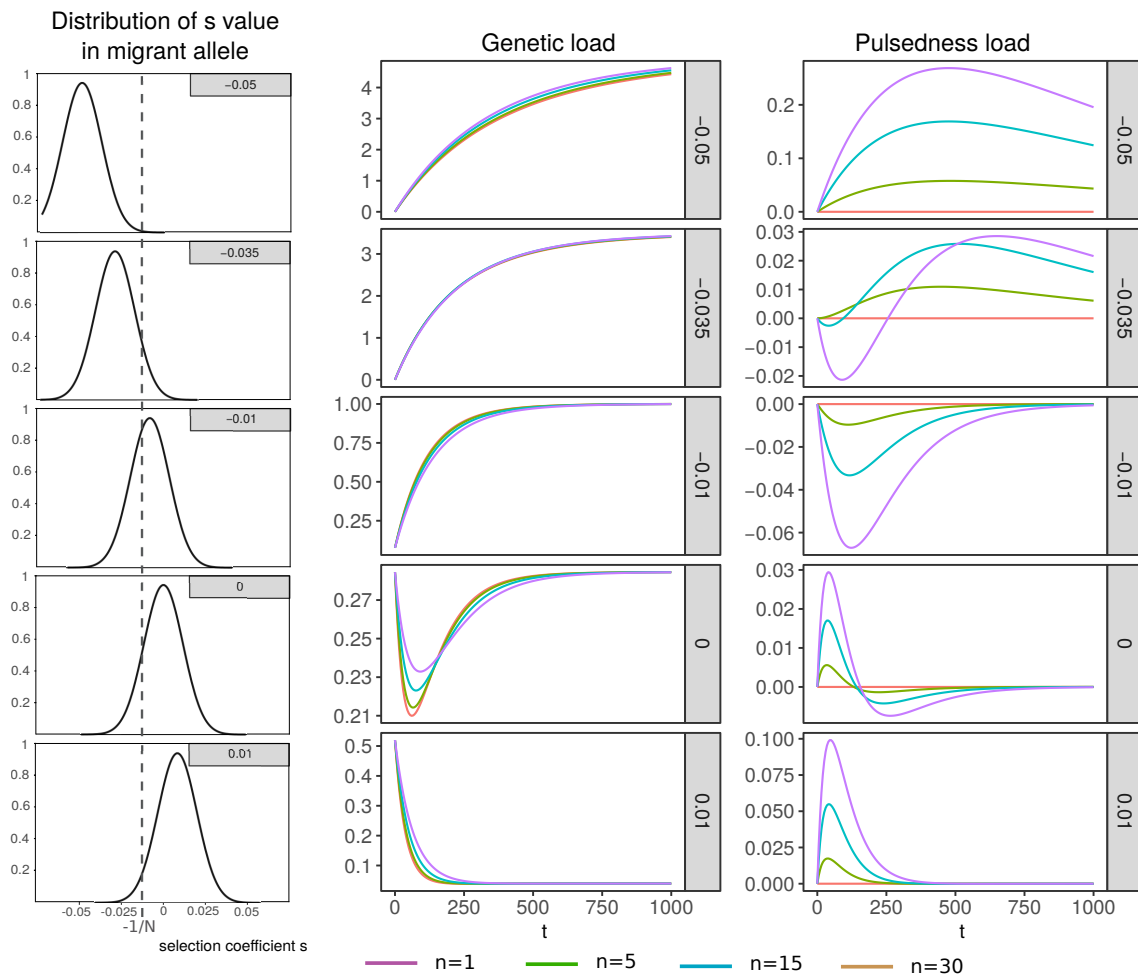


Figure C.6: Genetic load and pulsedness load for various allelic distribution of the migrant pool. From the top to the bottom, the mean of the distribution of s value in migrant allele is respectively -0.05 , -0.035 , -0.01 , 0 , 0.01 . Standard deviation is 0.01 and island population size is $N = 60$.

Bibliography

- Bajeux, N., Grognaud, F. & Mailleret, L. (2019) Influence of the components of propagule pressure, Allee effects, and stochasticity on the time to establish introduced populations. *Journal of Theoretical Biology*, **471**, 91 – 107.
- Goel, N.S. & Richter-Dyn, N. (1974) *Stochastic models in biology*. Academic Press., New York, San Francisco, London.
- Kimura, M. (1962) On the probability of fixation of mutant genes in a population. *Genetics*, **47**, 713–719.
- Kimura, M. & Ohta, T. (1969) The average number of generations until fixation of a mutant gene in a finite population. *Genetics*, **61**, 763–771.
- Otto, S.P. & Whitlock, M.C. (2013) Fixation probabilities and times. *eLS*. American Cancer Society. ISBN 978-0-470-01590-2.
- Peniston, J.H., Barfield, M. & Holt, R.D. (2019) Pulsed Immigration Events Can Facilitate Adaptation to Harsh Sink Environments. *The American Naturalist*, **194**, 316–333.
- Wallace, B. (1970) *Genetic load: its biological and conceptual aspects*. Englewood Cliffs, New Jers.: Prentice-Hall, Inc.
- Whitlock, M.C. (2003) Fixation Probability and Time in Subdivided Populations. *Genetics*, **164**, 767–779.

Appendix D

Inferring migration pulsedness from a genomic dataset

Thinking about the possibility to detect the migration pulsedness genomic signature, two questions arise following the Chapter 3 study. First, if we deviate from the limits of the mathematical model used in Chapter 3, will the genomic signature be as pronounced and detectable? And secondly, what would be the minimum genetic data set required to detect the signature in a real genomic dataset? What sample size, number of loci and external information would be needed? And what would be the statistical power of the approach in practice? All these questions require specific investigations to be addressed.

D.1 Type of data needed

We would need to consider a population (the “island”) that is known to be connected by migration to another population (the “mainland”). The island population effective size N does not have obligatory to be known, but this information could improve the quality of the analysis. Information on the date of contact of the two populations considered could also help, but is not mandatory either. The date of contact is the date at which the connection was made possible (through land or sea bridge for instance).

In this population, we would need to know the proportion of several alleles that we know to originally come from another population. “Several” is pretty vague, and this appendix is intended to provide a method that might help make this less vague. All that we know for now is that those several alleles must belong to different loci, and get different selection coefficient in the focal population. In other words, the genetic data set will be here defined by a number of loci, and by the distribution of mainland allele to each loci across selection coefficient. As we will perform a fit of the proportion of mainland allele present in the island as a function of selection coefficient, we must have sufficiently different selection coefficient represented, but also sufficiently loci per selection coefficient (to reduce the noise).

To answer the questions asked, we need simulated data sets (that can violate the mathematical assumptions of Chapter 3), and a suitable model that can fit

those data. Indeed, imposing strong constraints on migration rates, the model in Chapter 3 only allows access to a probability of fixation at time t , not the probability of having a given proportion of a given mainland allele on the island. We need to introduce a model that alleviates the hypothesis that fixation is fast relative to the inter-migration interval.

We first present such a model that describes the change in mainland allelic frequency in the island through time. We then compare this model with both the mathematical model and the stochastic simulations described Chapter 3, before exposing a method to estimate whether migration was pulsed or not.

D.2 Model description

As in Chapter 3, we consider a mainland-island system, in which there is a continuous migration from the mainland to the island. The system state is described by the number i of mainland alleles that are present in the island. We consider diploid individuals and one locus (see Chapter 3), and the population to be at its carrying capacity $N = K$, so that there are $2N + 1$ possible states for this system: $i \in \{0, 1, 2, \dots, 2N\}$.

The changes in the state of the system can be described as a Markov process. The probabilities to move from one state to another (transition probabilities) are controlled by migration, birth (selection) and death processes. Let's imagine we have two alleles: A from the mainland and a from the island. The possible transition are (see also fig. D.1):

- $i \rightarrow i - 1$ occurs if $AA \rightarrow Aa$ or if $Aa \rightarrow aa$ (birth-death). The transition probability is denoted $l_1(i)$.
- $i \rightarrow i - 2$ occurs if $AA \rightarrow aa$ (birth-death). The transition probability is denoted $l_2(i)$.
- $i \rightarrow i + 1$ occurs if $Aa \rightarrow AA$ (migration or birth-death) or if $aa \rightarrow Aa$ (birth-death). The transition probability is denoted $g_1(i)$.
- $i \rightarrow i + 2$ occurs if $aa \rightarrow AA$ (migration or birth-death). The transition probability is denoted $g_2(i)$.

We note $p_i(t)$ the probability to be in state i at time t . The master equation describing the change in state with time is:

$$\begin{aligned} \frac{dp_i(t)}{dt} = & -p_i(t)(l_1(i) + l_2(i) + g_1(i) + g_2(i)) \\ & + p_{i+1}(t)l_1(i+1) + p_{i+2}(t)l_2(i+2) \\ & + p_{i-1}(t)g_1(i-1) + p_{i-2}(t)g_2(i-2) \end{aligned} \quad (\text{D.1})$$

We note w_i the relative fitness of the mainland allele compared to the island allele, or in other words, the probability that a new gamete in the island is A .

$$w_i = \frac{\left(\frac{i}{N}\right)^2 (1+s) + \left(\frac{i}{N}\right) \left(1 - \frac{i}{N}\right) (1+hs)}{\left(\frac{i}{N}\right)^2 (1+s) + \left(\frac{i}{N}\right) \left(1 - \frac{i}{N}\right) (1+hs) + \left(1 - \frac{i}{N}\right)^2}$$

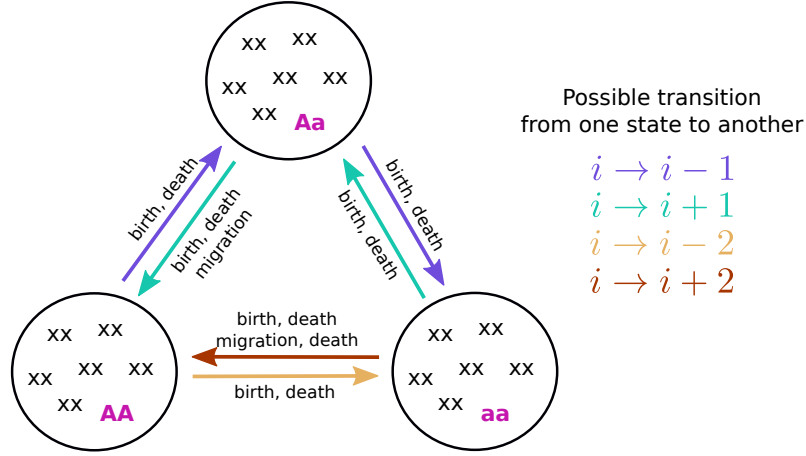


Figure D.1: Possible transition of the system. The system state i is the number of allele A in the island. A is the mainland allele and a the island allele. xx denotes any kind of genotype, either AA , Aa or aa .

with s the selection coefficient applied on allele A in the island. If $s = 0$, then w_i is simply equal to i/N . If $i = 0$ or $i = N$ then w_i is respectively 0 or 1. We note r the growth rate (probability of having a birth-death event per unit time) in the island, and m_r the migration rate (probability of having a migrant AA arriving on the island per unit time). The four transition probability write:

$$l_1(i) = 2r \left(\frac{i}{N} \right)^2 w_i(1 - w_i) + 2r \left(\frac{i}{N} \right) \left(1 - \frac{i}{N} \right) (1 - w_i)^2$$

$$l_2(i) = r \left(\frac{i}{N} \right)^2 (1 - w_i)^2$$

$$g_1(i) = 2r \left(1 - \frac{i}{N} \right)^2 w_i(w_i - 1) + 2r \left(\frac{i}{N} \right) \left(1 - \frac{i}{N} \right) (w_i)^2 + 2m_r \left(\frac{i}{N} \right) \left(1 - \frac{i}{N} \right)$$

$$g_2(i) = r \left(1 - \frac{i}{N} \right)^2 (w_i)^2 + m_r \left(1 - \frac{i}{N} \right)^2$$

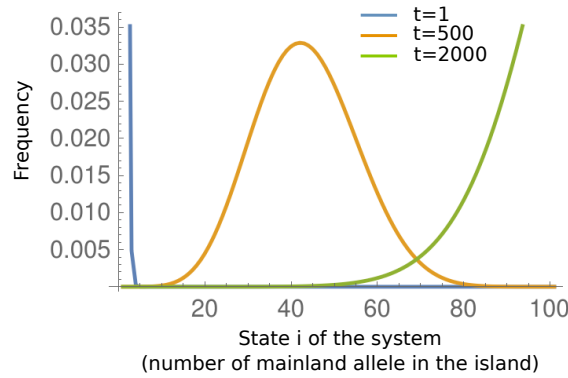


Figure D.2: Distribution of state i of the system for different times.

Here, we consider a continuous migration. Describing a pulsed migration this way would be more fastidious as it would imply to consider much more possible

transition. Finally precisizing an initial state (e.g. $p_i(0) = 0$) completes the set of equations that describes the distribution of allele A frequency in the island within time. We use Mathematica to numerically solve the differential equations (function *NDSolve*). Figure D.2 illustrates the distribution of allelic frequency for different time and the probability to be in state $i = N$ (“fixed”) within time.

D.3 Comparison with stochastic simulations and Chapter 3’s mathematical model

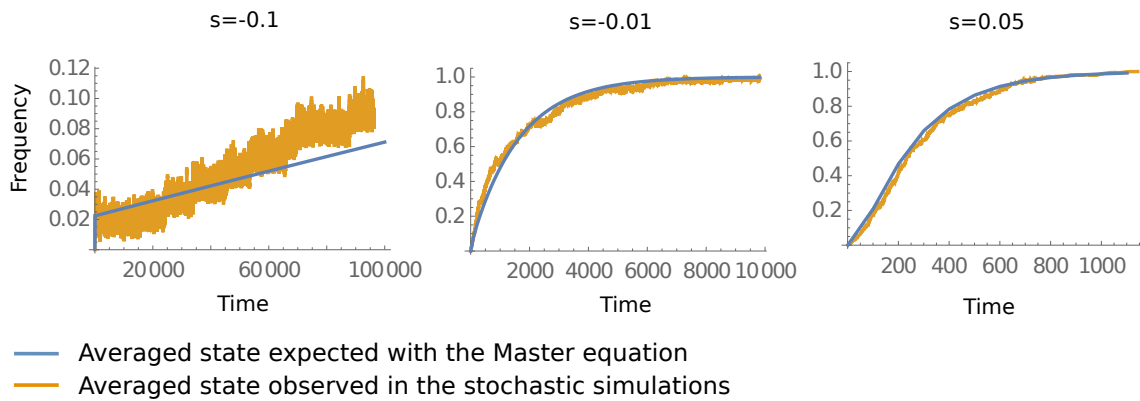


Figure D.3: Averaged state i expected with the Master equation and observed in the stochastic simulations as a function of time for different selection coefficient s . Here, $N = 100$ (equivalent to 50 individuals), $m_r = 0.1$, $r = 1/2$, $h = 0.5$.

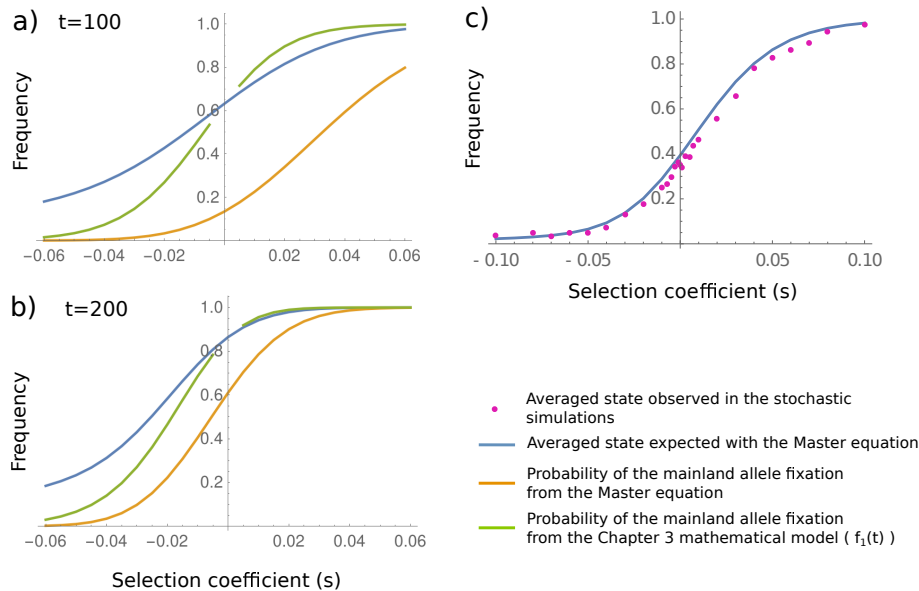


Figure D.4: Average state and probabilities of the mainland allele fixation as a function of s compared against each other. (a) and (b) are the same curves plotted at two different times ($t = 100$ and $t = 200$). (c) compares the average state observed in simulation and expected with the Master equation at time $t = 50$. Here, $N = 200$ (equivalent to 100 individuals), $m_r = 0.1$, $r = 1/2$, $h = 0.5$.

Comparing those results with the stochastic simulations in the continuous case shows a good concordance (see fig. D.3). It should thus in principle be possible to use the master equation to fit some simulation outputs and estimate whether the latter were realized under a pulsed or a continuous migration scheme.

Figure D.3 shows the averaged state i as a function of time. But in practice, we will only have access to a temporally local sample, and could not use the temporal dynamic to estimate parameters. Yet, as demonstrated in Chapter 3, it is possible to use the differential impact of migration on various unlinked loci, and to consider the averaged state as a function of selection coefficients. Figure D.4c illustrates this. We remark the good agreement between simulation and the Markov model.

Figure D.4a and b compares the averaged state (from the Markov model) and probability of the mainland allele fixation (from both the Markov model and the Chapter 3 model). We observe that the probability f_1 used in Chapter 3 is rather close to the average state calculated with the Markov model, but does not perfectly match it. It will therefore be preferable to use the model based on the Markov process to fit the data.

D.4 Fit by a maximum likelihood method

Equipped with this equation, we can now fit data sets. For this we will use a maximum likelihood approach.

Let's imagine the following situation. We consider a sub-sample of size N' of a population of size N (size not necessarily known). This population is referred here as the "island" population. We know several unlinked loci of the organism that composes this population, and we know that some of the alleles carried by those loci come from another population (referred here as the "mainland" population). We also know the selection coefficient applied, in the island, to each of the considered mainland alleles. We can measure, for each locus, to the number k of mainland alleles found in the sub-sample of size N' . We know that the two population (island and mainland) are connected by migration, but we don't know the migration rate m , and we don't know the time t since they are in contact. We do not know the pattern (pulsed or not) of this migration either.

We can make a guess of the different unknown parameters: N , m , t . By default, in the Master equation exposed above, the migration is considered as being continuous ($n = 1$). We can calculate the likelihood of this guess for our data set:

$$L = \prod_x L_x \quad (\text{D.2})$$

where x stands for one specific locus, which carries a mainland allele with selection coefficient s in the island, and found in k copies in the sub-sample N' . L_x is the likelihood for this specific locus. We define the likelihood L_x as

$$L_x = \sum_{i=0}^N p_i(t) P_{bin}(k, N', i, N) \quad (\text{D.3})$$

The sum is over the possible value of the system state i , and P_{bin} is the binomial probability which gives the probability to find k copies in a sub-sample of size N' knowing that the probability to pick a copy in the total population is $\frac{i}{N}$.

$$P_{bin}(k, N', i, N) = \binom{N'}{k} \left(\frac{i}{N}\right)^k \left(1 - \frac{i}{N}\right)^{N'-k}$$

For a given data set, we calculate the likelihood L for several combination of parameters N , m and t (several guess). The maximum likelihood obtained indicates which parameters combination most fits the data.

We then can observe whether the obtained fit really fit the data set or not. To render this observation more quantitative, we could for instance estimate the probability for the data set to have been generated by the model with the estimated parameters. If the estimated parameters does not fit the data set, we can conclude that the latter was generated by a pulsed migration process.

To estimate the minimal data set required to observe a pulsedness signature into them, we would have to test different scenarios for the data set. A scenario is a set of different selection coefficient, and a number of loci per selection coefficient value. In principle, we would have a large number of different scenario to test. A possible way to optimize the research could be to first determine the minimal number of loci required per selection coefficient, before focusing on the set of selection coefficient required.